Study of the feasibility and diagnostic accuracy of Proteomics and Next Generation Sequencing (NGS) for the investigation of neurosurgical cerebrospinal fluid infections.

Thesis submitted in accordance with the requirements of the University of Liverpool for the degree of Doctor in Philosophy

by

Libby van Tonder (née Ennis)

BA BAO BCh MB (Trinity College Dublin)

MSc (Trinity College Institute of Neuroscience)

MRCS(England)

January 2022

Abstract

Neurosurgical cerebrospinal fluid (CSF) infections continue to affect a small portion of patients despite clinical and technological advances in the field.. An infected neurosurgical implant like a ventriculoperitoneal shunt will need an operation to remove it whilst the CSF infection is treated and a repeat surgery performed once the CSF is sterile. Using proteomics and next generation sequencing (NGS) we explored novel approaches to the diagnosis of CSF infection.

Bottom up-proteomics (samples broken down by enzymatic digestion prior to liquid chromatography with tandem mass spectrometry LC-MS/MS) was used for biomarker screening in infected and uninfected neurosurgical CSF collected prospectively and also salvaged from routine microbiological testing. Lactoferrin, NPTXR, IGF2 and NEGR1 were identified as potential biomarkers and were tested using ELISA on further clinical CSF samples. The behaviour of proteins over the course of an infection (using samples from patients where multiple CSF samples were taken during a case of infection) was then examined using LC-MS/MS and ELISA. The pattern of differential expression of proteins seen in the first proteomic experiment was not reproduced but interesting trends emerged on cluster analysis of the sample cohort.

30 clinical CSF samples underwent NGS analysis. We were able to identify all the bacteria originally identified on routine in-hospital culture for clinically infected samples using NGS. Unexpectedly, *Prosthecochloris sp.* (a green sulphur bacterium) was identified in the definitely infected (cases where infection was clinically suspected and a bacterium was identified on routine in-hospital culture) and possibly infected (clinical suspicion of infection but no bacterium was identified on routine testing) samples but not in the uninfected (no infection suspected and all routine testing was negative for infection) samples tested. *Ralstonia spp.* also emerged as a potential pathogen in these samples.

The future of neurosurgical CSF infection diagnostics will require mass testing, great coordination, and big data but there will be a time when a proteomic profile combined with NGS testing will be able to reliably identify infection.

Acknowledgements

I would like to thank my PhD supervisors Conor Mallucci, Heather Allison and Mirren Iturriza-Gomara for their guidance and support (Mike Griffiths and Tom Solomon were involved at the beginning of my project). I would particularly like to thank Heather Allison and Mirren Iturriza-Gomara for stepping in and helping when circumstances required it. I would also like to acknowledge the great work and support given to me by our postdoctoral fellow Tessa Prince. My sanity was maintained throughout the delays and frustrations of research bureaucracy by my regular on call shift with the amazing Alder Hey paediatric neurosurgery department, led by the great hortator, Conor Mallucci.

I was able to collect the samples necessary to actually compete this project because of the Neurosurgery departments in Alder Hey Children's NHS Foundation Trust (Dawn Williams, Benedetta Pettorini, Chris Parks, Ajay Sinha, Sasha Burn and all the neurosurgical fellows who passed through during my time there), the Walton Centre NHS Foundation Trust and especially Colin Chisnall BSc (Hons) CSci FIBMS, Technical Manager, Medical Microbiology, Liverpool Clinical Laboratories- without whom I would have no project.

Proteomic analysis would not have been possible without Roman Fischer, Sarah Bonham and Svenja Hester in the Target Discovery Institute - University of Oxford. Next generation sequencing was completed with the Darby group in the Centre for Genomic Research, University of Liverpool. Statistical analysis of proteomics data was aided by Arturas Grauslys, Data Scientist, Computational Biology Facility, Technology Directorate, Life Sciences Building, University of Liverpool and also Nicolas Garron, lecturer in mathematics and computer science, Liverpool Hope University (and ukulele enthusiast).

Mostly I need to thank my husband, Martin van Tonder, who moved to a new country for me to do this PhD and was a constant support with culinary skills and research advice.

My final year sucked. My original primary supervisor had a second heart attack. My saving grace supervisor was poached to an NGO and my remaining supervisors were clinician academics who were suddenly even more busy than usual due to COVID 19. I no longer had a lab group or lab meetings. All non-COVID work halted. I worked in the ISARIC CCP CL3 lab during lockdown which allowed me to feel useful and part of a team but otherwise this final year has been lonely. I look forward to working as a team again and would love to lead a research team in the future- there are plenty of things I would make sure to be done

differently. In each job I have ever worked in I have learned many things. I have certainly learned a lot.

Declaration

Except for the assistance outlined in the acknowledgements, the work described is my own work and has not been submitted for a degree or other qualification to this or any other university.

List of Abbreviations

AIC	Antibiotic Impregnated Catheter
AUC	Area Under Curve
AUREA	Adaptive Unified Relative Expression Analyzer
AM	Aseptic Meningitis
BASICS	British Antibiotic and Silver Impregnated Catheters for ventriculoperitoneal Shunts
BBB	Blood Brain Barrier
BCE	Before the Common Era (previously BC- before Christ)
BCSFB	Blood CSF Barrier
βHCG	Beta-human chorionic gonadotropin
BLAST	Basic Local Alignment Search Tool
BM	Bacterial Meningitis
Bracken	Bayesian Re-estimation of Abundance after Classification with KrakEN
CAM	Cell Adhesion Molecule
CDC	Centers for Disease Control and Prevention
CE	Conformité Européenne
CGR	Centre for Genomic Research
CID	Collision Induced Dissociation
CNS	Central Nervous System
CoNS	Coagulase Negative Staphylococci
CP	Choroid Plexus
CSF	Cerebrospinal Fluid
CRP	C-Reactive Protein
CT	Computed Tomography
Da	Dalton or unified atomic mass unit
DES	DNA extraction solution
DNA	Deoxyribonucleic Acid
DMSO	Dimethylsulfoxide

ECM	Extracellular Matrix
EDTA	EthyleneDiamineTetraacetic Acid
ELISA	Enzyme-Linked Immunosorbent Assay
EPR	Electronic Patient Record
ESI	Electrospray Ionisation
ETV	Endoscopic Third Ventriculostomy
FBC	Full Blood Count
FCGR3A	Low affinity immunoglobulin gamma Fc region receptor III-A
FDA	Food and Drug Administration
FDR	False Discovery Rate
GCS	Glasgow Coma Scale
HCD	Higher-energy Collisional Dissociation
HRA	Health Research Authority
HRP	Horseradish Peroxidase
HSV	Herpes Simplex Virus
HTA	Human Tissue Authority
ICP	Intracranial Pressure
IFN-γ	Interferon-γ
IGF2	Insulin-like Growth Factor 2
IGH	Institute of Infection and Global Health
IIH	Idiopathic Intracranial Hypertension
IL-6	Interleukin 6
IL-1β	Interleukin 1β
IRAS	Integrated Research Application System
ISPN	International Society of Pediatric Neurosurgeons
IVD	In Vitro Diagnostic
Kilon	Kindred of IgLON
LCL	Liverpool Central Laboratories
LC-MS/MS	Liquid Chromatography with tandem mass spectrometry
LP	Lumbar Puncture

LTF	Lactoferrin
MALDI	Matrix-Assisted Laser Desorption/Ionization
MC&S	Microscopy, Culture and Sensitivity
mL	Milliliter
mmHg	Millimeters of mercury
MMP	Matrix Metalloproteinase
MS	Mass Spectrometer/Spectrometry
MTA	Material Transfer Agreement
NCBI	National Center for Biotechnology Information
NEGR1	Neuronal Growth Regulator 1
NGS	Next Generation Sequencing
NHS	National Health Service
NICE	National Institute of Health and Clinical Excellence
NPH	Normal Pressure Hydrocephalus
NPTXR	Neuronal Pentraxin Receptor
NPV	Negative Predictive Value
PBS	Phosphate-Buffered Saline
PCA	Principal Component Analysis
PCR	Polymerase Chain Reaction
PCT	Procalcitonin
POCT	Point of Care Test
PPM	Parts per million
PPV	Positive Predictive Value
PRM	Pattern Recognition Molecule
PTM	Post Translational Modification
RCC	Red Cell Count
RCF	Relative Centrifugal Force
REC	Research Ethics Committee
RNA	Ribonucleic Acid
ROC	Receiver Operating Characteristic Curve

RPM	Revolutions Per Minute
RPM	Reads Per Million
rRNA	Ribosomal Ribonucleic Acid
SAM	Significance Analysis of Microarray
SAP	Serum Amyloid P Component
SCG2	Secretogranin II
SCG5	Secretogranin V
SSI	Surgical Site Infection
TBE	Tris Borate EDTA
TDI	Target Discovery Institute
TIMP	Tissue Inhibitor of Metalloproteinase
TNF-α	Tumour Necrosis Factor-α
TMB	Tetramethylbenzidine
TOF	Time of Flight
UK	United Kingdom
UoL	University of Liverpool
UPLC	Ultra-performance liquid chromatography
USA	United States of America
U&E	Urea and Electrolytes
VA	Ventriculo-Atrial shunt
VGF	Vereinigte Glanzstoff-Fabriken (nerve growth factor inducible)
VM	Viral Meningitis
VPlS	Ventriculopleural Shunt
VPS	Ventriculoperitoneal Shunt
VSG	Ventriculo-SubGaleal shunt
WCC	White Cell Count
WHO	World Health Organisation
µL	Microliter
2D-PAGE	Two-Dimensional Polyacrylamide Gel Electrophoresis

List of Figures

List of Tables

Table of Contents

Chapter 1. Introduction

1.1 Neurosurgery

"It has often been said that the two oldest living professions are prostitution and neurosurgery. I would assume that the ancient warrior realized very early on that it was easiest to annihilate, or at least slow down, his opponent with a blow to the head. Therefore, the concept of head injury remains as ancient as the powers of solicitation of the opposite sex."

James Goodrich commenting on; Stone Age Skull Surgery in Mecklenburg-Vorpommern: A Systematic Study[1].

Neurosurgery, also sometimes referred to as neurological surgery, is a specialty concerned with diagnosis, assessment and surgical interventions of the central nervous system (CNS; brain and spinal cord) and the peripheral nervous system (PNS; peripheral nerves) [2].

Despite neurosurgery being a highly technological and modern practice, it has existed for millennia. The earliest evidence of trepanation (removing fragments of bone from the skull using man made instruments) comes from North Africa, dating back to the Neolithic period to approximately 10,000 BCE[3]. Archaeological evidence of trepanation has been found on every continent. Recently Peruvian excavations have discovered that 6% of mummies there had undergone trepanation and that many of these skulls showed bony remodelling as evidence of postoperative survival[4].

With the advent of reliable anaesthesia and antisepsis in the 19th century, neurosurgery became a more realistic clinical option for surgeons. All the while, knowledge of the anatomy and physiology of the brain advanced. The specialty principally took shape in the 20th century when neuroimaging (computed tomography [CT], magnetic resonance imaging [MRI]) and antibiotics became available[3].

Globally neurosurgery continues to grow apace. Worldwide there are an estimated ~50,000 neurosurgeons, mostly based in developed nations in Europe, North America, and Australia. Japan has the highest density with 58.95 neurosurgeons per 1 million population but there

are at least 33 countries which have no known neurosurgeons [2]. Worldwide, annually there are an estimated 13.8 million cases that require neurosurgical operations and 22.6 million cases needing neurosurgical opinion. There is an estimated deficit for 5.2 million neurosurgical cases annually, due to lack of lack of surgical capacity. Africa for example makes up 15% of neurosurgical disease worldwide but only has 1% of the neurosurgeons [5].

Whilst these numbers show the extent of neurosurgery worldwide, it can also be noted that neurosurgery is a very niche area (50,000 consultant neurosurgeons on the planet).

The act of breaching the CNS to operate for whatever reason, introduces the risk of infection. This risk is even higher when a device is implanted into the CNS (ventriculoperitoneal shunts for example- which will be discussed in section 1.4). Infection has been a grave concern to neurosurgeons from prehistoric times to present. In the past, the Sumerians used wine and turpentine-soaked head bandages in an effort to avoid infection. In medieval times boiling oil was applied to wounds. Silver tubes were inserted into brain abscesses to drain pus in the 18th century in a recognition of the metals antimicrobial properties [6]. Postoperative neurosurgical infections is a major source of morbidity and mortality, and with a better appreciation of the consequences of CNS infection, the need for swift, conclusive diagnosis of infection for the instigation of appropriate treatment is of ever more pressing importance.

1.2 The Central Nervous System (CNS)

The central nervous system (CNS) is comprised of the brain and spinal cord, anatomically they are housed and protected in bony structures; the skull and spine [7]. Very broadly, the brain is made up of cerebrum, cerebellum and brainstem. The cerebrum is divided into two hemispheres (left and right) and functionally there are four lobes (frontal, parietal, temporal and occipital) (Fig. 1) [8]. Within this, there are an estimated 86 billion neurons in the average brain [9].

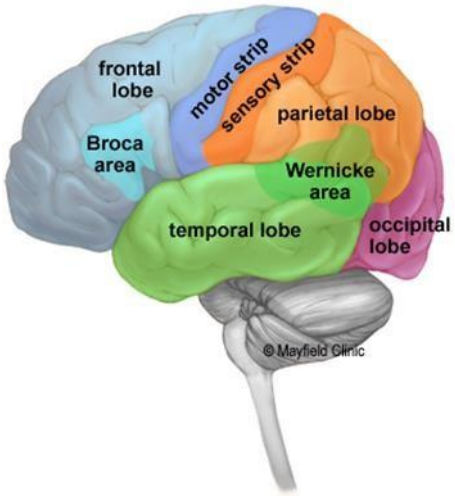

Figure 1 The lobes of the cerebrum; Frontal lobe (with Broca area for speech and motor strip), parietal lobe (with sensory strip), temporal lobe (with Wernicke area for language) and the occipital lobe[8].

Within the matter of the brain there are fluid filled spaces, ventricles. In the depths of each cerebral hemisphere is a c-shaped lateral ventricle, these connect with the midline, slit-like, third ventricle via the Foramen of Monro. The third ventricle connects to the fourth ventricle though the Aqueduct of Sylvius (cerebral aqueduct) (Fig. 2).

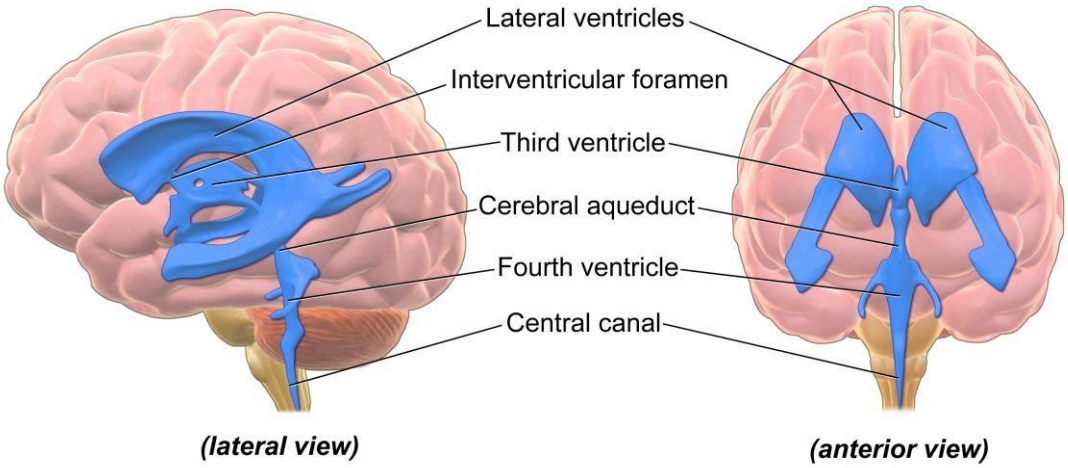

Figure 2 Anatomy of the ventricles within the brain [10]. Illustrating the position of the two lateral ventricles within each hemisphere of the brain. These lateral ventricles communicate medially with the midline third ventricle, which continues inferiorly to the fourth ventricle (via the Cerebral Aqueduct). The fourth ventricle narrows and continues as the central canal within the spinal cord[10].

1.3 Cerebrospinal Fluid (CSF)

As cerebrospinal fluid (CSF) is one of the most important components of investigation of neurosurgical infections, its physiology will be explored here.

1.3.1 Definition

CSF is a clear, colourless fluid contained in the ventricular system of the brain and between the arachnoid and pial layers of the meninges surrounding the brain and spine (Fig 3 & 4). The intracranial space of an average adult typically measures 1500 mL-consisting of 87% brain (all the nervous tissue- neurons, supporting glial cells and connective tissue etc), 9% CSF and 4% blood [11, 12].

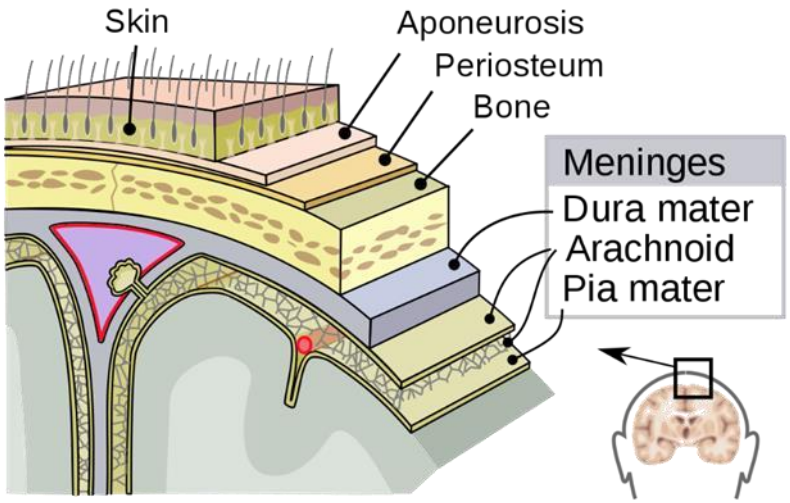

Figure 3 A diagram of the layers of the scalp (skin, aponeurosis, periosteum), skull and the covering of the brain- the meninges (three layers: dura mater, arachnoid mater and pia mater) [10]. These are the protective layers that separate the brain and spinal cord from the external world.

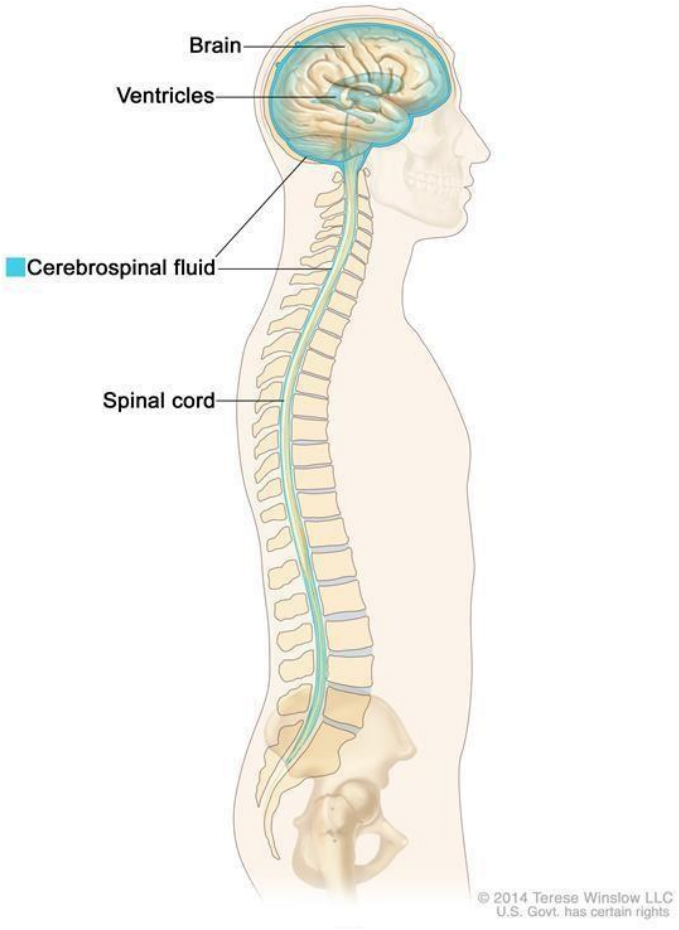

Figure 4 CSF circulating throughout the CNS [12]. This diagram shows the physically dispersed nature of CSF but as seen in Fig. 3 this CSF is very much separate from the rest of the body. This separation prevents microbes that are commonly encountered in daily life from entering the CNS (discussed in more detail in section 1.5).

The earliest known description of CSF comes from an ancient Egyptian text discovered in the 17th century (known as the Edwin Smith surgical papyrus) [13]. The anatomy of the brain and the ventricles received more attention in antiquity and it was not until 1747 that a Swiss physiologist, *Albrect von Haller*, described CSF secretion within the ventricles and absorption by veins [13].

Harvey Cushing described CSF as the "third circulation" in 1925 [14], to others it was a "nourishing liquor" and even analogous to the lymphatic system as being part of the "glymphatic system"[15, 16] but it was *François Magendie*, the French physiologist, who in 1842 first called *it "le liquide céphalo-rachidien ou cérébro-spinal"* or cerebrospinal fluid in English [17].

1.3.2 CSF production

It is traditionally taught that CSF is produced in the choroid plexus (CP) of the ventricles, but the reality is more nuanced than that simplistic explanation. The CP is a well vascularised, highly branched structure that projects into the ventricles. The CP is covered by specialised ependymal cells (choroidal epithelium) whose surface area are further increased by numerous villi [18]. The capillaries of the CP receive ten times the blood supply compared to that received by the brain cortex [19].

CSF is formed when hydrostatic pressure pushes plasma ultrafiltrate through the fenestrated walls of the CP capillaries, it then requires an active metabolic process to allow this ultrafiltrate to pass through the choroidal epithelium. CSF is actively secreted into the ventricles and the osmotic gradient is carefully controlled via sodium/chloride/bicarbonate ion transport [15]. This capillary-choroidal epithelium is also known as the blood-CSF barrier (BCSFB) as it forms part of an important physical barrier separating the CNS from the rest of the body [15]. This will be discussed in more detail in section 1.5.1.

It is thought that approximately 80% of CSF is formed by the CP [12, 20-22]. There are other sites of CSF production; the ventricular ependyma [11, 23] and possibly the brain parenchyma (interstitial fluid). CSF is produced continuously at a rate of 0.3 – 0.4 mL/min which means that the total production per day is about 430 – 580 mL, depending on body size and gender. Based on the total CSF volume of ~160 mL in the CSF system, it takes about six and a half to nine hours to replace this volume of fluid [18].

CSF is said to flow from the lateral ventricles through the Interventricular Foramina of Monro to the third ventricle, then onwards via the Cerebral Aqueduct of Sylvius to the fourth ventricle, it then enters the Cisterna Magna via the Foramina of Magendie (median foramen) and Luschka (lateral foramen). CSF then circulates in the subarachnoid space around the brain and spinal cord (Fig. 5). Its production is counterbalanced by its absorption into the cerebral vessels via the arachnoid villi by means of a hydrostatic gradient [14]. The intricacies of the production, flow and absorption of CSF continue to be discovered and remain somewhat unclear. Research is ongoing and with advancing imaging and experimental design, the reality is slowly emerging [18].

1.3.3 CSF Function

CSF forms a major portion of the extracellular fluid of the CNS, and it is well recognised for its vital role in brain health. The role of CSF has traditionally been thought to physically

protect the brain through buoyancy and to remove brain metabolites through the drainage of CSF [12]. Indeed, CSF buoyancy is said to reduce the effective weight of the brain from 1500 g to approximately 50 g via the Archimedes effect [24]. More recently the choroid plexus - CSF system has been recognised to play a much more active role in the development, homeostasis, and repair of the CNS [25]. A list of some of the known functions of CSF is seen in Table 1.

Table 1 Functions of CSF in the brain adapted from Neuroscience in Medicine, Johanson 2008*[12].*

CSF functions	Examples
Buoyancy effect	Brain weight is effectively reduced by >95%, shearing and tearing forces on neural tissue are greatly minimized.
Intracranial volume adjustment	CSF volume can be ↑or ↓ acutely in response to blood volume changes or chronically in response to tissue atrophy or tumour growth.
Micronutrient transport	Nucleosides, pyrimidines, vitamin C and other nutrients are transported via CSF to brain cells.
Protein & peptide supply	Transthyretin, insulin-like growth factor, and thyroxine are transported by CSF to target cells in the brain.
Source of osmolytes for brain volume regulation	In acute hypernatremia, there is bulk flow of CSF with osmolytes, from ventricles to surrounding tissue. This promotes water retention by shrunken brain, i.e., to restore volume.
Buffer reservoir	Shifts in brain interstitial H+, K+, and glucose concentrations can by buffered by CSF
Sink or drainage action	Waste products are cleaned from the CNS by active transporters in the choroid plexus or by bulk CSF drainage pathways to venous blood and the lymphatics.
Immune system mediation	Cells adjacent to ventricles have antigen-presenting capabilities. Some CSF protein drains into cervical lymphatics, with the potential for inducing antibody reactions.
Information transfer	Neurotransmitter agents like amino acids and peptides may be transported by CSF over distances to bind receptors in the parasynaptic mode.
Drug delivery	Some drugs do not readily cross the blood-brain barrier but can be transported into the CSF by endogenous proteins in the choroid plexus epithelial membranes.

1.3.4 CSF composition

The clear colourless fluid that is CSF is more than just water (Table 2) and the concentrations of electrolytes etc differ from other body fluids (Table 3).

Table 2 CSF composition. A non-exhaustive list of substances found in CSF, adapted from Spector et al [15].

Composition of CSF	
Water	

Ions	Sodium Chloride Bicarbonate Calcium Magnesium Manganese
Vitamins	Vitamin C Folate Thiamine
Hormones transported from the blood	Leptin Prolactin IGF- 1
Proteins produced by the CP	Transthyretin IGF-2 BDNF (brain-derived neurotrophic factor)
Proteins that diffuse through BBB as a function of size	Albumin Immunoglobulins

Table 3 Concentrations of solutes in plasma and lumbar CSF. An historical study of the concentrations of electrolytes, urea and osmolality in the CSF and plasma of 40 healthy subjects. Adapted from Sambrook et al [26]. CSF is similar but not identical to plasma, these differences can be useful when testing CSF for infection (1.5.4.6).

Substance (unit)	CSF	Plasma	Mean concentration ratio CSF/plasma
Sodium (Na^+) (mmol/L)	138-151	146 – 156	0.95
Potassium (K^+) (mmol/L)	2.6-3.1	3.6 - 5.0	0.69
Chloride (Cl^-) (mmol/L)	111-126	103–118	1.09
Urea (mg/dL)	15-54	18-68	0.82
Osmolality (mOsm/kg)	277-300	282 – 296	0.99

1.3.5 CSF sampling

Given the intimate relationship of CSF to the brain and its function or dysfunction, there are many scenarios where CSF needs to be sampled for clinical testing and diagnosis. These can be broadly grouped into infection (meningitis, encephalitis- discussed in section 1.5), bleeding (e.g., subarachnoid haemorrhage), tumours and inflammatory disorders (e.g., multiple sclerosis). For most specialties CSF sampling is primarily done via lumbar puncture (LP) (Fig 5).

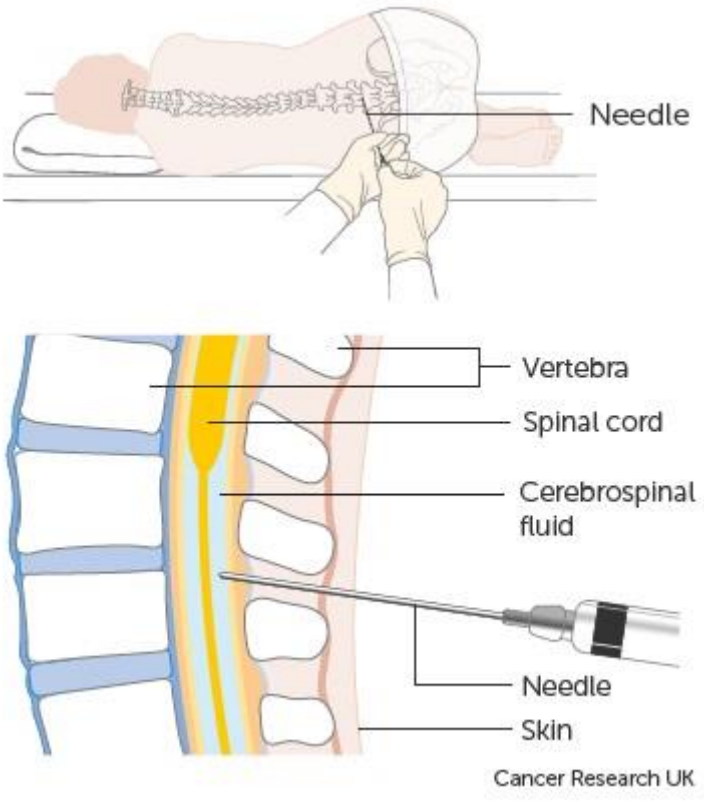

Figure 5 Diagram of the lumbar puncture procedure. The patient is usually lying, back facing the clinician, with knees pulled up to the chest. The spinous processes (bony prominences) of the lumbar spine are palpated by the clinician. A suitable entry point is chosen and marked. After decontaminating the skin and injecting local anaesthetic, a spinal needle is introduced to the space between the spinous processes. A" give" is felt when the needle passes through the dura of the meninges and CSF may then flow [26].

1.4 Hydrocephalus

1.4.1 Introduction

The CNS (brain and spinal cord) is enclosed in the meninges and protected by a rigid bony skeleton of skull and spine as described in section 1.2. The space contained within the CNS is therefore of fixed volume. Intracranial pressure (ICP) is the term used to describe the pressure within this space. Normal ICP ranges between 5-10 mmHg in adults and older children, with an upper limit of 15mmHg often being cited. There are normal transient

elevations in ICP up to 30-50mmHg with actions like coughing or sneezing but the ICP rapidly returns to normal levels[11].

The Monroe-Kellie Doctrine, one of the founding tenets of neurosurgical theory, states that the volume of the intracranial compartment is constant due to the rigid bony coverings. The contents are made up of brain, blood and CSF. If there is an increase in volume of any one of these constituents, there will be a counteracting decrease in volume of the other parts. Once the system is no longer capable of compensating for the rise in one component with the decrease in another component, the ICP begins to rise[27].

Derangements in ICP can have serious clinical consequences. A persistent elevation of ICP is a pathological and potentially life-threatening state. Infection of the CSF can cause hydrocephalus (see Table 4) and treatments for hydrocephalus can cause CSF infection.

Table 4 Causes of Hydrocephalus. Pathologies causing hydrocephalus grouped as non-communicating and communication (columns). This is further divided by timing of onset of hydrocephalus, whether congenital or acquired. Adapted from Youmans Neurological Surgery [28].

Non communicating (obstructive)	***Communicating***
Congenital	
Aqueduct Stenosis Dandy Walker Cyst Benign intracranial cysts (arachnoid cysts) Vascular malformations (vein of Galen malformations)	Arnold Chiari Malformation Encephalocoeles Skull base deformity
Acquired	

Tumour Other mass lesions (giant aneurysms, abscesses) Ventricular scarring	**Infection** Haemorrhage Venous hypertension (venous sinus thrombosis, arterio-venous shunts) Meningeal carcinomatosis (diffuse tumour) Overproduction of CSF (choroid plexus papilloma)

1.4.1.1 Definition of Hydrocephalus

Hydrocephalus as a term comes from the Greek; ὕδρο- (hydro-, from ὕδωρ, “water”) and κεφαλή (kephalé, “head”); literally “water on the brain”[29]. It makes sense that the word is Greek as the first description of it and use of the term comes from Hippocrates (466-377 BCE)[30]. Just as there is evidence of neurosurgery over the millennia there is evidence of hydrocephalus. Skeletons dating back to 10,000 BCE have been found with paleo pathological features of hydrocephalus[31].

Hydrocephalus is not a disease or diagnosis in itself; it is a pathophysiological condition that has many causes. Its definition has therefore been controversial over the years and highly changeable from publication to publication[32].

Orešković et al asserted the following in *Paediatric Neurosurgery* in 2017;

> *“A new definition suggests that hydrocephalus is a pathological state in which CSF is excessively accumulated inside the cranial part of the CSF system, predominantly in one or more brain ventricles as a consequence of impaired hydrodynamics of intracranial fluids between CSF, brain, and blood compartments.”[33]*

Since 2008 and through to today, *Rekate* has argued that hydrocephalus should be defined as;

> *“an active distension of the ventricular system of the brain related to inadequate passage of cerebrospinal fluid (CSF) from its point of production within the ventricular system to its point of absorption into the systemic circulation”[34]*

No one definition has managed to encompass all the scenarios considered to be *Hydrocephalus*. Definitions fail to include some commonly seen conditions like Idiopathic Intracranial Hypertension (IIH), a condition where the ventricles are normal size but the ICP is significantly elevated and can threaten eyesight[35]. Or Slit Ventricle Syndrome, where a patient who has had long term hydrocephalus can sometimes develop unresponsive ventricles – so that the ventricles do not enlarge (they remain slit like) even when the ICP is extremely elevated, even to life-threatening levels[36]. In Normal Pressure Hydrocephalus (NPH) the ventricles are often distended but the measured ICP is not elevated and curiously symptoms (classically a triad of gait disturbance, dementia and urinary incontinence) are ameliorated by CSF drainage[37].

Hydrocephalus was originally classified, in the early 20th century, as either

"communicating" or "noncommunicating" by another doyen of the neurosurgery world- *Professor Walter Dandy*[38]. Contemporary publications, including the National Institute of Neurological Disorders and Stroke (NINDS), continue to use this definition.

Handbook of Pediatric Surgery (2010)

"Communicating – full communication exists between the ventricles and subarachnoid space. *Noncommunicating* – CSF flow is obstructed within the ventricular system or in its outlets to the arachnoid space."[39]

Neuroendoscopy (2014)

"Noncommunicating hydrocephalus (NCH) is related to an obstacle on the CSF pathways, whereas communicating hydrocephalus (CH) concerns a pathological ventricular dilatation without identified obstacle."[40]

Hydrocephalus (2017)

"The term more frequently used nowadays is an obstruction in the ventricular system (obstructive or noncommunicating type) or alternation in CSF absorption or flow (communicating type)"[41]

Table 5 Proposed revised classification of causes of hydrocephalus based on site of obstruction. In a recent proposal for revised classification of hydrocephalus Rekate found only 6 attempts since 1990 at newer classification systems[34]. ETV= endoscopic third ventriculostomy, this will be discussed in section 1.4.2.4.1

Site of Obstruction	Pathology	Treatment
None	Choroid plexus papilloma	Removal
Foramen of Monro	Tumour, congenital anomaly, post-shunt ventricular asymmetry	Tumour removal, septum pellucidotomy, ventricular shunt
Aqueduct of Sylvius	Congenital lesion, tumour-secondary to extraventricular obstruction	ETV, ventricular shunt
Outlets of fourth ventricle	Chronic meningitis, Chiari II malformation	ETV, ventricular shunt
Basal cisterns	Meningitis, post subarachnoid haemorrhage	ETV, ventricular shunt, spinal thecal shunt
Arachnoid granulations	Haemorrhage or infection in infancy	Ventricle or thecal shunt

Venous outflow	Skull base anomalies, congenital heart disease	Ventricular or thecal shunt, treatment of vascular anomaly if possible

1.4.1.2 Prevalence, Incidence, Cost

Dewan et al estimated that worldwide there were 400,000 new cases of *childhood* hydrocephalus in 2019[42]. To put this in context, we can compare these numbers to another pathology that is considered as a worldwide health threat; HIV[43]. In 2019 there were an estimated 160,000 children with a new diagnosis of HIV[44].

The global prevalence of hydrocephalus was recently estimated by meta-analysis to be 85 per 100,000 population. This ranges from 11/100,000 in adults, 72/100,000 in the paediatric population to 175/100,000 in the elderly [25]. If this calculation is true then scaling up to a global population of 7.7 billion [45] there are 6.5 million people with hydrocephalus on the planet. The Hydrocephalus Clinical Research Network in the USA estimated that in 2003 up to $2 billion was spent on treating *paediatric* hydrocephalus in the USA alone[46].

1.4.1.3 Clinical Presentation

The presentation of hydrocephalus is that of raised ICP. Raised ICP can occur acutely or chronically, producing slightly different signs and symptoms (Table 4) [29]. Presentation also depends on the age of the sufferer. In young infants the skull is still growing, and the bones are not fused, allowing raised ICP to be compensated for by the skull expanding. In these cases, the head circumference is seen to increase at a rate beyond what would be expected for a child of the same gestational age and sex[47, 48].

Table 6 Common Initial Features of Acute versus Chronic Hydrocephalus. Signs and symptoms observed in patients with acute and chronically raised intracranial pressure. Adapted from Youmans Neurological Surgery, 2011 [29].

Acute	***Chronic***
• Headaches • Nausea and vomiting • Deterioration in gait or balance • Papilledema • Upgaze palsy—setting sun sign • Parinaud's syndrome—pressure on the suprapineal recess causing abnormalities of eye movement and pupil dysfunction.	• Headaches • Deterioration in gait or balance Urinary incontinence • Cognitive and attention deficits (subcortical dementia) • Personality changes (e.g., aggression, apathy) • Empty Sella Turcica (the space where the pituitary gland sits in the base of the skull) • Impingement or atrophy of the corpus callosum (the bundle of nerve fibres connecting the two cerebral hemispheres)

1.4.2 Treatment

Methods for treating hydrocephalus and raised ICP were developed in the 1890s – 1930s but widespread and effective use of these methods essentially was not possible until the advent of sterile technique, silicone catheters, adequate anaesthesia and antibiotics later in the twentieth century[38].

Overall ventriculoperitoneal shunts are considered the standard of care for long-term treatment of hydrocephalus but superiority of particular treatment modalities continues to be controversial[49]. The following sections will introduce the different treatment modalities.

1.4.2.1 External CSF Drainage

An external ventricular drain (EVD; also known as a ventriculostomy-a purpose made opening into the ventricle) is a temporary measure to deal with hydrocephalus or raised ICP secondary to cerebral swelling. A catheter is placed in the lateral ventricle and CSF may be allowed to drain to an external reservoir (Fig. 6). Via the resultant column of CSF in the catheter, ICP can be accurately measured. It remains the gold standard for measurement of ICP, particularly in the USA [50, 51] where there are approximately 25,000 EVDs placed annually [41].

An EVD is also useful for routine sampling of CSF. Samples are taken using a sterile technique to access a port on the drain tubing. CSF is taken regularly in some units for infection surveillance[52-54].

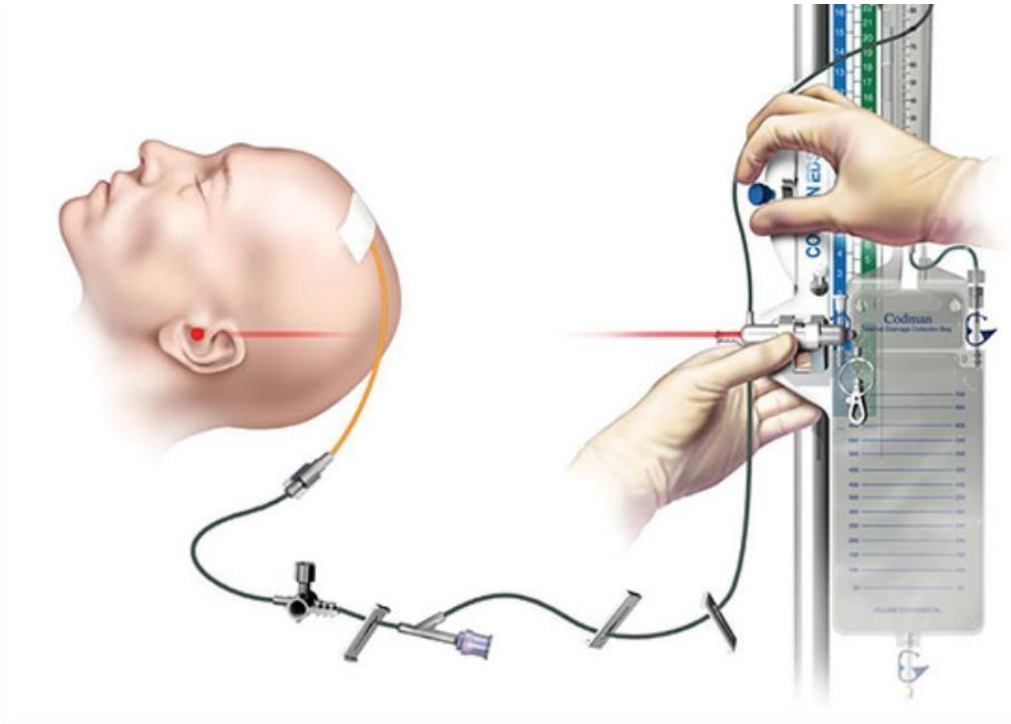

Figure 6 External appearance of an EVD. A silicone catheter placed in the ventricle is secured at its exit from the scalp with a suture and dressing. The catheter drains CSF to an external collection bag. The level of the collection bag is in line with the external auditory meatus (ear) [55].

An alternative to an EVD is a lumbar drain, which performs the same function as an EVD except that the proximal catheter is placed in the lumbar spine in much the same way as a lumbar puncture. It is contraindicated in cases where there is obstructive hydrocephalus [55].

1.4.2.2 Ventriculoperitoneal Shunt

A ventriculoperitoneal Shunt (VPS) is a permanent implant used to divert excess CSF from the ventricle of the brain to the intraperitoneal space in the abdomen where it can be absorbed readily into general circulation, Fig. 7[56]. It is the commonest permanent CSF diversion. In an international study of first ever neurosurgical shunt implant, 97.7% of shunts were VPS[57].

Approximately 3,500 VPS operations are performed annually in the UK and Ireland [58]. In the USA approximately 29,000 patients had ventricular shunt related procedures in 2000 at an estimated cost of $1.1 billion[59].

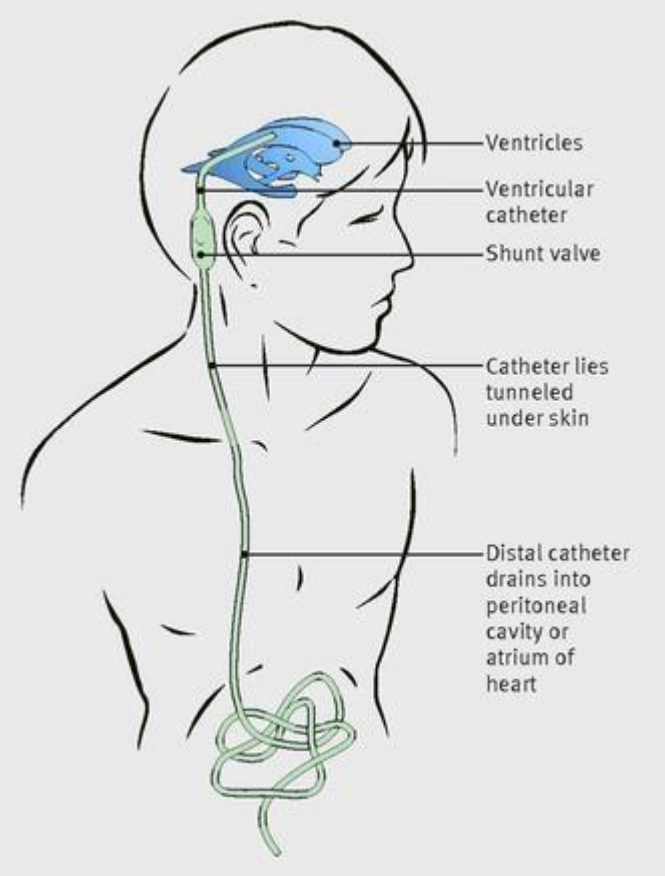

Figure 7 Diagram of a VP shunt. The shunt (light green) is made up of a ventricular catheter (seen within the ventricle, coloured blue) which is connected to a shunt valve and onwards to the distal catheter that is inserted

in the intraabdominal cavity. The excess length of distal catheter allows for the growth in height of children over time.

1.4.2.3 Other Shunts

Neurosurgical shunts have been placed into many cavities to drain CSF from the intracranial space to be absorbed. There are reports of shunts being sited distally into the suprahepatic space, [60] the gallbladder, [61] sagittal venous sinus of the brain, [62] urinary bladder, [63] and the ureter[64]. These sites are exceptionally rare, the more commonly used alternatives to the peritoneum are now considered.

Ventriculo-Atrial Shunt (VA)

A VA shunt redirects CSF to the cardiac atrium, Fig. 8. They are reserved for clinical scenarios where the peritoneal (abdominal) cavity is not amenable to distal catheter placement (e.g., necrotising enterocolitis in premature infants). The first VA shunt was placed by *Dr Pudenz* in Pasadena, California in 1955[65]. It was initially a more commonly used type of shunt, but studies later showed that the VP shunt is superior as it causes less morbidity (e.g. infective endocarditis and clots are risks of VA shunt implantation) [66-68].

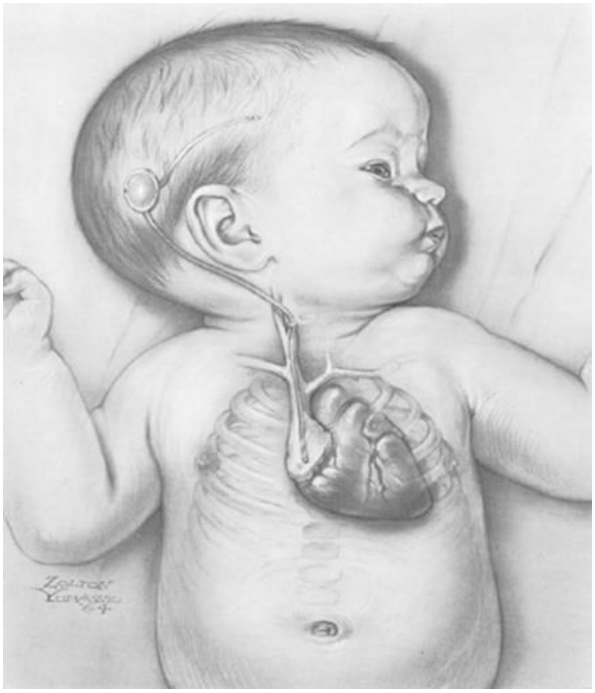

Figure 8 Sketch of a VA shunt. The distal catheter is seen to enter the atrium of the heart via the superior vena cava vessel. VA shunts are reserved for clinical scenarios where the abdominal cavity is not an appropriate site for distal catheter insertion. Premature babies can suffer from abdominal complications like necrotising enterocolitis, necessitating VA shunt [59, 60].

Lumboperitoneal Shunt

A lumboperitoneal shunt drains CSF in the same manner as a VP shunt but the *proximal* catheter is placed into the CSF space of the lumbar spine, Fig. 9. They are contraindicated in non-communicating/obstructive hydrocephalus.

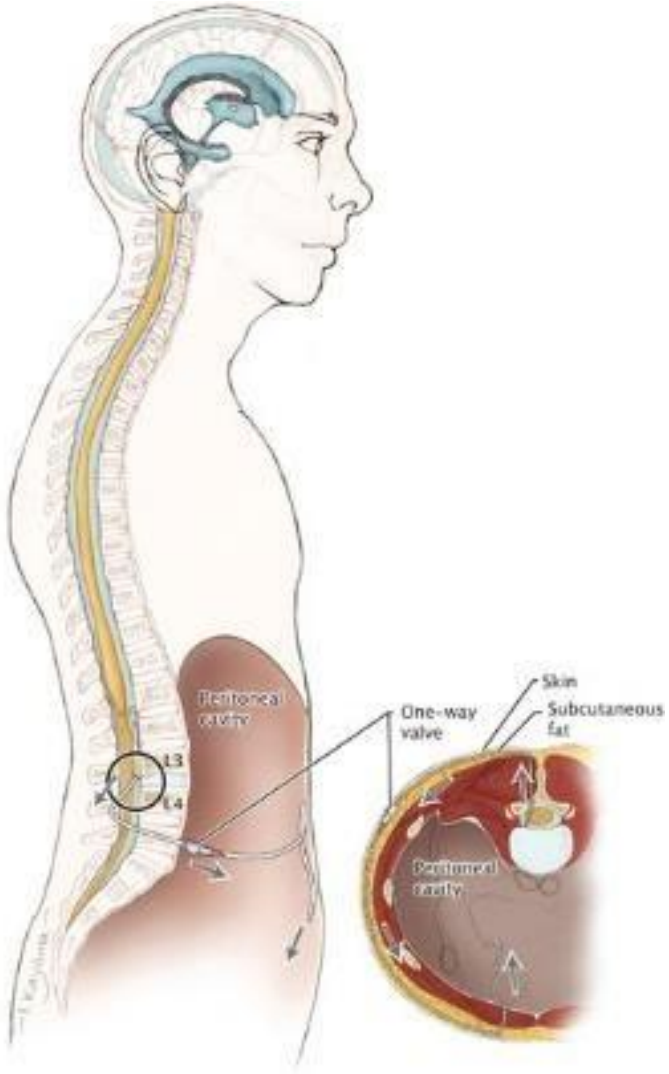

Figure 9 Diagram of a LP shunt. This avoids accessing the cranial space by placing the proximal catheter in the sub arachnoid space of the lumbar spine. The distal catheter drains to the intraabdominal cavity in the same way a VP shunt does [62].

Ventriculo-Pleural Shunt (VPl)

The VPl shunt redirects CSF to the pleural (chest) cavity, Fig. 10. They are never used as a first line treatment for hydrocephalus in modern neurosurgery due to the risk of pneumothorax (a potentially life threatening build-up of air between the lung and the chest wall due to lung injury at the time of implantation) and the limited capacity of the pleura to absorb CSF[69]. VPl shunts were first reported in 1914 by Heile in Germany[70]

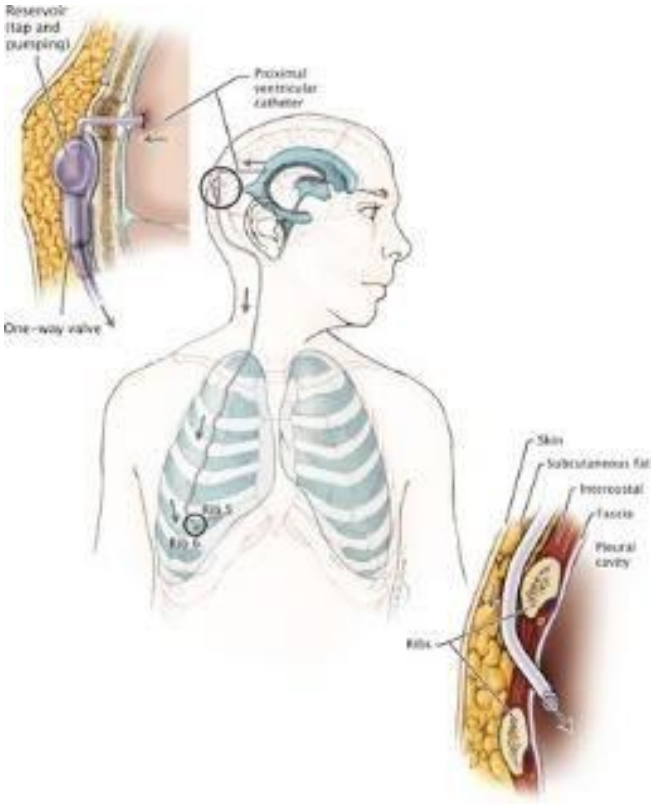

Figure 10 Diagram of a VPl shunt. The upper left enlargement shows the reservoir in detail. The reservoir is palpable under the scalp and can be accessed to test the shunts patency and sample CSF. The distal catheter of a VPl shunt enters the chest cavity between the rib, CSF is absorbed by the pleura (the covering of the lungs and inner chest wall)[71].

Ventriculo-SubGaleal Shunt (VSG)

The VSG shunt diverts CSF to the sub-galeal layer of the scalp, Fig. 11. The procedure was first performed by von Mikulicz in 1896 and continues to be used to this day [72]. VSG shunts

are a temporising measure used predominantly in preterm babies who are deemed unsuitable for a definitive VP shunt due to size and clinical state.

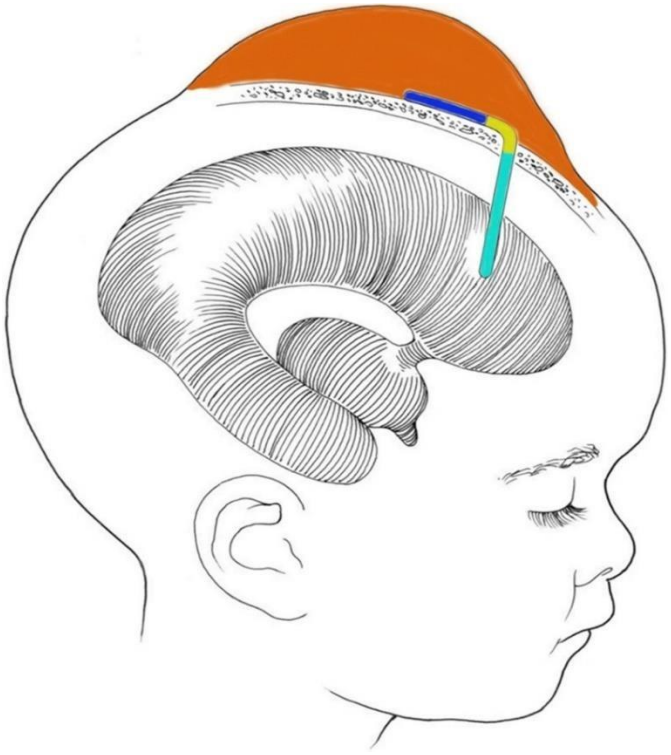

Figure 11 Diagram of a VSG shunt. The ventricular catheter (aqua) connects to a reservoir (yellow) and onwards to a distal catheter (blue) in a sub galeal pocket (orange). This is a temporary CSF diverting strategy, if a longterm shunt is required a VP shunt is placed one the infant is larger and clinically more resilient. VSG Shunt [61].

1.4.2.4 Other Management Options for Hydrocephalus

Endoscopic Third Ventriculostomy (ETV)

ETV is a "keyhole" surgery that creates an opening in the floor of the third ventricle, forming an alternative route for CSF drainage, Fig. 12. In carefully selected cases, ETV is successful in up to 75% of patients, therefore avoiding insertion of a VP shunt[73-75]. In children less than six months old more than half of ETVs will fail and require further surgery to implant a shunt[76].

The prospect of avoiding a permanent shunt and thus avoiding complications (infection or malfunction- which may not be treated in a timely manner due to geography or resources)

changes the risk- benefit ratio in low- and middle-income countries. In Nigeria and Uganda a recent review of cases showed a ~55% success rate for ETV (failure may be due to the ventriculostomy closing/scarring or the volume of CSF production cannot be absorbed adequately) , which was recommended by the authors as a reasonable public health policy locally[77].

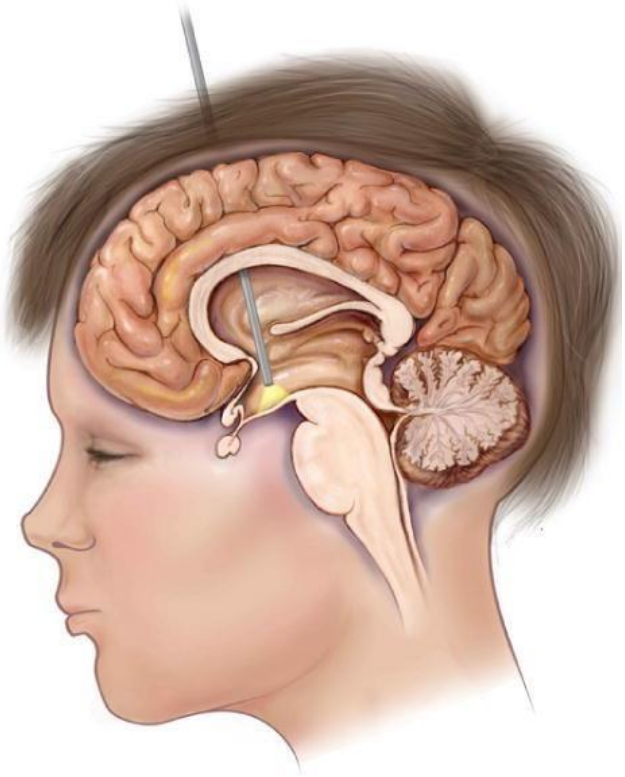

Figure 12 Illustration of an ETV. The endoscope is seen within the ventricular space with the tip illuminating the floor of the third ventricle. This will be the site of the ventriculostomy [62].

Repeat CSF drainage

In new-born babies with hydrocephalus, CSF can be drained acutely via lumbar puncture or by accessing the ventricle percutaneously via the anterior fontanelle (skull soft spot). Up to 20% of *pre-term* infants develop intraventricular haemorrhages [78] and of those approximately 10% develop long term hydrocephalus[79].

Ventricular access devices are like a VSG shunt except there is no distal catheter under the scalp, Fig. 13. They allow percutaneous access to ventricular CSF and were originally developed to allow delivery of drugs to the CNS [80]. Ventricular access devices are commonly referred to

as Ommaya reservoirs after the Pakistani neurosurgeon who developed the device in the 1960s [81, 82].

A Cochrane review of serial lumbar or ventricular punctures and drainage of CSF has shown that it does not decrease the need for long term CSF diversion; i.e. VP shunt [83]. Each instance of CSF drainage carries with it the risk of introducing infection.

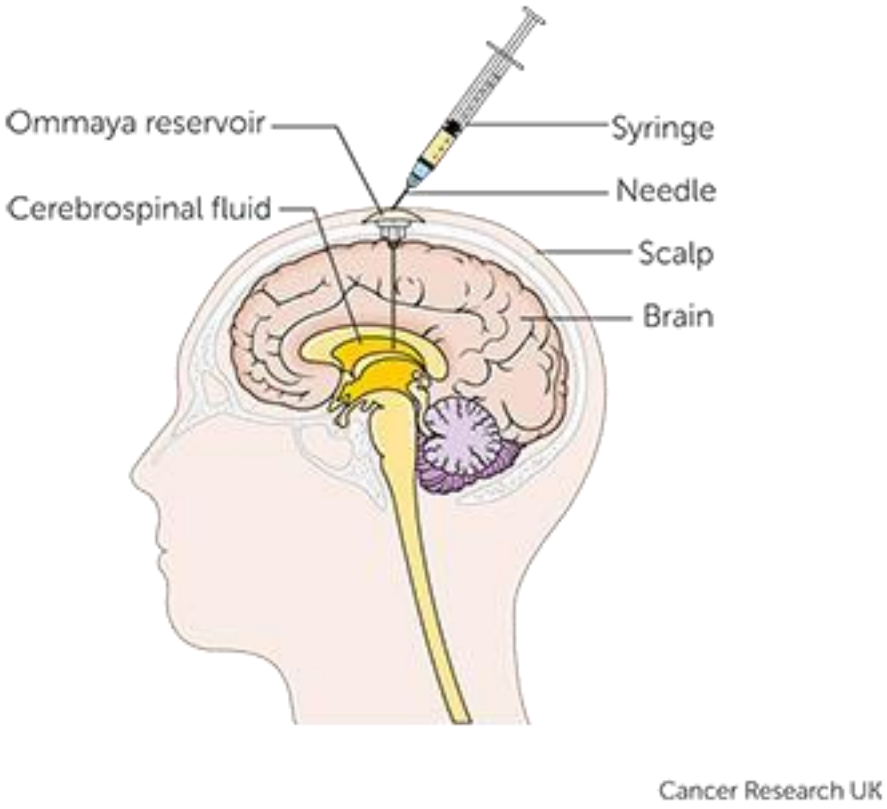

Figure 13 Diagram of a ventricular access device. This is alternately referred to as an Ommaya reservoir. The device can be percutaneously accessed to sample CSF or to deliver therapeutic drugs to the brain, bypassing the blood brain barrier [73].

Choroid Plexus Coagulation

Endoscopic coagulation or removal of the choroid plexus as a treatment for hydrocephalus was first reported by one of the founding fathers of neurosurgery, *Walter Dandy*, in 1918 [84]. The first choroid plexus coagulation was actually performed by an Urologist in Chicago in 1910 but not published [85]. It is not a generally accepted treatment however, due to the high rate of failure to control hydrocephalus long term. There is no standard amount of choroid plexus to coagulate and the ability of choroid plexus to regenerate or compensate

for such interventions is not understood. Reviews of reported choroid plexus coagulation case series shows the success rate between 30-50% [86].

Medical Management

In a small number of cases of hydrocephalus, medical management without surgical intervention may be possible. Idiopathic intracranial hypertension is a form of raised ICP that occurs without enlarged ventricles and no underlying cause is found. It mainly effects women and is strongly associated with obesity. IIH consensus guidelines recommend weight loss for patients with a BMI >30kg/m^2 and acetazolamide (a carbonic anhydrase inhibitor which reduces the production of CSF) in the first instance where eyesight is normal. This is not appropriate in the setting of reduced/threatened eyesight [35].

1.4.3 Morbidity & Mortality

Morbidity associated with hydrocephalus

Headache affects most children with shunted hydrocephalus to some extent and 10-20% suffer with severe headache [87]. Over 40% of adults with shunted hydrocephalus report serious chronic headache. 45% of adults who had hydrocephalus treated in childhood are treated for depression in later life, though the causes of this are poorly understood [88].

Up to one third of children who develop hydrocephalus after infection and require surgical intervention go on to develop seizures[87, 89]. Children who have hydrocephalus due to infection or intraventricular haemorrhage have significantly different intellectual outcomes compared to their peers- almost 60% go on to need special schooling. Congenital hydrocephalus without infection or bleed as a cause shows better outcomes with 29% requiring special schooling [90].

Extremely low birth weight premature babies are a group who have been intensively researched in recent years, due to rising survival rates. Whilst a relatively small number are impacted, 3% of the cohort who develop more severe intracranial bleeds receive a shunt. It is these infants that are disproportionately affected by neurodevelopmental problems and neurocognitive impairment over time [91].

In neonatal hydrocephalus where a shunt is inserted, the neurodevelopmental outcomes at 2 years is poorer in 47% of infants with a shunt in comparison to their unshunted peers [92]. In a study of a similar cohort of congenital hydrocephalus patients with shunts, the shunted children scored ~1 standard deviation lower than age matched controls in general intellectual functioning, verbal intellectual skill development and visuospatial and perceptual-organisational skill development [93]. In fact, only 20% of children with hydrocephalus feel they have near-normal quality of life [94].

Mortality associated with hydrocephalus

Untreated, hydrocephalus either results in death or extremely poor neurological outcomes. Studies from the 1960's of historical case series showed that two thirds of children with untreated hydrocephalus die by 18 months, rising to 80% by 25 years of age [95]. Mortality rates have improved for hydrocephalus with the introduction of surgical treatments [28,

30]. For example, the childhood hydrocephalus mortality rate declined by 60% between 1979 and 1998 in the USA [96].

A long-term follow up (minimum 20 years) of paediatric hydrocephalus patients in Austria treated with a shunt showed a mortality rate of 38.7%, of those deaths at least 43.4% were directly attributable to hydrocephalus or shunt complications [97]. Notably this study excluded tumour and complex cardiac patients. In a Norwegian study which followed 128 paediatric shunts for 40 years, excluding tumour, showed shunt-related mortality rate was 7% before age 20 and at 8.6% by age 40 [98]. These studies include periods where shunt technology was evolving, and management of shunt related problems may not have been as widely practiced as it is now. The International Society for Paediatric Neurosurgery cites the mortality rate for paediatric hydrocephalus as 1-2% [37].

Historical studies of hydrocephalus treated with shunts show that patients who develop a shunt infection almost double their long term mortality [99].

1.5 CNS Infection

1.5.1 Natural Barriers to CNS infection

In any other part of the body, when an infection takes hold there is an inflammatory response locally to fight the infection, resulting in *rubor* (redness), *calor* (heat), *dolor* (pain), *tumour* (swelling/oedema) and sometimes *functio laesa* (loss of function) [100]. As the CNS is enclosed in a rigid bony covering these inflammatory responses could potentially cause more harm than they prevent and so the CNS employs different strategies to the rest of the body. It is in this setting that the CNS is said to have “Immune privilege”. Experimentally, immune privilege is defined as the lack of or altered cell-mediated response to instilled antigens (antigens being substances that cause an immunological response- specific and adaptive response by immune cells in a tissue) [101].

Innate, non-specific immunity for the CNS consists of the anatomical barriers to pathogen entry; skin, bone, meninges, and the CNS immune barrier (blood brain barrier [BBB] and blood-cerebrospinal fluid barrier [BCSFB]). The BBB (1. In Fig. 14) and BCSFB (2. And 3. In Fig. 14) restrict pathogens and circulating immune cells from entering the CNS [102].

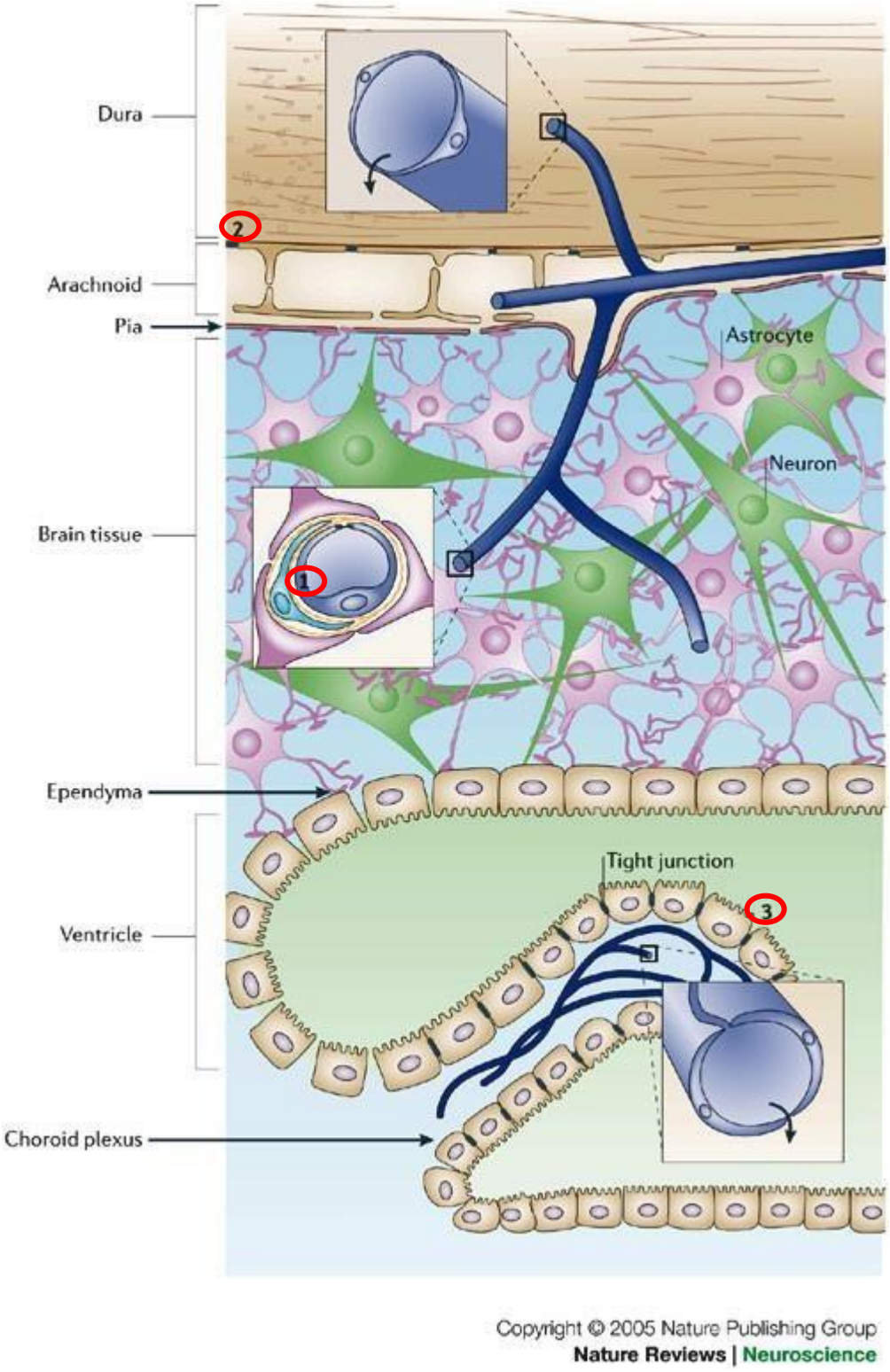

Figure 14 CNS immune barriers: the brain endothelium forming the blood–brain barrier (BBB) (1), the arachnoid epithelium (2) forming the middle layer of the meninges, and the choroid plexus epithelium (3), which secretes cerebrospinal fluid (CSF). At each site, the physical barrier is caused by tight junctions that reduce the permeability of the paracellular (intercellular cleft) pathway [92].

The CNS lacks a cell-mediated response to instilled antigens and also is notable for its absence of lymphatic vessels and its dearth of major histocompatibility complex (MHC) class

II- expressing antigen presenting cells (APC) [102]. The only immune cells present in the CNS parenchyma are microglia- highly specialised tissue macrophages [101].

The CSF is thought to be an immunologically active body fluid. It is widely in contact with the CNS and drains not only to the blood but also along cranial and spinal nerves to their local lymphatics. CSF therefore performs a function equivalent to that of lymphatics for the CNS [102].

1.5.2 Sites of access for pathogens

The CNS is protected from most interactions with everyday pathogens by the anatomy and physiology described in 1.5.1. It exists in a world apart from that of the rest of the body which through minor damage to the skin/nasopharynx/respiratory tree/ gastrointestinal tract comes in regular contact with bacteria and other pathogens.

Infection in the CNS occurs when pathogens gain entry via indirect or direct routes. Indirect inoculation is via haematogenous spread, whereby pathogens need to have adaptations to circumvent the BBB, or the BBB must be otherwise disrupted. Direct inoculation occurs when pathogens pass into the CNS via contiguous structures like nerves, penetrating veins or sinuses (most notably frontal sinusitis and mastoiditis complicating a middle ear infection). Direct inoculation is also a risk of neurosurgery, which intentionally breeches the anatomical barriers [103].

1.5.3 Types of CNS Infection

1.5.3.1 Meningitis and Ventriculitis

Meningitis is an inflammation of the meninges, it can be caused by bacteria, viruses, fungi, parasites, autoimmune conditions, cancer or by reactions to medications. Ventriculitis, as the name suggests, is an inflammation of the ventricles- more specifically the ventricular ependyma, which can be focal or diffuse. Clinically there is no way to differentiate between meningitis and ventriculitis, with ventriculitis being a diagnosis of contrast enhanced neuroimaging or pathology [104].

Definition & Diagnosis

Table 7 Centers for Disease Control and Prevention (CDC) criteria for the diagnosis of Meningitis/Ventriculitis [105].

Patient has organisms cultured from cerebrospinal fluid (CSF)	
> 1 of the following signs/ symptoms with no other recognized cause: • **fever (>38°C)** • **headache** • **stiff neck** • **meningeal signs** • **cranial nerve signs** • **irritability**	> 1 of the following: Increased WCC, protein, +/- decreased glucose in CSF Organisms seen on Gram stain of CSF Organisms cultured from blood Positive antigen test of CSF, blood, or urine Diagnostic single antibody titre (IgM) or 4-fold increase in paired sera (IgG) for pathogen If diagnosis is made antemortem, physician institutes appropriate antimicrobial therapy
Patient ≤1 year of age has >1 of the following signs or symptoms with no other recognized cause: • **fever (>38°C rectal),** • **hypothermia (<37°C rectal)** • **apnoea** • **bradycardia** • **stiff neck** • **meningeal signs** • **cranial nerve signs** • **irritability**	> 1 of the following: • Positive CSF examination with increased WCC, protein, +/- decreased glucose • Positive Gram stain of CSF • Organisms cultured from blood • Positive antigen test of CSF, blood, or urine • Diagnostic single antibody titre (IgM) or 4-fold increase in paired sera (IgG) for pathogen If diagnosis is made antemortem, physician institutes appropriate antimicrobial therapy

CSF analysis is a vital part of meningitis diagnosis as clinical characteristics fail to differentiate between CNS infection and other diagnoses. Even with full access to all available laboratory tests 15-29% of meningitis cases never have a definitive pathogen identified [71, 72].

Epidemiology. Morbidity, Mortality

The majority of meningitis cases are *not* associated with neurosurgery and most meningitis research is in relation to *community* acquired meningitis. Worldwide community acquired bacterial meningitis continues to pose a major public health challenge and progress has persistently lagged behind other vaccine-preventable diseases. Global deaths from meningitis decreased by 21% between 1990 and 2016 but incidence has increased from 2.5 million cases in 1990 to 2.82 million in 2016. The Sahel region – the so-called African meningitis belt- has the highest disease burden and mortality rates for community acquired meningitis[71].

Despite advances in diagnostics and treatments, meningitis continues to cause serious morbidity. A recent study in Denmark showed that 27% of children surviving community

acquired bacterial meningitis suffered from neurological sequelae. 15% had hearing deficits, 12% cognitive impairment and 9% had motor or sensory nerve deficits [74]. 32% of adult survivors of bacterial meningitis have demonstrable cognitive impairment [72]. Case fatality varies by location, 2.4% mortality in Singapore in comparison to 32.7% in Swaziland. Overall average case fatality is estimated as 15.9% worldwide [106].

Of particular concern to neurosurgeons is the fact that worldwide it is estimated that 7.1% of people who get bacterial meningitis develop hydrocephalus [73]. Meningitis in the setting of neurosurgery is the main area of interest for this thesis. The risk of meningitis in relation to neurosurgical intervention begins the moment the intracranial/intraspinal space is breeched. Bacteria may be seeded at the time of surgery or postoperatively via the wound or via an external CSF drainage system. Other microbial of CNS infection (viruses, fungi, prions) after neurosurgical interventions are very rare and are discussed briefly in section 1.5.4.3.

The clinical presentation may be the same as community acquired meningitis but may be complicated by the underlying pathology that prompted the original surgery. Blood from the surgery may irritate the meninges, mimicking meningitis and complicate the interpretation of CSF tests [104].

1.5.3.2 Encephalitis

Encephalitis is an inflammation of the brain parenchyma and clinically it can be difficult to differential between encephalitis and meningitis.

Definition & Diagnosis

Table 8 Diagnostic criteria for encephalitis [107].

Major Criterion (required):
• Patients presenting to medical attention with altered mental status (defined as decreased or altered level of consciousness, lethargy, or personality change) lasting ≥24 h with no alternative cause identified
Minor Criteria (2 required for possible encephalitis; ≥3 required for probable or confirmed encephalitis):

- Documented fever ≥38° C (100.4°F) within the 72 h before/after presentation
- Generalized/partial seizures not fully attributable to a pre-existing seizure disorder
- New onset of focal neurologic findings
- CSF WBC count ≥5/cubic mmd
- Abnormality of brain parenchyma on neuroimaging suggestive of encephalitis that is either new from prior studies or appears acute in onset
- Abnormality on electroencephalography that is consistent with encephalitis and not attributable to another cause

Epidemiology, Morbidity, Mortality

Each year there are approximately 6,000 cases of encephalitis diagnosed in the UK alone [108]. Historically up to 70% of encephalitis cases resulted in death [109]. With the advent of antiviral agents and autoimmune disease therapies, mortality is currently thought to be between 5-15% with morbidity being common [110]. Between 37% and 62% of encephalitis cases have no causative organism identified [111, 112].

Encephalitis related to neurosurgery is rare and not widely reported in academic literature. There are occasions when neurosurgery may be required to help manage hydrocephalus secondary to encephalitis affecting the cerebellum and causing obstruction to the outflow of CSF, but this is rare [113].

Reactivation of viral infections causing encephalitis postoperatively has been documented and will be discussed in section 1.5.4.3

1.5.3.3 Intracranial Abscess

A brain abscess is a space-occupying lesion of loculated infected matter (pus) in the brain. The abscess initially starts as a smaller but diffuse area of infection of the brain matter-cerebritis. This organises into a collection of pus with a highly vascular capsule [103]. For the purpose of diagnosis, brain abscesses are often considered along with other loculations of pus that occur in the CNS, namely subdural and epidural abscesses. Sources of infection causing these abscesses can be seen in Table 9.

Table 9 Sites of spread of infection causing brain abscess, adapted from Youmans Neurological Surgery [103].

Related to infection of the paranasal sinuses or the ear/mastoid
Related to dental infection
Related to lung abscess or empyema
Haematogenous spread from distant sites (e.g., endocarditis)
Direct inoculation (trauma, neurosurgery)
Cryptogenic (no source found)

Definition & Diagnosis

Table 10 Diagnostic criteria for intracranial abscess, subdural or epidural infection, adapted from Horan et al 2008 [114].

Patient has organisms cultured from brain tissue or dura.
Patient has abscess/evidence of intracranial infection seen during a surgical operation or histopathologic examination.

Patient has > 2 of the following signs or symptoms with no other recognized cause: • Headache • Dizziness • fever (>38°C) • localizing neurologic signs • changing level of consciousness, or confusion	And > 1 of the following: • organisms seen on microscopy of brain/abscess tissue obtained by needle aspiration/biopsy during operation or autopsy • positive antigen test on blood/urine • radiographic evidence of infection, (e.g., abnormal findings on ultrasound, CT scan, MRI, radionuclide brain scan, or arteriogram) • diagnostic single antibody titre (IgM) or 4-fold increase in paired sera (IgG) for pathogen If diagnosis is made antemortem, physician institutes appropriate antimicrobial therapy
Patient ≤1 year of age has >2 of the following signs/symptoms with no of other recognized cause: • fever (>38°C rectal) • hypothermia (<37°C • apnoea • bradycardia • localizing neurologic signs • changing level of consciousness	And > 1 of the following: organisms seen on microscopic examination brain/abscess tissue obtained by needle aspiration/biopsy during an operation/autopsy positive antigen test on blood/urine rectal) radiographic evidence of infection, (e.g., abnormal findings on ultrasound, CT scan, MRI, radionuclide brain scan, or arteriogram) diagnostic single antibody titre (IgM) or 4-fold increase in paired sera (IgG) for pathogen If diagnosis is made ante mortem, physician institutes appropriate antimicrobial therapy

Epidemiology, Morbidity, Mortality

An estimated 1.1 million people are affected by intracranial abscesses every year globally [106]. Patients present with headache, fever, vomiting, focal neurological deficits, papilloedema, meningeal signs, hemiparesis, change in mental status, ataxia and coma [115]. 25-45% of patients with a brain abscess present with seizures [115, 116] and approximately a third will develop long-term seizures (epilepsy) [117].

Prior to the late 19th century brain abscesses were almost invariably fatal. A Scottish neurosurgeon, *William McEwan*, pioneered neurosurgical drainage of brain abscesses in the

1876. Of the 19 cases he operated on only 1 died, a record that wasn't matched for many years [118]. In fact, up until the 1970's mortality from brain abscess ranged from 3060% [119]. The introduction of CT and MRI brain imaging, stereotactic and minimally invasive surgical techniques and advancing antibiotics have reduced mortality to approximately 0-10% [120-123].

Abscess rupture into the ventricular system results in ventriculitis, often leading to hydrocephalus, and is associated with high mortality (ranging from 27 to 85%) [124].

1.5.4 CSF Infections related to neurosurgery

A surgical site infection (SSI) is a postoperative infection that occurs within 30 days of a surgical procedure, this is extended to one year in the case of permanent implants (e.g., a neurosurgical shunt). SSI is the third most common hospital acquired infection. The economic cost of SSIs in Europe is estimated to be up to €19 billion annually [125].

Neurosurgical SSI rates vary enormously within the academic literature. One large cohort of 10,634 neurosurgeries in Montreal, Canada in the 1960/70's showed an overall infection rate of 0.65% but 30% of cases were spinal (ordinarily considered very low risk for infection) and they excluded EVDs (as discussed later in this section this is a high-risk procedure for infection) [126]. In a paper from 1985 which reviewed 1,517 operations in Helsinki, Finland, researchers found that the overall rate of infection was 7%. In this cohort spinal cases made up only 11% of surgeries and EVDs were included [127]. A more recent French paper showed an overall infection rate of 1.1% after all neurosurgeries (31% spinal and including EVD) [128].

Focusing on the rate of meningitis post craniotomy, rates are also variable in academic literature. Large European studies found rates of infection post intracranial surgery running at 4-9% [129-131] which contrasts with North American studies that cite infection rates less than 1% [132-134].

A meta-analysis of large cohort studies of postoperative intracranial infection rates, found that there were nearly three times more infections in Europe versus North America [135]. The reasons for this discrepancy are not clear but the variability of the definition of postoperative neurosurgical infections may contribute. Active surveillance for postoperative infections by an infection control professional has been shown to increase the rate of pick-up- neurosurgeons missed 36% of cases in one study in Virginia, USA [136].

1.5.4.1 Neurosurgical implant-related CSF infections

EVD infections

In the UK and Ireland, a recent nationwide prospective study of EVD infections showed rates running at 9.3% [137]. This compares favourably with most of the literature. A recent meta-analysis of EVD infection rates between 1984 and 2018 showed an average of 23% of EVDs became infected [138]. Of particular concern is the fact that if an EVD becomes infected the risk of needing long-term CSF diversion (i.e. a permanent VPS) is doubled [139].

Shunt Infections

George et al, in Johns Hopkins Department of Neurosurgery reviewed shunt infections between 1952 and 1976 and beautifully showed the progressive decline in shunt infection rates over time after surgery (Fig 15) [140]. They noted the relationship of infection to time of surgery and this trend continues to this day, with most infections occurring within 3 months of surgery [130]. 90% of infections occur within 6 months of surgery [141].

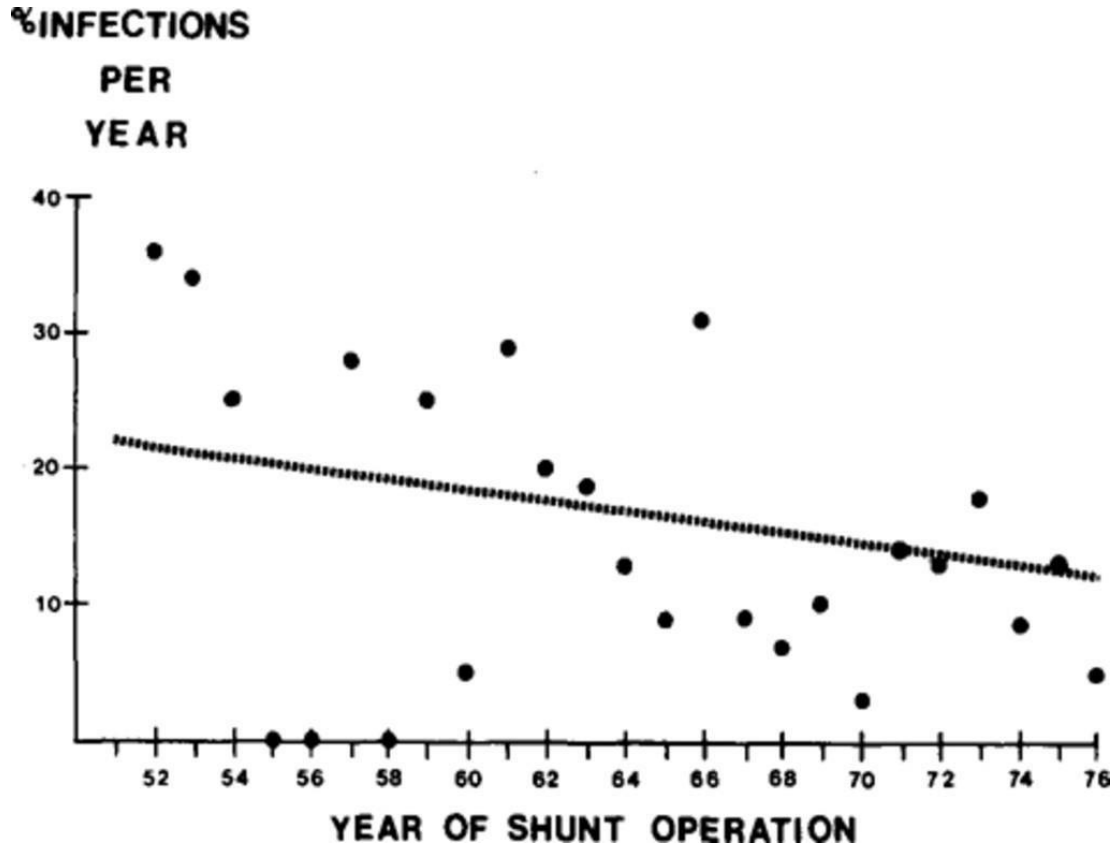

Figure 15 Graph of trend in shunt infections over time. The percentage of shunts inserted that went on to develop infection is seen on the x axis and the year is seen on the y axis of this graph from Johns Hopkins department of Neurosurgery from 1952-1976 [126].

One of the seminal papers on neurosurgical shunt outcomes is that by *Kestle et al* in 2000, this was a shunt design trial in children up to 18 years old. 344 participants were followed until first shunt failure for any reason or until 1999 (maximum follow up was 6 years). 8.4% of all shunts failed due to infection, rising to 16% infection rate for all participants that underwent a reoperation (second shunt failure) [142]. A second shunt failure that is confirmed to be caused by infection raises a question- was the first shunt failure due to an infection and missed, or did the operation to revise the shunt introduce an infection that then caused a second shunt failure?

The *British Antibiotic and Silver Impregnated Catheters for ventriculoperitoneal Shunts* (BASICS) trial, published in 2019 [143], was the first ever randomised controlled trial of shunt catheters. It compared the three types of shunt catheter available (plain silicone, silver impregnated, and antibiotic impregnated). The BASICS trial showed that of the 1,594 participants analysed (1605 were randomised, 11 dropped out) who were randomised and followed between 2013 and 2017, 5% developed a shunt infection [143]. Plain silicone

shunts had a 6% infection rate, silver impregnated shunts similarly had a 6% infection rate and antibiotic impregnated shunt had a 2% infection rate.

Thus, despite ongoing improvements in surgical techniques and shunt engineering the rate of infection remains a significant problem. Mortality related to shunt infection also remains significant. In 2006 ,*Vinchon et al* showed 10.1% of shunt infection patients die with almost all of these being infants with significant pre-existing neurological damage [144].

The economic toll of shunt infections is very significant. The health economics analysis included in the BASICS trial showed that *each episode* of shunt infection costs the NHS approximately £135,753 [143]. Each year in the UK 3500 shunts are implanted [58]. Extrapolating from the BASICS trial findings, the NHS could expect to treat ~210 shunt infections annually at a cost of approximately £28.35 million using plain silicone or silver impregnated catheters. By reducing this to 140 infections with the standard use of antibiotic impregnated shunt catheters the cost is reduced to £18.9 million. A saving of £9.45 million per year.

1.5.4.2 Causative Organisms of Neurosurgical CNS infections

This section will explore organisms associated with neurosurgical infection as the causative organisms differ somewhat from community acquired CNS infections. The vast majority of neurosurgical CSF infections are caused by bacteria, especially bacteria that are found normally on the skin. Data on specific sub species causing neurosurgical CSF infections is scarce. As described in section 1.1, neurosurgery is a rare event overall in healthcare and coordinated research programmes for infection (an uncommon event in neurosurgery) do not, as yet exist.

Bacteria

Bacterial CNS infections as a consequence of neurosurgery are caused mostly by skin commensals. Gram-positive cocci and more particularly *Coagulase negative staphylococci* (*CoNS*) are the commonest groups of pathogens causing bacterial infection in neurosurgical shunts[145, 146]. *Staphylococcus aureus* and *Staphylococcus epidermidis* account for up to 60% of all shunt infections [141, 144, 147]. *Enterococcus spp., Proprionibacterium and other Staphylococci spp.* are among the less commonly identified infecting organisms. Gramnegative

bacteria are also occasionally causative but less common (namely: *Acinetobacter spp., Enterobacter spp., Pseudomonas spp.*).

The proportion of infections caused by *CoNS* varies by geographical location (Fig. 16). A recent study of a Kenyan neurosurgical practice's shunt infections showed a larger proportion of infections due to gram-negative bacilli (almost 40%) [148]. With *CoNS* and other gram-positive infections being prevented with impregnated shunt catheters, there are concerns over the proportion of infection caused by gram-negative bacteria increasing [149].

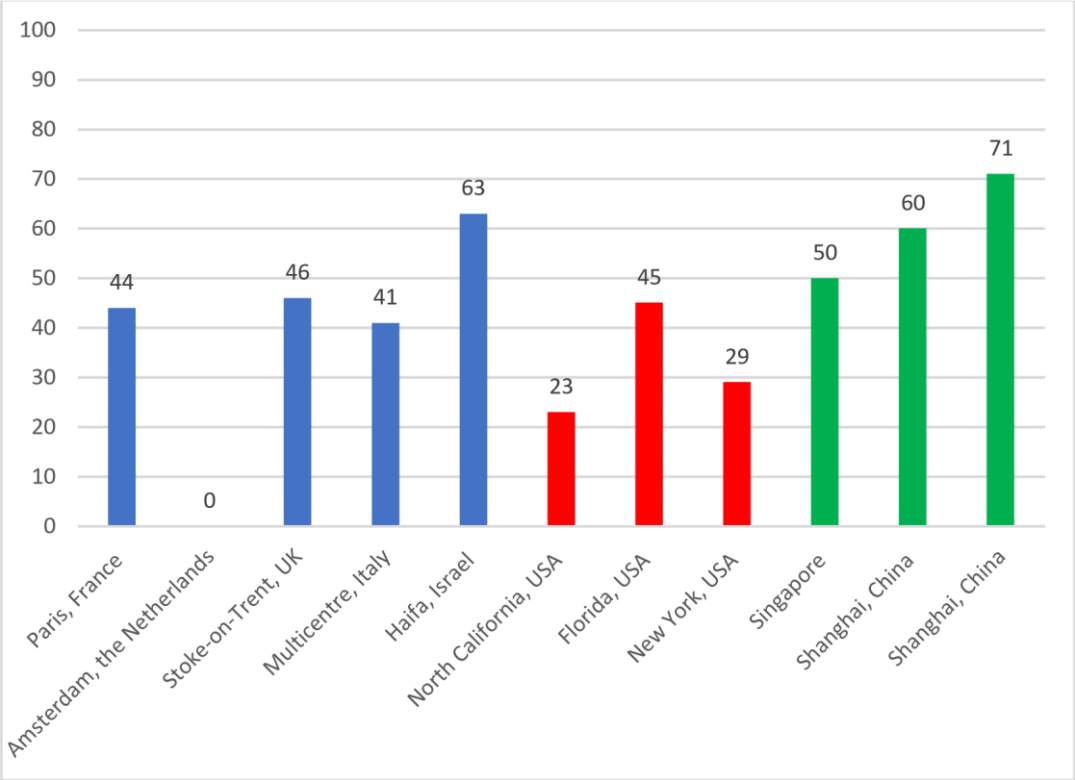

Figure 16 Percentage of neurosurgical CSF infections caused by gram-negative bacteria in adult-only studies of post neurosurgical meningitis. European studies are in blue, American studies are in red and Asian studies are in green. Adapted from Hussein et al *2019[149]. Given the dearth of neurosurgical services in the African continent it is unsurprising that no African data were available to be included.*

Viruses

Viral infection associated with neurosurgery is not a common occurrence. When it does arise, it is usually the reactivation of an old infection. *Herpes simplex virus (HSV)* has been shown to reactivate postoperatively [150-159], several reports of post neurosurgical HSV infection are related to vestibular nerve manipulation- causing an inflammatory response locally and

reactivating a dormant infection. Encephalitis due to *Varicella* is an even more rare event post neurosurgery but has been reported [160].

Fungi

Fungi can cause rare but serious infections after neurosurgery. *McClelland et al* found no fungal infections in over 2000 neurosurgical procedures reviewed in 2007 [132]. Beaumont Hospital in Dublin, Ireland reviewed 20 years of microbiological data for its neurosurgical patients and found 12 cases of *Candida* species postoperative neurosurgical infection. Notably there was a 27% mortality rate associated with these infections [161].

Most invasive fungal infections are found in premature infants but are also associated with immunosuppression (due to HIV, drug induced immunosuppression in organ transplant recipients or high dose steroid treatment) [162]. Given the rarity of fungal neurosurgical CSF infections it is not often examined in the medical literature.

Prions

Prions are small misfolded proteins that are pathogenic and transmissible. They cause Creutzfeldt Jakob disease (CJD), a progressive neurodegenerative disease that is ultimately fatal.

The first ever reported iatrogenic transmission of CJD occurred in 1974 with the implantation of an infected cadaveric corneal transplant. In total, there have been 236 surgical cases of iatrogenic CJD. Most infections came from cadaveric dural graft and corneal graft, with surgical instruments and electrodes only accountable for six cases [163].

1.5.4.3 Prevention of Neurosurgical CSF Infection

Skin preparation

In elective, planned procedures screening for *S. aureus* carriage with microbiology swabs and eradication with antiseptic wash (e.g. chlorhexidine) and nasal ointment (e.g.

mupirocin) has been repeatedly shown to be effective at preventing SSI in any specialty [164] and more specifically in neurosurgery [165, 166].

Universal application of eradication measures has been introduced by some specialties in high-risk procedures/populations. This includes cardiothoracic surgery [167] and intensive care [168]. The use of eradication measures for all preoperative patients is cost effective but controversial due to the potential for the development of resistant bacterial strains [169-172].

Preoperative skin preparation begins the night before an elective procedure with the patient washing with an antiseptic wash. It is not possible to completely sterilise the skin in preparation for surgery [173]. This is due to the structure and crevices where microbes reside in the skin (Fig. 17).

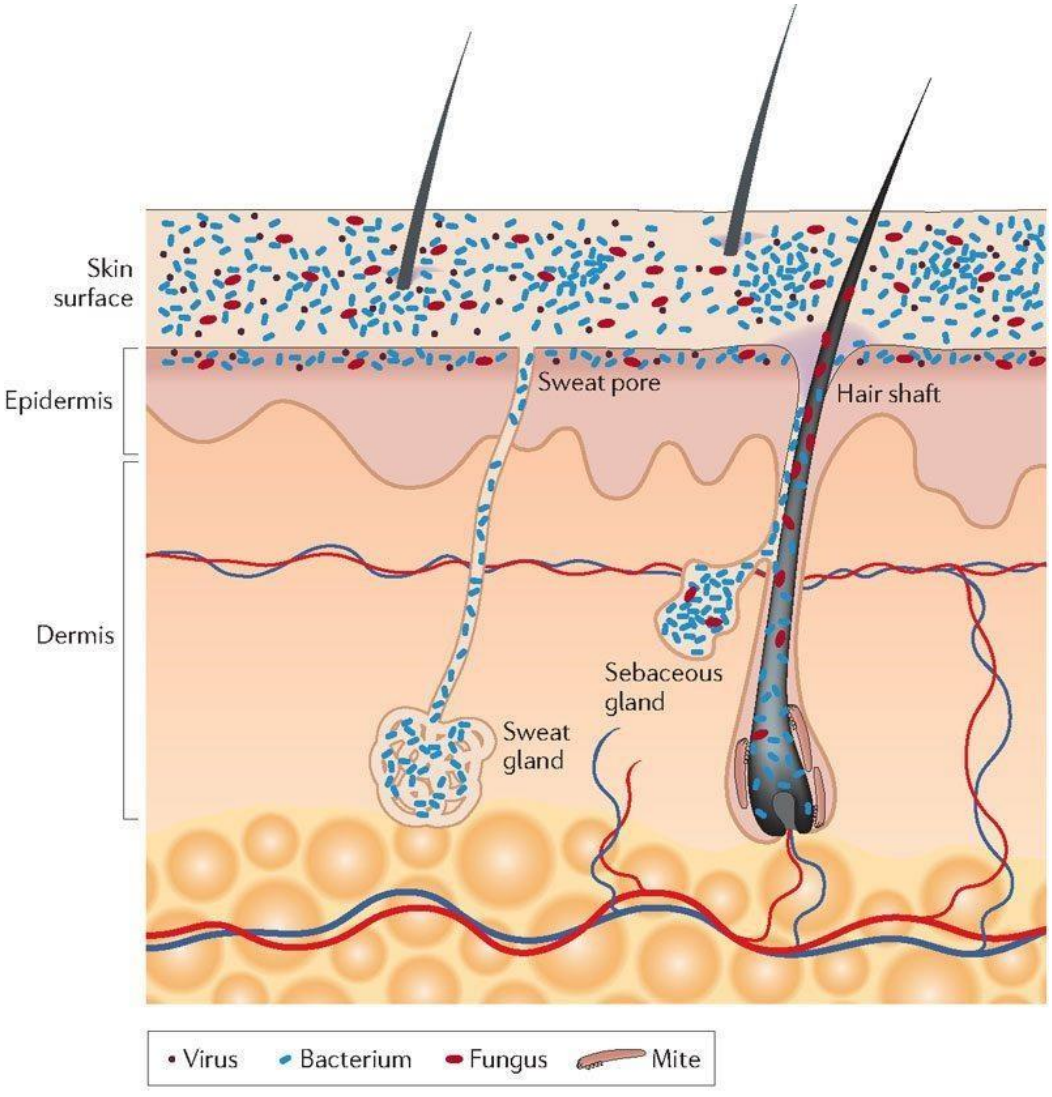

Figure 17 A diagram of the locations of pathogens on skin. Bacteria (blue rods) are seen on the skin surface, epidermis, sweat gland, sebaceous gland and hair follicle. Viruses (black dots) are confined to the skin and epidermis. Fungi (red oblong) are on skin surface, epidermis, sebaceous gland and hair follicle. Mites reside in the hair follicle in association with the hair [159].

Shaving hair in preparation for a neurosurgical procedure is no longer advocated as it does not reduce the risk of infection. Indeed, the trauma to the skin created by the passing of a razor may increase the risk of infection [174, 175]. National Institute for Health and Care Excellence (NICE) guidelines discourage shaving preoperatively and in cases where hair needs to be removed it should be done with clean clippers only [176].

Interestingly, *Cronquist et al* in a 2001 prospective study, found no relationship between colony forming units of bacteria on pre and post preparation skin swabs with subsequent infection [177]. More recently a combination of skin preparation agents (chlorhexidine and povidone iodine) has been found to reduce postoperative neurosurgical site infections when compared to preparation with one agent [178].

Preoperative Antibiotics

The use of prophylactic antibiotics in surgery has been debated for decades. Within neurosurgery their use is proven to be of benefit in preventing postoperative meningitis in craniotomy [129, 179-181] and shunt insertion [182, 183].

Operating Theatre Design and Management

Just as the patients' skin cannot be fully sterilised, the operating staff cannot be sterilised and constitute a source of microbes. People continually shed skin particles throughout the day- at a rate of ~ 10,000 per minute when walking. Up to 10% of shed skin particles will have viable bacteria [184].

A study of domestic air/ventilation/floor dust/HVAC (heating, ventilation and air conditioning) filter dust showed 17%, 17.5%, 20%, and 3% respectively, of the total bacterial abundance was comprised of human associated taxa — *Streptococcus spp*., *Staphylococcus spp*., *Propionibacterineae spp., Enterobacteriaceae spp.,* and *Corynebacterineae spp.* [185].

Ultraclean air filtration systems (high efficiency particulate air [HEPA] filters) are widely used in orthopaedics and neurosurgery. *Lidwell et al* proved the efficacy in the 1980s by comparing conventional ventilation with ultraclean air and showed a reduction of total hip/knee replacement infections from 1.5% to 0.6% [186]. More recently a study of postoperative neurosurgical infections showed a reduction in rates after the introduction of an air-filtration system in neurosurgery theatres in a regional hospital in India [187].

Laminar air flow in association with these air-filtration systems has been shown to reduce the colony forming units detectable at the neurosurgical site [188] but remains somewhat controversial for its effect on infection rates [189, 190].

The number of personnel in theatre is minimised in neurosurgery particularly in shunt implantation operations. It has been shown that the number of bacteria carrying particles found in theatre increases with the number of people present [191]. Similarly, traffic in and out of theatre (e.g., door opening) also increases the microbial air contamination [192, 193].

A small study of neurosurgeon glove contamination in 2008 showed that within 15 minutes of starting an operation, 100% of surgeon gloves cultured *Cutibacterium acnes* (formerly known as *Proprionibacterium acnes*) and 80% cultured *CoNS [194].* Previously, *Tulipan et al* (2006) had observed a neurosurgical shunt infection rate of 15.2% in cases where only one set of gloves were worn, versus 6.7% where the surgeon double-gloved [195]. In fact 15.2% of gloves are perforated during surgery when worn as a single layer, if 2 pairs of gloves are worn only 1.17% get a through and through perforation [196].

Communication within the operating team is essential in theatres. Surgical checklists (including team brief, patient sign-in, time-out before commencing procedure and sign-out) introduced in the first decade of the new millennium have proven to be effective on many levels. The landmark New England Journal of Medicine paper by *Haynes et al* in 2009 showed improvement of all outcomes after the introduction of a surgical checklist (including surgical site infection which decreased from 6.2% to 3.4%) [197]. Surgical checklists have since been introduced in most operating theatres worldwide, neurosurgery included. Neurosurgical teams have independently found a decrease in infection with the introduction of a checklist [198].

CSF catheters

Foreign bodies of any sort serve as a nidus for infection when implanted into the body. CSF diversion, whether temporary or permanent, breeches natural CNS barriers and places the person at risk of infection. Antimicrobial substances have been used for millennia in medicine to prevent infection. Even prehistoric neurosurgeons employed the tactic by using gold to form an implant for skull defects [3].

Shunt catheter design has evolved to include the use of silicone catheters with antimicrobials impregnated within the tubing: silver and antibiotics. Part of the reason that bacteria flourish in the setting of a neurosurgical implant is a "biofilm" that is produced by bacteria to adhere to the catheter and to evade the immune system. Impregnated catheters were developed after it was noted that a mucoid film (a biofilm) was very often found on infected shunts [199].. Biofilms are known to be produced by *S. epidermidis* and *Cutibacterium spp.* [200].

Which catheter type is most effective in preventing infection has been debated for years. Silver-impregnated catheters have been shown to decrease the rate of infection with EVDs. An EVD catheter trial, published in 2012, showed silver-impregnated catheters had an infection rate of 12.3% versus plain silicone catheters (21.3%) [139, 201, 202]. A more recent Swedish study, failed to show that silver-impregnated EVD catheters changed rates of infection [203].

Antibiotic-impregnated catheters (AIC) yielded variable results in the literature. A large American study of 1,935 shunt operations in the Hydrocephalus Clinical Research Network failed to show an improvement in infection rates after AICs were added to the standard care bundle [204]. The superiority of AICs for the prevention of infection in shunt surgery has been definitively proven by the BASICS trial [143]. AICs had a 2.2% infection rate versus 5.9% infection in silver-impregnated shunt catheters and 6% infection rate in standard plain silicone catheters.

Intraoperative Intraventricular Antibiotic

Systemic antibiotics penetrate the CNS poorly in the absence of infection/inflammation and so many neurosurgical centres give a dose of intraventricular antibiotic (vancomycin +/- gentamicin) at the time of shunt implantation. This has not been extensively studied, though one retrospective study of this practice in Utah, USA showed a significant reduction in CSF

device infection with the use of intraventricular vancomycin in combination with gentamicin (0.41%) versus systemic intravenous antibiotics alone (~6%) [205].

Wound Care

Local administration of antibiotic to a surgical wound has become widespread in spinal surgery and orthopaedic surgery where large implants are common. A recent meta-analysis of the use of intrawound vancomycin in non-spinal neurosurgery found very few high quality studies but pointed towards a benefit in reducing SSI [206].

The traditional head bandages of postoperative cranial neurosurgery patients are increasingly a thing of the past. Whilst not formally studied, retrospective reviews of SSI in departments who do not use bandages versus those that do show no difference in infection rates [207].

Chlorhexidine impregnated local wound dressings have proven to reduce the rate of blood stream infection in central venous catheters in a recent meta-analysis [208] and is gaining traction in EVD care [209, 210]. In a study in Denmark, it was shown that with the impregnated dressings had 1.70 infections per 1000 EVD days versus 6.98 per 1000 EVD days in the control phase [209].

After 72 hours, most neurosurgical units will advise patients that it is possible to gently wash the head and hair. Small studies have shown no increase in infection with this practice [211, 212].

Care Bundles

A care bundle consists of 3-5 evidence-informed practices that are known to improve patient outcomes when applied consistently [213]. There are increasing reports of significant decreases in EVD related infection with the introduction of standardised care bundles for the management of EVDs [214-217].

Singapore managed to reduce EVD infections from 4.8% to 2% with the introduction of an EVD care bundle [87]. In France, *Champey et al (2018)* have shown even more impressive results with the introduction of an EVD care bundle in Grenoble achieving infection rates of 1.4%. This is compared to Saint-Etienne and Marseille where the bundle was not used in the

same period and EVD infection rates were 9.2% and respectively 7.2% [53]. Never to be outdone, American centres report rates close to zero [216]. The introduction of formal shunt implantation protocols/care bundles have further improved the rate of shunt infection [218].

1.5.4.4 Risk Factors for Neurosurgical CSF Infection

Patient Factors

There are unalterable risk factors that some patients possess that increase the risk of developing a postoperative neurosurgical CSF infection. In these populations the clinician must be especially vigilant for signs and symptoms of infection (Table 11).

Table 11 List of patient factors that increase the risk of postoperative infection in neurosurgery.

Prematurity (<40 weeks gestation at the time of shunt insertion) [147]
Age less than 6 months [146, 219, 220]
Female sex [220]
Intraventricular haemorrhage [221]
History of meningitis[144]
Preoperative gastrostomy tube in situ[222]
Myelomeningocele [220]
Cardiac co-morbidity [219]
African American/ Asian race[221, 223]

Obesity has been shown to be a risk factor for postoperative infection in spinal surgery but not in cranial or shunt surgery, although it is associated with increased rates of distal shunt catheter migration and wound breakdown in posterior fossa tumours [224].

CSF leakage

CSF can occasionally leak from neurosurgical wounds. This may be a sign if increased ICP or of wound breakdown/infection. It is mentioned separately due to the significant risk its leakage places patients at for CSF infection. When CSF is able to exit a wound there is a pathway for entry for bacteria into the normally sterile intracranial space.

In the paediatric setting CSF leakage post shunt insertion is statistically significant for an increased risk of shunt infection [147, 225]. In a Great Ormond Street study, 57.1% of

patients with CSF leak developed an infection versus 4.7% in patients without leak [226]. As mentioned in section 1.5.4.1, the risk of developing another shunt infection is doubled once a patient experiences a shunt infection.

Surgical Factors

There are also factors that impact on infections rates that are specific to the surgery/surgeon (Table 12).

Table 12 List of surgical factors that increase the risk of postoperative infection in neurosurgery.

Previous Shunt revision [222, 227]
Surgeon experience [218]
Case volume of the hospital/surgeon[221]
Breech of surgical gloves[147]
Timing of surgery- e.g. overnight, after 9pm* [228] *risk of complication increase by more than 50%

1.5.4.5 Diagnosis of Neurosurgical CSF Infection

Like most diagnoses, the process of diagnosing a neurosurgical CSF infection is multipronged, involving clinical assessment, blood tests, CSF sampling and occasionally polymerase chain reaction (PCR) testing and radiological tests. Delays in diagnosis and appropriate treatment of a neurosurgical CSF infection has real-world consequences for patient length of stay in hospital, developing recurrent infections, the need for repeated surgeries and complications from prolonged complex CSF infections (e.g., seizures, neurological damage and even death).

Clinical Assessment

Clinically, postoperative CSF infection is similar to community acquired meningitis. Patients with shunt infections have been seen to have fever (~80%), nausea/vomiting (~55%), lethargy (~30%), neurological change/symptoms (~24%), headache (~10%). More specific to

the neurosurgery patient is surgical site changes (redness, swelling, tenderness, pus- in up to 58% of cases) which can occasionally leak CSF (23%) [229]. Clinical signs and symptoms often appear insidiously and can be difficult to distinguish from underlying pathology or routine postoperative fluctuations [230].

Serological Tests

In any scenario where infection is suspected clinically, baseline blood tests are usually taken. *Conen et al* showed only 33% of shunt infections had a raised serum WCC, though 77% had a CRP >5 mg/L [231]. When infection is suspected with a VA shunt, blood cultures are recommended due to the location of the distal catheter within the circulatory system [232].

CSF Microscopy, Culture and Sensitivity (MC&S) and Differential

CSF sampling in the context of neurosurgery often depends on whether intervention has already been performed, especially in the case of hydrocephalus. Many of the CSF diverting devices implanted in neurosurgery have access points to allow for sampling of the CSF (Fig. 18).

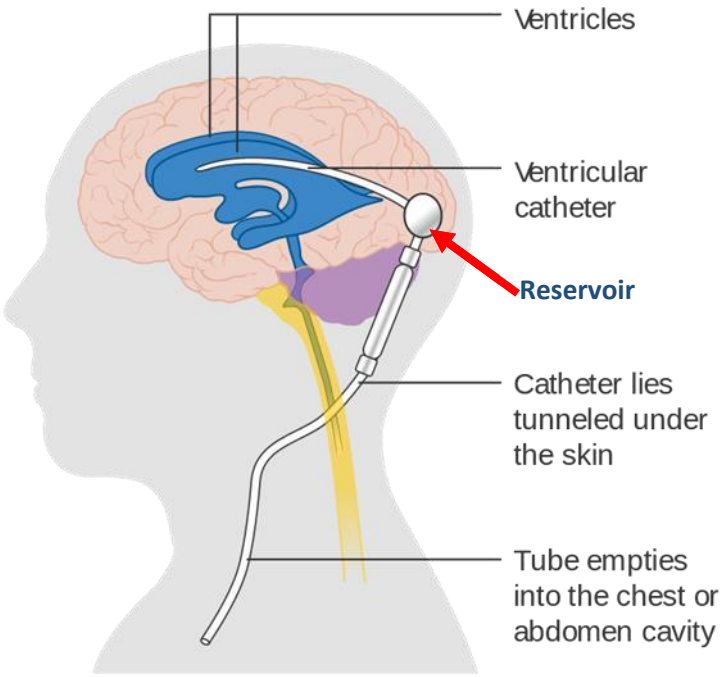

Figure 18 Diagram of a neurosurgical shunt. CSF may be sampled from a shunt via the reservoir [233].

CSF sampling where a patient has a neurosurgical shunt is quite simple. Though due to concerns about damaging or infecting the implant, sampling is ordinarily performed by a neurosurgeon or neurosurgical nurse specialist. It is a sterile procedure- the clinician dons a sterile surgical gown, mask, and gloves. The access point is decontaminated with antiseptic solution (usually chlorhexidine). Shunts include a "reservoir" to allow for CSF sampling and pressure measurement (Fig. 18). This reservoir is attached to the ventricular catheter proximally and the valve distally. It is usually easily palpated under the scalp. Once located, the pliable silicone dome of the reservoir can be gently depressed and felt to refill. If the proximal ventricular catheter is blocked the reservoir may fail to refill or return to its normal domed shape very slowly.

A fine bore butterfly needle can then be introduced to the reservoir through the prepared skin of the scalp. A pressure measurement is normally performed once CSF is seen, by attaching a manometer and allowing the CSF to level off with the zero measurement of the manometer held at the external auditory meatus (ear). A CSF sample can then be collected into a sterile specimen pot [234].

Conventional CSF parameters for infection that are used in community acquired meningitis are less reliable in the postoperative neurosurgery setting. Most laboratories will cite a white cell count (WCC) >5 cells/mm^3 in CSF as pleocytosis, but WCC exceeding this is often found in neurosurgery patients [235]. Whilst *Conen et al* found that 80% of shunt infections had a CSF WCC >5 cells/mm3, that still left 20% with a "normal" WCC who had an infection proven [231]. It is particularly difficult to interpret cell counts in neonates as shown by *Lenfestey et al* [236] when they compared neonates with and without CSF shunts or drains. The presence of a shunt significantly increases RCC, eosinophil count, protein, and glucose concentration. The changes in CSF parameters due to the presence of a shunt reduces their diagnostic sensitivity and specificity.

The degree of WCC rise also depends on the bacteria causing infection, gram-negative organisms are known to provoke a more pronounced WCC rise in comparison to less virulent bacteria like *S. epidermidis* or *C. acnes* [237]. As a group, shunt infections appear to follow a similar pattern over the course of the infection and treatment. There is an initial peak of polymorphonuclear leukocytes, this is later followed by a rise in lymphocytes, monocytes and eosinophils, and all WCC trend towards zero over the course of treatment [237].

Gram staining is performed on all CSF samples sent for microbiological examination but its' utility in neurosurgery is limited. 80% of CSF samples that had a positive culture in one study were Gram stain negative on initial examination [238].

The site of CSF access affects results. Microorganisms are isolated more often from reservoir puncture CSF specimens (91% of specimens) and ventricular CSF specimens (70%) than from lumbar CSF specimens (45%) [24]. Some labs have added extra processes to improve the yield of bacteria from suspected neurosurgical CSF infection cases. Sonication (low-frequency, long wave ultrasound used to disrupt biofilms) of shunt components has been employed by some to increase culture yields. A recent meta-analysis of sonication in neurosurgical infections has shown a dearth of studies but points towards its utility [239].

Contaminated samples (samples that grow bacteria on culture but that are not clinically infected) are often samples that take a prolonged time to grow the bacteria [240]. But neurosurgical CSF samples also need to be incubated for prolonged periods of time to assess for indolent anaerobic infections like C*. acnes*. Some protocols suggest 14 days incubation before a sample can be called truly negative [241] though *Arnell et al* (2008) showed in their series of shunt infections that no CSF culture turned positive after 7 days when they extended their incubation to 10 days [242]. All this makes the decision to classify a bacterium on positive culture as an infective organism somewhat challenging. Alternative methods are needed to identify pathogens causing neurosurgical CSF infection in a shorter timeframe than the current traditional tests.

Other laboratory tests

PCR was developed in the 1980's- gaining its inventor *Cary Mullis* a Nobel prize. PCR targets a specific sequence of nucleic acid which is then copied repeatedly. Through cycles of heating and cooling the nucleic acid of the target is copied, by adding a fluorescent dye quantification of the target is possible[243].

Multiplex PCR test kits for a panel of pathogens are widely available for many infections, with the panel targeting common causes of that type of infection (Table 13). Commercially available test panels have been developed for community acquired meningitis/encephalitis. The FilmArray® meningitis/encephalitis panel (BioFire Diagnostics, USA) is one multiplex assay that has been evaluated extensively, shown to be sensitive and specific and has even been approved for use by the United States Food and Drug Administration (FDA) [244, 245].

The Allplex™ Meningitis Panel (SeeGene Technologies, South Korea) is a similar assay which is approved by the European regulatory authority with a CE-IVD (in vitro medical diagnostic devices) mark [246].

Loop mediated isothermal amplification (LAMP) based tests like the Eazyplex® CSF direct panel (AmplexDiagnostics, Germany) have also been adopted by some laboratories. LAMP is similar to PCR except it does not require cycles of heating and cooling to achieve amplification, it is isothermal. It also employs 4-6 primers that target 6-8 distinct sequences in the target [247]. LAMP is cheaper and often marketed as particularly useful in resource limited settings. Eazyplex® tests cost less than half the price of FilmArray® ME Panel and showed ~91% sensitivity for all meningitis cases (4 cases caused by bacteria not included in the panel) [248].

Multiplex PCR assays have been compared to CSF culture, *Rath et al* showed a 92% concordance between the tests [240]. The issue with discordant samples was felt to be due to the high sensitivity of the PCR for *CoNS*, which are often contaminants in clinical specimens. This contrasts with *Banks et al* who examined PCR in neurosurgical CSF infection and found only 56% concordance between culture and PCR [231].

Whilst these multiplexed PCR assays have utility in the diagnosis of community acquired meningitis they do not test for bacteria commonly found in neurosurgery-related meningitis/CSF infections. Also, as mentioned in 1.5.4.2, viruses and fungi are exceedingly rare pathogens in neurosurgery. Thus, these assays are of limited use in neurosurgical CSF infections.

Table 13 Pathogens tested by the BIOFIRE® FILMARRAY® Meningitis-Encephalitis (ME) Panel[249] ,Allplex™ Meningitis Panel[250] and Eazyplex® CSF direct panel[248].

	BIOFIRE® FILMARRAY® ME Panel	Allplex ™ Meningitis B Panel	Eazyplex® CSF Direct Panel
Bacteria	Escherichia coli K1 Haemophilus influenzae Listeria monocytogenes Neisseria meningitidis Strep agalactiae Strep pneumoniae	Escherichia coli K1 Haemophilus influenzae Listeria monocytogenes Neisseria meningitidis Group B Streptococcus Strep pneumoniae	Escherichia Coli Haemophilus Influenzae Listeria monocytogenes Neisseria meningitidis Strep agalactiae Strep pneumoniae
Viruses	Cytomegalovirus Enterovirus Herpes simplex virus 1 Herpes simplex virus 2 Human herpes virus 6 Human parechovirus Varicella zoster virus	***Available in separate assays*** Cytomegalovirus Epstein-Barr virus Herpes simplex virus type 1 Herpes simplex virus type 2 Human herpes virus 6 Human herpes virus 7 Varicella-zoster virus Adenovirus Enterovirus Human parechovirus Mumps virus Parvovirus B19	
Fungi	Cryptococcus neoformans/gattii		

Radiology

CT of the brain is often performed in patients with a suspected shunt infection, this assesses the position of the ventricular catheter and function of the shunt but can also sometimes show signs of infection. On contrast enhanced CT, 12% of shunt infections in one study showed either meningeal enhancement or abscess [231].

1.5.4.6 Treatment of Neurosurgical CSF Infection

As with community acquired meningitis if a post neurosurgical CSF infection is suspected empirical treatment with antibiotics is instigated as soon as possible. This is directed at common causative bacteria. Vancomycin (targeting gram-positive bacteria- e.g., *Staphylococcus spp., Proprionibacterium spp.*) and a cephalosporin with good gramnegative bacteria coverage are often the antibiotics of choice [149]. When there is a VP shunt in situ and an infection is confirmed or highly likely, the shunt should be removed and an EVD placed whilst antibiotic therapy is ongoing. When a bacterium is identified on culture it is further tested for sensitivity to different antibiotics. Antibiotics are refined once sensitivity results are available, this is of increasing importance in the era of antimicrobial resistance (overuse of broad-spectrum antibiotics has likely contributed to bacteria evolving which are no longer treatable with standard antibiotics).

A review of all treatment strategies and clinical scenarios is beyond the scope of this thesis. However, a rapid and accurate diagnosis is critically important to treat infection. Local microbiology guidelines based on local bacterial prevalence data are widely available. Hussein et al have produced a thorough review of the management of post neurosurgical meningitis [149].

1.6 Improving the Diagnosis of CSF Infections

The processes and procedures for diagnosing a neurosurgical CSF infection have not changed in decades. Most of the research on diagnostics for CSF is targeted at community acquired meningitis and encephalitis. This is understandable given the numbers that contract community acquired meningitis worldwide, but the consequences of neurosurgical CSF infections are significant both biologically and economically (~£135,000 per shunt infection in the UK) [143]. In many tertiary hospitals the proportion of nosocomial meningitis being treated in comparison to community acquired meningitis is much larger. A now historical review of all episodes of meningitis in Massachusetts General Hospital, USA over almost 30 years, found that nosocomial meningitis accounted for 40% of cases [251].

Biomarker is the term used for a biological marker which can be “objectively measured and evaluated as an indicator of normal biological processes, pathogenic processes, or pharmacologic responses to a therapeutic intervention” [252]. They can be molecular,

histological, radiographical or physiological characteristics that can be measured as an indicator of normal/pathological biological processes or the response to an exposure of intervention (this may be therapeutic)[253].

Traditional CSF culture continues to be important, but the need for a test/biomarker that confirms the presence/absence of a CSF infection in a clinically actionable timeframe is ever more pressing.

Neurosurgical patients can contract other nosocomial infections. Chest infections secondary to aspiration or prolonged ventilation, urinary tract infections due to catheterisation and phlebitis from cannulae. The complexities of the neurosurgical patient are profound and clinical decision making presents many dilemmas to those caring for them. As *Puttgen* and *Shah* put it in their commentary in Critical Care Medicine in 2015, we remain in "dire straits for biomarkers of neurosurgery associated meningitis" but with collaborative effort, hope remains [254].

1.6.1 Biomarkers of Neurosurgical CSF Infections

A biomarker that consistently and reliably diagnoses neurosurgical CSF infection could be developed into a point of care test similar to a pregnancy test. A pregnancy testing strip is a form of lateral flow device where a biological fluid (urine) is placed on the strip. If beta human chorionic gonadotropin (βHCG) is present in the urine it causes a colour change to a section of the strip. This principle could be applied to a CSF biomarker at the time of surgery, so that whilst the VP shunt was being finished, a sample of the CSF could be tested on a lateral flow device in theatre. The presence or absence of an infection could be confirmed within theatre and guide ongoing treatment immediately.

Biomarkers are often proteins, which are up or downregulated in the presence of a particular disease state. Proteomics is the study of the protein profile of a biological sample and is being increasingly applied to clinical samples. There are only a handful of proteomic studies of neurosurgical CSF composition in different disease states [255-260] making the field ripe for exploration.

Some biomarkers for infection have emerged sporadically from small, often single institution studies. Some noteworthy candidates have emerged in the academic literature.

1.6.1.1 Lactate

Lactate is the electrically charged form of lactic acid. Lactic acid is formed by tissues producing energy via anaerobic pathways when they experience inadequate oxygen supply.
This means that in health, lactate/lactic acid concentrations are very low [261].

Lactate is found in the CSF as a product of anaerobic metabolism in bacteria and also cerebral ischaemia [262]. Lactate does not readily cross the BBB and as such the CSF lactate concentration is independent of the serum concentration [263].

Lactate or lactic acid as a suggested marker for *meningitis* has been around since the 1970's [264]. *Sakushima et al* performed a meta-analysis of the diagnostic accuracy of lactate for differentiating between bacterial meningitis and aseptic meningitis (Table 14).

Table 14 Summary of the findings of the Sakushima et al meta-analysis of Lactate as a biomarker for meningitis. HSROC: hierarchical summary receiver operating characteristic (ROC) curve. [a] Bacterial meningitis proven by culture or Gram stain. [b] Not available because of unextractable data. The sensitivity of Lactate to differentiate bacterial meningitis is seen to almost halve when antibiotics have be administered prior to CSF sampling [265].

	Sensitivity (95% CI)	Specificity (95% CI)
Overall analysis		
HSROC model	0.93 (0.89–0.96)	0.96 (0.93–0.98)
Random effect model	0.94 (0.92–0.96)	0.97 (0.96–0.99)
Subgroup analysis		
Bacteria proven BM[a]	0.96 (0.93–0.98)	0.97 (0.96–0.99)
Pre-treated BM	0.49 (0.23–0.75)	NA[b]
Untreated BM	0.98 (0.96–1.00)	NA[b]
Cut off around 35 mg/dl	0.93 (0.89–0.97)	0.99 (0.97–1.00)
Cut off around 27 mg/dl	0.90 (0.85–0.94)	0.94 (0.90–0.98)

The UK joint specialist societies guideline on the diagnosis and management of acute meningitis and meningococcal sepsis in immunocompetent adults advise testing lactate in the serum of all patients and in the CSF of patients who have not received antibiotics prior to CSF sampling [266]. *Sakushima* showed that the sensitivity of CSF lactate decreases by more than half if patients have received antibiotics prior to testing [265].

CSF lactate is weakly recommended in the UK joint specialist societies guidelines as there is only moderate quality evidence for its use whereas serum lactate is strongly recommended

despite low quality evidence- serum lactate >4 is associated with higher risk of fatal outcome in meningococcal meningitis (caused by *N. meningitidis*) [266].

It follows then, that CSF lactate level has been repeatedly reported in the literature as a potential biomarker of *post neurosurgical* meningitis [267-272]. A recent meta-analysis of Lactate as a diagnostic for post-neurosurgical meningitis by *Xiao et al* in 2016 showed a pooled sensitivity of 0.92 (95 % CI 0.85–0.96), a pooled specificity of 0.88 (95 % CI 0.84–0.92 with significant heterogeneity) [273].

More recently *Roth et al* investigated the value of CSF lactate levels in paediatric shunt infections. They measured lactate levels from 61 shunt aspirations, 6 infections were identified. The sensitivity of lactate was only 83%, with a specificity of 83% and positive predictive value of only 50%. However, the negative predictive value was 96%. They concluded that lactate could be a useful additional marker for the diagnosis and confirmation of shunt infections [274].

Lactate as a biomarker is referenced by many reviews of post-neurosurgical CSF infection diagnostics [149, 235, 275, 276]. In the neurosurgical setting it has limitations that need to be appreciated– notably cerebral ischaemia/traumatic brain injury and seizures [235].

1.6.1.2 Procalcitonin

Procalcitonin is the precursor form of the hormone calcitonin, a regulator of serum calcium and phosphate. The production of procalcitonin/calcitonin is usually confined to the C cells if the thyroid gland in the neck and neuroendocrine cells. Again, procalcitonin is absent from CSF in health [262]. During a bacterial infection procalcitonin/calcitonin production can be activated in any affected parenchymal tissue by cytokines (interleukin-6 (IL-6), tumour necrosis factor-α (TNF-α) and interleukin-1β (IL-1β)) [277] thus making it an attractive biomarker for infection.

Procalcitonin has a half-life of 22-29hr [278]. Experimental administration of endotoxin to healthy volunteers showed undetectable levels of procalcitonin in their sera at zero, one, two hours, it was detectable at four hours and peaked at six hours with a subsequent plateau from eight to 24 hours [279]. Reassuringly there does not appear to be a significant difference in the concentrations of procalcitonin in infections with gram-positive versus gram-negative bacteria [280].

Hailed initially as a silver bullet test for bacterial infection it soon became evident that there are potential confounders to its utility- hepatic dysfunction, heat stroke, fungal infection, anti-T cell therapy, burns, trauma (within 3 hours of injury). It is now known that it is not discriminatory for sepsis, but it may be useful as a marker for meningitis [281-284] and more specifically as a marker for meningitis related to neurosurgery [268, 285, 286].

1.6.1.3 CRP

C reactive protein (CRP) is a widely used biomarker of a systemic response to tissue damage- be that infection or inflammation of any cause. It is an acute phase reactant, mainly produced by the liver. CRP binds a wide range of ligands most of which are not available for binding in healthy states. Phospholipids like phosphocholine in bacteria and sphingomyelin or phosphatidylcholine in eucaryotic membranes are exposed only when the cells are damaged or apoptotic. Serum concentrations of CRP can rise 1000-fold during acute inflammation or infection, but this response is non-specific. It has pro and antiinflammatory effects depending on the scenario and its activation. Ligand-bound CRP or aggregated CRP activates the classical complement pathway and phagocytic cells and forms part of the innate immune system [287, 288].

Early work on CRP in CSF as a marker for bacterial meningitis often involved a qualitative test (latex agglutination) and yielded promising results. For example, in 1981, *Corrall et al* found that 100% of their 24 definite bacterial meningitis cases tested positive for CRP in CSF in comparison to 2/8 (25%) of the viral meningitis cases and 1/24 (4%) of specimens where no pathogen found in the setting of a pleocytosis [289]. A Danish group performed a meta-analysis of data available between 1980 and 1998 on the utility of CRP to diagnose bacterial meningitis. They included 35 studies, of which 25 tested CRP in CSF. 66% of the studies included <100 patients. The studies were highly variable geographically, for age groups included, study design and methods for CRP evaluation. They concluded that the post-test probability of not having bacterial meningitis in the setting of a negative CSF CRP test was very high at over 97% but given the data available they were unable to conclude that CRP is clinically useful for the management of suspected bacterial meningitis [290].

Table 15 Summary of the studies included in the meta-analysis of CSF CRP, adapted from Gerdes et al, 1998 [290]. BM: bacterial meningitis cases.

Year		Population	Quantitative	BM	Sensitivity	Specificity

1981	USA	1m-16y		24	0.99	0.07
1983	USA	2h-6w	Y	11	0.18	0.18
1983	Finland		Y	11	0.62	0.01
1984	France	1m-15y		21	0.85	0.05
1984	USA	1w-18y	Y	21	0.66	0.16
1985	Jamaica	0-adult		34	0.96	
1985	USA	1d-15y	Y	11	0.44	0.02
1985	South Africa	Children	Y	27	0.70	0.06
1985	USA	1d-87y		74	0.97	0.06
1986	Netherlands	1m-13y	Y	17	0.99	0.05
1986	Kuwait	12d-12y	Y	19	0.36	0.08
1986	USA	5d-16y	Y	49	0.85	0.07
1986	USA	1w-18y		17	0.81	0.04
1987	India			100	1.00	0.06
1987	Thailand	1m-14y		4	0.94	0.20
1988	Malawi	4d-adults	Y	28	0.81	
1988	Sweden	2w-85y	Y	57	0.91	0.01
1988	Spain	2m-10y	Y	27	0.11	0.05
1989	Indonesia			20	0.89	0.09
1990	India	15d-12y		22	0.90	0.00
1994	India	1w-18y		130	0.97	
1994	England		Y	15	0.85	0.25
1995	India	1m-10y		25	0.83	0.01
1995	Poland	19-82	Y	30	0.69	0.11

More recent studies continue much in the same way as those included in *Gerdes'* metaanalysis. There are small cohorts included, the study design is not always clear, the age range varies widely (Table16) [291-300].

Table 16 Summary of CSF CRP as a biomarker for meningitis 2010-2020.BM=numbers of bacterial meningitis cases included in the study, PTBM= partially treated bacterial meningitis, M=months, Y=years, W=weeks, NC= not calculated.

Year	Country	Population	Quantitative	BM	Sensitivity	Specificity	Ref
2020	India	>18y	Y	24	NC	NC	[294]
2019	Iran	<2m	y	20	95%	86%	[292]
2018	India	1m-14y	Y	31 BM 61 PTBM	87% 88.5%	94.8% 94.8%	[295]
2018	China	<4w	Y	74	NC	NC	[296]

2018	Spain	6-86y	Y	18	89.9%	83.3%	[301]
2018	Pakistan	0-12y	N	92	NC	NC	[297]
2016	India	>12y	Y	19	90%	97%	[302]

There is no conclusive study showing the utility of CSF CRP for the diagnosis of bacterial meningitis. CSF CRP is significantly higher in cases caused by gram-negative bacteria than caused by gram-positive bacteria ($P < 0.001$), which may impact on its utility in neurosurgical CSF infections.

More specific to neurosurgery, *Schuhmann* et al saw no difference in CSF CRP in infected VPS CSF versus uninfected CSF[300] whereas the Cardiff group showed the association of a raised CRP with SSI post craniotomy [303].

1.6.2 Pathogen Testing

The existing meningitis panels are designed for community acquired infections and omit the pathogens that commonly infect neurosurgical cases. The bacteria targeted by the FilmArray®, Allplex™ and Eazyplex® meningitis panels are not common in neurosurgical CSF infections and so are of little use.

Some UK units will send CSF samples for 16S sequencing when they have a particularly difficult case of possible neurosurgical CSF infection. Rather than test for specific pathogens with individual primers for each bacterium (as is the case for the multiplex PCR assays), it uses primers for an evolutionarily preserved section of the bacterial genome (the 16S rRNA gene) to amplify bacterial nucleic acid that can then be sequenced and identified [304]. This method is far more precise but currently it is only available in a few centres and very rarely used in clinical practice.

As discussed in 1.5.4.4 prophylactic intraoperative antibiotics are now standard for implant surgeries and the BASICS trial has proven that antibiotic impregnated catheters should be the international standard. Whilst prevention is undeniably better than cure, the consequences of widespread use of antibiotics in other fields has resulted in multiply resistant bacteria emerging. The WHO has named antimicrobial resistance as a major threat to global health [305]. Another fact to consider is that in the last 50 years over 50 new and

reemergent pathogens have been identified [306]. The possibility of bacteria that are not currently culturable emerging as pathogens in shunt infection is real.

In his original thesis, Koch anticipated the scenario where his criteria for identifying a causative organism of infection would not be possible to meet [307]. The conditions to be met to prove a microorganism causes a particular disease (Table 17) were always meant as a framework to promote scientific rigour. Newer technologies for the identification of bacteria may not be able to meet all of Koch's postulates but that should not prevent their use.

Table 17 Koch's Postulates. The three conditions to be met to prove a microorganism causes a disease [261, 307].

1. The microorganism occurs in every case of the disease in question and under circumstances which can account for the pathological changes and clinical course of the disease.
2. The microorganism occurs in no other disease as a fortuitous and non-pathogenic microorganism.
3. After being fully isolated from the body and repeatedly grown in pure culture, the microorganism can induce the disease anew.

Studies of postoperative CSF infections employ many different definitions of infection; one analysis of EVD related CSF infections found 17 different definitions in use [308]. Many definitions include a requirement for bacteria to grow on CSF culture- whilst this increases the likelihood that an infection is correctly identified it does exclude cases where there is likely to have been an infection but due to pre-treatment with antibiotics no bacteria were culturable. Therefore, there is very little data published on probable infections where the culture was negative but due to clinical concern the patient was treated as infected.

1.7 Aims and Objectives of my PhD Project

For my project I wanted to explore potential biomarkers in neurosurgical CSF for infection. The prospect of a lateral flow device that could be used in theatre or at the bedside when a neurosurgeon is assessing a shunt or CSF drain is exceptionally desirable.

The hypothesis is that the protein profile (proteome) of CSF in infection is significantly different to healthy/uninfected CSF. By comparing the proteome of multiple infected samples with the proteome of multiple uninfected samples, proteins (biomarkers) that can differentiate between the two states should be identifiable.

We know that bacterial identification is limited in traditional culture and that commercial multiplexed PCR assays for meningitis do not test for common neurosurgical CSF infection pathogens. Any bacteria present in CSF should be identifiable using newer sequencing technologies. I wanted to explore the utility of next generation sequencing (NGS) for neurosurgical CSF infections, to better characterise the bacteria present (the microbiome).

I therefore set out to:

- Investigate the proteome of neurosurgical CSF in the setting of infection.
- Identify potential candidate biomarkers of infection from that proteomic data.
- Investigate the performance of candidate biomarkers of infection using more targeted assays (i.e., enzyme-linked immunosorbent assay; ELISA)
- Investigate the proteome of CSF from neurosurgical cases over time.
- Investigate candidate biomarkers variation over time in neurosurgical CSF using more targeted assays (i.e., ELISA)
- Investigate the reproducibility of routine CSF culture result with NGS
- Examine the neurosurgical CSF microbiome with NGS

Chapter 2. Materials and Methods

With two busy neurosurgical departments within miles of each other, Liverpool is well placed as a site for CSF research. Alder Hey Children's Hospital NHS Foundation Trust is a dedicated paediatric hospital with 270 beds. Every year it cares for >270,000 children from a large catchment area from North Wales and Northwest England- serving a population of approximately 7 million people. The paediatric neurosurgery team perform more than 600 surgeries and approximately 4,000 outpatient reviews annually [313]. The Walton Centre NHS Foundation Trust is the only neurological disease specialist centre in the UK. Their

neurosurgery department is one of the busiest in the country, performing approximately 2,000 emergency surgeries and 3,000 elective surgeries every year. It serves a population of 3.5 million adults across Merseyside, Cheshire, Lancashire, Greater Manchester, the Isle of Man and North Wales and beyond [314].

The composition of CSF and its examination in suspected cases of CSF infection were discussed in Chapter 1. As previously mentioned, most research on CSF infection concerns community acquired meningitis or encephalitis. The normal ranges for WCC, RCC, protein, glucose etc. are based on this. We know that bacteria causing CSF infection in neurosurgery differ significantly from community acquired meningitis and that the immune response to different bacterial species differs. So, what does neurosurgical CSF look like? Do the pathologies that neurosurgery patients present with alter the CSF composition?

2.1 Research Governance

The full title of the research project for administrative purposes was:

"Study of the feasibility and accuracy of Next Generation Sequencing and Proteomics for improving the diagnosis of neurosurgical cerebrospinal fluid infection."

Sponsorship

Sponsorship was applied for and confirmed on the 25th of July 2016 with the Clinical Research Governance Office in the University of Liverpool (Waterhouse Building, 3 Brownlow Street, L69 3GL, sponsor@liv.ac.uk). Protocol number: UoL001216.

Research Ethics Committee

The project was submitted on the integrated research application system (IRAS) and reviewed by Wales Research Ethics Committee (REC) 7, REC reference: 16/WA/0263, IRAS project ID: 213305, on Wednesday 21st September 2016. Ethical approval was confirmed on the 16th of November 2016.

Health Research Authority

Health Research Authority (HRA) approval was confirmed on the 14th of December 2016.

Local NHS Trust

Local NHS trust research and development departmental approval and material transfer agreements (MTA) were obtained from Alder Hey Children's Hospital NHS Foundation Trust and recruitment commenced on the 17th March 2017. The same process was completed in the Walton Centre NHS Foundation Trust and recruitment commenced on 10th April 2017.

Data Management

A data management plan was formulated with the help of *Ms Elin-Rhian Southwell* in the Centre of Archive Studies in accordance with the University of Liverpool Research Data Management Policy ref: CSD-010, NHS confidentiality policy; 'Confidentiality: NHS Code of Practice'.

Clinical Sample Management

All clinical samples were stored in the Ronald Ross Building, Institute of Infection and Global Health, University of Liverpool which is a Human Tissue Authority (HTA) licenced body. *Professor Tom Solomon* is the custodian of all stored samples.

Research Funding

Funding for experimental consumables was obtained from the BASICS trial, the Hugh Greenwood Trust and the Alder Hey Children's Hospital NHS Foundation Trust Neurosurgical Fund.

2.2 Materials

2.2.1 CSF

Clinical Data

Salvaged CSF

Due to the nature of the samples salvaged from the Walton Centre NHS Foundation Trust via Liverpool Central Laboratories (LCL) limited clinical data were available; differential cell count (WCC, red cell count (RCC), and percentage polymorphonuclear leukocytes versus lymphocytes), culture reports, clinical indication, antibiotic prescription at the time of sampling (if recorded) and source of CSF (Shunt/EVD/LP/Lumbar drain) (appendix a).

The medical record number for the patients was included in this data and as such, multiple samples from the same patient were collected on occasion. Basic information regarding the site of sampling, reason for sampling and antibiotics were available from the ordering system/electronic patient record system (EPR).

This information was sent electronically by Colin Chisnall BSc (Hons) CSci FIBMS, Technical Manager, Medical Microbiology in LCL periodically over the course of this project, usually every two to three months.

Prospectively Collected Neurosurgical CSF

Participants in the prospectively collected neurosurgical CSF study arm consented to demographic and clinical data being recorded prospectively at the time of CSF collection. In addition to the clinical data as detailed in 2.2.1.1 age, sex, serological test results if applicable (Full blood count (FBC), C-reactive protein (CRP)) were recorded for all patients recruited (appendix b).

Classification of CSF samples

Definite Infection

A CSF sample was classified as a definite infection if the clinical impression were infection, the WCC was greater than 10 per µL and there was a positive bacterial culture on routine testing.

As discussed in Chapter 1, section 1.5.4.5, the diagnosis of neurosurgical CSF infections is similar to the diagnosis of meningitis but is complicated by the underlying pathologies being treated and the post-operative state. The clinical impression of infection was as stated by the treating neurosurgical team.

Uninfected

A CSF sample was classified as definitely not infected if the clinical impression was not related to infection, the WCC was less than 5 per µL and the routine culture result was negative.

Possible Infection

A CSF sample was classified as possibly infected if the clinical impression was infection, the WCC was greater than 10 per µL and the routine culture was unclear or negative.

Salvaged CSF

CSF from the Walton Centre NHS Foundation Trust not utilised by routine clinical testing in the Liverpool Central Laboratories (LCL) was immediately transferred (unspun, whole CSF only) to sterile 1.5 mL cryotubes and placed in -80 °C freezers.

The sample number, differential cell count, culture and clinical indication was compiled without patient identifiers and transferred electronically via secure NHS email. All data were maintained throughout as per the data management plan approved by REC and HTA.

Bacterial identification was confirmed by the LCL by a process of macroscopic examination of the culture and then further analysis. Colonies that grew on culture were examined for size, shape, growth on different media and in different atmospheric conditions (CO_2 etc). The colonies would then be subjected to common antibiotics to assess sensitivities. Latex agglutination tests and biochemical tests were also be applied to further aid identification.

Matrix assisted laser desorption/ionization coupled with time-of-flight mass spectrometry (MALDI-TOF, this technique is explained more detail in Chapter 3, section 3.1.1) was then used to analyse the molecular weight of the bacteria to confirm identity. The identification process for individual CSF samples was not included in the data provided for these samples.

CSF sample numbers and pathologies

Between February 2017 and July 2018, 1000 CSF samples were salvaged, from 715 patients. The recorded pathology involved for these samples are seen in Fig. 19.

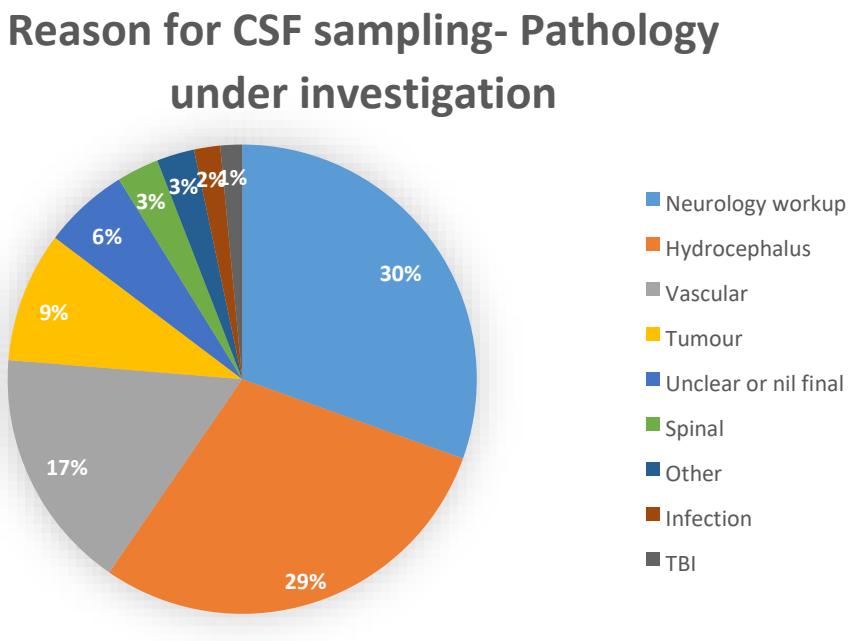

Figure 19 Pathologies being investigated or treated requiring CSF sampling. TBI= traumatic brain injury. The group labelled "Unclear or nil final" were samples where there is no pathology recorded in the EPR for that patient.

Clinically infected CSF with bacteria identified on culture

There were 37 cases of clinically diagnosed infection (Fig. 20, Table 18), where there was a bacterium identified on routine CSF culture and the clinical impression was infection. The commonest causative bacterium of confirmed neurosurgical CSF infection was *S. epidermidis* (13), followed by P. acnes (6), *S. aureus* (6), *E. coli* (3), K. pneumoniae (3), *S. haemolyticus* (3). There were two cases each for *Enterococcus faecalis, Pseudomonas aeruginosa, Staphylococcus hominis* and one case *involving Acetinobacter sp., Citrobacter koseri, Enterococcus cloacae, Enterococcus faecium, Staphylococcus capitis, Proprionibacterium granulosum, Staphylococcus saprophyticus* and *Staphylococcus simulans*. 79% of bacteria grown were gram-positive.

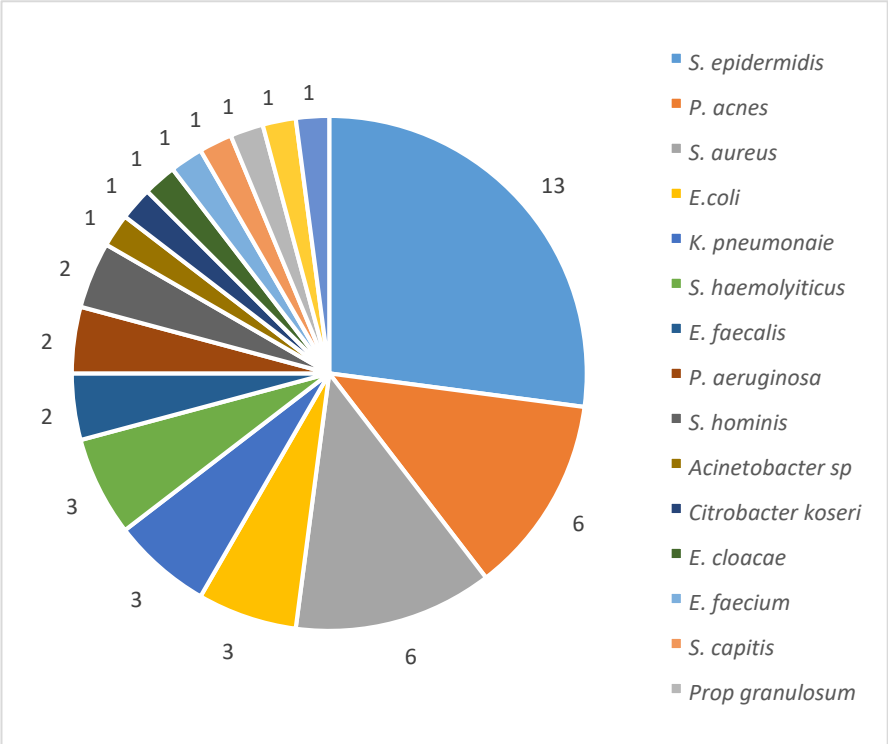

Figure 20 Causative organisms grown on CSF culture from clinically infected cases. These were identified by routine CSF culture by LCL, results of culture and cell counts (WCC and RCC and differential WCC) were provided by the laboratory without patient names/identifiers. These results are the same as reports provided to the clinicians treating the patients.

Table 18 Bacteria causing neurosurgical CSF infections. Data from salvaged CSF samples from LCL.

Bacterium	Number of cases
Staphylococcus epidermidis	8
Staphylococcus aureus	6
Proprionibacterium acnes	5
Klebsiella pneumoniae	3
Escherichia coli	2
Staphylococcus haemolyticus	2
Citrobacter koseri	1
Enterococcus faecalis	1
Enterococcus faecium	1
Pseudomonas aeruginosa	1
Staphylococcus capitis	1
Staphylococcus saprophyticus	1
Staph simulans	1
Mixed	4
Total	37

For *clinically infected*, *culture positive* samples the median WCC was 120 (mean=818.4, range=0 - 7,380) and the median RCC was 320 (mean=3023, range=0-43,400). For eight samples where there were bacteria grown on culture, there were no cell counts available due to clotted samples.

19 cases were being treated with antibiotics at the time of sampling (where that data was available). This ranged from 1 day to 19 days, median duration of antibiotics was 2 days (mean=3.7 days). 25 cases were not receiving antibiotics at the time of sampling.

Culture positive, clinically infected CSF samples where a *CoNS* (N=24) was identified had a mean WCC of 684. *S. epidermidis, S. haemolyticus, S. capitis, S. hominis, S. simulans, S. saprophyticus* are examples of CoNS. They form a significant portion of the skin's bacterial microbiome with *Cutibacterium spp.* and *Corynebacterium spp.* [316].

Culture positive, clinically infected samples with *S. aureus*(N=7) on culture had almost double that of the *CoNS* group, with a mean WCC of 1206. *P. acnes culture positive, clinically infected* samples (N=5) had a mean WCC of 29.5 in contrast to the three samples with *K. pneumoniae* which had a mean WCC of 705. The 11 samples with gram-negative bacteria on culture (five *K. pneumoniae*, two *E. coli*, one *C. koseri* and one *P. aeruginosa*) had a mean WCC of 487.

As mentioned in Chapter 1, cranial CSF has yielded more culture positive samples in the academic literature than lumbar CSF, this is seen in this collection also (Fig. 21).

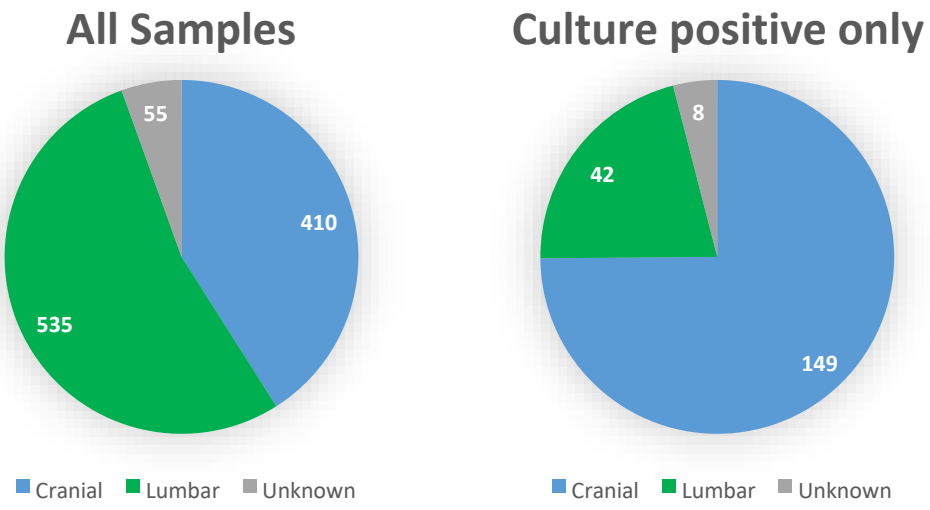

Figure 21 CSF sources. Of the 1000 samples there were 535 (53%) CSF samples from lumbar punctures/drains, 410 (41%) samples were from cranial sources (EVD, VPS, ETV, ommaya) and 55 (6%) samples did not have a source documented. Looking at culture positive CSF samples the proportions change- 75% of samples were cranial CSF, 21% were lumbar CSF and 4% the source was unknown/undocumented.

15% of CSF samples from lumbar sources were bloody in comparison to cranial CSF samples which were bloody in 22% of samples, the breakdown of percentage of infection by sampling site is seen in Fig. 21 and Fig 22. Again, as mentioned in Chapter 1, EVDs are known to have a significant risk for developing a CSF infection.

Proportion of culture positive samples by site of CSF sampling

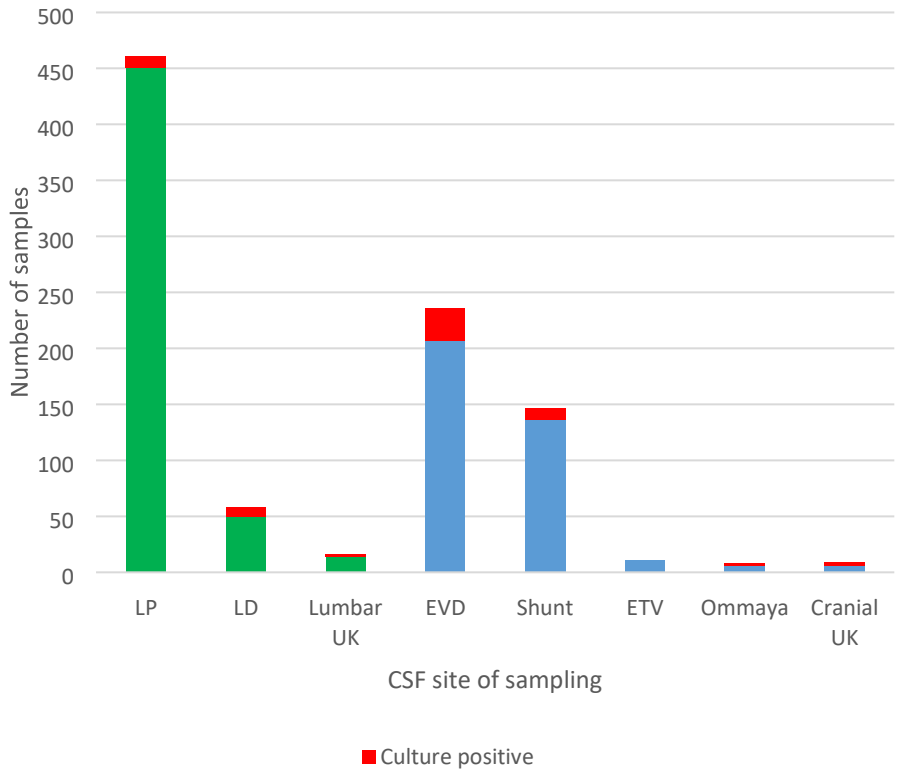

Figure 22 CSF samples grouped by specific site of sampling and including the fraction of that group that was culture positive (red) on routine microbiological testing. ***Lumbar*** *CSF is in green, LP= lumbar puncture, LD= lumbar drain and lumbar UK= lumbar CSF samples where the specific site is unknown. Cranial CSF is in blue, EVD= external ventricular drain, ETV= endoscopic third ventriculostomy and cranial UK= cranial CSF samples where the specific site is unknown. As mentioned in Chapter 1, section 1.5.4.1 there is a known risk of infection with any neurosurgical implant- EVD's in particular.*

The proportion of samples that were culture positive from each sampling site is seen in Fig. 23. Whilst this shows lumbar drains, ommayas and samples from an unknown site as being high risk for growing bacteria on culture, it must be noted that there are very few of these samples (Fig. 22).

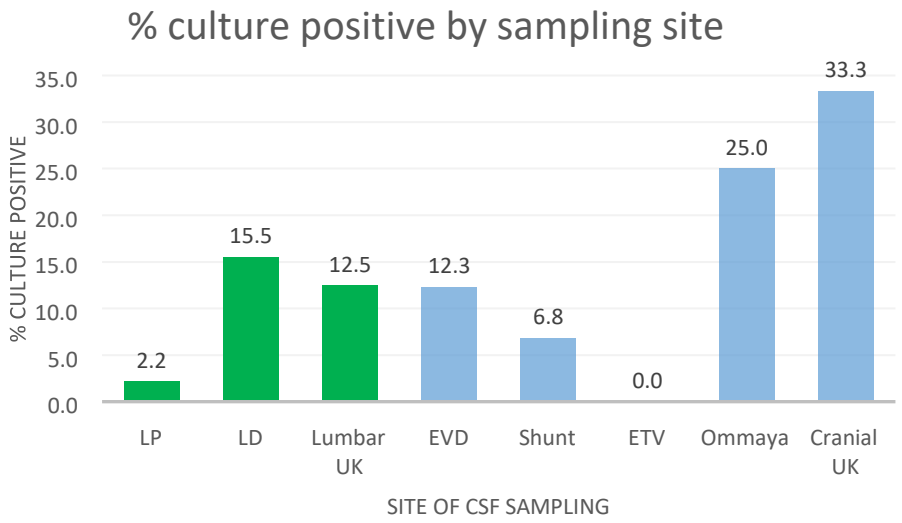

Figure 23 Percentage of culture positive CSF samples by site of sampling. LP= lumbar puncture, LD= lumbar drain, Lumbar UK= lumbar unknown, EVD= external ventricular drain, Shunt= any neurosurgical shunt, ETV= endoscopic third ventriculostomy, Cranial UK= cranial sample, unknown site of sampling. For example, 2.2% of lumbar puncture CSF samples were culture positive (10 out of 461 total).

Blood stained or clotted CSF

Normal, healthy CSF does not contain RCCs but up to 20% of lumbar punctures are "traumatic" and introduce blood into samples taken. As mentioned in Chapter 1, section 1.5.4.5 neurosurgical CSF samples are often contaminated with RRC's post operatively. General consensus on the definition of a bloody CSF sample is not well established but a cut-off of >500 RCC/µL has been suggested for the biobanking of research CSF samples [309]215 of the samples collected had a RCC ≥500 (i.e., a bloody sample) and 57 samples were noted to be bloodstained or to contain a clot (unsuitable for cell count). Most of these samples were from vascular cases, i.e., patients who were being treated for a vascular disease of the CNS, either a subarachnoid haemorrhage (SAH) or another acute intracranial bleed. 10 of the clotted samples were culture positive (one of these was deemed a contaminant as it was from a sample taken at shunt insertion and one was a duplicate sample from the same case on the same day). Six of these infected culture positive samples were taken from vascular cases.

Table 19 Culture positive samples which contained clot. A foraminotomy is a lumbar spinal procedure for sciatica. SAH= sub arachnoid haemorrhage, EVD= external ventricular drain, IIH= idiopathic intracranial hypertension, ASDH= acute subdural haematoma, IT= intrathecal (given into the CSF space).There were ten samples from 7 patients. In sample 2 on this table the K. pneumoniae was identified on 16S PCR.

	Organism	Pathology	Site	History

1	*E. faecalis, E. coli*	Spinal	LD	L5 foraminotomy. antibiotics started for infection
2	*K. pneumoniae* by I6S PCR	SAH	EVD	SAH-HCP-EVD, treated for meningitis
3	*P. acnes*	Infection	EVD	Ventriculitis with abscess- EVD inserted, and abscess drained.
4	*P. acnes*	IIH	Shunt	IIH- insertion of VP shunt
5	*P. aeruginosa*	ASDH	EVD	ASDH. Decompressive craniectomy, EVD, redo subdural drain. Infected
	P. aeruginosa			
	S. epidermidis			
6	*S. aureus*	SAH	EVD	SAH with intraventricular haemorrhage. Coiling of an aneurysm, vasospasm. EVD associated ventriculitis. VP shunt inserted.
7	*S. simulans*	SAH	EVD	SAH– required EVD. Coil aneurysm, EVD, new EVD for IT antibiotics
	S. simulans			

.

There were 63 cases where there was a neurosurgical CSF infection recorded. There isn't complete data on all these cases as the ethical approval did not include a case notes review. As mentioned above, 37 cases had documented clinically infected, culture positive CSF samples within this series. The remaining cases may have had culture positive samples taken but there was not a large enough volume of CSF to allow for routine tests as well as this study.

Prospectively Collected Neurosurgical CSF

CSF samples were collected prospectively in Alder Hey Children's NHS Foundation Trust and The Walton Centre NHS Foundation Trust between January 2017 and December 2018.

Participants or their parent/guardian/nominated consultee signed a consent or assent form, CSF and clinical data were collected prospectively in the neurosurgery departments of Alder Hey Children's Hospital NHS Foundation Trust and the Walton Centre NHS Foundation Trust for patients undergoing CSF procedures (Shunt insertion/revision, EVD insertion, Shunt/EVD access for routine clinical CSF sampling).

CSF was collected in sterile 25 mL clinical sample tubes and transferred to the Ronald Ross building. Paper record of consent and patient details were stored in a locked filing cabinet in a locked office of the relevant neurosurgery department.

An electronic record of all samples, minus patient identifiers was compiled on a secure NHS computer at the local site and transferred via secure email to the research office in Ronald

Ross. All data were maintained throughout as per the data management plan approved by REC and HTA.

148 of these samples were collected in Alder Hey, from 50 children (from premature babies to teenagers, ranging from two days to 16 years old). The 28 samples from adults in The Walton Centre came from 18 patients aged between 28 and 71 years old. The data for these samples is included in the appendix.

Discussion of CSF sample collection

The range of pathogens causing CSF infection in this collection is very similar to what is seen in the literature. *S. aureus, S. epidermidis* and *C. acnes* caused more than half of all clinical CSF infections (Chapter 1, section 1.5.4.3). The usual suspects emerge again and again, lending credence to the theory that skin commensals are gaining entry to the intracranial space at surgery and are taking advantage of a foreign object like a shunt to evade the normal immune response.

Cranial CSF samples make up a larger proportion of culture positive samples in comparison to the entire collection. Lumbar samples are predominantly made up of lumbar puncture CSF which are performed for a variety of reasons, particularly in a neurosurgery/neurology centre- often for the investigation of neurological diseases other than infection. A LP is a very low risk procedure with regards to infection- actual rates are difficult to find in academic literature but the rate of meningitis post spinal/epidural anaesthesia is between 0.2-1.8/10,000. [317-320]

In the Walton Centre, there is a much larger team of neurosurgeons and nurses and nurse specialists and ITU staff. Building up a working relationship with such a large group spread across multiple wards and theatres is tough even when you are full-time on-site. Trying to develop that when you visit once a day, Monday to Friday is nearly impossible. The sample yield from the Walton was disappointing but with retrospect it is not possible for one PhD student to capture all the clinical events where a potential CSF sample might be taken (even if they are based full time in that hospital).

Having never worked in the Walton and with my being based primarily in the University of Liverpool and Alder Hey it was never going to be simple to slot in. In retrospect support from the research department in the Walton with research nurse time would have facilitated a more successful project. This was not possible with my study as it was not NIHR portfolio adopted, something that my original supervising team advised was not feasible

within the time allotted to a PhD. Given the average timescales for sponsorship in the University of Liverpool, I would argue that there is ample time to get a project adopted.

CSF Storage and Handling

Aliquoting

Salvaged CSF samples with confirmed infection and an equal number of confirmed uninfected (clinically uninfected, low WCC and culture negative) samples were aliquoted and total volumes confirmed. Initially this was using 1.2 mL cryogenic vials, after December 2018 all samples were aliquoted into 0.5 mL LoBind Eppendorf tubes (Eppendorf UK Limited, catalogue number 0030108094). All prospectively collected CSF was aliquoted prior to December 2018 into cryogenic vials. All samples were stored in the -80 °C freezers in the ground floor storage room of the Ronald Ross building in the University of Liverpool.

2.2.2 Bacterial Control Samples

Staphylococcus aureus

S. aureus (US300 strain) cultured in Luria-Bertani (LB) broth was kindly provided by *Dr Tessa Prince* (post-doctoral researcher, Liverpool Brain Infection Group, University of Liverpool). This broth was frozen with glycerol for storage. This broth was used as a positive control for all nucleic acid extractions.

Bacterial DNA

ZymoBIOMICS™ Microbial Community DNA Standard (Cambridge Bioscience, UK) was used as a positive control for amplification of extract, to confirm that amplification was functioning if extraction failed.

2.3 Methods

2.3.1 Protein Digestion

To prepare samples for protein analysis they underwent protein digestion to fragment large proteins into smaller peptides that could be more easily analysed.

CSF samples were prepared for proteomic analysis with an optimised, heat stable enzymatic protein digestion kit; SMART Digest kit with SOLAμ HRP, SPE plate (ThermoFisher Scientific, USA, catalogue number:15317-298).

CSF samples were defrosted on ice. SMART digest tubes were prepared by spinning at 1000rpm for 1 minute prior to use.

150 μL of SMART Digest buffer and 50 μL of CSF was placed in a SMART Digest tube and held at 70°C on a heater/shaker for one hour (after the heater was equilibrated for 5mins). The tubes were then, once again spun at 1000rpm for 1 minute.

In the case of a **high complexity** protein/peptide clean up, the SOLAμ SPE plate was then used. The plate was positioned on a vacuum manifold (Vacuum Pump, P/N 60104-241, Thermo Scientific™, USA). 200 μL of acetonitrile (Sigma Aldrich, Germany) was added to each well, vacuum was applied until the liquid was seen to have emptied from each cell and the effluent was discarded. 200 μL of 0.1% trifluoroacetic acid (Sigma Aldrich, Germany) in water was added to each cell, the vacuum was applied, and the effluent discarded.

The SMART Digest kit digested CSF samples were diluted 1:1 with 0.1% trifluoroacetic acid in water transferred to the SOLAμ plate and individual sample plate positions recorded. The vacuum was applied, and the effluent discarded. 500 μL of 0.1% trifluoroacetic acid in water was added, the vacuum re-applied, and effluent discarded. 25 μL of 70% acetonitrile in water was then added to each well and the effluent collected in Eppendorf Protein LoBind tubes (Eppendorf, Germany, catalogue number:0030108094), this process was repeated to yield a 50 μL total volume for further analysis (LC-MS/MS or ELISA).

Finally, 50 μL of 0.1% formic acid was added to each sample prior to analysis.

For **low complexity** protein/peptide clean up the smart digest tubes containing the SMART Digest buffer and sample was placed in a benchtop centrifuge and spun at 1000rpm for one min. The supernatant was carefully pipetted, taking care not to disturb the beads, and transferred to a LoBind Eppendorf tube.

2.3.2 Liquid Chromatography Tandem Mass Spectrometry (LC-MS/MS)

This step was performed under the supervision of Dr Sarah Bonham (Postdoctoral researcher in the TDI, Oxford) for the initial proteomics analysis discussed in Chapter 4. For the experiment in Chapter 5 this work was done by Dr Svenja Hester (Postdoctoral researcher in the TDI, Oxford).

LC-MS-MS analysis was performed in the TDI laboratory in Oxford using a Dionex Ultimate 3000. This is nano-ultra high-pressure reverse phase chromatography which is coupled online to a Q Exactive mass spectrometer (Thermo Scientfic, USA). The analysis was performed over a 60-minute gradient of 2-35% acetonitrile in 5% DMSO, 0.1% formic acid at a rate of 250nL/min.

MS1 scans were acquired at a resolution of 70,000 at 200 m/z and the top 15 most abundant precursor ions were selected for higher-energy collisional dissociation (HCD) fragmentation. MS1 Filtering is a label-free quantitative software application that processes full-scan mass spectral data from proteomic experiments by extracting MS1 ion intensity chromatograms across multiple experiments [310].

Liquid chromatography – mass spectrometry/mass spectrometry (LC-MS/MS) analysis was performed using a Dionex Ultimate 3000 ultra-performance liquid chromatography (UPLC) coupled on-line to a Q Exactive HF mass spectrometer (Thermo Scientific, USA). Samples were separated on an EASY-Spray PepMap C18 column (500 mm × 75 µm, 2 µm particle size, Thermo Scientific, USA) over a 60-minute gradient of 2–35% acetonitrile in 5% DMSO 0.1% formic acid at 250 nL/min. MS1 scans were acquired at a resolution of 60,000 at 200 m/z and the top 15 most abundant precursor ions were selected for HCD fragmentation. Protein quantitation was performed using Progenesis QI for proteomics (Non-linear Dynamics, version 2.0). MS/MS data was searched using Mascot (Matrix Science, version 2.5.1) against the human Swissprot database (retrieval date 15.10.14) allowing one missed cleavage. Mass tolerances were 10 ppm for precursor and 0.05 Da for fragment masses. Carbamidomethylation of cysteine was set as a fixed modification. Oxidation of methionine, deamidation of asparagine and glutamine were set as variable modifications. Identified peptides scoring below 20 following application of a 1% false discovery rate (FDR) were discarded and the Mascot search results were imported back into Progenesis for label-free protein quantitation.

Peptide & Protein Identification

MaxQuant is a freely available software package used in the TDI for analysing large massspectrometric proteomic data sets (http://www.maxquant.org) [311, 312].

Perseus is also a freely available software platform that is used in the TDI for interpreting protein quantification, interaction, and post-translational modification data. It has a comprehensive portfolio of statistical tools including for normalization [313].

2.3.2.2 Data Analysis

Cluster & Java TreeView

Using "Cluster 3.0"[314],data were filtered for proteins present across 80% of samples and adjusted to centre data on the median, to allow for outlying data. Data were then clustered (unsupervised) on proteins in a hierarchical manner with un-centred correlation and using average linkage. The outputted file was then opened in Java TreeView [315] to visualise.

AUREA

Relative expression of proteins was analysed using an open-source software; AUREA (Adaptive Unified Relative Expression Analyzer) [316].

Within AUREA samples were classified e.g., as either Group 1 (control- uninfected) or Group 2 (case- infected). Top Scoring Pairs (TSP), k-Top Scoring Pairs (k-TSP) and Top Scoring Triplets were identified.

Using a small set of controls and cases, classifiers were tested to assess accuracy.

Statistical Packages

Analysis was performed using R and RStudio [317]. Cluster analysis was performed on the LC-MS/MS data without any classification of samples using R statistical analysis software, with "stats", "gplots", "heatmap.plus", "Heatplus" packages [318] with the assistance of Dr. *Enrique Gonzalez Tortuero*, University of Liverpool.

2.3.3 ELISA

Candidate proteins identified in the proteomics experiment in Chapter 3 with commercially available enzyme-linked immunosorbent assays (ELISAs) were brought forward for further analysis.

- Lactoferrin
- Neuronal Pentraxin Receptor (NPTXR)
- Tissue Inhibitor of Metalloproteinases 2/ Metalloproteinase inhibitor 2 (TIMP2)
- Insulin-like growth factor II (IGF2)
- Neuronal Growth Regulator 1 (NEGR1)
- Fc Fragment of IgG Low Affinity IIIa Receptor (FcGR3A)
- Vereinigte Glanzstoff-Fabriken (VGF)
- Secretogranin II (SCG2)
- Secretogranin V (SCG5)

Due to the restricted volumes of infected CSF available for testing and to allow for testing of multiple ELISAs, pools of infected and uninfected CSF were used initially for ELISA optimisation. 5 infected CSF samples were pooled, and 5 uninfected CSF samples were pooled (Table 20).

Table 20 CSF samples used for pools. The result of culture is seen in the Organism column.In sample 4 there were no cell counts recorded/provided. It is not possible to calculate cell counts in clotted samples.

Sample	Volume (µL)	Organism	WCC (cells/mm^3)	RCC (cells/mm^3)
1	200	*P. aeruginosa*	Clotted	Clotted
2	200	*S. epidermidis*	26	<1
3	200	*E. faecium*	2240	70
4	200	*S. aureus*	No cell counts recorded	No cell counts recorded
5	200	*S. aureus*	3960	70
6	200	Negative	4	304
7	200	Negative	<1	160
8	200	Negative	<1	18
9	200	Negative	Clotted	Clotted
10	200	Negative	<1	44

Sample Preparation:

200 µL aliquots of pooled infected CSF samples and pooled uninfected CSF samples were aliquoted in LoBind tubes and stored at -80 °C. A 200 µL aliquot of pooled infected CSF and a 200 µL aliquot of pooled uninfected CSF was defrosted on ice whilst kit reagents equilibrated

to room temperature. None of the ELISAs chosen had specific instructions for sample preparation of human CSF. Initially samples were centrifuged at 800 relative centrifugal force (RCF) for ten minutes to remove debris and the supernatant was used for analysis. Due to the relatively low cell counts of these samples it was felt that this step was unnecessary going forward.

None of the ELISAs used had specific *dilution* recommendations for human CSF samples either, therefore the pooled samples were tested using a range of dilutions to optimise the assays. The individual kit protocols for all ten ELISAs are detailed below.

Lactoferrin

Lactoferrin was tested using a Human Lactoferrin CatchPoint® SimpleStep ELISA® Kit from Abcam®, UK, catalogue number ab229392. The stated range for this kit is 15.6 -1000 pg/mL and sensitivity is 6 pg/mL as per the Abcam® material.

Reagent Preparation:

All reagents were brought to room temperature prior to use. This is a sandwich enzymelinked immune-sorbent assay (ELISA). The anti-Lactoferrin antibody comes pre-coated on the 96 well plate.

Wash Buffer:

50 mL of wash buffer was prepared by adding 5 mL of ten times concentrated wash buffer to 45 mL of deionised water. This solution was mixed gently and thoroughly and labelled.

Antibody Cocktail:

3 mL of antibody cocktail was prepared by adding 300 µL of ten times concentrated capture antibody to 300 µL of ten times concentrated detector antibody and 2.4 mL of antibody diluent 5BI. This was then mixed gently and thoroughly and labelled.

CatchPoint® HRP Development Solution:

6 mL of CatchPoint® Horseradish Peroxidase (HRP) development solution was prepared by adding 60µ of one hundred times concentrated StopLight Red™ substrate to 12 µL of five hundred times concentrated hydrogen peroxide and 5.928 mL of StopLight Red™ substrate buffer. This was mixed gently and thoroughly and labelled.

Standard Preparation:

The lyophilised human Lactoferrin protein was reconstituted with 1000 µL of sample diluent NS and mixed gently and thoroughly. This solution was kept at room temperature for 10 minutes before gently mixing again to yield a 15,000 pg/mL stock standard solution.

Eleven standard tubes were then labelled 1-11. 240 µL of the stock standard solution was added to the Standard 1 tube with 60 µL sample diluent NS. This mixture was then mixed gently and thoroughly.

150 µL of the sample diluent was added to Standard 2-8 tubes. Standard 2 was prepared by adding 150 µL of standard 1 to the Standard 2 tube. This mixture was then mixed gently and thoroughly. Standard 3 was prepared by adding 150 µL of standard 2 to the Standard 3 tube. This mixture was then mixed gently and thoroughly.

The above was repeated sequentially for Standards 4-10. Standard 11 was a blank control (Table 21).

Table 21 Lactoferrin ELISA preparation of standards

Standard Number	Dilution Sample	Volume to Dilute (µL)	Volume of Sample Diluent (µL)	Starting Conc. (pg/ mL)	Final Conc. (pg/ mL)
Standard 1	Stock Standard Solution	240	60	15,000	12,000
Standard 2	Standard 1	150	150	12,000	6,000
Standard 3	Standard 2	150	150	6,000	3,000
Standard 4	Standard 3	150	150	3,000	1,500
Standard 5	Standard 4	150	150	1,500	750
Standard 6	Standard 5	150	150	750	375
Standard 7	Standard 6	150	150	375	187.5
Standard 8	Standard 7	150	150	187.5	93.75
Standard 9	Standard 8	150	150	93.75	46.88
Standard 10	Standard 9	150	150	46.88	23.44
Standard 11	N/A	0	150	0	0

Assay Procedure:

50 µL of each standard and each sample for testing was added to wells and their position recorded. 50 µL of antibody cocktail was then added, the plate was sealed, and it was incubated at room temperature for one hour on a plate shaker at 400rpm.

The plate was then washed three times in an automatic plate washer with 350 µL wash buffer per well, with complete aspiration of buffer between washes.

100 µL of CatchPoint® HRP development solution was then added to each well. The wells were then sealed and incubated at room temperature for 10 minutes in the dark. 100 µL of Stop Solution was then added to each well and the plate was placed on a plate shaker for 1 minute to mix.

The fluorescence was measured on a ThermoFisher™ Varioskan™ (ThermoFisher, USA); excitation=530, cut-off=570, emission=590. Results were saved on a Microsoft Excel spreadsheet.

NPTXR

Neuronal Pentraxin Receptor (NPTXR) was tested using RayBio® Human NPTXR ELISA Kit, catalogue number ABIN4883974. Detection Range is between 0.410 ng/ mL and 100 ng/ mL, with a sensitivity of 0.4ng/ mL or 400pg/ mL.

Reagent Preparation:

All reagents were brought to room temperature prior to use. This is a sandwich ELISA. The anti- NPTXR antibody comes pre-coated on the 96 well plate.

Wash Buffer:

400 mL of wash buffer was prepared by adding 20 mL of the twenty times concentrated wash concentrate to 380 mL of deionised water. This solution was mixed gently and thoroughly and labelled.

Assay Diluents D and B:

Assay Diluent D was prepared by adding 15 mL of the Assay Diluent D concentrate to 60 mL of deionised water. This solution was mixed gently and thoroughly and labelled.

Assay Diluent B was prepared as Assay Diluent D above.

Detection Antibody Working Solution:

A vial of NPTXR detection antibody was briefly spun and then reconstituted with 400 µL of assay diluent B. This was mixed gently and thoroughly by pipette. This detection antibody

concentrate was diluted 80-fold by adding it to 3.2 mL of assay diluent B. This solution was mixed gently and thoroughly and labelled.

HRP-Streptavidin Working Solution:

A vial of HRP-Streptavidin concentrate was first briefly spun, then mixed by pipette and finally diluted 500-fold by adding 100 µL of the concentrate to 5 mL of assay diluent B. This solution was mixed gently and thoroughly and labelled.

Standards:

The NPTXR standard protein vial was briefly spun before 400 µL of assay diluent D was added to the lyophilised protein. The contents were gently and thoroughly mixed to yield a 100ng/ mL solution (Standard 1).

Seven standard tubes were then labelled 2-8. 180 µL of the stock standard solution was added to the Standard 2 tube with 270 µL assay diluent D. This mixture was then mixed gently and thoroughly.

270 µL of assay diluent D was added to Standard 3-8 tubes. Standard 3 was prepared by adding 180 µL of standard 2 to the Standard 3 tube. This mixture was then mixed gently and thoroughly.

The above was repeated sequentially for Standards 4-7. Standard 8 was a blank control (Table 22).

Table 22 NPTXR ELISA standard preparation

Standard Number	Dilution Sample	Volume to Dilute (µL)	Volume of Diluent D (µL)	Starting Conc. (ng/ mL)	Final Conc. (ng/ mL)
Standard 1	Lyophilised NPTXR	N/A	400	N/A	100
Standard 2	Standard 1	180	270	100	40
Standard 3	Standard 2	180	270	40	16
Standard 4	Standard 3	180	270	16	6.4
Standard 5	Standard 4	180	270	6.4	2.56
Standard 6	Standard 5	180	270	2.56	1.024
Standard 7	Standard 6	180	270	1.024	0.41
Standard 8	N/A	0	270	0	0

Assay Procedure:

100 µL of each standard and each sample was added to individual wells and their position recorded. The plate was then sealed and incubated at room temperature for two and a half hours on a plate shaker. Thereafter the solution was discarded, and the plate was washed four times on an automatic plate washer with 300 µL of wash buffer per well, ensuring complete aspiration of buffer after each wash.

100µL of antibody working solution was then added to each well, the plate covered and incubated at room temperature for one hour on a plate shaker. The plate was then washed four times as above.

100 µL of HRP-Streptavidin working solution was then added to each well, the plate covered and incubated at room temperature for 45 minutes on a plate shaker. The plate was then washed four times as above.

100 µL of tetramethylbenzidine (TMB) One-Step Substrate Reagent was then added to each well, the plate covered and incubated at room temperature for 30 minutes in the dark. 50 µL of stop solution was finally added before optical density absorbance was measured at 450nm on a ThermoFisher™ Varioskan™ (ThermoFisher, USA). The results were saved to a Microsoft Excel spreadsheet.

TIMP2

Tissue Inhibitor of Metalloproteinases 2/ Metalloproteinase inhibitor 2 (TIMP2) was tested using an Abcam® TIMP2 Human SimpleStep ELISA®Kit, catalogue number: ab188395. The published range for this kit is 15.6pg/ mL- 1000pg/ mL, with a sensitivity to 6pg/ mL.

Reagent Preparation:

All reagents were brought to room temperature prior to use. This is a sandwich ELISA. The anti-TIMP2 antibody comes pre-coated on the 96 well plate

Wash Buffer:

Wash buffer was prepared by diluting 5 mL of 10x wash buffer PT with 45 mL of deionised water to produce a 1x wash buffer PT. This solution was mixed gently and thoroughly and labelled.

Antibody Cocktail:

Antibody cocktail was prepared by adding 300 µL of 10x capture antibody to 300 µL of 10x detector antibody and 2.4 mL of antibody diluent 5BI. This solution was mixed gently and thoroughly and labelled.

Standards:
The TIMP2 human lyophilised purified protein was reconstituted with 1000 µL of sample diluent NS and mixed gently and thoroughly. This solution was kept at room temperature for 3 minutes before gently mixing again to yield a 5000pg/ mL stock standard solution.

Eight standard tubes were then labelled 1-8. 60 µL of the stock standard solution was added to the Standard 1 tube with 240 µL sample diluent NS. This mixture was then mixed gently and thoroughly.

150 µL of the sample diluent was added to Standard 2-8 tubes.

Standard 2 was prepared by adding 150 µL of standard 1 to the Standard 2 tube. This mixture was then mixed gently and thoroughly.

Standard 3 was prepared by adding 150 µL of standard 2 to the Standard 3 tube. This mixture was then mixed gently and thoroughly.

The above was repeated sequentially for Standards 4-7. Standard 8 was a blank control (Table 23).

Table 23 TIMP2 ELISA preparation of standards

Standard Number	Dilution Sample	Volume to Dilute (µL)	Volume of Diluent (µL)	Starting Conc. (pg/ mL)	Final Conc. (pg/ mL)
Standard 1	Stock Standard	60	240	5,000	1,000
Standard 2	Standard 1	150	150	1,000	500
Standard 3	Standard 2	150	150	500	250
Standard 4	Standard 3	150	150	250	125
Standard 5	Standard 4	150	150	125	62.5
Standard 6	Standard 5	150	150	62.5	31.3
Standard 7	Standard 6	150	150	31.3	15.6
Standard 8	N/A	0	150	-	0

Assay Procedure:

50 µL of each Standard solution (1-8) and sample was added to individual wells and their position recorded. 50 µL of antibody cocktail was added to each well. The wells were then sealed and incubated at room temperature for 60 minutes on a plate shaker set at 400rpm.

The plate was then washed three times in an automatic plate washer with 350 µL 1x wash buffer, with complete aspiration of contents between washes.

100 µL of TMB substrate was then added to each well. The wells were then sealed and incubated at room temperature for 10 minutes in the dark. 100 µL of Stop Solution was then added to each well and the plate was placed on a plate shaker for 1 minute to mix.

The OD was recorded at 450nm on ThermoFisher™ Varioskan™ (ThermoFisher, USA). Results were saved on a Microsoft Excel spreadsheet.

IGF2

Insulin-like growth factor was tested using a Human IGF2 (Insulin-like growth factor II) ELISA Kit from FineTest, Wuhan Fine Biotech Co., Ltd, catalogue number EH0166. The stated detection range is between 62.5ng/ mL and 4000pg/ mL with a sensitivity <37.5pg/ mL.

Reagent Preparation

All kit components were brought to room temperature for 20 minutes before use. This is a sandwich ELISA. The anti-IGF2 antibody comes pre-coated on the 96 well plate.

Wash Buffer:

30 mL of concentrated wash buffer was diluted into 720 mL of deionised/distilled water. Unused buffer can be stored at 4°, if crystals form in the buffer it can be warmed to 40°C in a water bath and mixed thoroughly to dissolve crystals. The solution is then cooled to room temperature before use

Standards:

1 mL of the sample/standard dilution buffer was added to the lyophilised standard. This was left to stand at room temperature for 10minutes and then mixed thoroughly to produce a 4000pg/ mL standard solution.

Serial dilutions of the standard were made as indicated in the table below and mixed thoroughly at each step (Table 24).

Table 24 IGF2 ELISA standard preparation

Standard Number	Dilution Sample	Volume to Dilute (µL)	Volume of Diluent (µL	Start conc. (ng/ mL)	Final conc. (ng/ mL)
Standard 1	Lyophilised IGF2	1000	N/A	N/A	4000
Standard 2	Standard 1	300	300	4000	2000
Standard 3	Standard 2	300	300	2000	1000
Standard 4	Standard 3	300	300	1000	500
Standard 5	Standard 4	300	300	500	250
Standard 6	Standard 5	300	300	250	125
Standard 7	Standard 6	300	300	125	62.5
Standard 8	N/A	300	N/A	0	0

Standards were prepared immediately before the experiment.

Biotin-Labelled Antibody Working Solution:

A 1:100 dilution solution of Biotin-labelled antibody working solution was prepared by adding 1 µL of Biotin-detection antibody to 99 µL of antibody dilution buffer for each well to be used (i.e., 45ul plus 4455ul for 45 wells) and mixing thoroughly. This was prepared within an hour before use.

HRP-Streptavidin Conjugate (SABC) Working Solution:

A 1:100 dilution solution of SABC working solution was prepared by adding 1 µL of SABC to 99 µL of SABC dilution buffer for each well to be used and mixing thoroughly. This was prepared within 30 minutes before use.

Assay Procedure:

All wells were washed 3 times with 350 µL of wash buffer with a one minute soak prior to use. 100 µL of each standard and each sample was added to individual wells and their position recorded. The wells were then sealed with a plate cover and incubated at 37°C for 90 minutes.

The plate cover was removed, contents were discarded, and the plate washed twice as in before. 100 µL of Biotin-Labelled antibody working solution was added to each well, the plate was sealed cover and incubated at 37°C for an hour.

The plate cover was removed, contents were discarded, and the plate washed three times as before. 100 µL of SABC working solution was added to each well, the plate was sealed and incubated at 37°C for 30 minutes.

TMB substrate was allowed to equilibrate at 37°C for 30 minutes. The plate cover was removed, contents were discarded, and the plate washed five times as before. 90 µL of TMB substrate was added to each well, the plate sealed and incubated at 37°C for 15 minutes in the dark. 50 µL of Stop Solution was added to each well.

The optical density absorbance was measured at 450nm in a microplate reader immediately after adding the Stop Solution. Results were saved on a Microsoft Excel spreadsheet.

NEGR1

Neuronal Growth Regulator 1 (NEGR1) was tested with the Human NEGR1 (Neuronal Growth Regulator 1) ELISA kit from MyBiosource, catalogue number MBS7607024. The stated detection range is between 78pg/ mL and 5000pg/ mL with a sensitivity of <46.9pg/ mL.

Reagent Preparation:

All kit reagents were equalised to room temperature before use. This is a sandwich ELISA. The anti-NEGR1 antibody comes pre-coated on the 96 well plate.

Wash Buffer:

Wash buffer was prepared by adding 30 mL of the concentrated wash buffer to 750 mL of deionised water. This was mixed thoroughly and labelled.

Biotin-Labelled Antibody Working Solution:

5 mL of Biotin-Labelled Antibody Working Solution was prepared within 1 hour of use by adding 50 µL of Biotin-Labelled Antibody to 4950 µL of Antibody Dilution Buffer (i.e., a 1:100 dilution to allow for 100 µL per well in 48 wells plus 200 µL extra). This was mixed gently and thoroughly and labelled.

HRP-Streptavidin Conjugate (SABC) Working Solution:

5 mL of HRP-Streptavidin Conjugate (SABC) Working Solution was prepared within 30 minutes of use by adding 50 µL of SABC to 4950 µL of SABC Dilution Buffer (i.e., a 1:100

dilution to allow for 100 µL per well in 48 wells plus 200 µL extra). This was mixed gently and thoroughly.

Standards:

1 mL of sample diluent was added to one standard tube (NEGR1 human lyophilised purified protein), kept at room temperature for ten minutes and mixed thoroughly (Table 25).

Table 25 NEGR1 ELISA standard preparation

Standard Number	Dilution Sample	Sample to Dilute(µL)	Sample Diluent DS(µL)	Start Conc. pg/ mL	Final Conc. pg/ mL
Standard 1	Lyophilised NEGR1	N/A	1000	N/A	5000
Standard 2	Standard 1	300	300	5000	2500
Standard 3	Standard 2	300	300	2500	1250
Standard 4	Standard 3	300	300	1250	625
Standard 5	Standard 4	300	300	625	312.5
Standard 6	Standard 5	300	300	312.5	156.25
Standard 7	Standard 6	300	300	156.25	78.1
Standard 8	N/A	NA	300	0	0

Assay Procedure:

The plate was washed twice with an automatic plate washer with 350 µL of wash buffer, allowing for a one-minute soak between washes.

100 µL of each standard and sample was added to the appropriate well and their position was recorded. The plate was then sealed and incubated for 90 minutes at 37°C. The seal was removed, the contents discarded, and the plate was washed twice as before.

100 µL of Biotin-Labelled Antibody Working Solution was added to the bottom of each well being careful not to touch the sidewall. The plate was then sealed and incubated for an hour at 37°C. The seal was removed, the contents discarded, and the plate was washed three times as before.

100 µL of SABC working solution was added to each well. The plate was then sealed and incubated for 30 minutes at 37°C. The seal was removed, the contents discarded, and the plate was washed five times as before.

90 µL of TMB substrate was added to each well, the plate sealed and incubated for 30 minutes at 37°C in the dark. 50 µL of Stop Solution was then added to each well. O.D. absorbance was measured immediately at 450nm on the ThermoFisher™ Varioskan™ (ThermoFisher, USA). Results were saved on a Microsoft Excel spreadsheet.

FCGR3A

Fc Fragment of IgG Low Affinity IIIa Receptor/ Human Fc γ R3A (FCGR3A) was tested using Human Fc γ R3A ELISA kit from FineTest, Wuhan Fine Biotech Co., Ltd; catalogue number EH3048. The detection range for this kit is between 7.813ng/ mL and 500ng/ mL, with a sensitivity down to at least 4.688ng/ mL.

Reagent Preparation:

All reagents were brought to room temperature prior to use. This is a sandwich ELISA. The anti- Fc γ R3A antibody comes pre-coated on the 96 well plate.

Wash Buffer:

Wash buffer was prepared by adding 30 mL of concentrated wash buffer to 750 mL of deionised water. This solution was mixed gently and thoroughly and labelled.

Biotin-Labelled Antibody Working Solution:

No more than one hour before the experiment, 5 mL of biotin-labelled antibody working solution was prepared by adding 50 µL of Biotin-labelled antibody concentrate to 4950 µL of antibody dilution buffer. This solution was mixed gently and thoroughly and labelled.

HRP-Streptavidin Conjugate (SABC) Working Solution:

No more than 30 minutes before the experiment, 5 mL of SABC working solution was prepared by adding 50µL of SABC to 4950 µL of SABC dilution buffer. This solution was mixed gently and thoroughly and labelled.

Standards:

The lyophilised human Fc γ R3A protein was reconstituted with 1000 µL of sample dilution buffer and mixed gently and thoroughly. This solution was kept at room temperature for 10 minutes before gently mixing again to yield a 500ng/ mL stock standard solution (Standard 1).

Seven standard tubes were then labelled 2-8. 300 µL of the stock standard solution was added to the Standard 2 tube with 300 µL sample dilution buffer. This mixture was then mixed gently and thoroughly.

300 µL of the sample dilution buffer was added to Standard 3-8 tubes. Standard 3 was prepared by adding 300 µL of standard 2 to the Standard 3 tube. This mixture was then mixed gently and thoroughly.

The above was repeated sequentially for Standards 4-7. Standard 8 was a blank control (Table 26).

Table 26 Fc γ R3A ELISA standard preparation

Standard Number	Dilution Sample	Volume to Dilute (µL)	Volume of Sample Diluent (µL)	Starting Conc. (ng/ mL)	Final Conc. (ng/ mL)
Standard 1	Lyophilised Fc γ R3A	N/A	1000	N/A	500
Standard 2	Standard 1	150	150	500	250
Standard 3	Standard 2	150	150	250	125
Standard 4	Standard 3	150	150	125	62.5
Standard 5	Standard 4	150	150	62.5	31.25
Standard 6	Standard 5	150	150	31.25	15.625
Standard 7	Standard 6	150	150	15.625	7.81
Standard 8	N/A	0	150	0	0

Assay Procedure:

The ELISA plate was washed twice in an automatic plate washer with 350 µL of wash buffer per well to be used, ensuring complete aspiration of contents after each wash.

100 µL of each standard and each sample was added to individual wells and the position recorded. The plate was then sealed and incubated at 37°C for 90 minutes. The contents were then aspirated, and the plate was washed a further two times as above.

100 µL of Biotin-labelled antibody working solution was added to the bottom of the wells with care taken to avoid touching the side walls. The plate was again sealed and incubated at 37°C for one hour. The contents were aspirated, and the plate was washed a further three times as above but with a one-minute soak between washes.

100 µL of the SABC working solution was added to each well, the plate was sealed and incubated at 37°C for 30 minutes. Thereafter the plate was washed 5 times as above, including a 1-minute soak time.

90 µL of TMB substrate was added, the plate sealed and incubated at 37°C in the dark for fifteen minutes. 50 µL of stop solution was added and the solution gently mixed.

Optical density absorbance was measured at 450nm on a ThermoFisher™ Varioskan™ (ThermoFisher, USA) and results saved on a Microsoft Excel spreadsheet.

VGF

Vereinigte Glanzstoff-Fabriken (VGF) an inducible nerve growth factor was tested using Human VGF (Neurosecretory protein VGF) ELISA kit from FineTest, Wuhan Fine Biotech Co., Ltd. The detection range for this kit is stated as being between 78pg/ mL and 5,000pg/ mL, with a sensitivity to at least 46.9pg/ mL.

Reagent Preparation:

All reagents were brought to room temperature prior to use. This is a sandwich enzymelinked immune-sorbent assay. The anti- VGF antibody comes pre-coated on the 96 well plate.

Wash Buffer:

Wash buffer was prepared by adding 30 mL of concentrated wash buffer to 750 mL of deionised water. This solution was mixed gently and thoroughly and labelled.

Biotin-Labelled Antibody Working Solution:

No more than one hour before the experiment, 5 mL of biotin-labelled antibody working solution was prepared by adding 50 µL of Biotin-labelled antibody concentrate to 4950 µL of antibody dilution buffer. This solution was mixed gently and thoroughly and labelled.

HRP-Streptavidin Conjugate (SABC) Working Solution:

No more than 30 minutes before the experiment, 5 mL of SABC working solution was prepared by adding 50 µL of SABC to 4950 µL of SABC dilution buffer. This solution was mixed gently and thoroughly and labelled.

Standards:

The lyophilised human VGF protein was reconstituted with 1000 µL of sample dilution buffer and mixed gently and thoroughly. This solution was kept at room temperature for 10 minutes before gently mixing again to yield a 5000pg/ mL stock standard solution (Standard

1).

Seven standard tubes were then labelled 2-8. 300 µL of the stock standard solution was added to the Standard 2 tube with 300 µL sample dilution buffer. This mixture was then mixed gently and thoroughly.

300 µL of the sample dilution buffer was added to Standard 3-8 tubes. Standard 3 was prepared by adding 300 µL of standard 2 to the Standard 3 tube. This mixture was then mixed gently and thoroughly.

The above was repeated sequentially for Standards 4-7. Standard 8 was a blank control (Table 27).

Table 27 VGF ELISA standard preparation

Standard Number	Dilution Sample	Volume to Dilute (µL)	Volume of Sample Diluent (µL)	Starting Conc. (ng/ mL)	Final Conc. (ng/ mL)
Standard 1	Lyophilised VGF	N/A	1000	N/A	5000
Standard 2	Standard 1	150	150	5000	2500
Standard 3	Standard 2	150	150	2500	1250
Standard 4	Standard 3	150	150	1250	625
Standard 5	Standard 4	150	150	625	312.5
Standard 6	Standard 5	150	150	312.5	156.25
Standard 7	Standard 6	150	150	156.25	78.1
Standard 8	N/A	0	150	0	0

Assay Procedure:

The ELISA plate was washed twice in an automatic plate washer with 350 µL of wash buffer per well to be used, ensuring complete aspiration of contents after each wash.

100 µL of each standard and each sample was added to individual wells and the position recorded. The plate was then sealed and incubated at 37°C for 90 minutes. The contents were then aspirated, and the plate was washed a further two times as above.

100 µL of Biotin-labelled antibody working solution was added to the bottom of the wells with care taken to avoid touching the side walls. The plate was again sealed and incubated at 37°C for one hour. The contents were aspirated, and the plate was washed a further three times as above but with a one-minute soak between washes.

100 µL of the SABC working solution was added to each well, the plate was sealed and incubated at 37°C for 30 minutes. Thereafter the plate was washed five times as above, including a 1-minute soak time.

90 µL of TMB substrate was added, the plate sealed and incubated at 37°C in the dark for 30 minutes. 50 µL of stop solution was added and the solution gently mixed.

Optical density absorbance was measured at 450nm on a ThermoFisher™ Varioskan™ (ThermoFisher, USA) and results saved on a Microsoft Excel spreadsheet.

SCG2

Secretogranin II (SCG2) was tested using a Human SCG2 (Secretogranin II) ELISA Kit from FineTest, Wuhan Fine Biotech Co., Ltd.; catalogue number EH3751. The stated detection range is between 1.25ng/ mL and 80ng/ mL with a sensitivity of sensitivity < 0.75ng/ mL.

Reagent Preparation

All kit components were brought to room temperature for twenty minutes before use. This is a sandwich enzyme-linked immune-sorbent assay. The anti-Secretogranin II antibody comes pre-coated on the 96 well plate.

Wash Buffer:

30 mL of concentrated wash buffer was diluted into 750 mL of deionised/distilled water. Unused buffer can be stored at 4°C, if crystals form in the buffer it can be warmed to 40°C in a water bath and mixed thoroughly to dissolve crystals. The solution is then cooled to room temperature before use

Standards:
1 mL of the sample/standard dilution buffer was added to the lyophilised standard. This was left to stand at room temperature for ten minutes and then mixed thoroughly to produce an 80ng/ mL standard solution.

Serial dilutions of the standard were made as indicated in the table below and mixed thoroughly at each step (Table 28).

Table 28 SCG 2 ELISA standard preparation

Standard Number	Dilution Sample	Diluent Volume (µL)	Volume of Sample Diluent (µL)	Start Conc. ng/ mL	Final conc. ng/ mL
Standard 1	Lyophilised standard	N/A	1000	N/A	80
Standard 2	Standard 1	300 of Std 1	300	80	40
Standard 3	Standard 2	300 of Std 2	300	40	20
Standard 4	Standard 3	300 of Std 3	300	20	10
Standard 5	Standard 4	300 of Std 4	300	10	5
Standard 6	Standard 5	300 of Std 5	300	5	2.5
Standard 7	Standard 6	300 of Std 6	300	2.5	1.25
Standard 8	N/A	N/A	300	0	0

Standards were prepared immediately before the experiment.

Biotin-Labelled Antibody Working Solution:

A 1:100 dilution solution of Biotin-labelled antibody working solution was prepared by adding 45 µL of Biotin-detection antibody to 4,455 µL of antibody dilution buffer and mixing thoroughly. This was prepared within an hour before use.

HRP-Streptavidin Conjugate (SABC) Working Solution:

A 1:100 dilution solution of SABC working solution was prepared by adding 45 µL of SABC to 4,455 µL of SABC dilution buffer and mixing thoroughly. This was prepared within 30 minutes before use.

Assay Procedure:

All wells were washed three times in an automated plate washer, with 350 µL of wash buffer per well with a one-minute soak, prior to use. 100 µL of each standard and each sample was added to individual wells and their position recorded. The wells were sealed with a plate cover and incubated at 37°C for 90 minutes. The plate cover was removed, contents were discarded, and the plate washed as twice before.

100 µL of Biotin-Labelled antibody working solution was added to each well, the plate was sealed and incubated at 37°C for an hour. The plate cover was removed, contents discarded, and the plate washed three times as before.

100 µL of SABC working solution was added to each well, the plate was and incubated at 37°C for 30 minutes. TMB substrate was allowed to equilibrate at 37°C for 30 minutes. The plate cover was removed, contents were discarded, and the plate washed five times as before.

90 µL of TMB substrate was added to each well, the plate was sealed and incubated at 37°C for fifteen minutes in the dark. 50 µL of Stop Solution was then added to each well. The optical density absorbance was measured at 450nm in a microplate reader immediately after adding the Stop Solution. Results were saved on a Microsoft Excel spreadsheet.

SCG5

Secretogranin V (SCG5) was tested using an ELISA kit for Secretogranin V (SCG5) from Cloud Clone Corp; catalogue number SEC834Hu. The stated detection range is between 7.8pg/ mL and 500pg/ mL with a sensitivity<2.8pg/ mL.

Reagent Preparation

All kit components were brought to room temperature for twenty minutes prior to use. This is a sandwich enzyme-linked immune-sorbent assay. The anti-Secretogranin II antibody comes pre-coated on the 96 well plate.

Wash Buffer:

Wash buffer was prepared by adding 20 mL of concentrated wash buffer to 580 mL of deionised/distilled water. This was thoroughly mixed and labelled.

Standards:

1 mL of the sample/standard dilution buffer was added to the lyophilised standard. This was left to stand at room temperature for ten minutes and then mixed thoroughly to produce a 1000pg/ mL stock standard solution.

Serial dilutions of the standard were made as indicated in Table 29 below and mixed thoroughly at each step.

Table 29 SCG5 ELISA standard preparation

Standard Number	Dilution Sample	Diluent Volume (µL)	Volume of Sample Diluent (µL)	Start Conc. Pg/ mL	Final conc. pg/ mL
Standard 1	N/A	N/A	1000	N/A	500

Standard 2	Standard 1	500 of Std 1	500	500	250
Standard 3	Standard 2	500 of Std 2	500	250	125
Standard 4	Standard 3	500 of Std 3	500	125	62.5
Standard 5	Standard 4	500 of Std 4	500	62.5	31.2
Standard 6	Standard 5	500 of Std 5	500	31.2	215.6
Standard 7	Standard 6	500 of Std 6	500	215.6	1.25
Standard 8	N/A	N/A	500	0	0

Standards were prepared immediately before the experiment.

Assay Procedure:

100 µL of each standard and each sample was added to individual wells and their position recorded. The plate was sealed with a plate cover and incubated at 37°C for an hour. The plate cover was removed, and contents were discarded.

100 µL of Detection Reagent A working solution was added to each well. The wells were sealed and incubated at 37°C for an hour. The plate cover was removed, contents were discarded, and the plate washed three times in an automated plate washer with 350 µL of wash buffer per cell with a one-minute soak.

100 µL of Detection Reagent B working solution was added to each well, the plate sealed and incubated at 37°C for 30 minutes. The plate cover was removed, contents were discarded, and the plate washed five times as before.

90 µL of Substrate Solution was added to each well, the plate sealed and incubated at 37°C for fifteen minutes in the dark. 50 µL of Stop Solution was then added to each well. The optical density absorbance was measured at 450nm in a microplate reader immediately after adding the Stop Solution. Results were saved on a Microsoft Excel spreadsheet.

2.3.4 Bacterial Genomic Analysis

Nucleic Acid Extraction

FastDNA™ Spin Kit for Soil (MP Biomedicals, USA, SKU 116560200) was used for all DNA extractions. This was used due to the experience of the research group with this kit for nucleic acid extraction in other relatively paucicellular samples, e.g., breast milk.

100 µL of CSF, 978 µL Sodium Phosphate buffer and 122 µL MT buffer was added to a lysing matrix E tube. This was homogenised in a bead beater (Qiagen) for 40 seconds at 6 m/sec, then centrifuged at 14,000 g for five minutes. This bead beating step was added due to the predominance of gram-positive bacteria causing neurosurgical CSF infections (as discussed in Chapter 1, section 1.5.4.2).

The supernatant was carefully transferred to a clean 2 mL microcentrifuge tube, where 250 µL protein precipitation solution was added and mixed by hand by inverting the tube ten times. Samples were then centrifuged at 14,000g for 5 minutes, the supernatant was transferred to a clean 15 mL tube. 1 mL of binding matrix suspension was added to the supernatant and inverted by hand for two minutes to allow DNA binding. The tube was then placed on a rack for three minutes to allow the silica matrix to settle. 500 µL of the resulting supernatant was carefully removed and discarded whilst avoiding the binding matrix. The binding matrix and remaining supernatant were then gently resuspended and transferred to a SPIN™ Filter. This was then centrifuged at 14,000 g for one minute, discarding the effluent.

Then, 500 µL SEWS-M (an ethanol-based wash solution used in extraction of DNA to remove impurities once the DNA is bound to the Binding Matrix) was added to the SPIN™ Filter tube and the pellet re-suspended, this was centrifuged at 14,000 g for one minute and then two minutes, discarding the effluent between spins. The Spin™ Filter tube was allowed to air dry at room temperature for five minutes.

At this point, 50 µL of DES (DNase/Pyrogen free water) elution solution was added, the pellet gently re-suspended and again this was centrifuged at 14,000 g for one minute using a clean collection tube. This was labelled and stored at -20 °C until needed.

Bacterial Nucleic Acid Amplification

Amplification of the extracted DNA was performed using 16S primers (V3/V4 region; oligos 319F, 806R, HPLC; Integrated DNA Technologies, USA) and the RoVI (Rotavirus Vaccine Immunogenicity: Impact of maternal antibodies & microbiota Study) standard operating procedure. This protocol was developed between Clinical Infection, Microbiology and Immunology, Institute of Infection and Global Health and Functional and Comparative Genomics, Institute of Integrative Biology in the University of Liverpool[319].

A PCR mix was first prepared; 12.5 µL of *NEBNext* Q5 Hot Start HiFi PCR Mastermix (New England Biolabs Inc, M0544S), 0.625 µL of 10 µM 319F primer, 0.625 µL of 10 µM 806R primer, 0.3 µL 2 mg/mL BSA and 4 µL nuclease free water per reaction required plus one reaction volume extra. Then, 21 µL of the PCR mix was added to 4 µL of whole DNA in a labelled PCR tube and briefly spun. PCR was performed in an Eppendorf Thermal Cycler using steps detailed in Table 30.

Table 30 PCR conditions for 16S amplification of CSF DNA extract

Step	Temperature	Time	Cycles
Initial Denaturation	98°C	30 sec	1 cycle
Denaturation	98°C	10 sec	
Annealing	55°C	15 sec	25 cycles
Extension	72°C	40 sec	
Final Extension	72°C	60 sec	1 cycle
Hold	4-10°C	indefinite	

Quantification of Nucleic Acid

Qubit (ThermoFisher Scientific, USA) fluorometric quantification was used to measure DNA yield with the high sensitivity dsDNA assay kit (ThermoFisher Scientific, USA, Q32851). This assay can detect dsDNA in concentrations from 10 pg/µL to 100 ng/µL.

Briefly, allowing 1 µL if qubit reagent plus 199 µL of buffer per sample to be tested, 2 µL of reagent plus 380 µL (190 µL*2) of buffer for the two standards and one extra volume (1 µL reagent plus 199 µL buffer), a test mix is prepared immediately prior to testing.

The Qubit was set to measure high sensitivity dsDNA assay and “Test Standards”. Then 10 µL of standard 1 and 190 µL of mix is added to a Qubit tube, mixed thoroughly by vortex and placed in the Qubit sample chamber. Standard 1 (low concentration standard) was recorded. The same process was repeated with Standard 2 (high concentration standard).

"Run Samples" was then selected with an original sample volume (i.e., sample volume to be added to test mix for qubit) of 1 µL. Sequentially, 1 µL of sample was added to 199 µL of test mix in a clean qubit tube, mixed thoroughly by vortex, measured and result recorded.

Gel Visualisation of Nucleic Acid

Extracted and amplified DNA was visualised using gel electrophoresis, this was performed to confirm that bacterial DNA had been extracted and amplified

For this process, 1.2 g of agar was added to 120 mL of 0.5% TBE buffer and heated in a microwave until all agar crystals had dissolved. Then 12 µL of SYBR™ safe DNA gel stain (ThermoFisher Scientific, USA, S33102) was added, and the gel poured into a multiwall gel form and allowed to cool and set. 5 µL of E-Gel™ 1 Kb Plus DNA Ladder (ThermoFisher Scientific, USA, catalogue number 10488090) was carefully pipetted into the first and last wells of the gel when the well comb was removed. For each sample 1 µL of GelPilot DNA Loading Dye (Qiagen, Germany, catalogue number 239901) and 5 µL of sample was carefully mixed and pipetted into a well and position recorded.

The gel was placed in an electrophoresis chamber (Appleton Woods, UK), TBE was topped up to cover the surface of the gel, Thermo EC 250-90 positive and negative electrodes were attached and machine was set to 100 V for one hour. The gel was then removed and placed in an UV trans-illuminator (Syngene Ingenius, UK).

Sanger Sequencing of Amplified Nucleic Acid

Extracted and amplified DNA was further assessed by Sanger sequencing to confirm that enough nucleic acid was extractable from CSF for sequencing with NGS. This was sent for commercial Sanger sequencing with Eurofins.

10 µL of sample, 2 µL 10µM of 319F primer, 2 µL of 10 µM 806R primer and 3 µL of nuclease-free water was added to an individually barcoded PCR tube and thoroughly mixed. This was sent via courier to Eurofins and sequence data was available within 24 hours.

FASTA files for each sample were then analysed in BLAST (https://blast.ncbi.nlm.nih.gov/Blast.cgi) using nucleotide BLAST for bacterial and archaea 16S ribosome.[320]

Shotgun/Deep sequencing; Illumina NovaSeq

Libraries prepared by Edith Vamos and sequenced by Charlotte Nelson in the Centre for Genomic Research, University of Liverpool.

DNA samples (DNA extracted from CSF but not amplified with 16S primers) were submitted for *Illumina NEBNext* Ultra II FS DNA Library Prep. Following the manufacturers protocol, 20ng of DNA was used as input material where available (many of the uninfected samples did not meet this threshold but were included anyway), followed by size selection of Adaptor-ligated DNA. Following 10 cycles of amplification the libraries were purified using Ampure XP beads. Each library was quantified using Qubit and the size distribution assessed using the Fragment analyser (Agilent, USA)

These final libraries were pooled in equimolar amounts using the Qubit and Bioanalyzer data. The quantity and quality of each pool was assessed by Bioanalyzer and subsequently by qPCR using the *Illumina* Library Quantification Kit from Kapa (KK4854) on a Roche Light Cycler LC480II according to manufacturer's instructions. Briefly, a 20 µl PCR reaction (performed in triplicate for each pooled library) was prepared on ice with 12 µl SYBR Green I Master Mix and 4 µl diluted pooled DNA (1:1000 to 1:100,000 depending on the initial concentration determined by the Qubit® dsDNA HS Assay Kit). PCR thermal cycling conditions consisted of initial denaturation at 95°C for 5 minutes, 35 cycles of 95°C for 30 seconds (denaturation) and 60°C for 45 seconds (annealing and extension), melt curve analysis to 95°C (continuous) and cooling at 37°C (*LightCycler*® LC48011, Roche Diagnostics Ltd, Burgess Hill, UK).

Following calculation of the molarity using qPCR data, template DNA was diluted to 300pM and denatured for 8 minutes at room temperature using freshly diluted 0.2 N sodium hydroxide (NaOH) and the reaction was subsequently terminated by the addition of 400mM TrisCl pH=8. To improve sequencing quality control 1% PhiX was spiked in. The libraries were sequenced on an *Illumina® NovaSeq 6000* (*Illumina®*, San Diego, USA) following the XP workflow on 1 lane of an S4 flow cell, generating 2 x 150 bp paired-end reads.

Data Analysis

Sequencing data analysis was performed by Matthew Gemmell in the CGR, University of Liverpool.

Initial processing and quality assessment of the sequence data was performed using an inhouse pipeline (developed by Richard Gregory). Briefly, base-calling, and de-multiplexing of indexed reads was performed by CASAVA version 1.8.2 (*Illumina*) to produce 10 samples sequence files, in FASTQ format. The raw FASTQ files were trimmed to remove Illumina adapter sequences using Cutadapt version 1.2.1[321]. The option "-O 3" was set, so the 3' end of any reads which matched the adapter sequence over at least 3 bp was trimmed off. The reads were further trimmed to remove low quality bases, using Sickle version 1.200 with a minimum window quality score of 20. After trimming, reads shorter than 20 bp were removed. If both reads from a pair passed this filter, each was included in the R1 (forward reads) or R2 (reverse reads) file. If only one of a read pair passed this filter, it was included in the R0 (unpaired reads) file.

Read length is important for *Kraken 2* taxonomic assignment and *Bracken* abundance estimation. For the benefit of the downstream processes filtering was carried out to remove read pairs where at least one of the reads had a shorter length than 100bp. This was carried out with the tool fastp using the option "--length-required 100"[322].

Prior to taxonomic classification a *Kraken 2* database was created[323] (Wood et al, 2019). The "bacteria", "viral", "archaea", and "human" Kraken libraries were added to the database. The *Kraken 2* database was created with a default k-mer length of 35. From the *Kraken 2* database a *Bracken* database was built. An ideal read length of 100 was used, hence the 100bp minimum length filtering.

Paired reads were classified with *Kraken 2* using the *Kraken 2* database [323]. *Kraken 2* carries out taxonomic classification of short DNA reads by examining the k-mers within a read and querying a database with those k-mers. *Bracken* (Bayesian Re-estimation of Abundance with KrakEN) was used with the results of the *Kraken 2* read classification to compute the abundance of classified species [324]. *Bracken* output only contains the name at the specified taxa level (e.g., species) and taxon id. Therefore, the tool Taxonkit was used in conjunction with the taxon id to generate the lineages of each classified species[325].

A relative abundance of species was generated with R based on the “Total Reads after Abundance Re-estimation” values generated by *Bracken* (Team R.C., 2013). Interactive clustered heat maps of the relative abundances were created with the R package ‘heatmaply’[326]. Hierarchical clustering was carried out on the rows and columns of the heat map with ‘heatmaply’ choosing the optimal dendrogram for the data using one of the following methods: "ward.D", "ward.D2", "single", "complete", "average" (= UPGMA), "mcquitty" (= WPGMA), "median" (= WPGMC) or "centroid" (= UPGMC).

Chapter 3. Protein analysis of infected & uninfected neurosurgical CSF

3.1 Introduction

> *“Proteomics attempts to bridge the knowledge gap between genomes and living cells, or rather, that constellation of proteins that gives living cells structure and function.”* [327]

Proteomics is a relatively new discipline, involving the study of the proteome (the full complement of proteins expressed by the genome of a cell/tissue/organism at a given time [328]). It is good modality for screening large numbers of samples for potential biomarkers.

Prior to the human genome project, it was estimated that there would be >100,000 protein-coding genes in the human genome, which would explain the diversity and complexity of the human body and all biological tissues/organisms. The actual number of protein-coding genes is closer to 20,000 [329] with an estimated 100,000+ proteins and their isoforms expressed by these genes [330], with some even estimating that there may be over one million [331].

A gene is *transcribed* into ribonucleic acid (RNA), which is then *translated* into a protein (Fig. 24). The genetic code (the sequence of nucleotides making up the strand of deoxyribonucleic acid [DNA]) can acquire mutations which may affect the resultant protein. An example is a single nucleotide polymorphism (SNP), where there is a substitution of a nucleotide [332]. There is a large amount of degeneracy in the genetic code so these SNPs may not result in the change in the amino acid translated – it is said to be synonymous.

When the SNP occurs in a coding region (an exon) and results in a change of amino acid translated subsequently, the SNP is said to be non-synonymous [333].

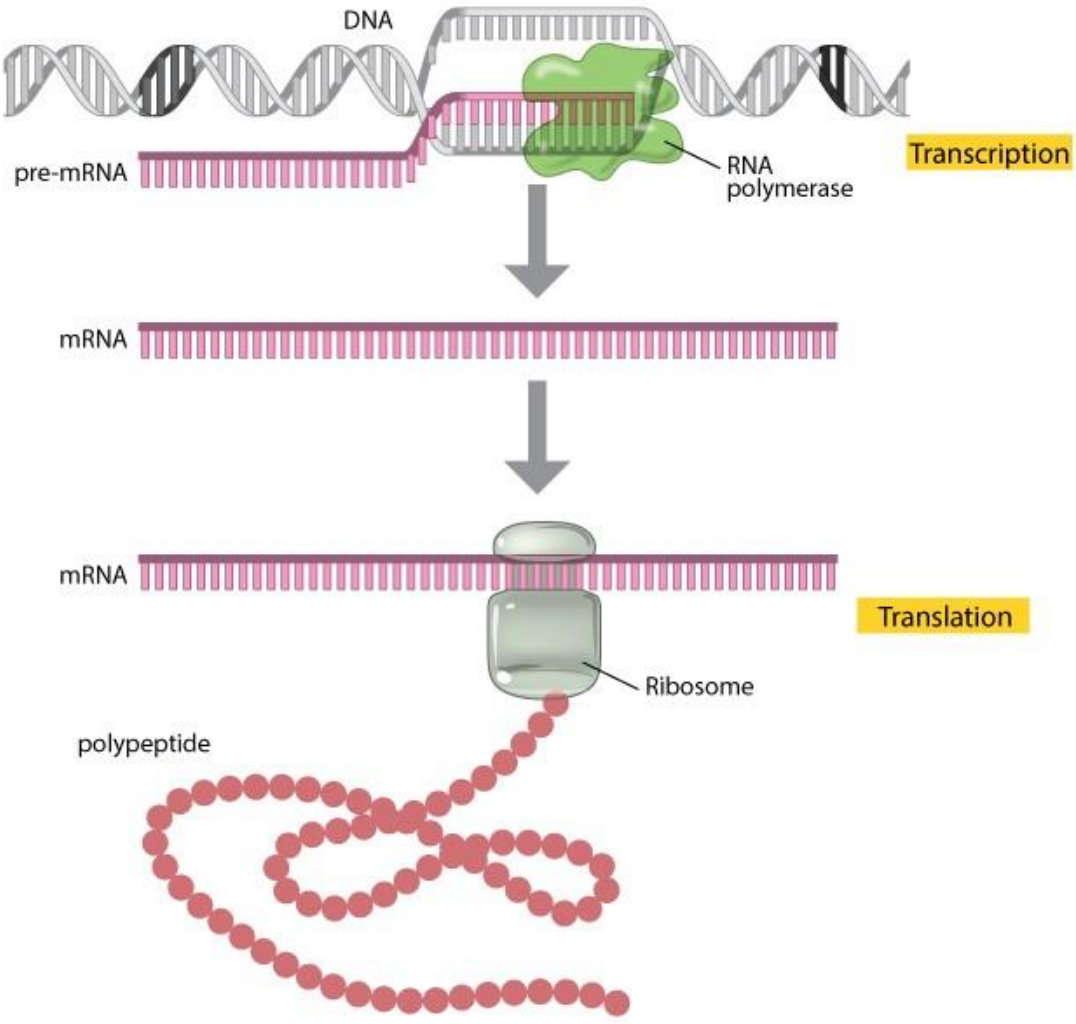

Figure 24 Protein synthesis from transcription *of the gene from DNA producing messenger RNA (mRNA) to* translation *by the* ribosome *of this mRNA into the polypeptide that will form the finished protein. Illustration taken from Nature Education, 2013 [334].*

The RNA that has been *transcribed* is processed prior to translation and it is at this point that it can undergo alternative splicing. Alternative splicing occurs via alternative splice sites, cassette exon inclusion or skipping and intron retention (non-coding sections which are ordinarily excluded prior to translation) (Fig. 25) [335].

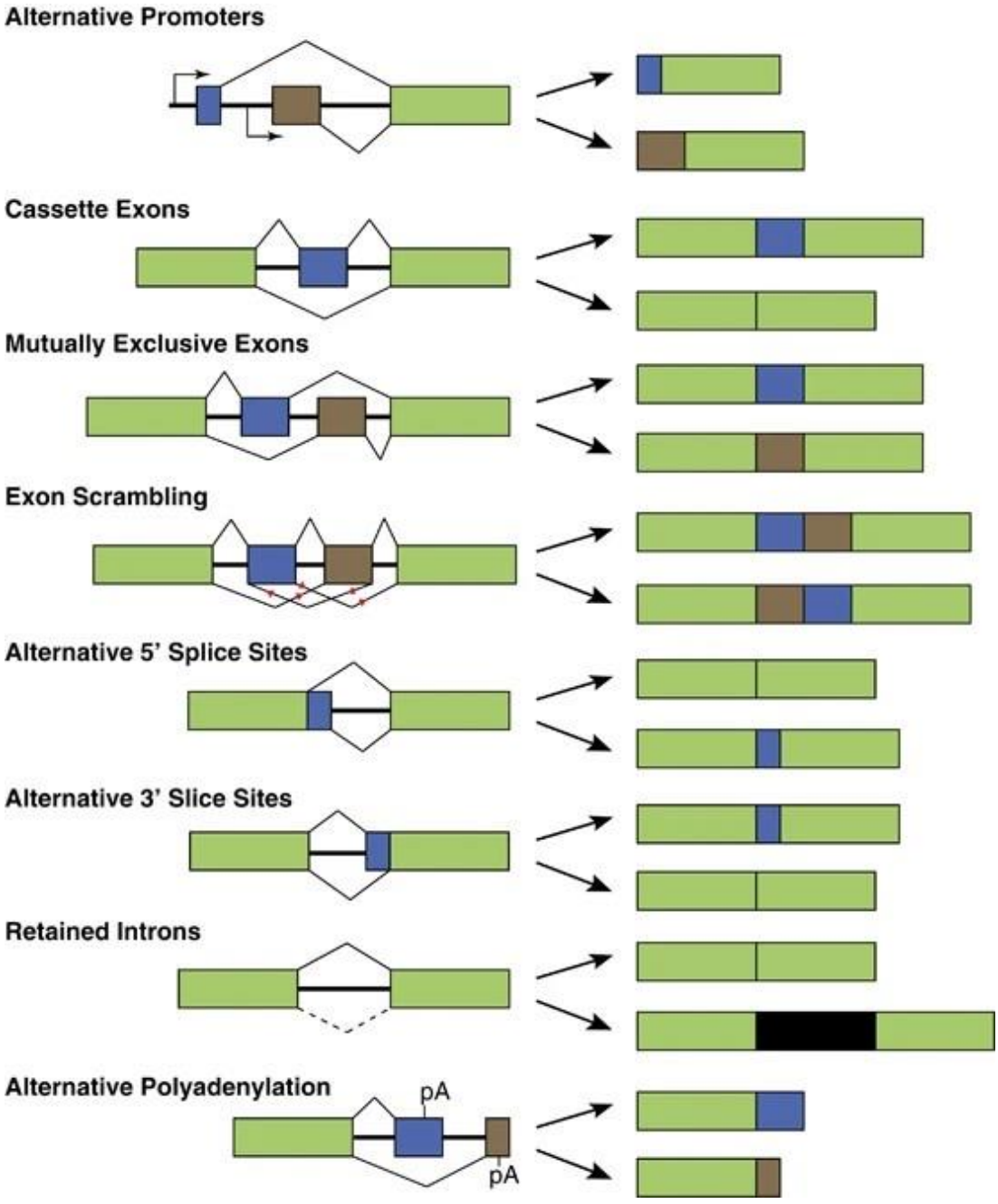

Figure 25 Alternative splicing. Common mechanisms of alternative splicing are shown. Alternative splicing can occur via several different processes and give rise to different mature transcripts (right). Exons (any part of a gene that will encode a part of the final mature RNA) and final transcripts are illustrated as boxes while lines represent introns (non-coding regions). Constitutively expressed exons are depicted in green, and alternatively spliced exons are depicted in blue or brown. Retained introns occur with the absence of splicing, with the intervening intron (black) included in the final transcript .pA= poly (A) tail, which is made up of multiple adenosine monophosphates. Illustration taken from Chen et al*,* Oncogene*, 2015 [336].*

After translation, proteins can be modified in a variety of ways (post translational modifications-PTMs), from cleavage of peptide bonds to the addition of chemical groups, lipids, carbohydrates and even entire proteins to an amino acid side-chain [337]. The vast repertoire of proteins and their isoforms can thus be explained by an organism's genetic variations, alternative splicing and PTMs (Fig. 26).

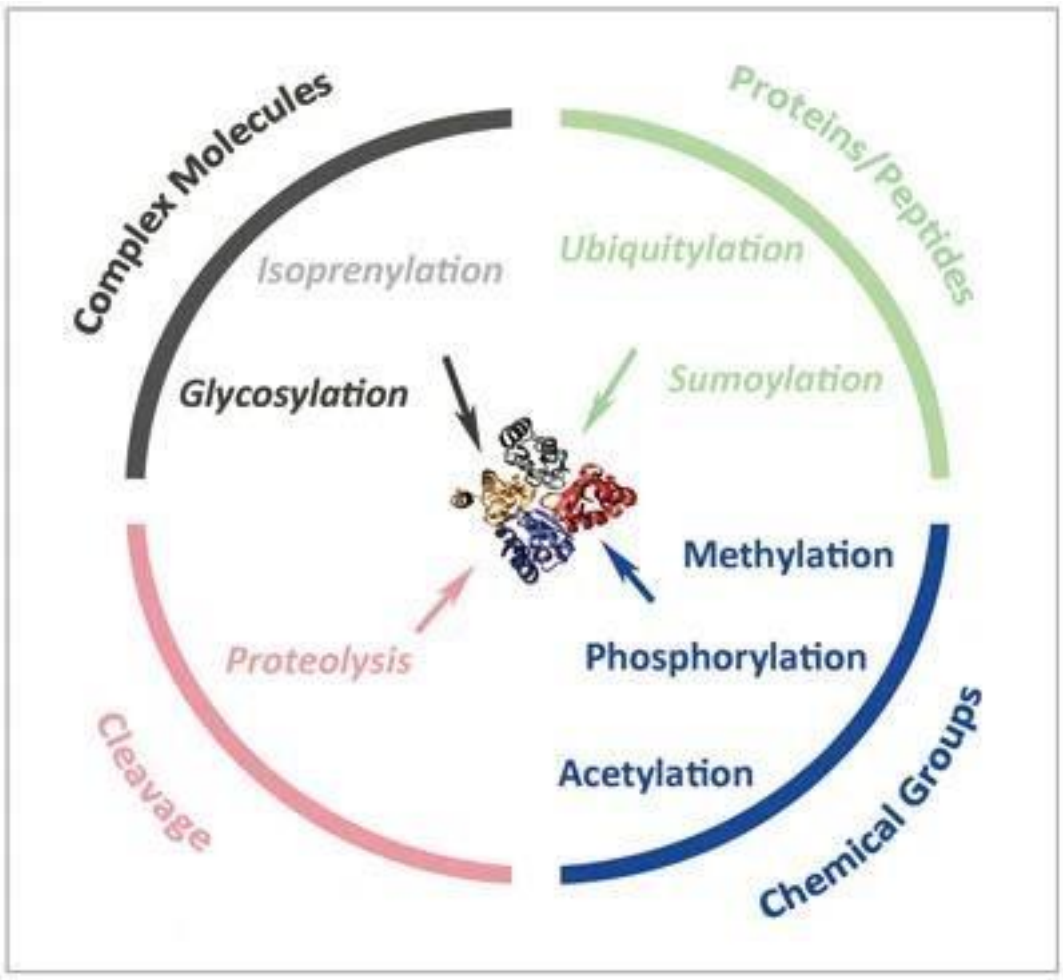

Figure 26 Post-translational modifications (PTMs) reversibly or irreversibly alter the structure and properties of proteins through biochemical reactions. This serves to diversify and extend protein function beyond what is dictated by gene transcripts. Illustration taken from Wang et al*,* Cell Research *2014 [338].*

3.1.1 Proteomics and CSF

CSF is an attractive biological fluid for proteomic analysis as it is known to be paucicellular and contains ~1/200th the protein content of blood [339]. CSF has been analysed in attempts to fully characterise its proteome. The most extensive examination of human CSF to date, was completed by *Zhang et al* in 2015. They identified 3,256 proteins using a bottom-up proteomic approach. To reduce the complexity of the sample it had highly abundant proteins removed with immunoaffinity depletion prior to protein digestion [340].

We know that protein content of CSF varies. Routine CSF analysis in clinical laboratories often includes the measurement of total protein content. High CSF protein content in association with a high WCC and low glucose concentration is associated with CSF infection (Table 31) [341]. An increase in CSF protein content is not exclusive to infection though, it is known to vary in a variety of neuropathologies (Table 32) making them ripe for study proteomically. The hypothesis of this experiment is that the proteome of a group of infected CSF samples is different to the proteome of a group of uninfected CSF samples. By comparing the two groups, candidate biomarkers that can differentiate between infection and no infection can be found.

Table 31 WCC, glucose and protein concentration patterns seen on CSF analyses. WCC = white cell count, PML = polymorphonuclear lymphocyte.

*Type **A** fluid is most commonly the result of bacterial meningitis.*

*Type **B** is characteristic of tuberculosis and other granulomatous meningitides.*

*Type **C** is produced by an assortment of disorders- viral meningitis, meningitis caused by* Listeria, Syphilis*,* Rickettsia, Leptospirosis, Trichinosis, Toxoplasmosis, Trypanosomiasis*, as well as cerebral* Malaria*, other intracranial infections not involving the meninges (subdural, epidural, brain and spine abscesses), toxic encephalopathy (associated with systemic bacterial infection), postinfectious and post vaccinal encephalitis. [341].*

Fluid type	WCC	Predominant cell type	Glucose	Protein (mg/dl)
Normal	<5	All mononuclear	Normal 40–80 mg/dl or at least 40% of the simultaneous blood sugar	<50
A	500–20,000	90% PMLs	Low in most cases	100–700
B	25–500	Mononuclear (PMLs early)	Low but may be normal	50–500

C	5–1,000	Mononuclear (PMLs early)	Normal, but rarely quite low	< 100

Table 32 Protein concentration (mg/dL) of CSF in different pathologies, adapted from Clinical Methods: The History, Physical, and Laboratory Examinations, Chapter 74. Cerebrospinal Fluid. BM + bacterial meningitis, TB = tuberculous, AM = aseptic meningitis, MS= multiple sclerosis [342]. These variations in protein depending on pathology are very relevant in neurosurgery, where CSF diversion may be necessary due to brain tumour or cerebral haemorrhage. The interpretation of CSF results where an infection may be suspected is therefore not simple in these cases.

Diagnosis	Total Cases	Normal (45 mg/dl or less)	Slightly (45–75 mg/dl)	Moderately (75–100 mg/dl)	Greatly (100–500 mg/dl)	Very greatly (500–3600 mg/dl)	Highest (mg/dl)	Lowest (mg/dl)	Average
BM	157	3	7	12	100	35	2220	21	418
TB meningitis	253	9	30	37	172	12	1142	25	200
Poliomyelitis	158	74	44	16	24	0	366	12	70
Neurosyphilis	890	412	258	102	117	1	4200	15	68
Brain tumour	182	56	45	22	57	2	1920	15	115
Brain abscess	33	9	15	3	6	0	288	16	69
AM	81	37	20	7	17	0	400	11	77
MS	151	102	36	9	4	0	133	13	43
Polyneuritis	211	107	33	17	44	10	1430	15	74
Epilepsy(idiopathic)	793	710	80	2	1	0	200	7	31
Cerebral thrombosis	300	199	78	13	10	0	267	17	46
Cerebral haemorrhage	247	34	41	32	95	45	2110	19	270
Cerebral trauma	474	255	84	43	73	19	1820	10	100

Proteomic analysis with a focus on biomarker discovery using CSF, to date, has predominantly targeted neurodegenerative diseases like Alzheimer's disease [343-348], amyotrophic lateral sclerosis (ALS) [349-351], Parkinson's disease [352-356], Lewy body dementia [357, 358], spinal muscular atrophy [359, 360] and multiple sclerosis (MS) [361363]. It can be noted that the average protein content of CSF in MS is lower than in aseptic meningitis and bacterial meningitis (Table 34) and yet has been successfully proteomically profiled.

In our experiment we were not interested in identifying every protein in the CSF, our experiment is one of expression proteomics. The hypothesis being that the proteins expressed by the body, and more particularly the brain/CSF, are uniquely altered in the setting of a systemic insult like infection. The performance of differentially expressed proteins to identify a CSF infection will then be further examined using more targeted testing: ELISA.

3.1.2 Proteomics technologies

Techniques for the study of proteomics have largely emerged over the last half century. No one analytical method or instrument can handle the vast dynamic range of the proteome. The concentration of proteins in plasma, for example, are estimated to vary in excess of ten orders of magnitude (Fig.27) [364].

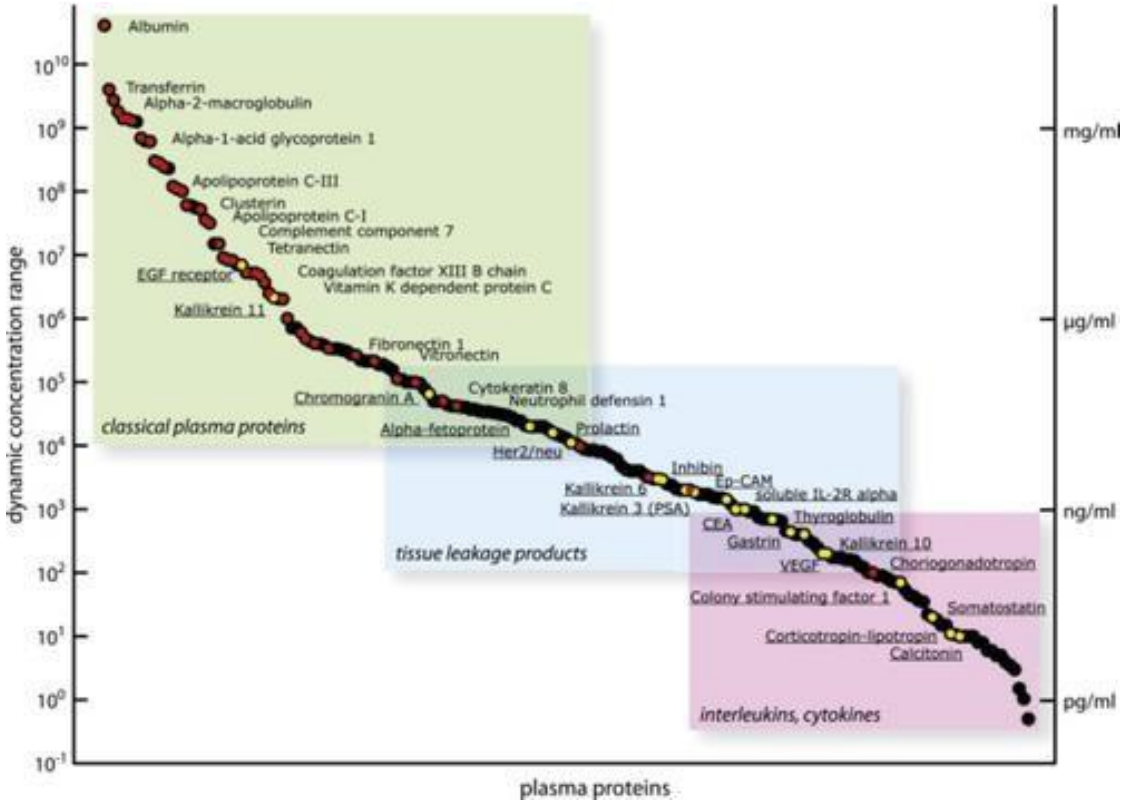

Figure 27 Dynamic range of some known proteins. Cytokines are seen to the right in the ng/mL to pg/mL range. [365]

Since the 1970's two-dimensional polyacrylamide gel electrophoresis (2D-PAGE) has been widely used to separate proteins by isoelectric point and by molecular mass and with the addition of dyes, quantitation is also possible. The separated proteins can then be cut out of the gel and identified (mainly by mass spectrometry [MS]) [366].

MS measures the mass to charge ratio of molecules with very high sensitivity to identify molecules. The mass spectrometer was invented by the great *J.J. Thompson* during his hunt for and discovery of the electron in 1897 [367]. There are three main ways of manipulating the analyte molecules to allow for separation and measurement in MS: time-of-flight (TOF MS), separation by quadrupole electric fields generated by metal rods (quadrupole MS), and separation by selective ejection of ions from a three-dimensional trapping field (ion trap or Fourier transform ion cyclotron MS) [368].

Notably, MS requires charged particles in a gaseous phase to perform analyses. MS used in protein identification was limited until the 1980's when "soft" ionisation technologies were developed. These allow peptides, polypeptides and larger proteins to be ionised and

therefore analysed with MS. The main techniques are matrix assisted laser desorption ionisation (MALDI) [369] and electrospray ionisation (ESI) [370].

MALDI produces ionised, gaseous molecules by coprecipitating the analyte with a matrix material (Fig. 28). The mix of analyte and matrix is pipetted onto a metal substrate and dried forming crystals. This solid is then irradiated with laser pulses. Proteins normally undergo fragmentation during MALDI resulting in loss of sensitivity [368]. MALDI is often paired with TOF detection (MALDI-TOF analysis), allowing peptide mass fingerprinting. In TOF analyses, ionised molecules are accelerated using a fixed energy, the smaller mass molecules reach the detector before the larger mass molecules and produce TOF spectra [368].

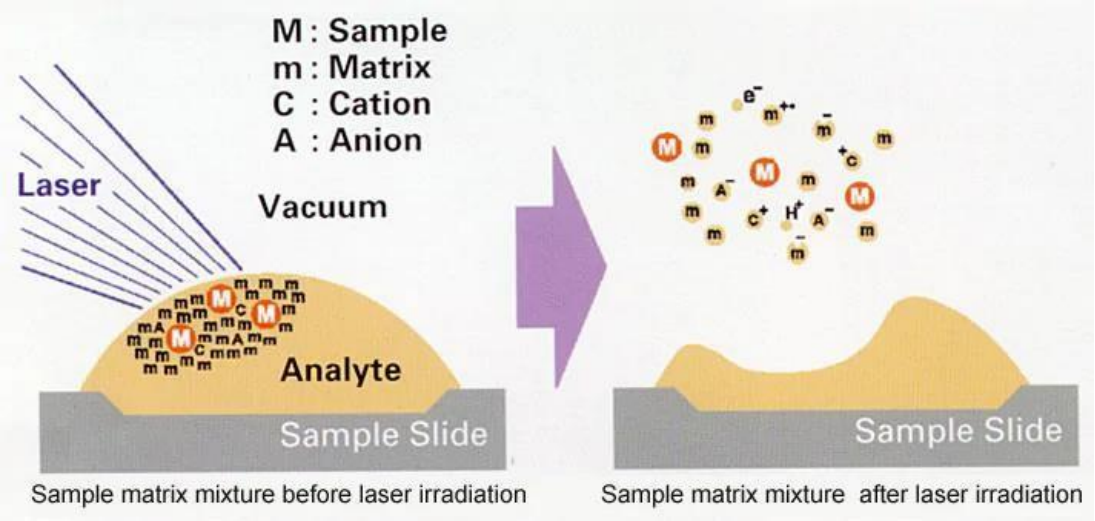

Figure 28 Diagram of matrix assisted laser desorption ionisation (MALDI). The coprecipitated analyte and matrix is irradiated with a laser causing the analyte to pass into a gaseous phase and to gain charge (ionisation). Illustration taken from commercial literature on The Principles of MALDI/TOF MS *by the* Shimadzu Corporation *[371].*

With electrospray ionisation (ESI), analyte in liquid is passed through a hypodermic needle with high voltage applied to it. This electrostatically disperses tiny micrometre sized droplets which evaporate and impart their charge to the analyte molecules (Fig. 29). These ionised molecules can then be passed through a mass spectrometer [368].

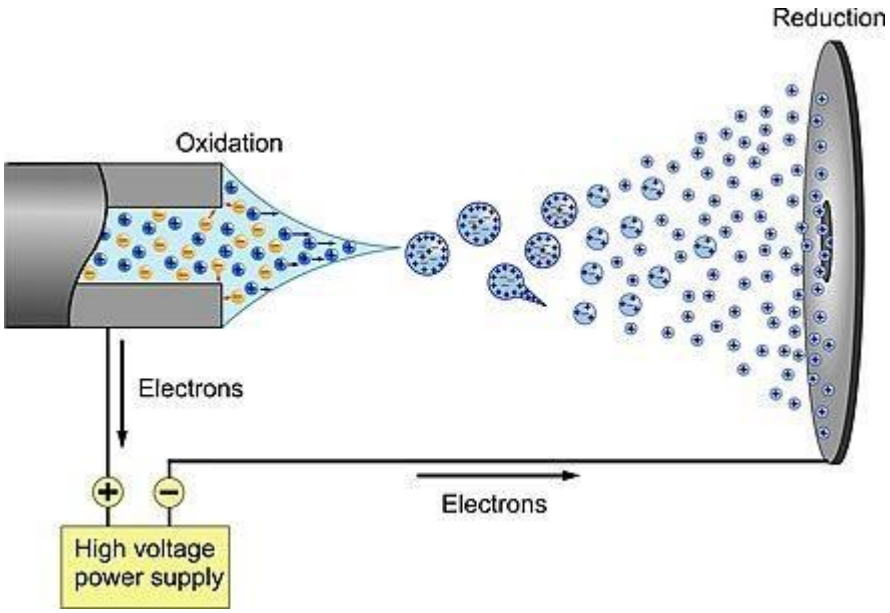

Figure 29 Diagram of electrospray ionisation. The analyte in solution is seen in the hypodermic needle on the left, which has a high voltage power supply attached. Illustration taken from Alymatiri et al*,* Analytical Methods *2015 [372].*

In comparison to ESI-MS, MALDI MS is very sensitive and more tolerant of contaminants like salts/small amounts of detergent [373]. MALDI and ESI can be coupled to any one of the three types of MS (TOF/quadrupole/ion trap). MALDI produces bursts of ions, whereas ESI gives a continuous beam of ions. This has meant that, typically, MALDI has been paired with TOF MS and ESI with quadrupole and ion-trapping MS [368].

Not only can MS identify peptides/proteins, it can also be used to determine amino acid sequence and PTMs. In tandem mass spectrometry (MS/MS) after initial mass determination, specific ions are selected and subjected to fragmentation by collision. These fragments are then analysed and the features of the peptides can be inferred from the masses [373].

Broadly speaking there are two schools of proteomic analysis: bottom- up and top-down. Bottom-up analyses identify proteins by first enzymatically breaking the proteins down into constituent peptides. This peptide mixture is passed through the MS and the mass spectra are compared with a reference proteomic database, e.g. UniProt [374]. Thereafter follows the process of peptide-protein inference. Protein inference is achieved by assigning peptide sequence to proteins [375]. This bottom-up strategy is the most commonly used approach for discovery proteomics [342]. Top-down analysis examines *intact* proteins with mass spectrometry. The proteins are analysed by fragmenting the protein within the MS to allow

measurement of the fragment ions and in this way it is possible to characterise PTMs of proteins [376] (Fig. 30).

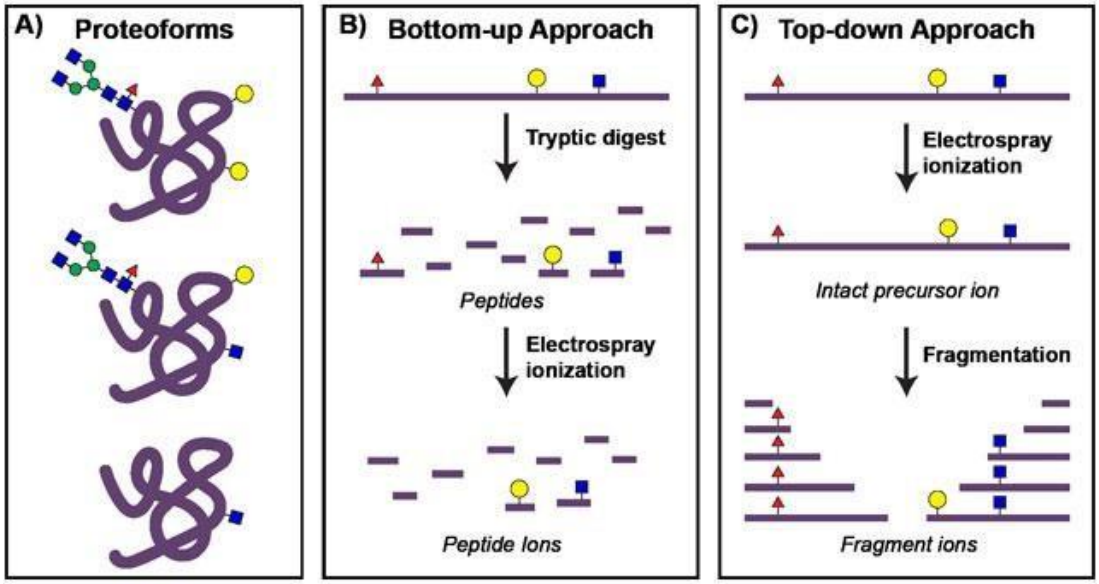

Figure 30 Diagram of proteomic approaches. Panel A) shows a protein with three different proteoforms (different post translational modifications (PTMs) can be seen- the coloured shapes representing carbohydrate/lipid/chemical groups that have been added to an amino acid side group), panel B) shows the Bottom-up proteomic approach where the protein is first digested enzymatically before analysis where the peptides undergo fragmentation by either by collision-induced dissociation [CID] or higher-energy collisioninduced dissociation [HCD], in panel C) Top-down proteomic analysis takes the intact protein through analysis , where the protein is fragmented by HCD or other dissociation techniques. Illustration taken from Bennett et al, Proteomics & Metabolomics *2020 [377].*

Proteomics elucidates the complex biological processes that occur in every cell/tissue/organ and that make up the integrated network that is organic life. But it not only provides basic knowledge, tantalisingly it now offers mass screening for the potential biomarkers of disease [378]. Expression proteomics harnesses the ability to both identify proteins **and** measure their relative quantity. In doing so, the data can be used to identify markers uniquely expressed in a disease state when compared to controls [379].

3.2 Materials & Methods

3.2.1 CSF

The clinical status, site of sampling (i.e., where it was sampled from), routine CSF culture result (Organism) and basic cell count results (WCC and RCC) of CSF samples used in this chapter are outlined in Table 33 (LC-MS/MS) and Table 34 (ELISA).

Table 33 CSF samples used for LC-MS/MS analysis. These samples were collected in the Walton Centre NHS

Foundation Trust in 2017/2018. The site of CSF sampling (source), outcome of routine microbiological culture (Organism), white cell count (WCC) and red cell count (RCC) are included. EVD= external ventricular drain, LD= lumbar drain, LP= lumbar puncture. The organisms found on routine culture are presented as reported by LCL.

Sample	Status	Source	Organism	WCC	RCC
1	Infected	EVD	*E. faecalis*	670	710
2	Infected	LD	*S. capitis*	7380	9540
3	Infected	EVD	*S. haemolyticus*	355	253
4	Infected	EVD	*E. faecalis*	434	62
5	Infected	EVD	*S. haemolyticus*	138	118
6	Infected	Shunt revision	*C. acnes*	Clotted	
7	Infected	EVD	*E. cloacae 2 types*	850	90
8	Infected	EVD	*S. epidermidis*	164	16
9	Infected	LP	*C. acnes*	22	12
10	Infected	Shunt revision	*C. acnes*	18	4
11	Infected	EVD	*E. coli*	46	1510
12	Infected	EVD	*S. epidermidis*	860	770
13	Uninfected	LP		4	<1
14	Uninfected	LP		<1	<1
15	Uninfected	LP		<1	<1
16	Uninfected	LP		<1	8
17	Uninfected	LP		<1	<1
18	Uninfected	LP		<1	<1
19	Uninfected	LP		<1	1
20	Uninfected	LP		<1	<1
21	Uninfected	LP		<1	<1
22	Uninfected	LP		3	268
23	Uninfected	LP		4	3
24	Uninfected	LP		1	120
25	Uninfected	LP		1	<1
26	Uninfected	LP		2	10
27	Uninfected	LP		2	558
28	Uninfected	LP		3	<1
29	Uninfected	LP		2	3
30	Uninfected	LP		3	20
31	Uninfected	LP		2	400

Table 34 CSF samples used for ELISA. The site if CSF sampling (Source), result of routine microbiological culture (Organism), white cell count (WCC) and red cell count (RCC) are included. EVD= external ventricular drain, LD= lumbar drain, TNP= test not performed.

Sample	Status	Source	Organism	WCC	RCC
1	Infected	EVD	*P. aeruginosa*	Clotted	
2	Infected	EVD	*S. epidermidis*	26	<1
3	Infected	LD	*E. faecium*	2240	70

4	Infected	LD	*S. aureus*	TNP	TNP
5	Infected	EVD	*S. Aareus*	3960	720
6	Uninfected	Shunt revision		<1	18
7	Uninfected	EVD		Clotted	
8	Uninfected	Shunt revision		<1	44
9	Uninfected	Shunt insertion		4	304
10	Uninfected	Shunt insertion		<1	160

3.2.2 Proteomic analysis

There were two groups for this experiment: infected and uninfected. The infected group included 13 infected samples with a clinical diagnosis of infection, high CSF WCC (where the ratio of WCC to RCC was >1:500) *and* positive routine culture. We would expect proteins involved in inflammation and fighting infection to be upregulated in this group. The uninfected group included 19 samples where there was no suspicion of infection, low WCC (<5), negative routine culture and where all other investigations were negative (Table 32).

Whole, unspun CSF was transported frozen, on dry ice to Target Discovery Institute (TDI) in Oxford. Samples were thawed on ice in preparation for analysis. The protocol for protein digestion with SMART digest kit (ThermoFisher Scientific, USA) (Ms Libby van Tonder) and subsequent LC-MS/MS (Dr Sarah Bonham) is described in detail in Chapter 2, section 2.2.2. This was all performed in the TDI laboratory in Oxford University.

Briefly, protein digestion was performed first. SMART Digest Tubes containing SMART Digest buffer and whole unspun CSF were clearly labelled and incubated at 70°C for one hour. The digestion was completed with a high complexity clean-up method using a SOLAμ SPE plate (ThermoFisher Scientific, USA, product code 60109-103). The plate was prepared, then digested samples were diluted with trifluoroacetic acid (Sigma Aldrich, Germany) in water before loading on the SOLAμ SPE plate. The plate was then washed with trifluoroacetic acid in water before peptides were eluted with acetonitrile (Sigma Aldrich, Germany). Finally, formic acid was added to each sample prior to analysis.

LC-MS-MS analysis was performed in the TDI laboratory in Oxford using a Dionex Ultimate 3000. The mass spectrometry proteomic data was analysed with MaxQuant[311] and the protein identification, quantification was performed using Perseus[313].

3.2.3 ELISAs

ELISAs for candidate proteins identified in the proteomic data were carried out initially using pooled CSF samples (two pools, one made up of five 200 µL aliquots of infected CSF and a second pool of five 200 µL aliquots of uninfected CSF) to allow for optimisation of the ELISAs tested.

The most sensitive, commercially available, ELISAs for the candidate proteins were chosen (i.e., the assays capable of detecting protein at the lowest possible concentration). ELISAs were optimised for sample dilution as none of the commercially available kits gives guidance on the dilution of CSF for testing. Details of the ELISA protocols are seen in Chapter 2, section 2.3.3.

A protein digestion step was added to the preparation of individual CSF samples for ELISA. This was added to control for any effect protein digestion may have had on the CSF sample. This was carried out as described above for LC-MS/MS. There were two control samples included with the CSF samples that were protein digested- an aliquot of ultra-pure laboratory grade water and an aliquot of phosphate-buffered saline (PBS). This was included to assess the effect of the protein digestion kit on the ELISA.

3.2.4 Statistical analysis

Cluster 3.0[314], TreeView[315] and AUREA[316] were used to analyse the LC-MS/MS data and created a shortlist of potentially interesting peptides for further analysis; i.e. proteins that are either upregulated or downregulated between the two groups and that can differentiate infected CSF from uninfected CSF.

The protein relative abundance data was interrogated using AUREA (Adaptive Unified Relative Expression Analyzer)[316]. AUREA is a software based on algorithms predominantly developed in cancer research using microarray data of gene expression[380]. The ranks of the relative expression of each entity (gene/protein) are used rather than the absolute expression values, thus avoiding issues around data normalisation techniques. The basic unit of comparison is the relative expression reversal, where the expression value between two biomolecules (e.g., genes) reverses between phenotypes. In this study that is infected and uninfected states. Top scoring pairs (TSP) or top scoring triplets (TST) of proteins can then be computed that best differentiate phenotypes (i.e., infected, and uninfected).

Using various combinations of subsets of infected and uninfected samples, AUREA was trained to differentiate infected CSF from uninfected CSF. For example, sample 1(*E. faecalis*), sample 3(*S. haemolyticus*), and sample 9(*C. acnes*) were classified as *Infected* whilst sample 16, sample 24, and sample 29 were classified as *Uninfected*. The remaining samples data were then analysed, and a list was produced of top scoring pairs and top scoring triplets of proteins that together differentiate between infected and uninfected samples.

The ID for proteins in the LC-MS/MS data identified by this process were searched for in UniProt[381] and the Human Protein Atlas [382]. Proteins that were expressed in brain tissue and had a commercially available ELISA were selected for further investigation.

ELISA results were then uploaded to MyAssays.com using the standard curve to calculate the target protein concentration via linear regression. This calculation adjusts for the dilution factor of the sample. All concentrations were converted to ng/mL at this point.

These results were converted to a long format data frame and uploaded to the RStudio[317], whereupon the infected and uninfected groups were compared using a t-test and described using the “psych” package. Data was then plotted using “ggplot2” and “ggsignif”. Each of these R packages are commonly used for basic statistical analyses.

3.3 Results

3.3.1 LC-MS/MS

A total of 683 proteins were identified (Appendix A). After data was filtered for proteins present across 80% of samples, 641 proteins remained. This ensured that proteins that were present in the majority of samples were included for further analysis, excluding any outlier values that may represent severe/unusual infection.

The relative abundance data for the identified proteins were median adjusted and then underwent hierarchical clustering on proteins with uncentred correlation and average linkage. This is visually represented below (Fig. 31) using Java TreeView. This analysis was repeated using R (Fig. 32).

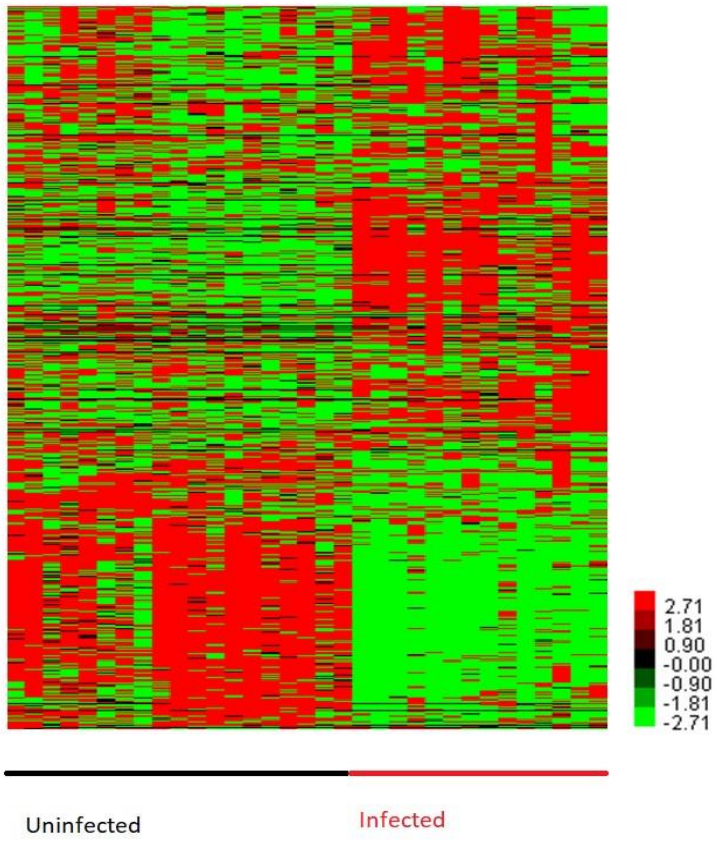

Figure 31 Heat map of relative abundance of proteins identified by LC-MS/MS. This was generated using Cluster 3.0 and TreeView. For clarity a section where there was no difference in the relative abundance of proteins between the groups were omitted. Red cells are proteins with increased expression, green is decreased expression, and black is no difference. The larger grouping on the left of the map is the group of uninfected samples and the right sided group is the infected samples.

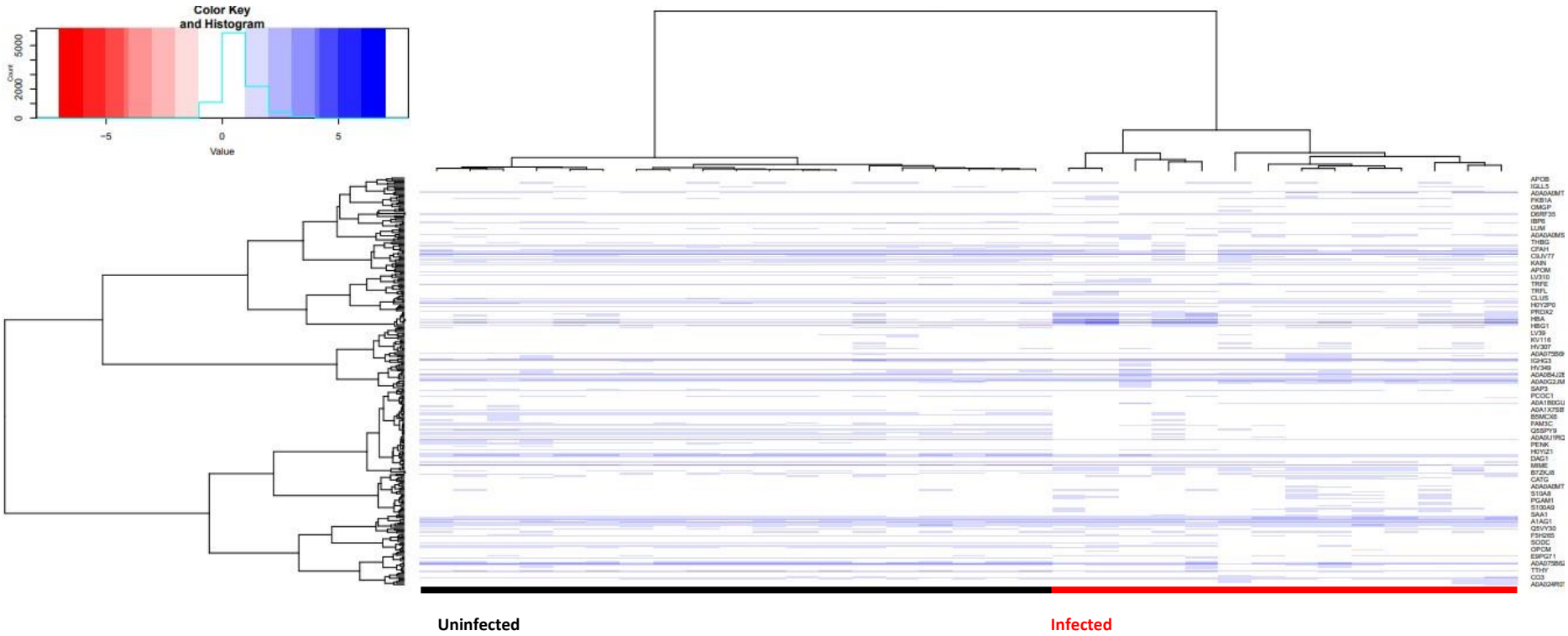

Figure 32 Heat map of relative abundance of proteins identified by LC-MS/MS. This was generated with R statistical analysis software, with "stats", "gplots", "heatmap.plus", "Heatplus" packages [318]. Samples were not categorised prior to cluster analysis but the two groups are clearly different. The ***uninfected*** *samples are the main cluster on the left (annotated with the* ***black*** *bar) and* ***infected*** *sample are on the right (red bar).The colour palate used for the colour key was inverted to more clearly show the pattern- upregulation of a protein is shown in shades of blue whereas downregulation is shown in reds.*

3.3.2 Candidate biomarkers of CSF infection

During the analysis of the relative expression data using AUREA many combinations of subsets of the infected and uninfected samples yielded an array of top scoring pairs and triplets of proteins. Different subsets of infected samples and uninfected samples were used to train AUREA to differentiate between infected and uninfected states.

Nine proteins were chosen as candidates for further investigation (Table 35). These were chosen due to the protein's expression in the brain and where there was a commercially available ELISA available (Table 36). The role of these proteins in vivo and any known relevance to meningitis will be explored in section 4.4. None of the three biomarkers (lactate, procalcitonin, CRP) for neurosurgical CSF infection discussed in Chapter 1, section 1.6.1 emerged as proteins of interest in this analysis, in fact they were not identified at all during proteomic analysis.

Table 35 List of proteins chosen from top scoring pairs and triplets of proteins identified by AUREA. ID: identification code used in LC-MS/MS data, Name: actual protein name (confirmed by searching UniProt for the LC-MS/MS protein ID).

	ID	Name
1	TRFL	Lactoferrin
2	A0A1X7SBT7	Neuronal pentraxin receptor (NPTXR)
3	TIMP2	Tissue inhibitor of metallopeptidase 2 (TIMP2)
4	IGF2	Insulin-like growth factor 2 (IGF2)
5	NEGR1	Neuronal growth regulator 1 (NEGR1)
6	A0A1W2PQB1	Fc of IgG low affinity IIIa receptor isoform 1 (FCGR3A)
7	VGF	Nerve growth factor inducible (VGF)
8	SCG2	Secretogranin II (SCG2)
9	7B2	Secretogranin V (SCG5)

Table 36 ELISAs used for testing CSF. ELISAs produced by RayBio®, FineTest and Cloud Clone Corp were procured via Antibodies-Online GmbH, Germany

Target	Assay type	Company	Catalogue No.	Range	Sensitivity

Lactoferrin	Sandwich	Abcam®	ab229392	15.6-1000 pg/mL	6 pg/mL
NPTXR	Sandwich	RayBio®	ABIN4883974	0.410-100 ng/mL	0.4 ng/mL
TIMP2	Sandwich	Abcam®	ab188395	15.6- 1000 pg/mL	6 pg/mL
IGF2	Sandwich	FineTest, Wuhan Fine Biotech Co.	ABIN2950563 EH0166	62.5-4000 pg/mL	<37.5 pg/mL
NEGR1	Sandwich	MyBiosource	MBS7607024	78-5000 pg/mL	<46.9 pg/mL
FCGR3A	Sandwich	FineTest, Wuhan Fine Biotech Co	ABIN5654105 EH3048	7.813-500 ng/mL	4.688 ng/mL
VGF	Sandwich	FineTest, Wuhan Fine Biotech Co.	ABIN4948129	78-5,000 pg/mL	46.9 pg/mL
SCG2	Sandwich	FineTest, Wuhan Fine Biotech Co.	ABIN850904 EH3751	1.25-80 ng/mL	< 0.75 ng/mL
SCG5	Sandwich	Cloud Clone Corp	ABIN418504 SEC834Hu	7.8-500 pg/mL	<2.8 pg/mL

3.3.2.1 Lactoferrin

Lactoferrin is a protein known to be involved with the response to bacterial infection. Lactoferrin expression was significantly higher in infected CSF samples than in uninfected samples, with a p-value <0.001 (see Fig. 33).

The relative abundance measurement for each protein identified is calculated from the LCMS/MS data, it is not measured in a standard unit and the data for each protein selected for further investigation is presented here for illustrative purposes only.

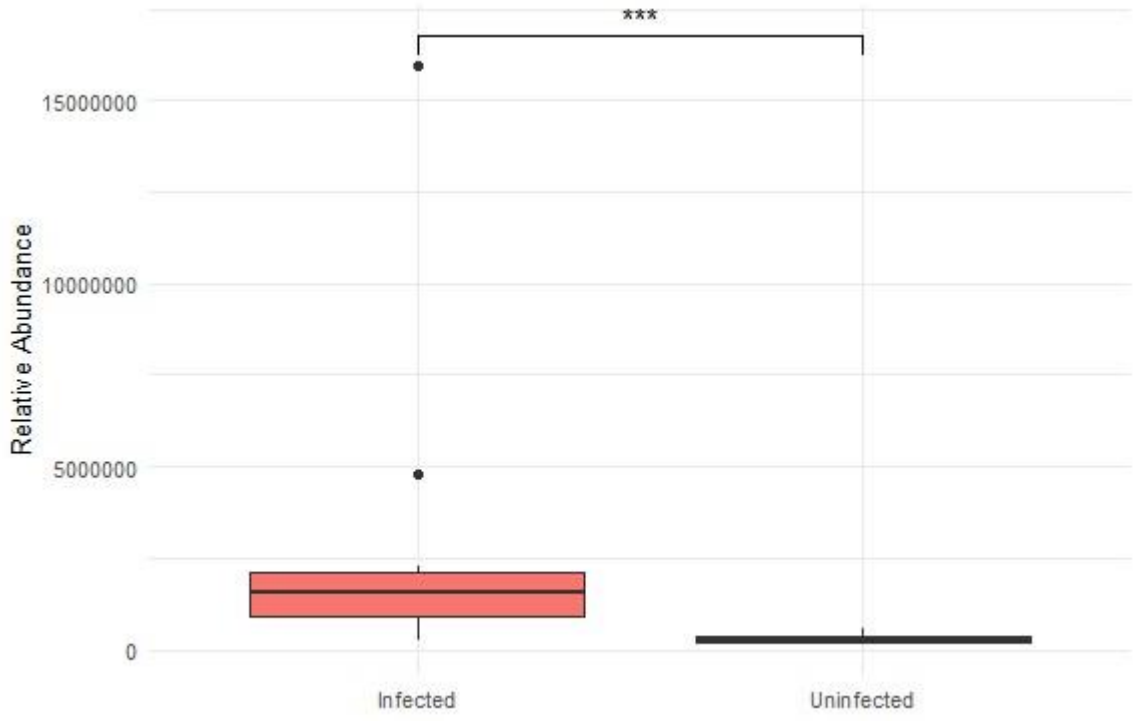

*Figure 33 Lactoferrin relative abundance in infected CSF samples and uninfected CSF samples, as measured by LC-MS/MS. *** P-value < 0.001. The relative abundance of Lactoferrin in infected samples was 1,287,919 (250,763 - 2,260,166). In uninfected samples the mean was 287,998.7 (119,402.8 - 589,507.1). A Welch two sample t-test was applied to this data. T test statistic was 5.0342 with 11.602 degrees of freedom and p-value of 0.0003239 (confidence interval 565,499.2 - 1,434,342.3).*

Pooled CSF Samples

The relationship between lactoferrin concentrations in infected samples versus uninfected samples was then examined using ELISA performed on pooled CSF samples (1 pool of infected CSF samples and a second pool of uninfected samples). This again showed that Lactoferrin is significantly higher abundance in infected CSF samples in comparison to uninfected samples (p-value <0.001, see Fig. 34).

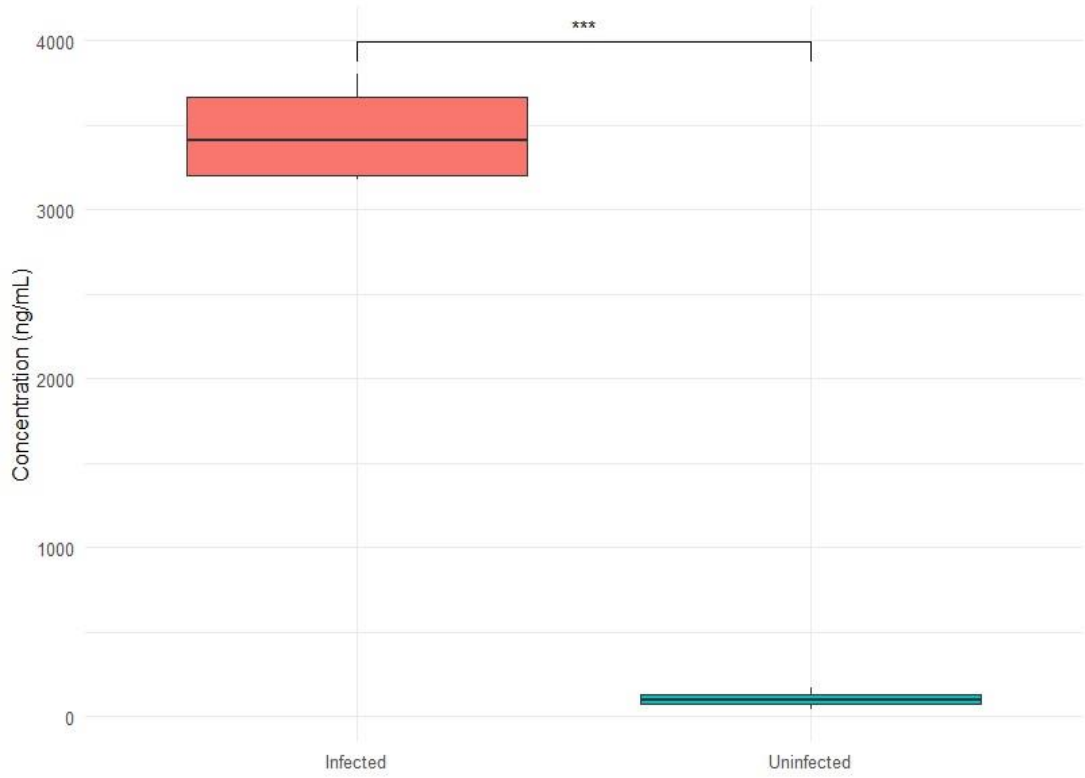

*Figure 34 Lactoferrin ELISA results of testing pooled CSF samples, one pool of infected CSF samples and another pool of uninfected CSF samples. *** P-value < 0.001. The mean concentration of lactoferrin in the four different dilutions of CSF, corrected for dilution, was 3,451.5 ng/mL (range=3,179 - 3,804 ng/mL, SD 308.85) for infected samples and 102.95 ng/mL (44.6 - 172.76 ng/mL, SD 54.26) for uninfected samples. Welch Two Sample t-test statistic was 21.357, df = 3.185, p-value = 0.0001512 (95% confidence interval: 2,865.574 - 3,831.531).*

Individual CSF Samples

The CSF samples that made up the pools used for the first ELISA were then individually tested. This failed to show a statistical difference between the groups (Fig. 35).

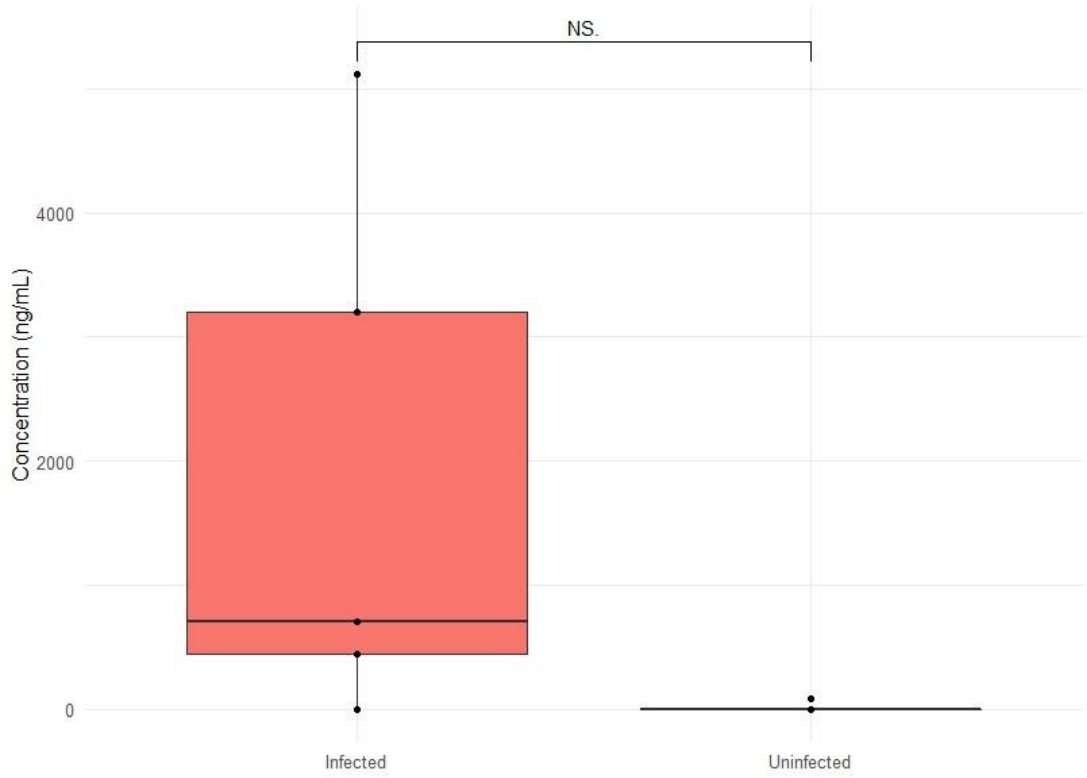

Figure 35 Lactoferrin ELISA results of individual CSF samples. NS= non-significant. The average Lactoferrin concentration for the infected samples was 1,895.44 ng/mL, (0 - 5,121 ng/mL, SD 2,192.69). Sample 2 was below the level of detection of the assay. In the uninfected group the average Lactoferrin concentration was 17.3 ng/mL, range 0 - 86.3 ng/mL, SD 38.6. Only sample 9 had a detectable level of Lactoferrin. Welch Two Sample t-test statistic was 1.915, df = 4.0025, p-value = 0.128 (95% confidence interval: -844,155.3 - 4,600,523.3).

The relationship between the concentration of Lactoferrin in infected CSF and uninfected CSF was maintained between testing modalities, i.e., LC-MS/MS and ELISA showed that there is a higher concentration of lactoferrin in infected CSF samples in comparison to uninfected CSF samples. This difference is highly statistically significant in the pooled CSF samples, but this significance was not seen in the individual samples tested. (Table 37, Fig. 36).

*Table 37 Summary of Lactoferrin LC-MS/MS, pooled sample ELISA and individual sample ELISA results. *** Pvalue < 0.001, NS=non-significant.*

	LC-MS/MS		ELISA pooled (ng/ mL)			ELISA individual (ng/ mL)		
Infected	High	***	High	3,450	***	High	1,895 (0 - 5,121)	NS
Uninfected	Low		Low	103		Low	17.3 (0 - 86)	

Discussion

Within the LC-MS/MS data relative expression analysis, Lactoferrin came out within a top scoring triplet. It can be seen in Fig. 33, there is a significant (p-value < 0.001) difference between Lactoferrin in infected versus uninfected CSF samples with infected CSF showing higher relative abundance of Lactoferrin in comparison to uninfected CSF. There is a wide range of values seen for the infected samples in this experiment, with the lowest value overlapping with the range of values seen for uninfected samples. This sample was an infected shunt with a neck abscess that grew *E. coli* on culture though the cell count was not especially impressive (WCC=46, RCC=1510).

ELISA testing of pooled infected CSF and uninfected CSF similarly showed that there is a significantly higher concentration of Lactoferrin measured in infected samples versus uninfected CSF (Fig. 34). This finding was further explored with testing of the individual CSF samples used in the respective CSF pools. Again, the concentration of Lactoferrin was higher in infected CSF in comparison to uninfected CSF (Fig. 35). The significance of this difference was reduced by sample 2 in the infected group, which measured below the limits of detection for the assay.

Sample 2 involved a definite infection with *S. epidermidis*, which is a very common skin commensal. In any other setting the finding of *S. epidermidis* on a sample would often be dismissed as a contaminant, introduced during sampling. In this case there had been clear clinical presentation of infection and the WCC was elevated in comparison to the RCC (WCC=26, RCC<1). The four other infected cases involved more aggressive pathogens: *P. aeruginosa, E. faecium* and *S. aureus* (x2). It may be that the systemic response to *S. epidermidis* fails to produce the rise in Lactoferrin expression seen in more aggressive pathogens.

The concentration of Lactoferrin seen in the pooled samples was within the range seen in the individual samples for *infected* CSF but the uninfected pool result was higher than the upper limit of individual sample results. Average Lactoferrin concentration for individual CSF is almost half of that seen in the pooled samples. Is this an effect of duration of storage without protease inhibitors?

The samples used for the pools were thawed, aliquoted and then 200 µL aliquots were combined to create the pool. This pool was aliquoted and refrozen. The individual sample aliquots were refrozen at the same time. These were stored at – 80 °C until needed for testing. Therefore, they all underwent equal numbers of freeze-thaw cycles. The only difference being the duration in storage. Ideally, all samples would have been tested in triplicate or when the

discrepancies arose between the pools and individual sample averages the tests should have been repeated. Unfortunately, due to the small volumes of CSF available (particularly for infected CSF) this was not possible.

Literature Review

Lactoferrin has been extensively studied. First identified in 1939 by *Sørensen et al* [383] in the whey of cow's milk, "the red protein" was later isolated in human milk, the red colour of the protein coming from its iron content [384]. It is constitutively produced and secreted by mucosal epithelial cells. It has been identified in saliva, tears, nasal mucus, bronchial secretions, hepatic bile, pancreatic secretions, seminal fluid, cervical mucus, urine, gastrointestinal secretions, joint fluid, blood serum and CSF [385, 386]. Some of the established concentrations of lactoferrin in different bodily fluids are listed in Table 38.

Table 38 Lactoferrin concentration (µM) in different body fluids. Table adapted from Weinberg*, 2009 [387].*

Fluid	Concentration (µM)	Underlying condition
Colostrum	100	Normal
Milk	20–60	Normal
Tears	25	Normal
Saliva	0.05	Normal children
	0.25	Children: cystic fibrosis
Cerebrospinal fluid	0	Normal children
	0.01	Children: viral meningitis
	0.13	Children: bacterial meningitis
Joint fluid	0.014	Non-inflammatory
	0.33	Inflammatory arthritis
Blood plasma	0.005	Normal
	2.5	Sepsis

Highest concentrations of Lactoferrin are seen in colostrum- milk produced by mothers in the first few days of a new born baby's life [388]. Interestingly, for this study of CSF, it is

also produced by secondary neutrophil granules [389]. In fact, it has been shown that 15µg of Lactoferrin can be produced by 10^6 neutrophils in the setting of infection or inflammation [390].

Lactoferrin is an 80kDa positively charged (cationic), glycosylated protein and a member of the transferrin family [391]. It is an avid iron binder and by scavenging iron from an environment it deprives many microbes of an essential factor for growth *[392].*

Lactoferrin has long been recognised for its bacteriostatic properties secondary to iron chelation but increasingly Lactoferrin is increasingly revealing other properties. Lactoferrin is a part of the innate immune system. It contains a bactericidal domain [393] and is transported across the blood brain barrier via receptor mediated transcytosis [394]. It has received a lot of attention as an antimicrobial peptide in the setting of rising antimicrobial resistance (one of the World Health Organisation -WHO's top ten threats to global health [305]). To this end, Lactoferrin has been employed as a nutraceutical (products that are used as medicines in addition to their nutritional role [395]) in clinical trials to reduce infection in pre-term infants [396] and more specifically to prevent late onset sepsis in preterm/low birth weight infants with positive effects [397, 398].

With such extensive research into Lactoferrin and its innate immunity roles, it is unsurprising that it has previously been identified as a protein of interest in meningitis. To date there are seven studies which look at lactoferrin as a biomarker for meningitis (Table 39). One was excluded here, as there is only an abstract available (*"Level of lactoferrin in serum and cerebrospinal fluid of patients with meningitis" Lykova et al* 2007 Zhurnal mikrobiologii, epidemiologii, i immunobiologii) [399]. All these studies involve community acquired meningitis which, as has been discussed in Chapter 1, is predominantly caused by *S. pneumoniae, N. meningitidis, H. influenzae.*

Table 39 Summary of literature dealing with Lactoferrin and bacterial meningitis (BM) [400-405].

Year	Author	Population	No. with BM	Lactoferrin concentration	Causative bacteria
1982	Hallgren et al[400]	Adult	5	360 µg/L (+/- 168)	Meningococcal (2), Staphylococcal (2), Pneumococcal (1)

1986	Gutteberg et al[401]	Paediatric	11	No mean/median provided Range ~5,00060,000 ng/mL	*S. pneumoniae* (3), *S. aureus* (1), gram-negative diplococci (1) and *N. meningitidis* (6)
1987	Visakorpi et al[402]	Mixed	15	139 ng/mL Range <10 - 8,685 ng/mL	Not provided
1999	Maffei et al[403]	Paediatric	19	Mean 13,209 ng/ mL ± 9,644 ng/ mL Range 184 - 31,412 ng/ mL	*S. pneumoniae* (9), *N. meningitidis* (5), *H. influenzae* type b (3), and *S. agalactiae* (2)
2010	Steinberg et al[404]	Paediatric	106	61.9 ±7.8 ng/L Range 37–135 ng/L	States BM caused mainly by *N. meningitidis*
2015	Dastych et al[405]	Adult	25	97.2 ng/mL 95% CI 92.3-100ng/ mL	*S. aureus* (8), Pneumococcus (8), *N. meningitidis* (4), *P. aeruginosa* (4), *E. coli* (3), and Meningococcus (2)

3.3.2.2 NPTXR

The relative abundance of Neuronal Pentraxin Receptor (NPTXR) in infected samples as measured by LC-MS/MS was statistically significantly lower ($p < 0.001$) in infected CSF samples than in uninfected CSF (Fig. 37).

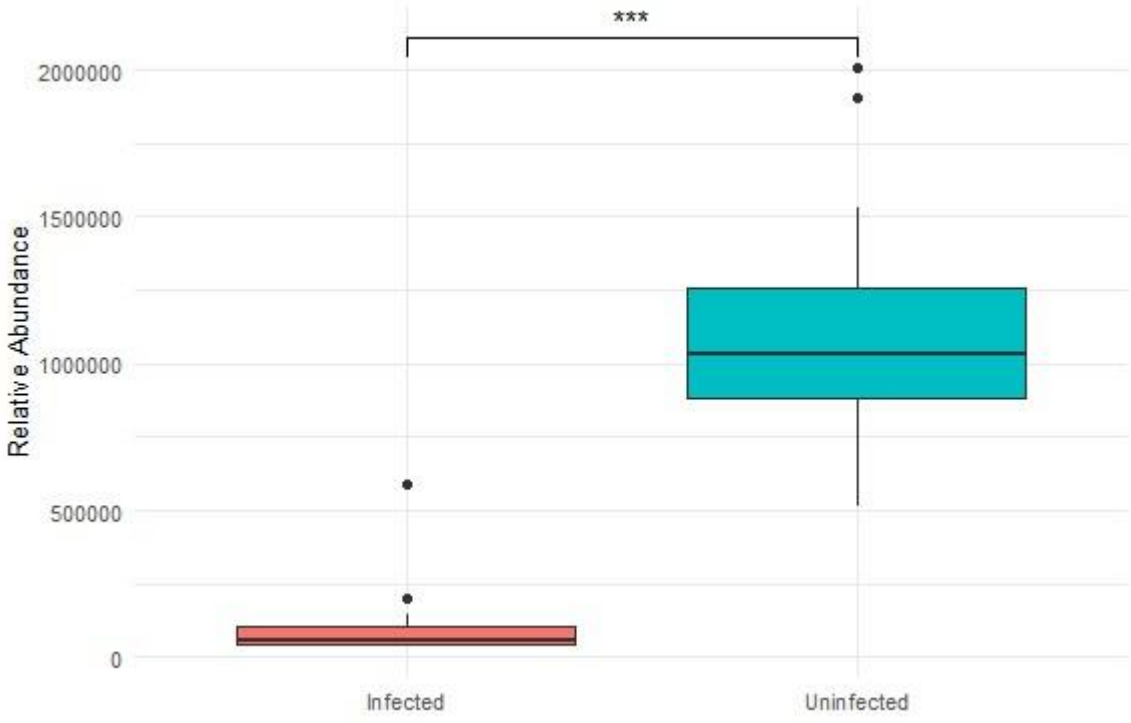

*Figure 36 NPTXR relative abundance as measured by LC MS/MS. *** p < 0.001.*

Pooled CSF Samples

Testing of pooled CSF for NPTXR using ELISA showed a similar relationship between infected and uninfected groups- NPTXR is in low abundance in infected CSF samples and in higher abundance in uninfected samples (p-value <0.01, Fig 38).

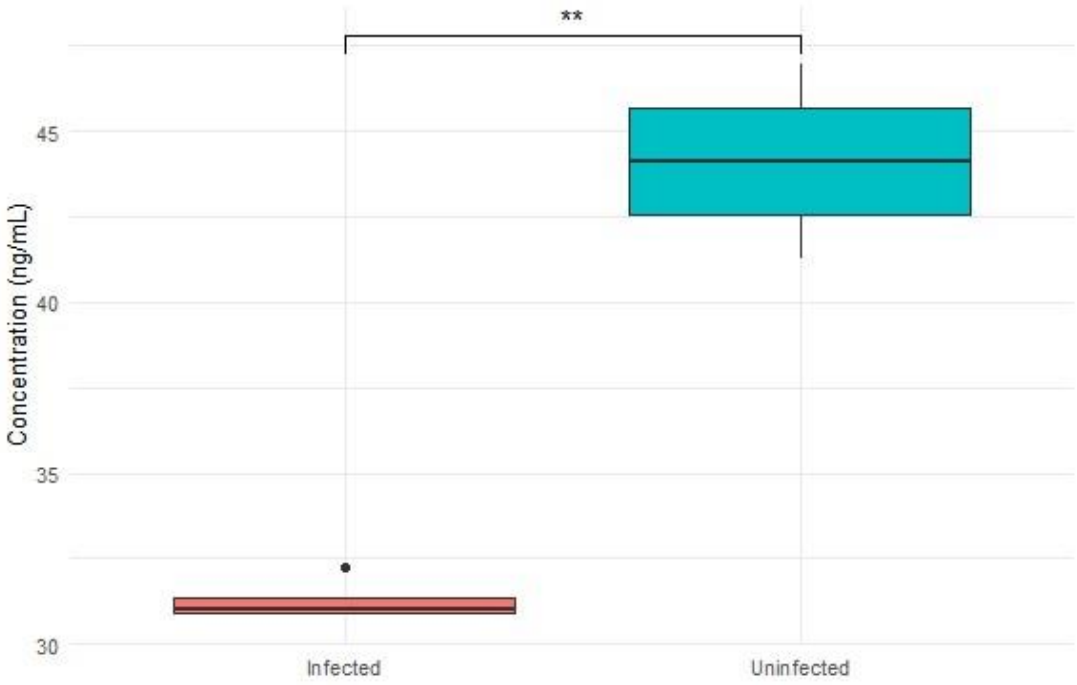

*Figure 37 NPTXR ELISA results of pooled CSF samples. ** P-value < 0.01. The mean concentration of NPTXR in the four different dilutions of CSF, corrected for dilution, was 31.27 ng/mL (range 30.83 - 32.26 ng/mL, SD 0.67) for infected samples and 44.11 ng/mL (41.25 - 46.96 ng/mL, SD 2.51) for uninfected samples. Welch Two Sample ttest statistic was -9.8715, df = 3.4181, p-value = 0.001248 (95% confidence interval: -16.71 - 8.97).*

Individual CSF Samples

Individual CSF samples tested with a NPTXR ELISA showed there was no difference in NPTXR concentration seen between infected and uninfected samples (Fig. 39).

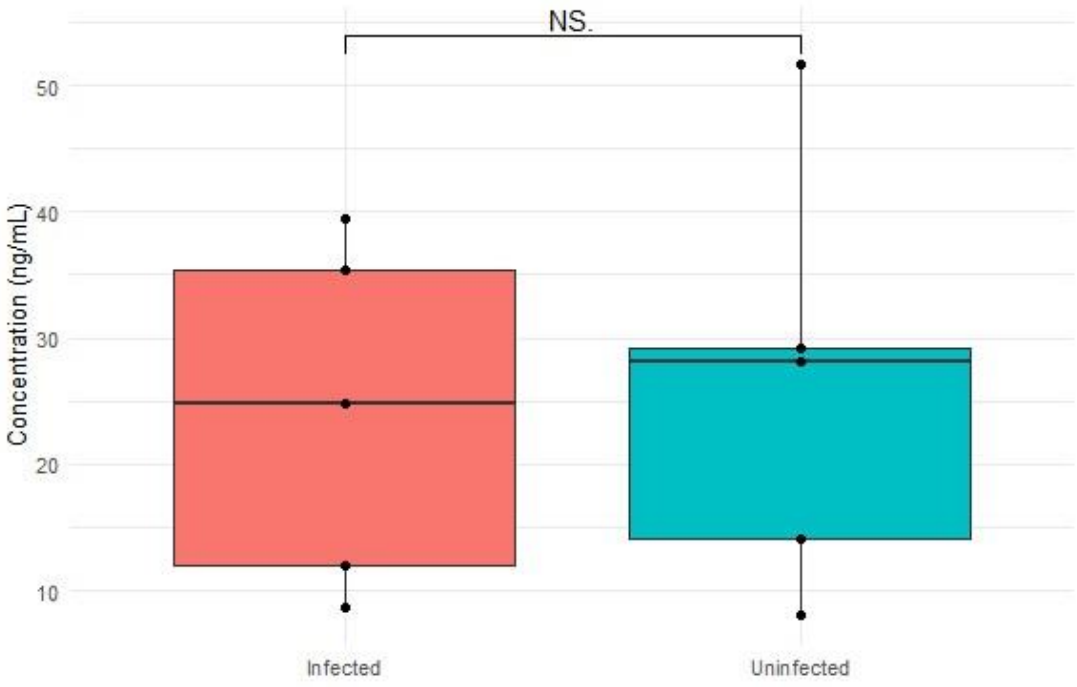

Figure 38 NPTXR ELISA results of individual CSF samples. NS= non-significant. The average NPTXR concentration for infected samples was 24.04 ng/mL (range 8.7 - 39.4 ng/mL, SD 13.65) whilst the average for uninfected samples was 26.21 ng/mL (range 8 - 51.69 ng/mL, SD 16.89). Welch Two Sample t-test statistic was -0.22302, df = 7.6634, p-value = 0.8293 (95% confidence interval: -24.73184 - 20.40024). Sample 2 (S. epidermidis infection) tested below the detectable range of the assay, though even when this result is excluded there is no statistically significant difference between infected and uninfected samples.

The relationship between the concentration of NPTXR in infected CSF and uninfected CSF was maintained between modalities but the individual CSF samples failed to show statistical significance (Table 40, Fig. 40).

Table 40 Summary of NPTXR LC-MS/MS, pooled sample ELISA and individual sample ELISA results

	LC-MS/MS		ELISA pooled (ng/ mL)			ELISA individual (ng/ mL)		
Infected	Low	***	Low	31	**	NS	24 ng/ mL (9-39)	NS
Uninfected	High		High	44ng/ mL		NS	26 ng/ mL (8-52)	

Discussion

Neuronal Pentraxin Receptor (NPTXR) showed the opposite of Lactoferrin, in that levels are low in infected samples and high in uninfected samples. NPTXR levels were low in infected sample analysis using LC-MS/MS, pooled sample ELISA and individual sample ELISA. In the LC-MS/MS one of the infected samples measured relatively highly and is seen as a point outlier on the boxplot of the data in Fig. 37. This sample was a *C. acnes* infection and whilst *C. acnes* is a skin commensal which is normally not seen as an invasive pathogen, it is encountered in neurosurgical SSI.

Pooled CSF samples had low NPTXR concentration in the infected CSF pool versus high concentration in the uninfected pool (Fig 38), p-value < 0.001. Testing of individual CSF samples did not yield results with a significant difference between infected and uninfected groups (Fig.39). Again, the average protein concentration for NPTXR was much lower for the individually tested samples in comparison to the pools.

Literature Review

In contrast to Lactoferrin, NPTXR has not yet been extensively studied in humans. It is a member of the evolutionarily conserved superfamily of proteins, the pentraxins (a key component in humoral innate immunity) [406].

Pentraxins share a conserved amino-acid sequence at the c-terminus and a “pentraxin domain” made up of similar 8 amino acid sequence. The N-terminal of the neuronal pentraxins is unlike other known human proteins [407]. There are two sub-families: short and long pentraxins. Short pentraxins include C reactive protein (CRP) and serum amyloid P component (SAP). NPTXR is a long pentraxin, included with neuronal pentraxin 1-4.

NPTXR is a ~53kDa protein composed of 500 amino acids and is mostly expressed in the brain. NPTXR is the only pentraxin that exists in at least one form that is anchored to the cellular membrane [408] in contrast to other pentraxins which serve as soluble pattern recognition molecules (PRM). These soluble PRMs are thought to be the functional ancestors of antibodies [406]. NPTXR has intracellular isoforms [409] and the transmembrane form can be enzymatically cleaved and released as a diffusible form [410].

Whilst the role of short pentraxins in human innate immunity is well documented, this has not been the case for long pentraxins [407]. NPTXR was only identified in 1997 [408] in

comparison to the short pentraxin CRP which was identified in 1930 [411]. The name is also misleading. NPTXR was initially named as a receptor due to the belief that it was the receptor for the other neuronal pentraxins. In fact, the neuronal pentraxins have not been shown to act primarily via NPTXR [412].

It is unsurprising given their expression in the brain that the neuronal pentraxins are involved in essential CNS roles: differentiation of pluripotent stem cells to neurons [413], synaptogenesis [414], synaptic plasticity and homeostasis [415, 416]. The breadth of function for neural pentraxins is being increasingly recognised. Their role in tumour progression is an area of great research activity [407] e.g. gastric cancer [417], neuroblastoma [418], and ependymoma [419].

NPTXR in recent years has emerged as a biomarker of interest for Alzheimer Disease [420425], Frontotemporal dementia [426-429] and dementia with Lewy bodies [357] mainly through proteomic analyses of CSF. It can thus be postulated that NPTXR may serve as a marker for neuroinflammation or damage, which would make its appearance in a proteomic analysis of infected and uninfected CSF logical- lower concentration levels of NPTXR are associated with Alzheimer Disease etc.

NPTXR is a relative newcomer in the biomarker world and the potential for cross reactivity of an ELISA to the common pentraxin domain is unknown but a possible confounder.

3.3.2.3 TIMP2

The relative abundance of Tissue Inhibitor of Metalloproteinases 2 (TIMP2) in the infected group was statistically significantly lower than the uninfected group ($p < 0.001$, Fig. 41).

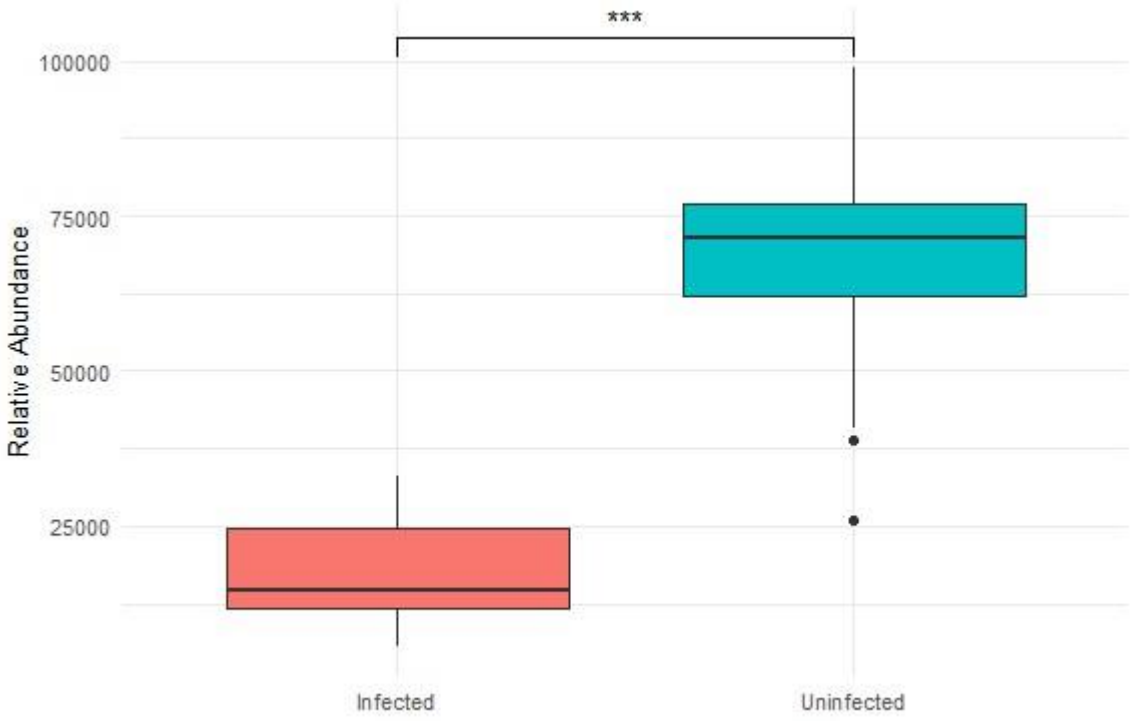

*Figure 39 TIMP2 relative abundance as measured by LC-MS/MS. *** P-value < 0.001.*

Pooled CSF Samples

ELISA testing of pooled CSF samples showed a reverse of the relationship seen in LC-MS/MS with higher concentration in infected CSF in comparison to uninfected CSF (Fig. 42), with a p value < 0.05.

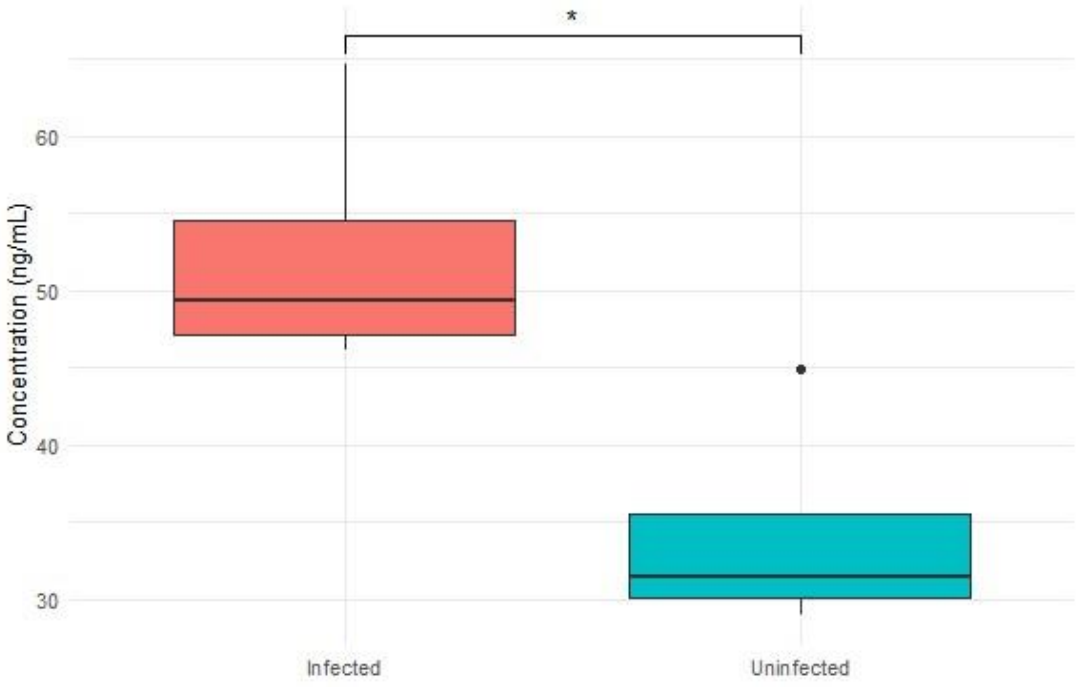

Figure 40 TIMP2 ELISA results of pooled CSF samples. P < 0.05. The mean concentration of TIMP2 in the four different dilutions of CSF, corrected for dilution, was 52.4 ng/mL (range 46.1 - 64.7 ng/mL, SD 8.46) for infected samples and 34.2 ng/mL (29 - 44.95 ng/mL, SD 7.3) for uninfected samples. Welch Two Sample t-test statistic was 3.2469, df = 5.8737, p-value = 0.01807 (95 percent confidence interval: 4.399 - 31.9).

Individual CSF Samples

Individual CSF samples underwent ELISA testing, infected CSF samples had higher concentrations overall, in comparison to the uninfected CSF samples but this was not statistically significant (Fig. 43). This experiment was performed twice- the samples were tested in duplicate, with one set having a protein digestion step performed prior to analysis with ELISA. This data is not included here as the protein digestion appears to have interfered with the ELISA (data in Appendix A). The data for the non-digested samples are presented here.

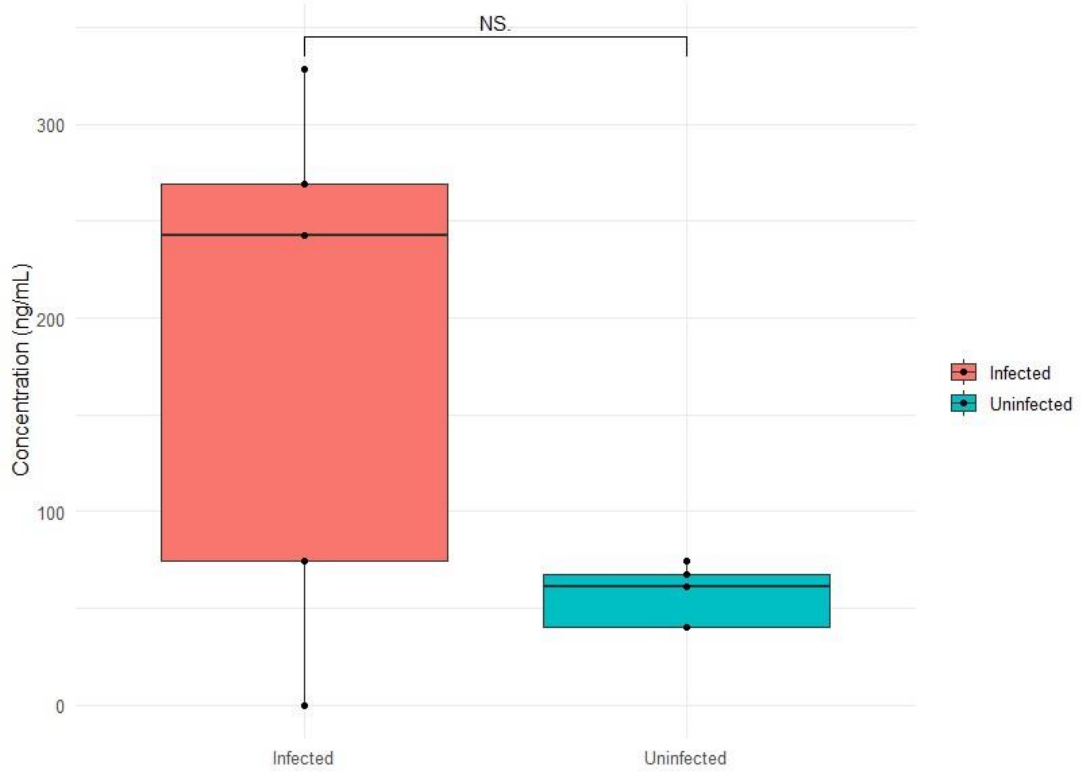

Figure 41 TIMP2 ELISA results of individual CSF samples, Experiment 1. The mean TIMP2 concentration in the infected samples was 182.99 ng/mL (range 0 - 328.6 ng/mL, SD 139.1). The mean for uninfected samples was 56.63 ng/mL (range 39.94 - 74.65 ng/mL, SD 16). There was no difference between infected and uninfected CSF samples statistically. Welch Two Sample t-test statistic was -0.95132, df = 7.4051, p-value = 0.3715 (95% confidence interval: -100.963 - 42.6 ng/mL).

The ELISA testing of individual CSF samples did not show a significantly different concentration of TIMP2 in infected versus uninfected samples (Table 41, Fig. 44). The TIMP2 protein concentration decreased between the two experiments using individual CSF samples (performed on separate days).

Table 41 Summary of TIMP2 results (Inf=Infected samples, Uninf=Uninfected samples, Exp1=Experiment 1, Exp2=Experiment 2,)

	LC-MS/MS		ELISA pooled			ELISA individual Exp1		
Inf	Low	***	High	52	*	Low	130 (78-222)	NS
Uninf	High		Low	34		High	159 (111-212)	

ELISA individual Exp2		
High	37(0-66)	NS
Low	11(8-15)	

Discussion

In LC-MS/MS analysis the relative abundance of TIMP2 was significantly lower in infected CSF in comparison to uninfected CSF, $p < 0.001$ (Fig. 41). This relationship was reversed in the ELISA results for pooled CSF (p-value < 0.05, Fig. 42).

It is peculiar that the relationship of the concentration of TIMP2 reversed between experiment 1 and experiment 2 (Table 41). It may be that the degradation/digestion of proteins in the CSF was occurring at different rates.

Literature Review

Tissue Inhibitor of Metalloproteinases 2 (TIMP2) protein is one of the four known TIMPs- tissue inhibitor of metalloproteinases. Metalloproteinases (MMPs) are enzymes that break down proteins important in the degradation of the extracellular matrix (ECM). TIMPs are thought to be the main regulators of MMPs during tissue remodelling [430]. Without regulation of their activities MMPs can cause extensive tissue damage.

TIMP2 was first identified in 1989 [431].It is a 21kDa unglycosylated protein. TIMPs are being increasingly recognised for functions beyond inhibition of MMPs, influencing apoptosis, angiogenesis, and cell proliferation. They have roles in oncogenesis which are complex and often contradictory. TIMPs angiogenic effects are known to be independent of MMPS [432].

The role of MMP and TIMPs in the degradation of the ECM prompted an explosion of interest in their significance in tumour invasion and metastasis in the 1990s onwards. In vitro studies showed inhibition of tumour cell invasion by TIMP2 [433, 434].There were high hopes for inhibitors of MMPs for cancer therapeutics but to date, this hasn't been a fruitful area [435], likely reflecting the complexity of the system of proteins that are involved with ECM.

TIMP2 has received attention in the last decade as a biomarker of acute kidney injury (AKI). This has led to it being studied in postoperative surgical patients [436-439], intensive care

unit patients [440-442] and as marker of delayed graft function in kidney transplant patients [443, 444]. This increase in TIMP2 is not a product of dead/dying cells as the gene expression of TIMP2 in urinary sediment (i.e. dead cells sloughing from the renal tubules) does not correlate with urinary TIMP2 concentration [445].

In neuroinflammatory disorders like multiple sclerosis, TIMP2 has been found to be elevated in the monocytes of patients- this TIMP2 acts with MMP14 to activate MMP2 and in doing so drives neuroinflammation [446]. MMPs are known to be involved in the disruption of the BBB and it has been shown experimentally that intraventricular administration of TIMP2 in an animal model (rat) can counteract this [447]. This knowledge in addition to the known role of MMPs and TIMPs in neuroinflammation has led to TIMP2 being explored in meningitis (in concert with the other MMPs and TIMPs).

Image analysis of post-mortem brain tissue from five bacterial meningitis cases, five viral meningitis cases and five controls showed a strong positive signal for MMP-9, TIMP1 and TIMP2 in leukocyte infiltrates in the thickened meninges of bacterial meningitis and viral meningitis cases [448].

Leppert et al examined the MMP and TIMP concentrations in a retrospective paediatric study of bacterial meningitis and controls in 2000, this showed >2.5 - fold increase in the MMP-9 concentration in CSF from patients who suffered long term neurological sequelae.
There was no difference in expression of TIMP2 seen between infected and control groups. The complexities of the MMP-TIMP network were commented on in this paper, manufacturers of their ELISAs informed investigators that TIMP1 is known to form heterodimers with MMP-9 and MMP-8 (The authors had been surprised to not be able to detect MMP-8 in bacterial meningitis CSF samples) [449]. Any study of a single TIMP/MMP is therefore complicated by the highly dynamic nature of this network/cascade of proteins.

Metalloproteinases and their inhibitors have been studied in South Africa in paediatric tuberculous meningitis, which is a severe form of Tuberculosis (TB) and significant issue in parts of the world where TB is endemic. Of interest in this study, CSF samples were taken from the ventricles of patients and from LP, thus allowing the comparison of TIMP2 concentrations in each site and with blood samples. TIMP2 was highest in serum, felt to reflect the systemic response to TB, but of particular interest to my study is the fact that TIMP2 concentration was seen to be higher in lumbar CSF than in ventricular CSF (Fig. 45) [450].

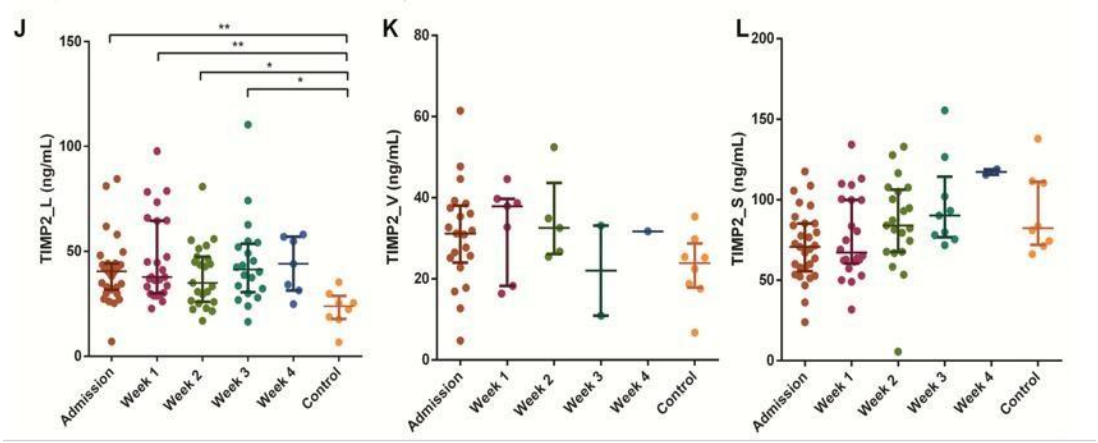

Figure 42 TIMP2 concentration in (J) Lumbar CSF, (K) Ventricular CSF and (L) Serum from paediatric TB meningitis cases and controls, adapted from Li et al 2019 [450]. Note the scale of the Y axis changes depending on the site of sampling.

3.3.2.4 IGF2

The relative abundance of insulin-like growth factor 2 (IGF2) in infected samples as measured by LC-MS/MS was statistically significantly lower than that measured in uninfected samples ($p < 0.001$, Fig 46).

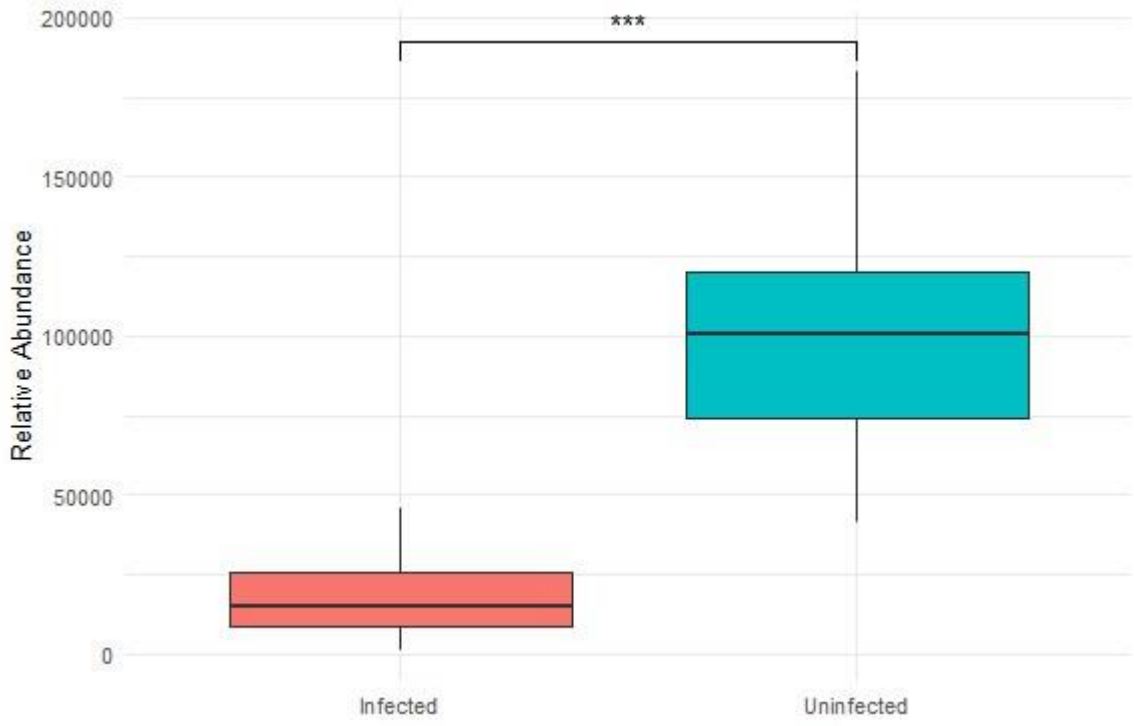

*Figure 43 IGF2 relative abundance as measured by LC MS/MS. *** P-value < 0.001.*

Pooled CSF Samples

ELISA testing of pooled CSF samples showed the infected pool had a significantly higher concentration of IGF2 than the uninfected pool (p-value<0.01, Fig. 47).

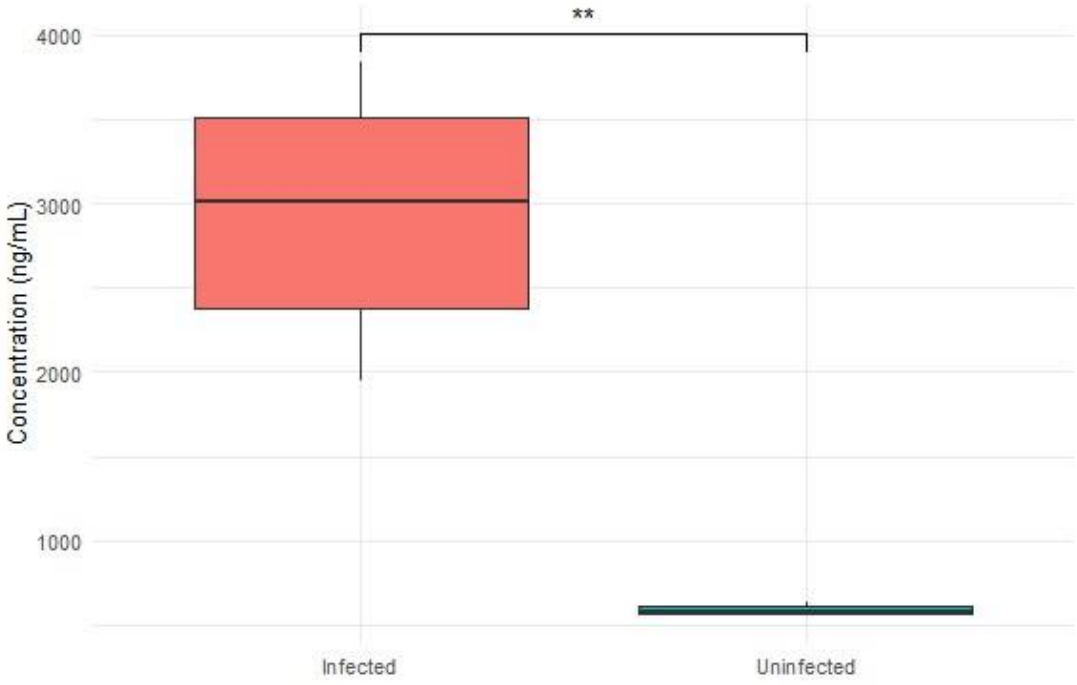

*Figure 44 IGF2 ELISA results of pooled CSF samples. ** P-value < 0.01. The mean concentration of IGF2 in the five different dilutions of CSF, corrected for each dilution, was 2,937.3 ng/mL (range 1,944.5 - 3,843.2 ng/mL, SD 783.96) for infected samples and 592 ng/mL (range 562.5 - 638.5 ng/mL, SD 34.21) for uninfected samples. Welch Two Sample t-test statistic was 6.6832, df = 4.0152, p-value = 0.002571 (95% confidence interval: 1,372.5 - 3,318.2).*

Individual CSF Samples

Individual infected CSF samples are higher in IGF2 concentration than the uninfected samples, but this failed to reach significance (p-value 0.078, Fig. 48).

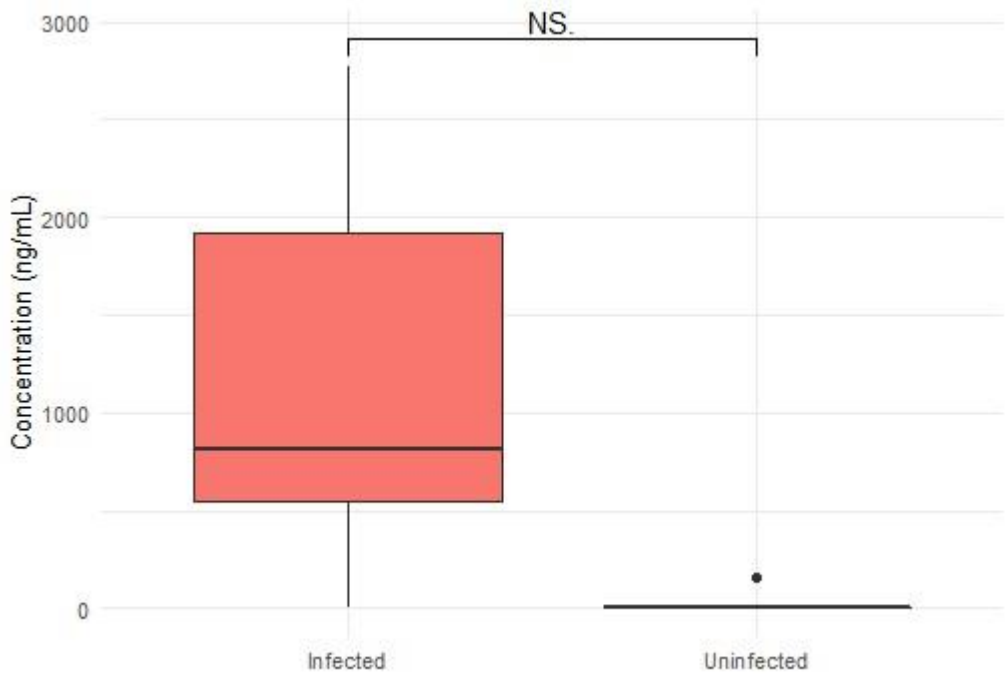

Figure 45 IGF2 ELISA results of individual samples

*Table 42 Summary of IGF2 results. LC-MS/MS, ELISA pooled (results of ELISA using pooled infected samples and pooled uninfected samples), ELISA individual (results of ELISA using individual samples from the pools of infected and uninfected samples), mean conc. ng/mL (mean concentration measured in ng/mL). *** p < 0.001, ** p < 0.01, N.S. = non-significant.*

	LC-MS/MS		ELISA pooled CSF mean conc. ng/mL(range)			ELISA individual CSF mean conc. Ng/mL(range)		
Infected	Low	***	High	2,937 (1,945-3,843)	**	High	1,210 (0-2,771)	N.S.
Uninfected	High		Low	592(563-639)		Low	30.68 (0-153.4)	

Discussion

Insulin-like growth factor 2 (IGF2) in the LC-MS/MS data showed high relative abundance in infected samples in comparison to the uninfected samples ($p < 0.001$) (Fig. 46). This relationship was reversed when pooled samples were tested with ELISA (Fig. 47).

The individual CSF samples showed higher concentrations in the infected samples (mean concentration 1,210 ng/mL, range 0 – 2,771 ng/mL) and lower concentrations in the

uninfected group (mean 30.68 ng/mL, range 0 - 153.4 ng/mL) (Fig. 48, Table 42). Yet again, the mean concentration of the infected group is less than half of the concentration of the infected pool and the uninfected group mean is a fraction of the concentration measured in the uninfected pool.

The IGF2 concentrations of the individual samples visually appear to be significantly different between groups (Fig. 48). The data is skewed again by sample 2 in the infected group, which has undetectable IGF2. In addition, sample 9 was the only uninfected sample to have a measurable IGF2 concentration. Sample 9 was a CSF sample taken at shunt insertion, but the cell count was not entirely normal (WCC = 4, RCC = 304).

Literature Review

IGF2 is a circulating peptide growth factor hormone that is important for normal development and growth [451]. As the name implies it has much in common with insulin, in fact it shares 47% of the same amino acid sequence [452]. IGFs are synthesised in most tissues, though circulating serum IGF2 is mainly produced in the liver [453].

Mature IGF-2 is a 67 amino acid (7.5 kDa) monomeric protein which has both autocrine and paracrine effects and has been implicated in many malignancies [454]. It has been found in CSF [455] and is known to be secreted by the choroid plexus [456]. Neither a PubMed nor a Scopus search for “IGF2” and “meningitis” yielded any academic literature on the subject.

3.3.2.5 NEGR1

The relative abundance of Neuronal growth regulator 1 (NEGR1) in infected samples as measured by LC-MS/MS was statistically significantly lower than the uninfected samples (Fig. 50).

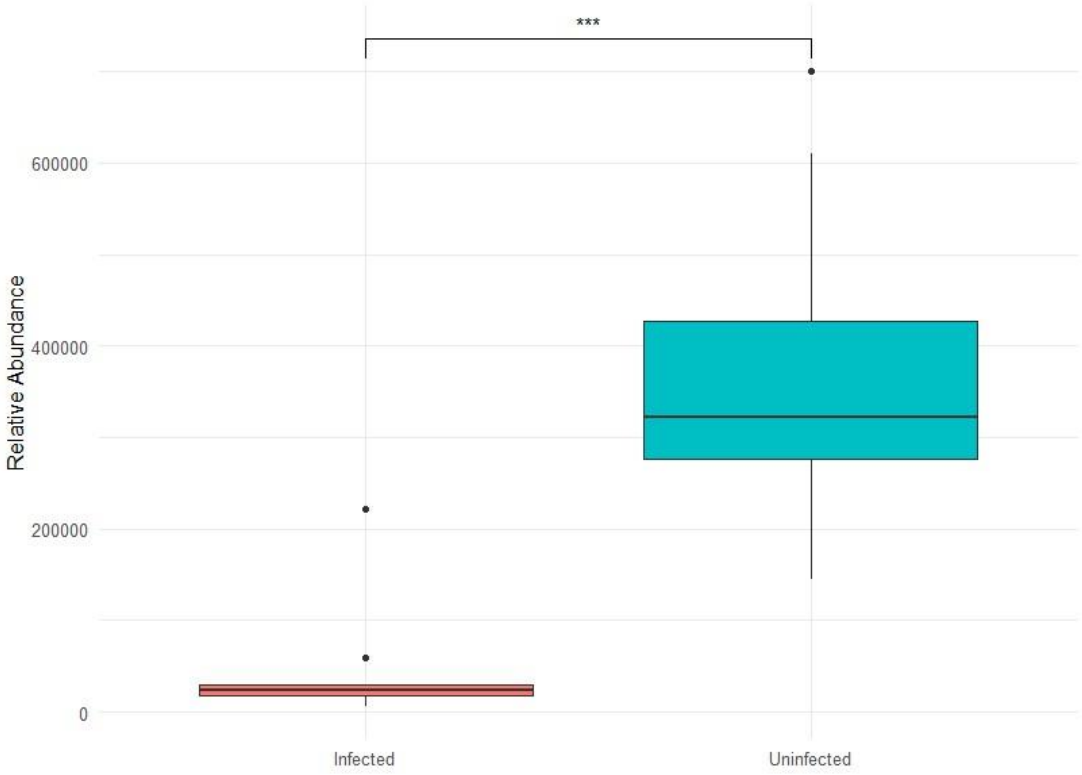

*Figure 46 NEGR1 relative abundance as measured by LC MS/MS. *** P-value < 0.001.*

Pooled CSF Samples

NEGR1 concentration was higher in infected CSF than in uninfected CSF but was only measurable in the 1/10 dilution of CSF pools for both groups and in the 1/20 dilution in the infected group only. Thus, the comparison failed to reach statistical significance (Fig. 51).

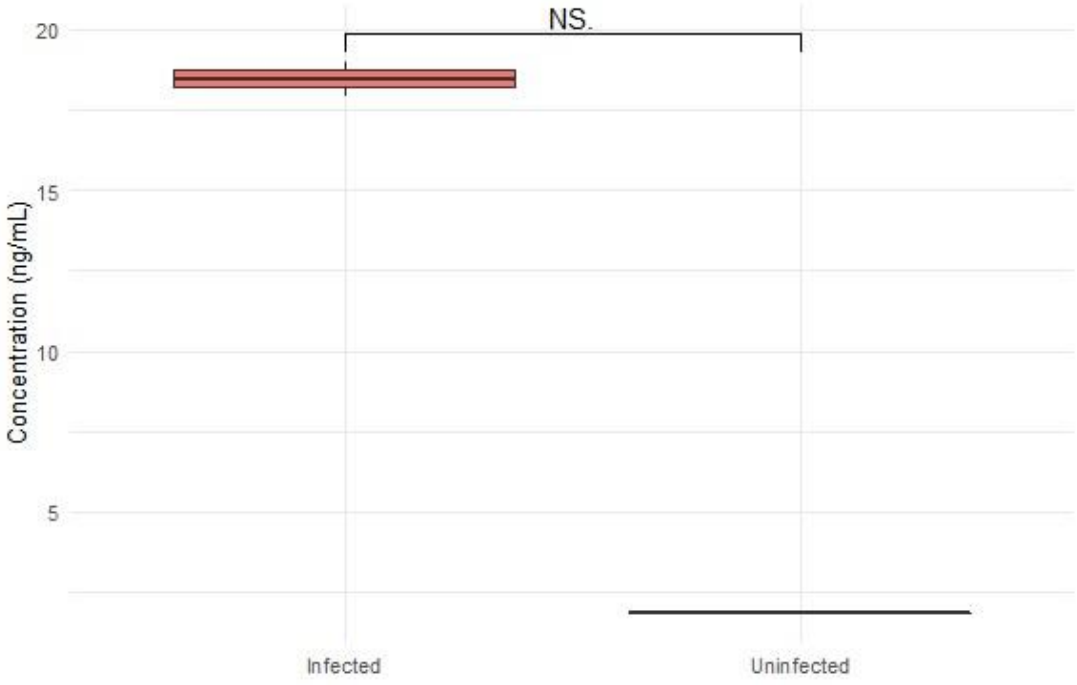

Figure 47 NEGR1 ELISA results of pooled CSF samples. NS: non-significant. The mean NEGR1 concentration, adjusting for dilution, of the infected pool was 18.5 ng/mL (17.9 - 19 ng/mL). In the 1/10 dilution of the uninfected pool the NEGR1 concentration was 1.8 ng/mL.

Individual CSF Samples

There was not a significant difference between groups when individual CSF samples were tested for NEGR1 concentration (Fig. 52).

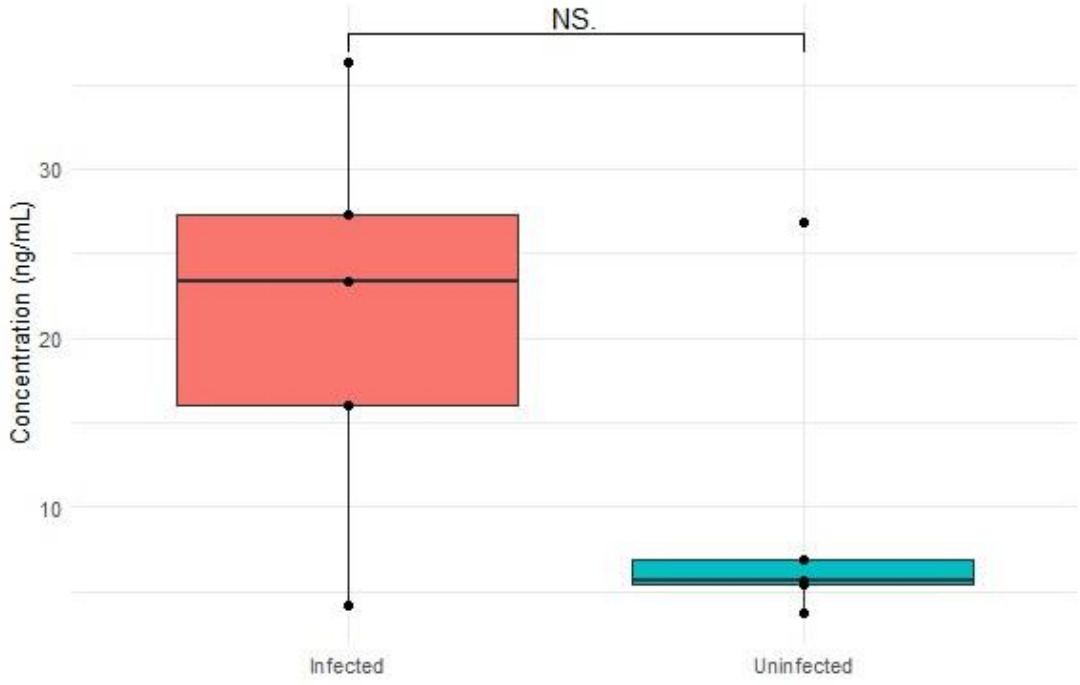

Figure 48 NEGR1 ELISA results of individual CSF samples. NS: non-significant.

The mean NEGR1 concentration of the individually tested infected samples was 21.4 ng/mL (range 4.2 - 36.3 ng/mL, SD 21.43) and the mean for uninfected samples was 9.7 ng/mL (range 3.7 - 26.8 ng/mL, SD 9.69).

T-test statistic was 1.6974, df = 7.6177, p-value = 0.13 (95% percent confidence interval: -4,351.259 - 27,838.459). Sample 2 (infected) was detected, the concentration measured was 4.2 ng/mL and Sample 9 (uninfected) measured 26.8 ng/mL.

Neither the pooled nor individual CSF samples ELISAs produced statistically significant results (Fig 51, 52, Table 43).

Table 43 Summary of NEGR1 results

	LC-MS/MS		ELISA pooled CSF mean conc. ng/mL(range)			ELISA individual CSF mean conc. ng/mL(range)		
Infected	Low	***	High	18.5 (17.9 - 19)	N.S.	High	21 (4-36)	N.S.
Uninfected	High		Low	1.8		Low	10 (4-27)	

Discussion

Relative abundance of Neuronal growth regulator 1 (NEGR1) was statistically lower in infected samples in comparison to uninfected samples in LC-MS/MS data ($p < 0.001$) (Fig. 50). The ELISA-measured concentration of NEGR1 in pooled CSF saw a reversal of the LCMS/MS relationship (Fig. 51). Testing of the individual CSF samples, like pooled samples showed higher concentrations in the infected CSF group in comparison to the uninfected group but the ranges of values for the two groups overlapped significantly (Fig 52, Table 43). Sample 2 was measurable in this experiment, 4.2 ng/mL, but was the lowest measurement

in the infected group. Within the uninfected group Sample 9 was again an outlier, measuring 26.8 ng/mL (the highest uninfected sample value).

Literature Review

NEGR1 was initially called Kilon (a **Ki**ndred of Ig**LON**) when it was first described in a mouse model by Funatsu et al in 1999 [457]. Marg et al called it neurotractin in their 1999 paper describing its increased expression during embryonic chick brain development, its persistence in the adult chick brain and its role in regulating neurite overgrowth [458].
Schäfer et al settled its human orthologue nomenclature as Neuronal growth regulator 1 (NEGR1) whilst further investigating its role in CNS regeneration after injury in another mouse model [459].

NEGR1 is a 46kDa glycosylphosphatidylinositol-anchored cell adhesion molecule and a member of the IgLON cell adhesion molecule family, a subfamily of the immunoglobulins [460]. NEGR1 is best known as a gene of interest for obesity, a meta-analysis of 15 genome wide association studies for body mass index (BMI) identified it as one of fourteen candidate genes [461]. NEGR1 has been repeatedly implicated in mental illnesses[462] like major depressive disorder[463-465], bulimia nervosa [466], and autism [467]. It shows significantly increased concentrations in Parkinson's disease [468].

3.3.2.6 Proteins that were not detectable by ELISA

Four proteins were further investigated with ELISAs using the pooled infected and uninfected CSF samples. These ELISAs worked (protein standard dilution series was detectable) but all sample measurements fell below the limits of the standard curve. These were FCGR3A, VGF, SCG2 and SCG5 (Fig. 54).

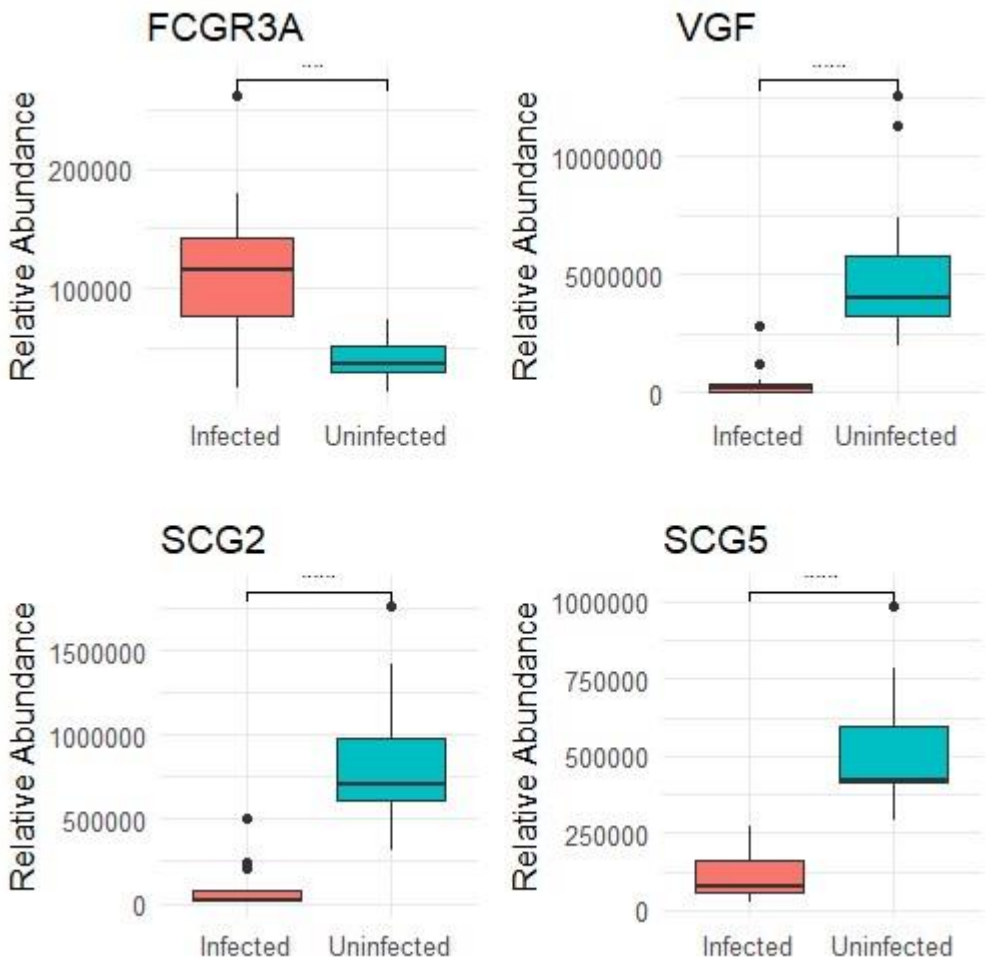

Figure 49 Relative abundance as measured by LC-MS/MS of FCGR3A, VGF, SCG2, and SCG5.

Table 44 Summary of protein concentrations as measured in LC-MS/MS versus ELISA.

	Status	LC-MS/MS	Pooled	Individual
LTF	Infected	High	High	High
	Uninfected	Low	Low	Low
NPTXR	Infected	Low	Low	Low
	Uninfected	High	High	High
TIMP2	Infected	Low	High	High
	Uninfected	High	Low	Low
IGF2	Infected	Low	High	High
	Uninfected	High	Low	Low
NEGR1	Infected	Low	High	High
	Uninfected	High	Low	Low

3.4 Discussion

To my knowledge, this is the first exploration of *neurosurgical CSF* for the discovery of biomarkers for *infection using proteomics*. Confident identification of *all* proteins present in these CSF samples is not possible with current technologies and indeed was not the aim of this project. The vast dynamic range of concentrations of different proteins and the size differences between proteins makes identification of all proteins in a sample impossible currently.

By identifying 683 differentially expressed proteins, ample data was provided to mine for potential biomarkers of infection. And whilst the numbers of samples analysed were not large (13 infected and 19 uninfected) they are comparable with exploratory proteomic analyses of bacterial meningitis CSF in the literature (see Table 45).

Protein analysis of clinical CSF will analyse all proteins in a sample including any from a pathogen. My focus was host protein response, but one could wonder whether bacterial proteome could impact on data. *Gomez-Baena et al* showed that even in cases of acute pneumococcal meningitis the increased protein load within the CSF of cases due to pathogen is no more than 0.001% to 0.1% of the total pool [461] and given that we did not deplete our samples of highly abundant proteins it is unlikely that bacterial proteins would have been present in high enough concentrations to be identified confidently.

Table 45 Literature review of proteomics and meningitis. BM=bacterial meningitis. 2D DIGE= Two-dimensional difference gel electrophoresis).MALDI-TOF= matrix-assisted laser desorption/ionization - time of flight. 2DPAGE=two-dimensional polyacrylamide gel electrophoresis. SWATH-MS=Sequential window acquisition of all theoretical fragment ion spectra- mass spectrometry..

Author & Year	***No. of BM cases***	***No. of proteins identified***	***Notes***
Jesse *et al* *2010* ***[469]***	*28*	6	2D DIGE produced ~2500 spots, MALDI-TOF used to ID proteins
Goonetilleke et al 2010 **[470]**	*20*	34	2D PAGE produced ~2500 spots, MALDI-TOF used to ID proteins
Cordeiro et al 2015 **[471]**	12	117	
Njunge et al 2017 **[472]**	37	52	
Gomez-Baena et al 2017 **[473]**	16	112-454	All BM involved *S. pneumoniae*

Thanh et al 2020 **[474]**	10	1012 729 specific for BM	7 *S. suis* 3 *S. pneumoniae*
Wall et al 2020 **[475]**	57	336	All BM involved *S. pneumoniae*
Bakochi et al 2021 **[476]**	35	771	17 *S. pneumoniae* 5 *N. meningitidis* 3 *S. aureus* SWATH-MS used to ID proteins

It was surprising not to find the three biomarkers discussed in Chapter 1 (lactate, procalcitonin, CRP) in these samples as all three are common proteins and we know from the literature that they are present in CSF (see chapter 1 section 1.6.1). One factor that may account for this is that these are large proteins that require longer periods of protein digestion to allow for identification by LC-MS/MS. According to the SMART digest manual, CRP requires 240 minutes of protein digestion, whereas we allowed only 60 minutes of incubation for protein digestion (as per the TDI standard operating procedure).

The protein candidates chosen from the LC-MS/MS data analysis were further explored using enzyme linked immunosorbent assays (ELISA). Candidate proteins which emerged in top scoring pairs (TSP) or triplets (TST) from relative expression analysis which were known to be expressed in the brain or which were related to infection or inflammation were shortlisted for further investigation. Each of the proteins within a TSP are discriminatory for infection status. The aim of combining elements of different TSP/TST is to create a panel of markers that can reliably and reproducibly discriminate infection status.

Due to time and financial constraints of a PhD project, it was decided to narrow the selection to proteins where there were ELISA kits are available commercially. This saved time on designing bespoke ELISAs that would require further optimisation before use. Also given the restricted volumes of neurosurgical CSF samples (especially infected CSF) available for testing, it was felt best to use ELISAs that were commercially established.

The proteins brought forward for ELISA were tested first on pooled CSF samples to make testing and optimisation of sample preparation possible for the nine assays. Using pooled

samples has limitations, in that it can and will mask outlier samples which can in turn make a potential marker look more discriminating than it really is for the disease under scrutiny.

Pooled CSF was tested using a range of dilutions to establish the optimal dilution for an assay. Four of the proteins tested on pooled CSF measured below the limits of the assay. FCGR3A, VGF, SCG2, SCG5 when tested on a range of dilutions proved to have undetectable concentrations of the target protein and were not re-tested on individual samples. All the ELISAs used were the highest sensitivity assays available at the time of testing.

There were two proteins that retained the same pattern of concentration in infected compared to uninfected CSF in ELISAs versus proteomic analysis (Lactoferrin and NPTXR). Three proteins (TIMP2, IGF2 and NEGR1) showed discordant results in pooled CSF ELISA analysis in comparison to the relationship seen between infected and uninfected samples in LC-MS-MS analysis.

There are many factors that can affect proteomic analyses. Klont et al, in "Proteomics for Biomarker Discovery: Methods and Protocols", argue that factors impacting on variability in biomarker discovery fall into 2 groups; pre-analysis factors (i. sample type, ii. biological variability, iii. sampling site, iv. sample storage, v. sample processing) and post-analysis factors [477].

Pre-analysis factors

i. Sample type

CSF is an ideal tissue to use in proteomics as it is a paucicellular fluid. It does not suffer to the same extent from the problems encountered with, say, blood. Proteomic analysis of blood is complicated by the dominance of albumin and other large proteins and identifying proteins in proportionally smaller concentrations is difficult. As previously mentioned, CSF has been estimated to contain 1/200th the protein content of whole blood [339].

CSF is known to reflect the state of neurons and glial cells, with up to 30% of CSF proteins thought to be derived from the brain specifically [478, 479]. Whilst in most clinical settings CSF is rarely sampled; in neurosurgery it is very regularly included in routine testing. CSF is quite easily sampled from a shunt reservoir as seen in section 1.5.4.6 of Chapter 1. It is therefore not unreasonable to use it for biomarker discovery and development.

ii. Biological variability of CSF

None of the putative biomarkers identified here discriminated between infected and uninfected CSF with statistical significance when tested on individual CSF samples. This is likely due to the small numbers of samples used. Except for NPTXR, the proteins tested visually appear as though they are differentially expressed in infection. With the small numbers of samples, outliers have a greater effect.

It is already appreciated that some bacteria cause a more pronounced cellular reaction in the CSF than others. The community acquired meningitides (*S. pneumoniae, N. meningitidis, L*. monocytogenes etc.) cause a pronounced neutrophilia whereas *C. acnes* rarely causes this. *S. epidermidis* and *C. acnes* are indolent infections that grow slowly over time and evade the immune system in the CNS. The spectrum of proteomic expression can be assumed to vary (possibly significantly) from pathogen to pathogen. In testing such a relatively small number of samples with a range of infecting bacteria a confounding variable was added.

With such small numbers of samples, it could have been more useful to focus on one or two common bacteria in neurosurgical CSF infections to reduce this variability. On a practical level that would have extended the time needed to collect adequate sample numbers to complete the experiments.

Ultimately any test for neurosurgical CSF infection will be applied to samples that could have any number of causative pathogens. For biomarkers to be of use in the neurosurgical setting, they need to differentiate infected from uninfected samples even in the setting of an indolent bacteria. If many hundreds/thousands of samples were available and tested it may be the case that the differential signal of putative biomarkers may shine through more clearly or flatten out. For examples, did sample 2 just not have detectable levels of Lactoferrin, NPTXR and IGF-2 or was that sample mishandled in the laboratory before storage (left on the scrub trolley in theatre for hours before transport to the laboratory?).

There are known age and gender specific differences in protein content of CSF [480]. CSF shows circadian variations in production [481] and the concentration of protein is known to decrease with advancing age [482]. These factors were not considered in this study as this information was not included in the data attached to the salvaged CSF samples. We can say that all the samples used in this chapter were taken from adults, but any further analysis of age as a confounder is not possible.

iii. Sampling site

As mentioned in Chapter 1, CSF is normally sampled via lumbar puncture in nonneurosurgical settings. In neurosurgical patients a lumbar puncture may be used, but if there is an indwelling CSF drain or shunt these will often be used instead. Neurosurgery is the only specialty to *commonly* sample ventricular CSF.

It can be seen in the heat map of the LC MS/MS proteomic data that there is a clear difference between the groups of samples tested. There are a couple of potential reasons for this difference. The effect of infection on the production of proteins and peptides is one and obviously this is the hypothesis we were testing. A potential confounding reason for the difference in the protein profiles of these groups is the site of CSF sampling. The CSF samples used for the non-infected group were all collected via lumbar puncture. In contrast, the infected samples were all ventricular CSF which were sampled either during a shunt surgery or via an EVD.

As outlined in the Chapter 1, section 1.3.2, CSF is produced mainly by the choroid plexus in the lateral ventricles, it circulates around the brain and spinal cord and is resorbed. It has been noted that the constituents of CSF vary slightly by site with some components having a rostro-caudal gradient [483]. This was seen in the South African study of TIMP2 in TB meningitis where lumbar CSF had higher concentrations of TIMP2 than ventricular (cranial) CSF (Fig. 46, section 4.4.2.2) [450].

The reality of the rostrocaudal protein gradient has been seen in other studies where successive portions of CSF sampled by lumbar puncture were analysed for protein content. The initial CSF withdrawn by LP showed the highest protein concentration, and this progressively declined as further volumes were withdrawn and analysed, with the later fractions being felt to be more representative of ventricular CSF [484]. There is no method to allow for this disparity or to assess the extent of the effect of the rostrocaudal gradient on the proteomic profile from our LC-MS/MS analysis, but it needs to be considered when planning future experiments and analysing results.

Another potential confounder is RCC contamination. Blood is not normally found in CSF.

Many authors recommend excluding CSF samples with RCC over 500 cells per mm^3 [485, 486] when storing CSF for research. Six of the CSF samples used for the LC-MS/MS experiment had RCC > 500 (Table 33, section 4.2.1), five of which were infected samples. Only Sample 5 (infected) of the CSF samples used for ELISA testing had a RCC > 500.

Traditionally it is taught that up to 20% of lumbar punctures for CSF sampling result in a "traumatic tap" [487-489]. This is where the CSF is bloody due to bleeding from the venous plexus in the spinal canal. More recent reports of traumatic tap rates are lower, ~10% and this rate falls to 3.5% for fluoroscopy-guided(x-ray guided) lumbar punctures [490]. The rate of traumatic taps is also dependent on operator experience and frequency of performing lumbar punctures [491].

There is no universally applied definition of a traumatic tap. It may be visibly blood tinged to the human eye or a red cell count limit may be applied (> 400/ > 500/ > 1000 RCC/mm^3) [488, 490, 492]. It is essential that analysis of samples is possible with bloody CSF samples.

Postoperatively it is not unusual for there to be RCC in the CSF. For any marker to be of utility in clinical practice it needs to be detectable even in bloody CSF.I could have excluded bloody samples from the proteomic analysis, as this step was always a discovery phase where the technique used is highly unlikely to be applied in daily practice but for any protein to function as a useful biomarker in clinical practice it needs to be measurable in bloody samples (which are frequently encountered in neurosurgical practice)

iv. Effect of storage

Ideally all testing would be done prospectively using fresh CSF, but this is highly impractical due to the nature of neurosurgical CSF infections (presenting at all hours of the day and night and being relatively infrequent events). It is therefore necessary to store CSF samples before experiments can be carried out.

It is known that there is a loss of protein via adsorption to storage containers- in Alzheimer's disease research an estimated 5% of beta amyloid is lost to adsorption per transfer of sample from one container to another [493]. Proteins also degrade over time when stored at -20 °C or when samples go through multiple freeze-thaw cycles [339]. This effect has been significant in the past. A truncated form of a protein cystatin C was identified as a potential biomarker in Alzheimer's disease but later it was shown that

cystatin C is cleaved when stored at -20 °C even after two months (This effect was not seen when CSF was stored at -80 °C). Truncated cystatin was therefore an artefact of storage related degradation and erroneously identified in proteomic studies [494].

Upon thawing, protein degradation is a fact of life for all biological samples. CSF is known to contain proteases and indeed the protease profile of CSF is very similar to that seen in serum [495]. With the protein content of CSF being a fraction of that in serum, the effects of proteases on the protein profile of CSF over even relatively short periods of time could be considerable. Some have suggested that protease inhibitors should be added to samples prior to storage but *Zhang et al* notes that many current protease inhibitors are known to have effects on sample analysis- e.g., aprotinin affects sample MS spectra for unknown reasons [496]. The Human Proteome Organisation (HUPO) ,an international consortium established in 2002 [497], which has attempted to establish consensus guidelines- the Proteomic Standards Initiative (PSI) [498], make no recommendation regarding protease inhibitors. Thus the strategy used in this study, of aliquoting CSF samples in LoBind tubes, storing them at - 80 °C and minimising freeze-thaw cycles is very much in keeping with international practice [339].

v. Sample processing

On reviewing the initial results of these pooled sample ELISAs, one thought that came to shape further testing was the role sample protein digestion may have had. Within the LCMS/MS proteomic analysis protocol in TDI, University of Oxford, there is always a protein digestion step. This is rather rigorous, using a heat stabilised lysozyme and incubating the sample for an hour at 70°C. This breaks large complex proteins down into more uniformly sized peptide fragments that allow for LC-MS/MS. In doing this, are there proteins identified that are not accessible to binding to the ELISA antibodies?

A protein digestion step was added to the sample preparations for TIMP2 and IGF2 ELISAs to see the effect of protein digestion on detectable protein levels. These assays were chosen at random as they arrived quickest from the manufacturer. The TIMP2 ELISA was affected by the protein digestion process (which included a high complexity protein cleanup step). This was likely to have been due to the acids used in the clean-up step which I did not neutralise prior to ELISA testing. This acidic solution may have interfered with the ELISA, resulting in all samples, including the controls, measuring as high concentration.

Protein digestion with a low complexity clean-up step was performed on samples in preparation for ELISA testing for IGF2. In this case all protein digested samples measured below the limits of the assay. It is likely that the binding site for the antibody used in the ELISA was cleaved by the protein digestion.

In retrospect, adding a protein digestion step to the sample preparation was unlikely to yield useful results. If the ELISA antibodies are unable to bind protein in a sample due to the protein being expressed intracellularly in any cells recruited into the CSF to fight an infection. A simpler approach would have been to disrupt cells mechanically.

It is difficult to find published research papers exploring the differences between LCMS/MS discovered biomarkers and ELISA. Most authors are preoccupied with examining the identification algorithms used or the calculations of quantity. Many are focused on promoting LC-MS/MS as a technique that could avoid ELISA [499-501](developing specific and sensitive antibodies for a protein can be extremely expensive and time consuming- indeed this is the reason I only explored proteins with commercially available ELISAs).

Overall, this reflects the relative infancy of proteomics as a scientific field.

Post-analysis factors

Bioinformatics for proteomic data is a PhD project in itself. The protein identification and relative quantification process was performed by *Roman Fischer et al* in the TDI in Oxford. The parameter settings and algorithms applied in proteomic data processing can have very significant effects on results. It has been difficult to replicate proteomics experiments in different labs, indeed *Zhang et al.* commented in a review of Alzheimer's Disease proteomics that the markers identified often behave very differently in other scientists experiments or are not identified at all [339]. As a clinician I will never personally set up and perform LC-MS/MS, but I need an appreciation of the factors that can impact on proteomic analysis and whether they can affect biomarker discovery.

The FDR set by the Oxford group is conservative and any protein that is identified by a single peptide has the spectrum of that peptide manually checked for quality and validity. The process is therefore more likely to exclude proteins than to include erroneous ones. Analysis of the relative abundance of proteins yielded a long list of potential biomarkers.

This process used a subset of the samples analysed to train an algorithm to classify samples (into infected or uninfected) and in doing so discriminative proteins were ranked. Proteins in TSP and TST were reviewed for their potential for further investigation. Those candidate proteins which were expressed by the brain, or which were intrinsically involved in the immune response and where there was a commercially available ELISA were chosen.

Conclusion

Label-free protein quantification by mass spectrometry was used here to identify potential markers of bacterial meningitis in neurosurgical CSF samples. This is an excellent modality for screening for biomarkers, but there are limitations the investigator must be aware of. The effect of pre-analysis sample processing for bottom-up proteomic analysis should not be underestimated. In digesting samples to allow for the mass tandem spectroscopy the resultant mixture is far removed from the sample encountered in the clinical setting. And whilst this may be acceptable for the purposes of biomarker discovery, there may ensue an even higher failure rate for these markers when validation experiments are performed.

The major challenge for any study is to verify the significance of markers emerging from LCMS/MS proteomic analysis. Any biomarkers identified need careful validation on another experimental platform. The numbers of samples needed for validation are significant and beyond the scope of a single PhD project to collect. The potential biomarkers identified in this project were therefore simply explored using ELISA. The biological variability of host response to different pathogens proved to be appreciable even with a small number of samples. Future experiments wishing to validate CSF biomarkers of infection should be carefully planned and ideally involve a large biobank of CSF.

Would one hope to find a standout single biomarker of infection in a study like this? Given the failure to date to identify a single marker that performs well enough to supplant traditional CSF microscopy, cell count and culture, it is unsurprising that no one marker performed strongly here. The future of BM diagnostics must include panels of markers that are interpreted informatically. The *clinical* diagnosis of BM is not a matter of identifying one symptom or sign, it is a weighing up of pre-existing risk, history, examination, and laboratory tests. The laboratory diagnosis of BM, therefore, should also embrace a

multifactorial analysis. To fully appreciate the range of protein expression depending on the pathogen many, many more CSF samples will need to be analysed.

In an ideal world, with limitless resources, I would collect neurosurgical CSF prospectively in multiple centres. Clinical data would be contemporaneously collected and linked with the samples. If I were doing this experiment again, I would test many more samples, in triplicate using LC-MS/MS. I would allow for a longer digestion time, as per the SMART digest manual, to ensure that large proteins like CRP would be analysable.

Hundreds if not thousands of neurosurgical CSF samples would be needed to properly assess for biomarkers of neurosurgical CSF infection. These samples would also need sufficient CSF sample volume to allow for follow-on ELISA testing for multiple proteins (again allowing for at least three replicates per protein tested). With large numbers of CSF samples, a sub-analysis of neurosurgical CSF infections caused by specific bacteria would be possible (to examine the proteome of CSF in a *P. aeruginosa* infection versus a S. epidermidis infection for example).

As infection is not a common event in neurosurgery, the numbers of CSF samples needed to capture enough infections to assess for a biomarker of neurosurgical infection would yield many, many uninfected CSF samples. This would allow for the analysis of the proteome in many neurosurgical pathologies (e.g., subarachnoid haemorrhage, brain tumours, hydrocephalus etc.).

Ideally, I would aim to recruit a minimum of 100 cases of neurosurgical CSF infection from each of the main causative bacteria of neurosurgical infections (*S. epidermidis, S. aureus, C. acnes, K. pneumoniae* etc.). All samples would be cranial CSF, collected for research and as such brought to a research sample storage facility immediately. Samples would be frozen to -80°C as soon as possible in Lo-bind tubes.

Chapter 4. Protein analysis of time course samples of infected neurosurgical CSF versus uninfected CSF

4.1 Introduction

While collecting the salvaged CSF samples from Liverpool Clinical Laboratories (LCL) it soon became apparent that the collection contained multiple samples from individual patients. Patients routinely have CSF taken at the time of any surgery that accesses the ventricles (e.g., shunt insertion or revision, EVD insertion etc.). Repeat CSF samples may be taken to monitor for developing CSF infections or to track the treatment of an established CSF infection. It can be assumed that not every sample from these patients' admissions was captured, but there was a group of patients where a series of samples taken over the course of treatment were stored. During the prospective CSF collection, a similar collection accrued with even better capture of multiple CSF sampling events. The opportunity to examine the pattern of protein expression in individual patients over time presented itself.

There are many biomarkers in medicine that are used to monitor the progression of a disease or the response to treatment. A prime example of a laboratory tested biomarker in routine use is C-reactive protein (CRP). CRP is primarily produced in the liver as an acute phase reactant. It is long established as an adjunct to diagnosis in infection and inflammatory diseases, and is also widely used to monitor response to treatment [502, 503]. CRP rapidly increases in concentration within 6-8 hours of initial stimulus, up to 10,000 fold [504] and once the inflammation or infection resolves it declines swiftly (elimination half-life of 4-9 hours)[502].

Originally identified in the 1930's in patients with *S. pneumoniae* chest infections, with increasingly sensitive assays for its detection, CRP has emerged as a marker of risk of coronary heart disease (CRP being produced as a presumed marker of chronic vascular wall inflammation in the development of atheroma or from the visceral adipose associated with metabolic syndrome) [505]. CRP is a standard blood test for many if not most patients presenting to hospital with suspected infection.

For any biomarker of CSF infection there are several questions;

1. Are the proteins that are candidate biomarkers in infection stable over time when there is no suspicion of infection?
2. Do they display a more restricted dynamic range over time if there is no infection present?
3. What is the behaviour of markers over the course of an infection?
4. Is the proteome at the time of reinsertion of shunt comparable to uninfected samples?

Chapter 3 approached neurosurgical CSF proteomics searching for a diagnostic biomarker. A follow up experimental hypothesis would be that a marker of infection will change over time, that this change would be predictable and there will be a value under which it can be confidently said that the infection has been adequately treated. This is of interest to all clinicians when treating a CSF infection when the question of duration of antimicrobial treatment arises but in neurosurgery another question is particularly important- when can the patient safely have a VP shunt reinserted? This has not been explored in neurosurgical CSF infections before, and it is not clear if the change in the proteomic profile of infected CSF is affected by the causative organism. The number of CSF samples needed to assess the difference between different pathogenic bacteria in neurosurgical CSF infection is beyond the scope of this project, and as such was not investigated.

Therefore, in this chapter we will analyse neurosurgical CSF that has been sampled at multiple serial time points in individual patients to investigate whether there are response/monitoring biomarkers of infection status.

4.2 Materials & Methods

4.2.1 CSF

Within both the salvaged CSF collection and the prospectively collected CSF there were patients who had been multiply sampled over time. The patients with the most samples with a clear history of neurosurgical CSF infection and then 2 controls (where there were

multiple samples but there was never a suspicion of infection, and all microbiological tests were negative) were chosen for analysis.

This collection was in no way ideal (Table 46). Patient 1 did not have a bacterium identified on culture; Patient 5 developed a second infection so there is no clear uninfected sample at the end of the time course. The data for these patients were incomplete but the series was felt to be unique and of sufficient interest to proceed.

CSF was thawed and carefully aliquoted in an extractor hood in a clean room in the IGH into LoBind Eppendorf tubes. These aliquots were stored at - 80°C until needed for analysis. An aliquot of each sample was sent on dry ice to the TDI, University of Oxford.

Table 46 CSF samples from patients who had a diagnosed CSF infection. Inf=infected, WCC=white cell count, RCC=red cell count, SAH= subarachnoid haemorrhage, EVD= external ventricular drain, HCP= hydrocephalus, ETV= endoscopic third ventriculostomy, VPS= ventriculoperitoneal shunt, IVH= intraventricular haemorrhage. TNP= test not performed. Day one is the first day of diagnosis. CoNS= coagulase negative staphylococci. The summary clinical details for these patients are included to illustrate the complexity of their cases.

Case	Day	CSF culture result	WCC	RCC	Clinical	Source
Patient 1	1		1580	2500	SAH, EVD complicated by ventriculitis	EVD
	6		42	1142		EVD
	11		2	190		EVD
	19		14	146		EVD
Patient 2	1	*C. acnes*	Clot		Ventriculitis, abscess- EVD inserted, and abscess drained	EVD
	10		Clot			EVD
	12		140	260		EVD
	14		360	9200		EVD
Patient 4	1	*P. aeruginosa, proprionibacterium*	248	452	*Pseudomonas* shunt infection requiring bilateral EVD insertion Background: West Syndrome, post meningitic HCP, ETV, then VPS, complex loculated HCP, cyst fenestration.	EVD
	1	*P. aeruginosa*	104	1170		Shunt tap
	4		TNP			EVD
	7		308	18		EVD
	10		392	4		EVD
	14		368	0		EVD
	19		TNP			EVD
	19		TNP			EVD
	19		1320	1800		EVD-left
	19	*CoNS*	18	14		EVD-right
	22		252	28260		EVD- left
	22		60	16		EVD-right
Patient 5	1	*CoNS*	320	16	Infected VPS requiring EVD after which VPS replaced.	Shunt tap
	5		1928	740		EVD
	14		8	268		EVD

	17	*CoNS*	6	78	Background: Ex prem, IVH, VPS	EVD
Patient 6	1	*S. aureus*	30	0	*S. aureus* infected shunt Background: TBI, decompressive craniectomy, VPS.	Shunt tap
	1	*S. aureus*	22	0		EVD
	3	*CoNS* on anaerobic culture - unlikely clinical significance	8	7290		EVD
	5		22	18		EVD
	7		TNP			EVD
	12		0	0		EVD
	16		12	21240		Shunt insertion
Patient 7	1	*S. aureus*	0	6	Presented as appendicitis- shunt externalised, confirmed shunt infection, VPS removed, EVD placed, later VPS reinserted. Background: Post meningitic HCP, ETV, VPS, previous VPS revision.	Ext shunt
	2	*S. aureus*	438	1450		EVD
	7		168	3640		EVD
	10		0	95		EVD
	20		8	6		EVD
	22		4	74		Shunt insertion

Table 47 Uninfected Samples used in this chapter. Uninf=uninfected, WCC=white cell count, RCC=red cell count.

Case	Day	WCC	RCC	Clinical	Source
Patient 3	3	10	9300	VPS revisions and externalisation, no CSF infection	EVD
	6	2	162		EVD
	12	14	5194		EVD
	13	4	2790		Shunt revision
	38	28	132		Shunt tap
	56	1	0		Shunt tap
Patient 8	1	32	45000	Anaplastic Infantile Ganglioglioma- cystic tumour, post op hydrocephalus-EVD, then VPS. Later had a seizure- shunt tapped.	EVD
	3	2	9000		EVD
	6	12	2520		EVD
	10	18	234		Shunt insertion
	10	18	234		Shunt insertion
	26	7	5280		Shunt tap

4.2.2 LC-MS/MS & ELISA

Sample preparation and LC-MS/MS procedure were as described in Chapter 2, section 2.3.1 and 2.3.2. This was again performed with Roman Fischer's group in the Target Discovery Institute in the University of Oxford by their post-doctoral fellow, Sonja Hester.

ELISAs were undertaken as detailed in Chapter 2, section 2.3.3

4.2.3 Statistical Analysis

Initial data analysis, as performed in Chapter 3 using Cluster 3.0[314] and TreeView[315], was undertaken on subgroups of the time course samples. These were *Infected* (clinical suspicion of infection, high WCC and culture positive) and *Uninfected* (no clinical suspicion of infection, low WCC and culture negative). The samples included in the *Infected* group were those samples taken at a time of clinical suspicion of infection and where a bacterium was grown on routine culture. The samples that were taken during the course of treatment of a CSF infection were neither included in the *Infected* nor the *Uninfected* groups.

The time points were not standardised for these samples and as such no formal analysis of trends over time was possible.

An unbiased cluster analysis was performed on the LC-MS/MS data without any classification of samples using R statistical analysis software, with "stats", "gplots", "heatmap.plus", "Heatplus" packages [318] with the assistance of Dr. Enrique Gonzalez Tortuero, University of Liverpool.

4.3 Results

4.3.1 LC-MS/MS

888 proteins were identified from LC-MS/MS analysis (Appendix B). Presenting the findings of the proteomic analysis for this collection of samples is not as straight forward as in Chapter 3. Whereas in Chapter 3 there were two groups- infected and uninfected, here there are eight patients with multiple samples over time. In effect, there are three groups; infected samples, samples where antibiotics were commenced but infection can be presumed to be ongoing/partially treated and uninfected samples.

If the samples where we can be surest about the clinical status are selected- i.e., samples where we are most certain there is an active infection (clinical suspicion, high WCC and culture positive) and samples where we can be confident there is no infection (no clinical suspicion, low WCC and culture negative)- it would be reasonable to subject that data to the same processing as used in Chapter 3. This failed to produce a similar heat map to that seen in 3.3.1 Fig. 31 & 32. The infected samples do not appear to have a clearly differential expression in comparison to the uninfected group as before (Fig. 55).

An unbiased cluster analysis of the relative abundance of all proteins identified on the LCMS/MS of *all* time course samples was performed without classifying the samples as infected or uninfected to aid visualisation of any trends (looking to identify if infected samples are more similar to other infected samples or if samples from one patient are more similar to other samples from that individual in comparison to other patients samples). The resulting heat map with patients identified is seen in Fig. 56. The colour palate for the heat map was reversed from the usual red for upregulated and blue for down regulated to aid pattern visualisation.

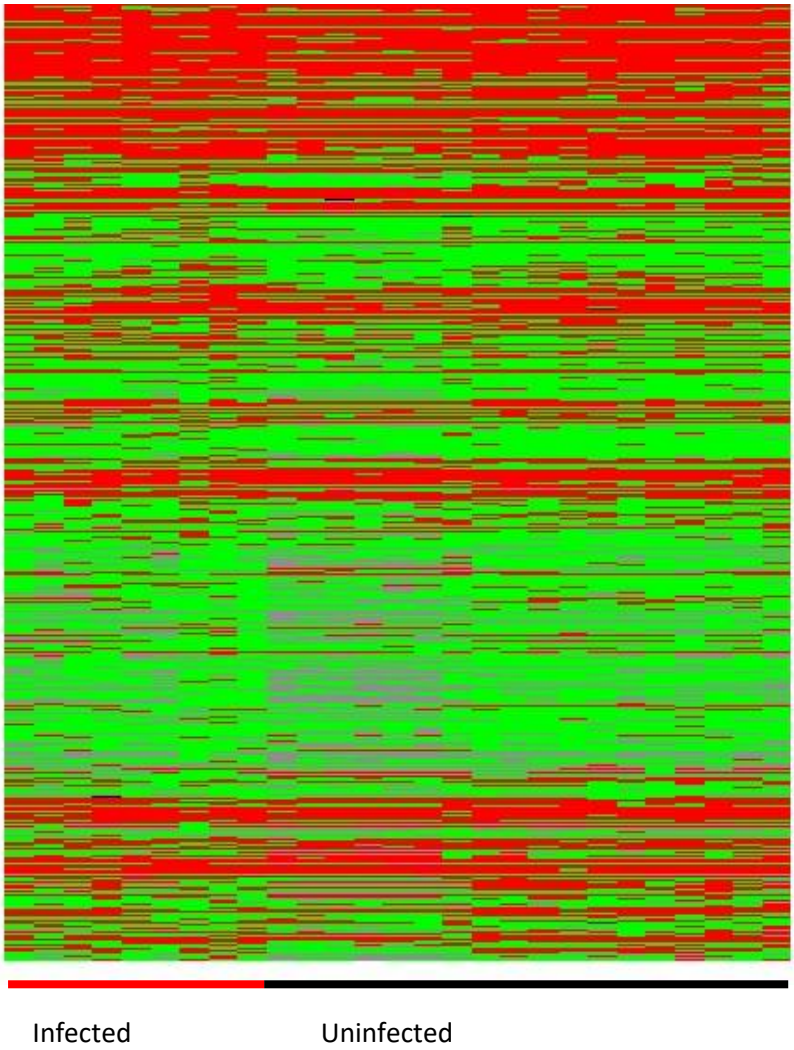

Figure 50 Heat map of proteins identified by LC-MS/MS. Infected *samples are on the right (red bar) and* Uninfected *samples are grouped on the right (black bar underscores the group). This heat map was produced, as in Chapter 3, with AUREA and TreeView as described in section 4.3.3.*

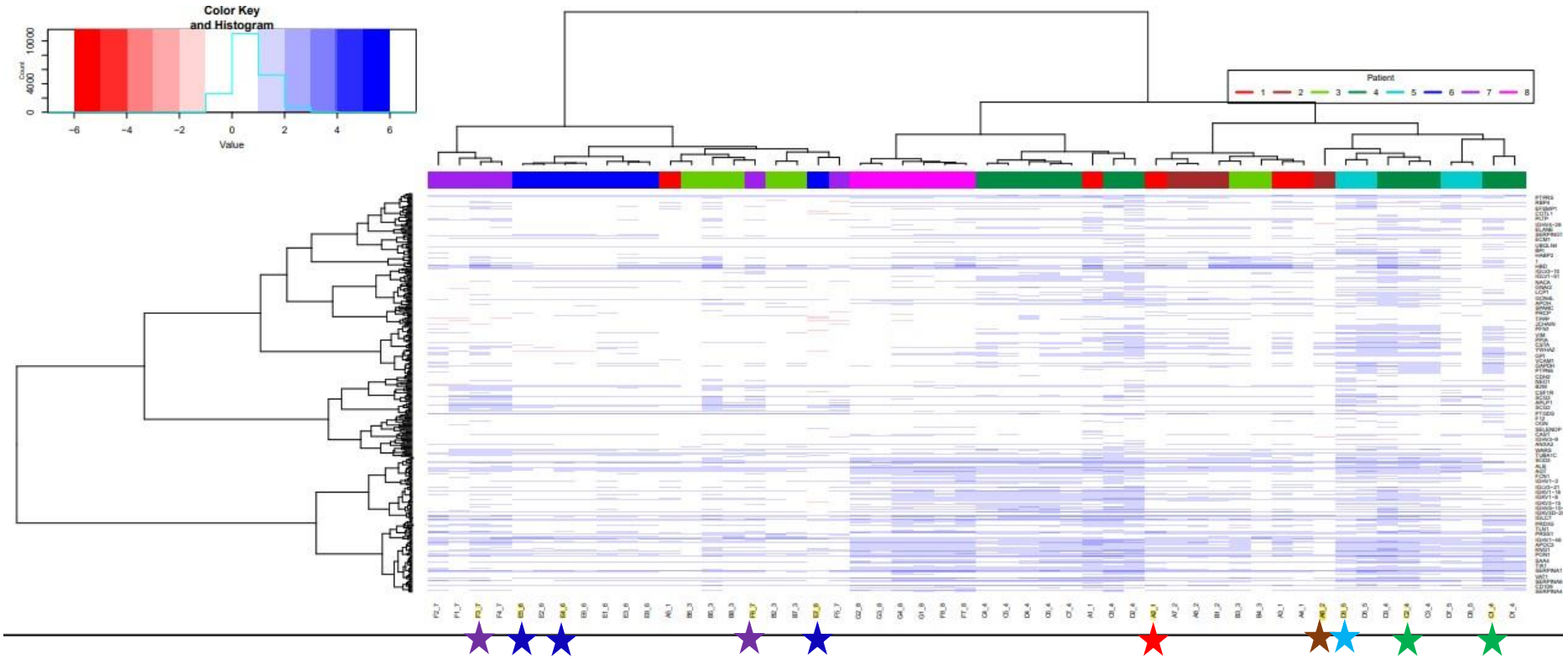

Figure 51 Heat map of proteins identified on LC-MS/MS for time course samples. This was an unbiased cluster analysis of relative abundance of each protein identified. The samples are colour coded by patient (Patient key on the top right). The infected samples for each patient are marked by a star below the heat map. The colour key (top left) indicates the relative abundance of proteins, with proteins in blue being expressed in greater abundance and proteins in red lesser abundance. The coloured bar directly above the heat map is coloured according to the patient; Patient 1 in red, Patient 2 in brown, Patient 3 in lime green, Patient 4 in green, Patient 5 in teal, Patient 6 in blue, Patient 7 in purple and Patient 8 in pink.

Patient 1

Patient 1's samples are seen on Fig.57 as bright red. This patient suffered a subarachnoid haemorrhage, requiring an EVD which was complicated by infection (ventriculitis). None of the samples salvaged for this case were culture positive but the first sample had a very high WCC (1580) and was included as it was felt that this was highly likely to be an infected sample.

The sample to the left in a very separate cluster to the other samples is CSF taken on Day 19 (WCC=14, RCC=146). The sample to the right of this, in a sub cluster, is a Patient 3 sample- a patient where infection was never suspected, taken on Day 13 with WCC= 4, RCC=2790. Both of these samples should be uninfected, but the Patient 1 sample has a relatively high WCC.

Patient 1 had a sample taken 18 days prior to the presentation with infection (WCC= 12, RCC=13500), marked as D* on Fig. 57. This clusters with Patient 4 (particularly with two Day 19 samples from Patient 4, one which had no cell count recorded and the second which had WCC=18, RCC=14 and grew a *CoNS* on culture). The Patient 1 sample from Day -18 should be uninfected but the two Patient 4 samples appear to be from a second infection for that patient- why these samples would be so similar is unclear.

The first sample that was salvaged from Patient 1 during their episode of infection, Day 1(WCC=1580, RCC=2500) is seen to cluster together with Patient 2 (Day 10 (clotted) and Day 12(WCC 140, RCC 260)). Whilst the Day 1 sample from Patient 1 was assumed to represent an early infected CSF sample this may not be the case and all three samples may be similar in that they are CSF samples taken from complex patients with ongoing antibiotic treatment for CSF infection.

The subsequent samples on Day 6 (WCC=42, RCC=1142) and Day 11 (WCC=2, RCC=190) cluster with uninfected Patient 3 (WCC=2, RCC=162). These three samples are all likely to be uninfected.

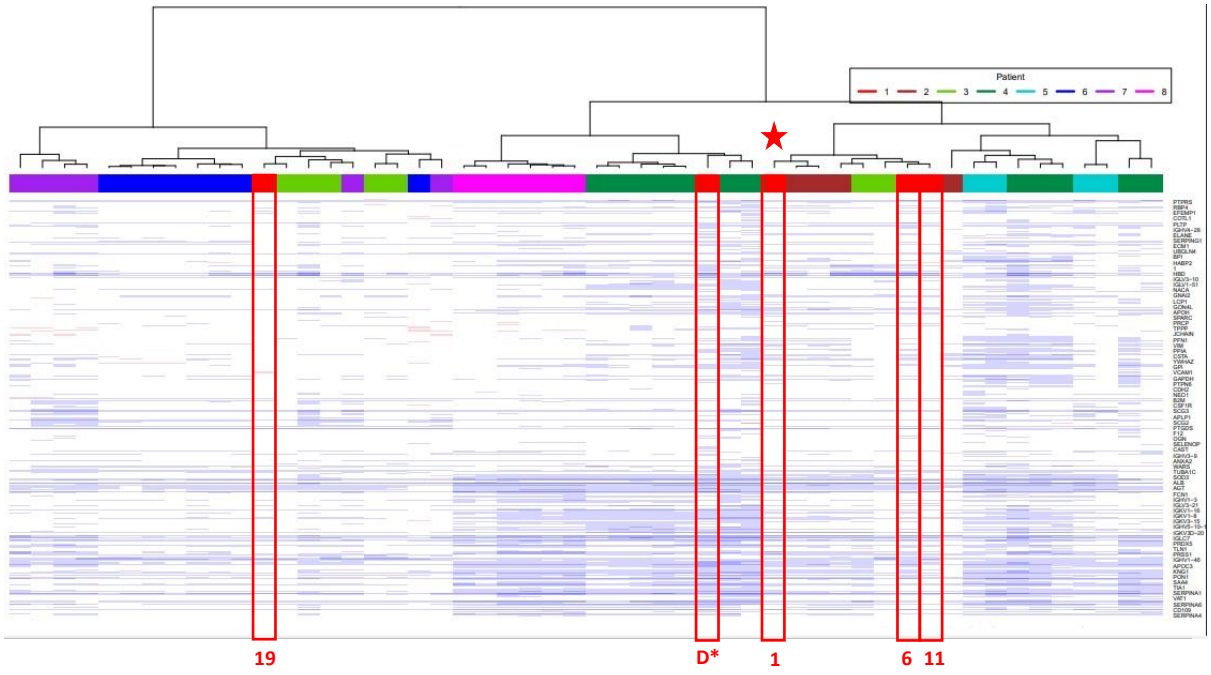

Figure 52 Patient 1. All 8 patients' data are presented here with Patient 1's samples highlighted with red outlines. The Day 1 samples which had a very high WCC but no bacteria on culture is marked with a filled red star and is assumed to be infected. The day of sampling in relation to day 1 is marked below each sample. As in Figure 56 the relative abundance of the identified proteins is denoted by colour, with increased abundance shown as deepening shades of blue, decreased abundance as deepening shades of red and no difference as white.

Patient 2

Patient 2 developed ventriculitis and an abscess- an EVD had been inserted and later the abscess was drained. The Day 1 sample for this patient grew *C. acnes*. The sample was clotted so cell counts were not available, it is therefore difficult to say whether *C. acnes* was the causative organism for what sounds like a long and complicated infection. The Day 1 sample clusters separately to the other samples (brown filled star, Fig 58).

Day 10 (clotted) and Day 12(WCC 140, RCC 260) are very similar to each other and Patient 1's sample from Day 1 which was culture negative but WCC 1580, RCC 2500 and so suspected to be infected- as discussed previously.

Day 14 (WCC 360, RCC 9200) is clustering with Patient 3, a case where no infection was suspected (Day 3, WCC 10, RCC=9300). Clinically both of these samples are thought to be uninfected.

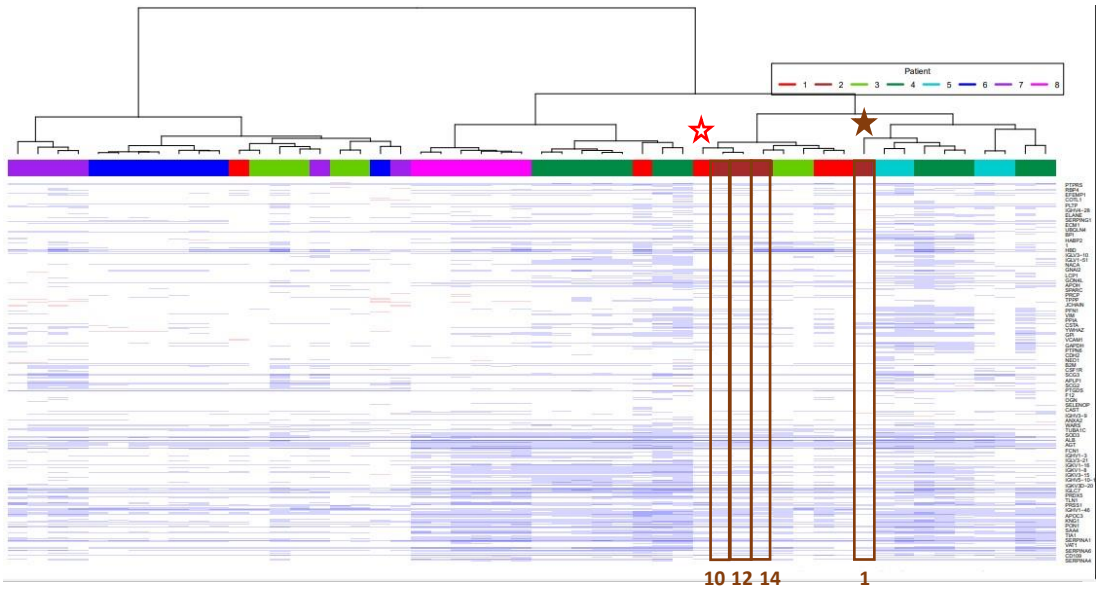

Figure 53 Patient 2. All 8 patients' data are presented here with Patient 2's samples highlighted with brown outlines. The Day 1 sample is marked with a filled brown star and the day of sampling relative to Day 1 is noted below each sample profile. The unfilled red star marks the Day 1 sample for Patient 1 which had a high WCC and was presumed to be infected. As in Figure 56 the relative abundance of the identified proteins is denoted by colour, with increased abundance shown as deepening shades of blue, decreased abundance as deepening shades of red and no difference as white

Patient 4

Patient 4 had a *P. aeruginosa* shunt infection (Fig. 59). This patient had two samples from

Day 1, one taken via shunt tap and another taken at EVD insertion. The shunt tap sample (marked as *1s* in Fig 60, WCC=114, RCC=1170) clusters with Day 22 (WCC=252, RCC=28260) and Day 4 (cell count not performed) and with two samples from Patient 5 (Day 1 sample which grew a *CoNS*, WCC=320, RCC=16 and Day 5 sample which was culture negative but WCC=1928, RCC=740). All these samples appear to be from the acute phase of infection. The Day 22 sample from Patient 4 could be thought of as Day 4 of the second infection that this patient developed. Similarly, the Day 5 sample from Patient 5 has a very elevated WCC.

The EVD sample (1e) from Patient 4, taken on Day 1 (WCC=248, RCC=452, culture grew *P. aeruginosa*) clusters with a Day 19 sample (marked 19^3 in Fig 58, WCC=1320, RCC=1800, culture negative). This cluster being of samples that are clearly infected, despite the 19^3 sample being culture negative.

There is a separate cluster of the other Patient 4 samples in the middle of the heat map. This is made up of 2 sub clusters. The one on the right was discussed with Patient 1 before. The one on the left is made up of:

- Day 7 WCC=308, RCC=18 □ Day 10 WCC=392, RCC=4 □ Day 22 WCC=60, RCC=16
- Day 14 WCC=368, RCC=0

All four of these samples were culture negative and were taken whilst the patient was receiving antibiotics. Which would point towards these samples being uninfected but there were two Day 22 samples and the other sample clusters with infected samples. This may represent the difference in CSF taken from different CSF compartment even when taken at the same time.

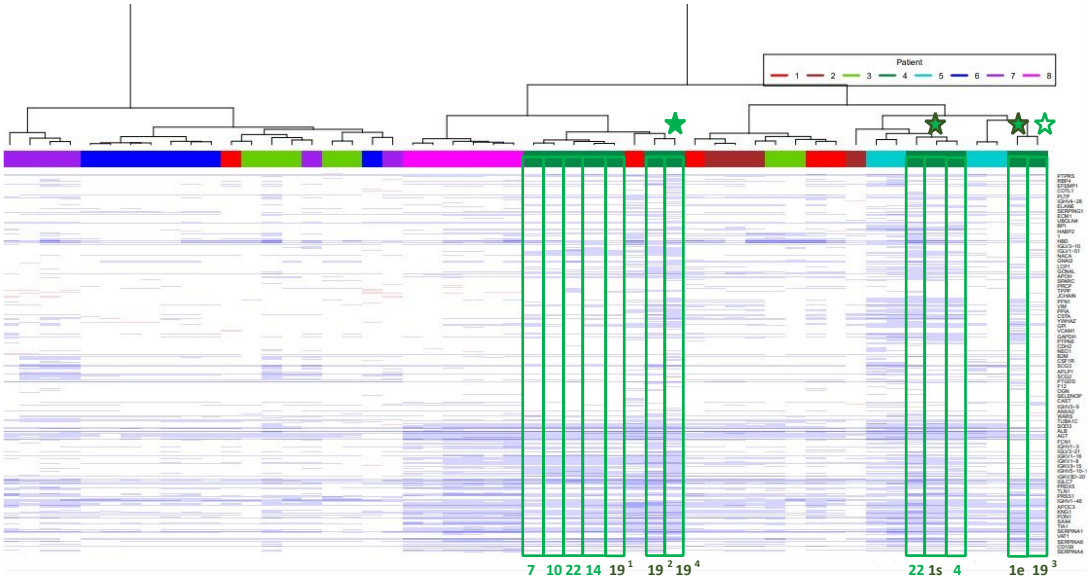

Figure 54 Patient 4. All 8 patients' data are presented here with Patient 4's samples highlighted with green outlines. The two Day 1 samples are marked with a green filled star outlined in dark green, both samples grew P. aeruginosa *on culture. The day of sampling relative to Day 1 is marked below each sample profile. 1s= shunt sample taken on Day 1. 1e= EVD samples taken on Day 1. There were four samples taken on Day 19, these are identified by the superscript numbers. Sample 19 [1] and 19 [2] had no cell counts recorded and did not grow bacteria on culture. Sample 19 [3] was taken from a* ***left*** *sided EVD and had an elevated WCC=1320, RCC=1800 (marked with a filled green star). Sample 19 [4] was taken from a* ***right*** *sided EVD and grew a CoNS, WCC=18, RCC=14 (marked with an unfilled green star). As in Figure 56 the relative abundance of the identified proteins is denoted by colour, with increased abundance shown as deepening shades of blue, decreased abundance as deepening shades of red and no difference as white*

Patient 5

Patient 5 had an infected VPS where the shunt was removed and an EVD placed and later replaced with another VPS. The Day 1 sample which was Gram-stain positive and grew a *CoNS* had WCC=320, RCC=16. This clusters with Day 5 (WCC=1928, RCC=740) (Fig. 60). As mentioned previously Patient 4's samples from Day 1(shunt sample, filled green star), Day 4 and Day 22 cluster with these samples.

Day 14 (WCC=8, RCC=268) and Day 17 (cultured a *CoNS*, WCC=6, RCC=78) appear very similar, at this point this patient was receiving intrathecal vancomycin for the infection.

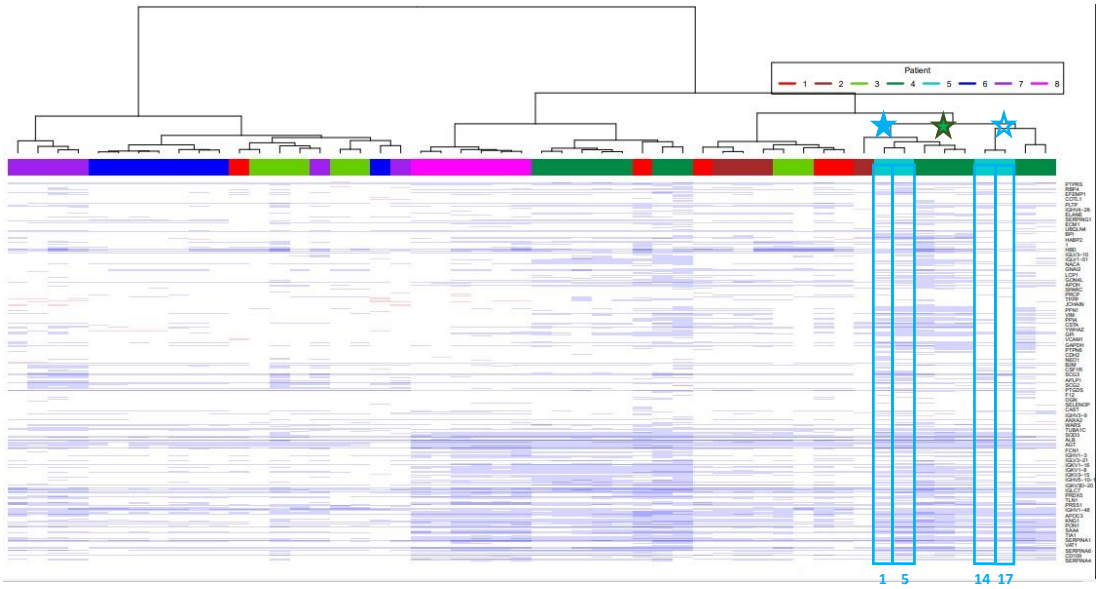

Figure 55 Patient 5. All 8 patients' data are presented here with Patient 5's samples highlighted with teal outlines. The Day 1 sample, which grew CoNS, *is marked with a teal filled star. The Day 17 sample also grew a* CoNS *and is marked with an unfilled teal star. The culture positive sample from Patient 4 is marked with a filled green star. As in Figure 56 the relative abundance of the identified proteins is denoted by colour, with increased abundance shown as deepening shades of blue, decreased abundance as deepening shades of red and no difference as white*

Patient 6

Patient 6, a *S. aureus* VP shunt infection, has one main cluster of samples and one outlier (Fig. 61). The main cluster from left to right consists of

- Day 1- a shunt tap sample, that grew *S. aureus* WCC=30, RCC=0
- Day 12-WCC=0, RCC=0
- Day 3- which grew a *CoNS*, WCC=8, RCC=7290
- Day 7-which had no culture or cell count results
- Day 16-WCC=12, RCC=21240
- Day 5-WCC=22, RCC=18
- D*-a sample taken 87 days prior to the shunt infection episode which again had no culture or cell count results.

Day 1, Day 12, Day 3 and Day 7 form one sub cluster. Day 1 is infected and it clusters with Day 3 (which is still growing bacteria on culture) but why these infected samples cluster with the Day 7 and Day 12 samples is unclear.

Day 16, Day 5 and D* are in a sub cluster together, the Day 16 and D* samples are very likely to be uninfected and the sample from Day 5, whilst it has an elevated WCC, it was taken when the patient had received antibiotics for 5 days.

The outlier sample was a second sample taken at the time of EVD insertion on Day 1, which also grew *S. aureus* with WCC=22 and RCC=0. This CSF had shown gram-positive cocci on immediate Gram stain. The protein profile appears similar to Patient 7's sample from Day 20 (WCC 8, RCC 6), which was also an EVD sample but which was taken two days prior to the reinsertion of a VP shunt (so it will have been thought to represent a non-infected CSF sample which was reassuring for a treated infection).

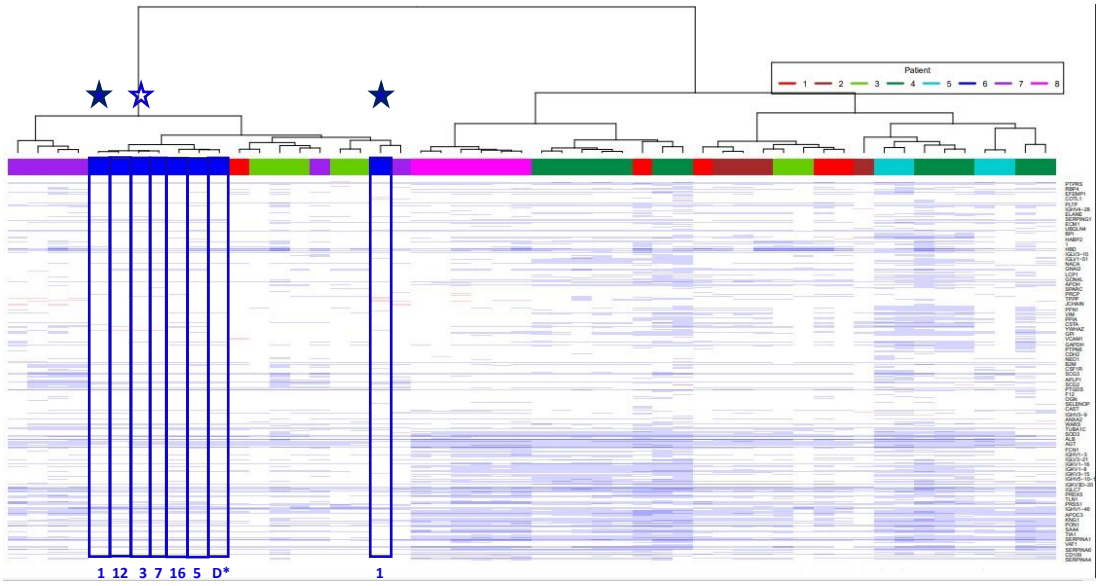

*Figure 56 Patient 6. All 8 patients' data are presented here with Patient 6's samples highlighted with blue outlines. The Day 1 sample taken from the shunt is marked with a filled **blue** star on the far left, the second Day 1 sample taken from the EVD insertion is marked with a filled **blue** star to the right of the main cluster of Patient*

6 samples. The Day 3 sample also grew a CoNS is marked with a unfilled **blue** star. As in Figure 56 the relative abundance of the identified proteins is denoted by colour, with increased abundance shown as deepening shades of blue, decreased abundance as deepening shades of red and no difference as white

Patient 7

Patient 7 had a *S. aureus* shunt infection that initially presented with presumed appendicitis (Fig. 62). The shunt was externalised at the time of appendicectomy, and it was from this externalised distal catheter that the first CSF sample was taken (Day 1). This patient had culture positive samples on Day 1 and Day 2. The Day 2 sample had a more pronounced WCC rise.

The cluster of samples from Patient 7, on the far left of the heat map, from left to right, were:

- Day 22 - culture negative, WCC=4, RCC=74, sample from the shunt re-insertion
- Day 7 - culture negative, WCC=168, RCC=3640, EVD sample
- Day 1 -gram-positive cocci in clusters on Gram stain, *S. aureus* on culture, WCC=0, RCC=6, distal catheter CSF sample at the time of externalisation of shunt
- Day 10- culture negative, WCC=0, RCC=95, EVD sample

The Day 2 sample was taken when the shunt was removed and an EVD was inserted. The WCC=438, RCC=1450 and *S. aureus* again grew on culture. It clusters with Patient 3 Day 56 (WCC 1, RCC <1) and then with Patient 3 Day 13 (WCC 4, RCC 2790), Day 12 (WCC 14, RCC 5194) and Patient 1 (Day 19, WCC 14, RCC 146). This infected sample from Patient 7 was taken after the patient had received at least 24 hours of antibiotics for appendicitis but why it clusters with apparently uninfected samples is not clear.

The final Patient 7 sample was taken from the EVD on Day 20 (WCC 8, RCC 6) in preparation for reinsertion of a VP shunt on Day 22. As mentioned earlier, this is similar to Patient 6's Day 1 sample which grew *S. aureus* (WCC 22, RCC 0).

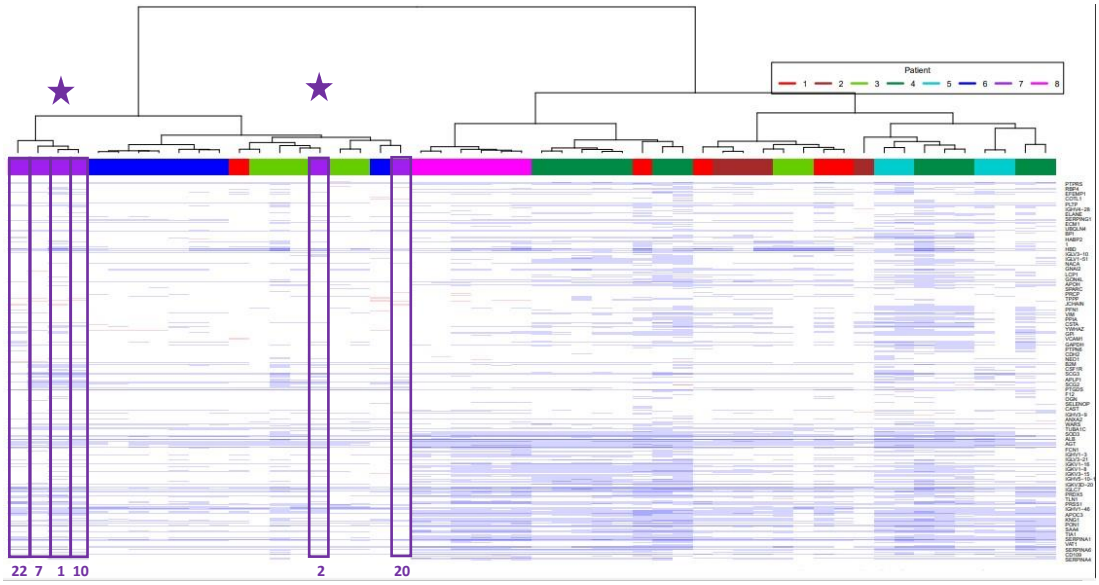

Figure 57 Patient 7. All 8 patients' data are presented here with Patient 7's samples highlighted with purple outlines. The Day 1 and Day 2 samples, which both grew S. aureus *on culture are marked with filled purple stars. As in Figure 56 the relative abundance of the identified proteins is denoted by colour, with increased abundance shown as deepening shades of blue, decreased abundance as deepening shades of red and no difference as white*

Patient 3 & Patient 8

Patient 3 was an adult who was not clinically suspected as having a CSF infection but who had a complicated history of shunt malfunction and non-CSF infections. This case is obviously not an ideal "control" as the patient has systemic infection at non neurological sources that may have impacted on the CSF proteomic profile, particularly because they needed repeated surgery. Patient 3 samples have been discussed previously with the other cases but are highlighted in Fig. 63.

Patient 8 was a child with a brain tumour that developed hydrocephalus post operatively, requiring an EVD. This child was never suspected of having a CSF infection and went on to have a VPS inserted. More than two weeks after the shunt insertion a CSF sample was taken from the shunt as part of the investigation of a seizure. None of these samples grew bacteria on culture. All this patients' samples neatly cluster together (Fig 63).

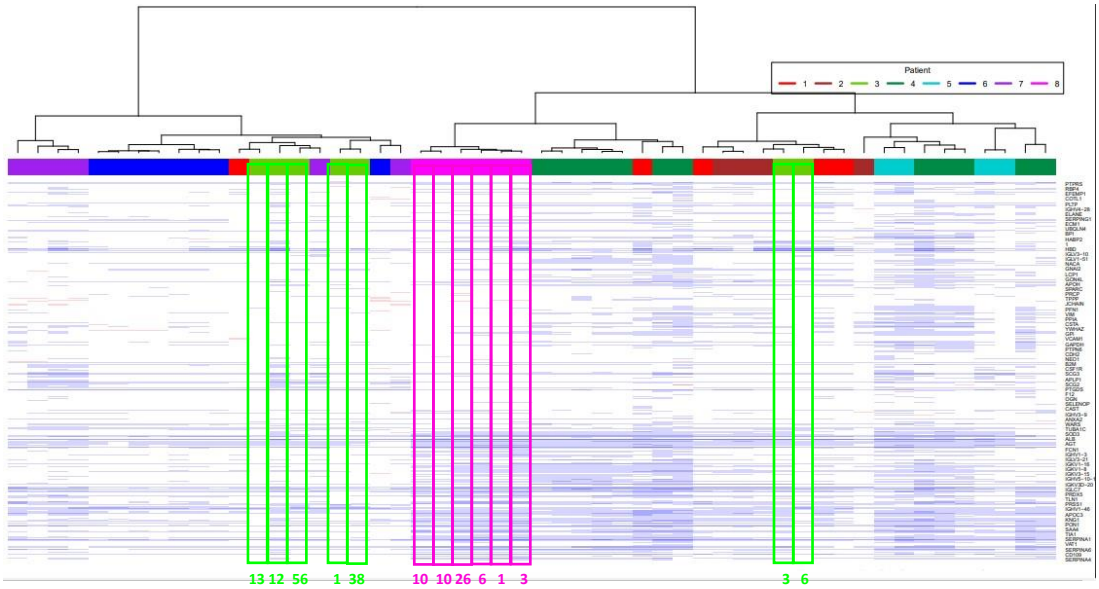

Figure 58 Patient 3 and Patient 8. All 8 patients' data are presented here with Patient 3 and Patient 8's samples highlighted with lime green and pink outlines respectively. There are no culture positive samples to highlight for these samples. Patient 3 samples are outlined in lime green and Patient 8's are outlined in pink. As in Figure 56 the relative abundance of the identified proteins is denoted by colour, with increased abundance shown as deepening shades of blue, decreased abundance as deepening shades of red and no difference as white

4.3.2 Proteins identified in Chapter 4

The differential expression of the proteins identified as potential biomarkers in the first LCMS/MS analysis in Chapter 3 may be reflecting something other than the infection status of the samples (i.e., it reflects the difference in proteome in cranial CSF versus lumbar CSF), but we have seen that there is biological reasoning for their candidacy as potential

biomarkers for infection. These proteins were therefore examined in this data despite the failure of the initial clustering and analysis of relative expression to identify them again.

Lactoferrin

When the relative abundance as measured by LC-MS/MS for Lactoferrin was isolated from the data, there was no significant difference between the infected samples and uninfected samples (see Fig 64). It failed to reproduce the pattern seen in Chapter 3 where Lactoferrin was significantly higher in infected samples in comparison to uninfected samples. (Fig. 65)

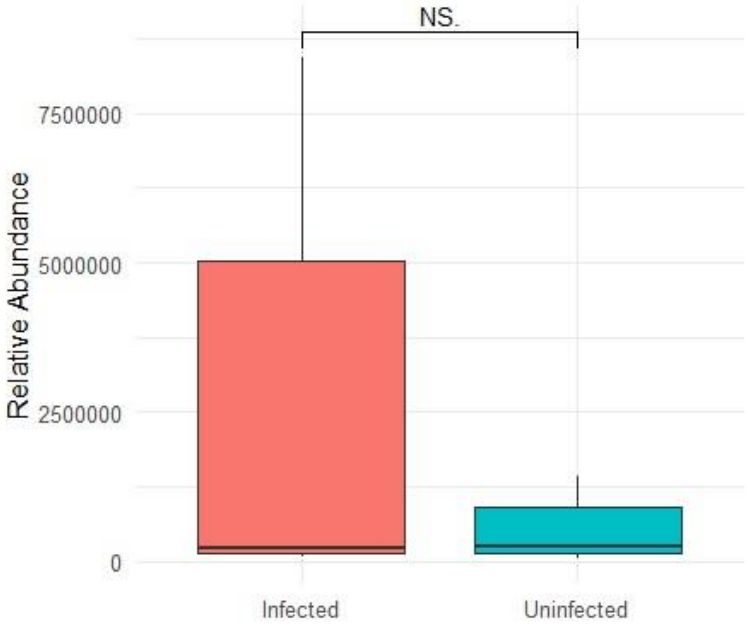

Figure 59 Relative abundance as measured by LC-MS/MS. Samples in the time course cohort where there was a positive culture and raised WCC were classified as infected and samples where the culture was negative, the WCC was less than 1 per 500 RCC and clinically there was no suspicion of infection were classified as uninfected.

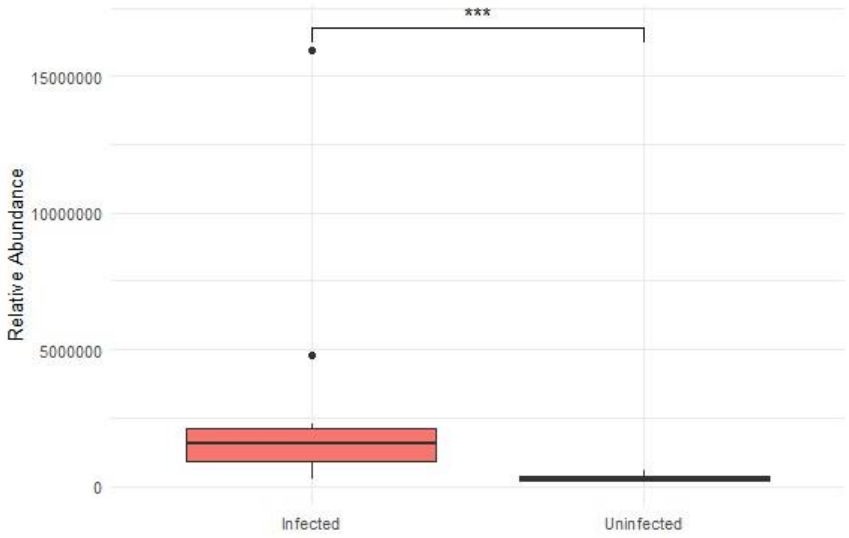

Figure 60 Relative abundance of Lactoferrin as measured by LC-MS/MS in the Chapter 3 experiment.

The individual results for all the samples grouped by patient were then examined (Fig. 66). The axes have been standardised throughout to make comparison simpler. As these

samples were not on set time points (e.g., consistently on Day 1, Day 3, Day 5 etc.) and with only eight patients, statistical comparison of trends was not attempted. The LC-MS/MS data shows changing Lactoferrin concentration over time for some samples (Infected case 2, 3, and 4) whereas in the other cases it is relatively stable over time (Infected case 1, 5, 6 and Uninfected 1 and 2) (Fig.66).

The individual CSF samples used in this chapter for LC-MS/MS were then tested for Lactoferrin concentration using ELISA (Fig. 67).

The data for NPTXR, TIMP2, IGF2, and NEGR1 were then examined in a similar manner, with similar results (see Appendix B).

LC-MS/MS

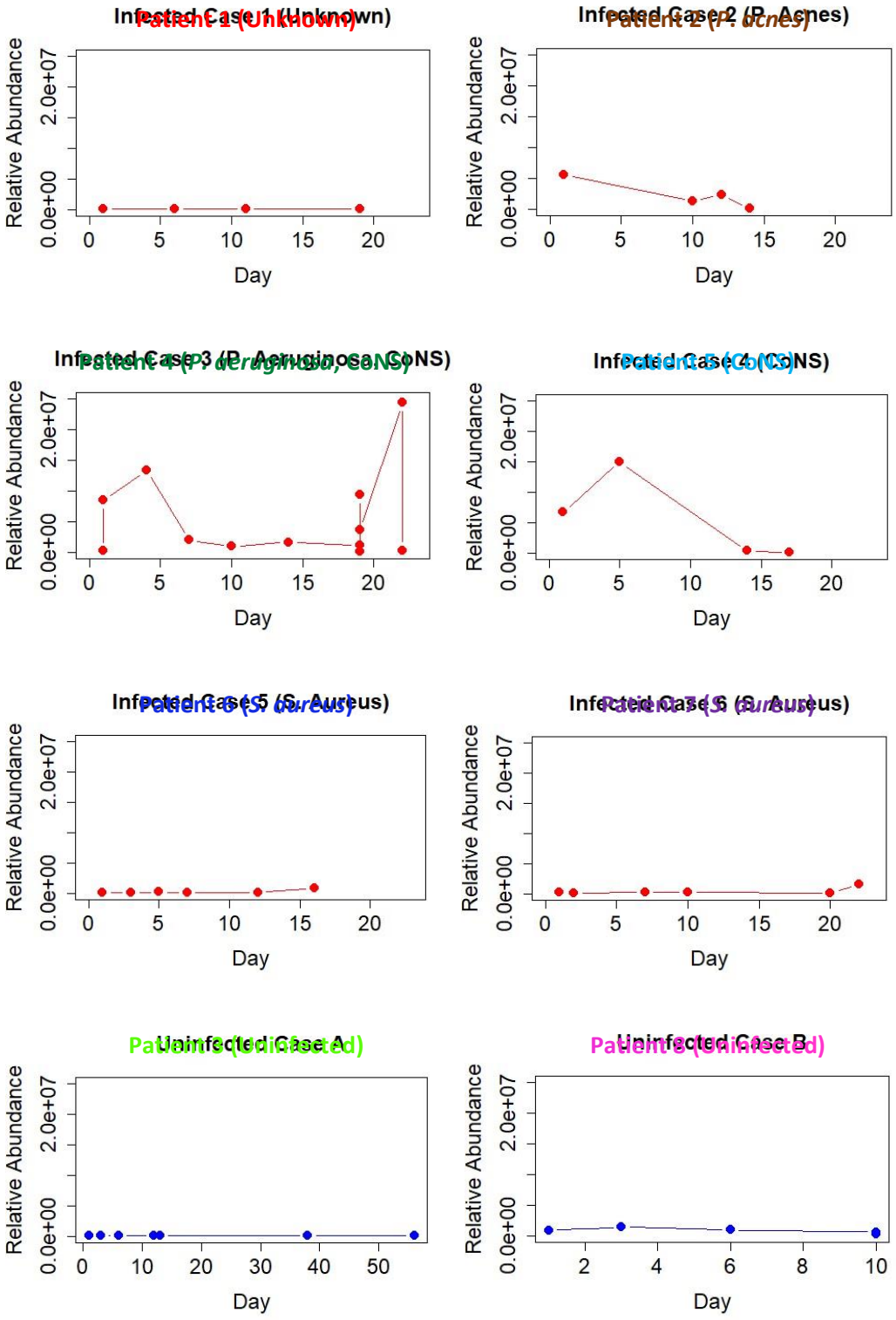

Figure 61 Relative abundance of Lactoferrin as measured by LC-MS/MS. Each patient is presented separately with the axes standardised throughout. Patient 4 had 2 samples taken on day 1, 4 samples taken on day 19 and 2 samples taken on day 22, the result for each sample is presented as a separate filled red dot. CoNS= coagulase negative staphylococcus.

ELISA

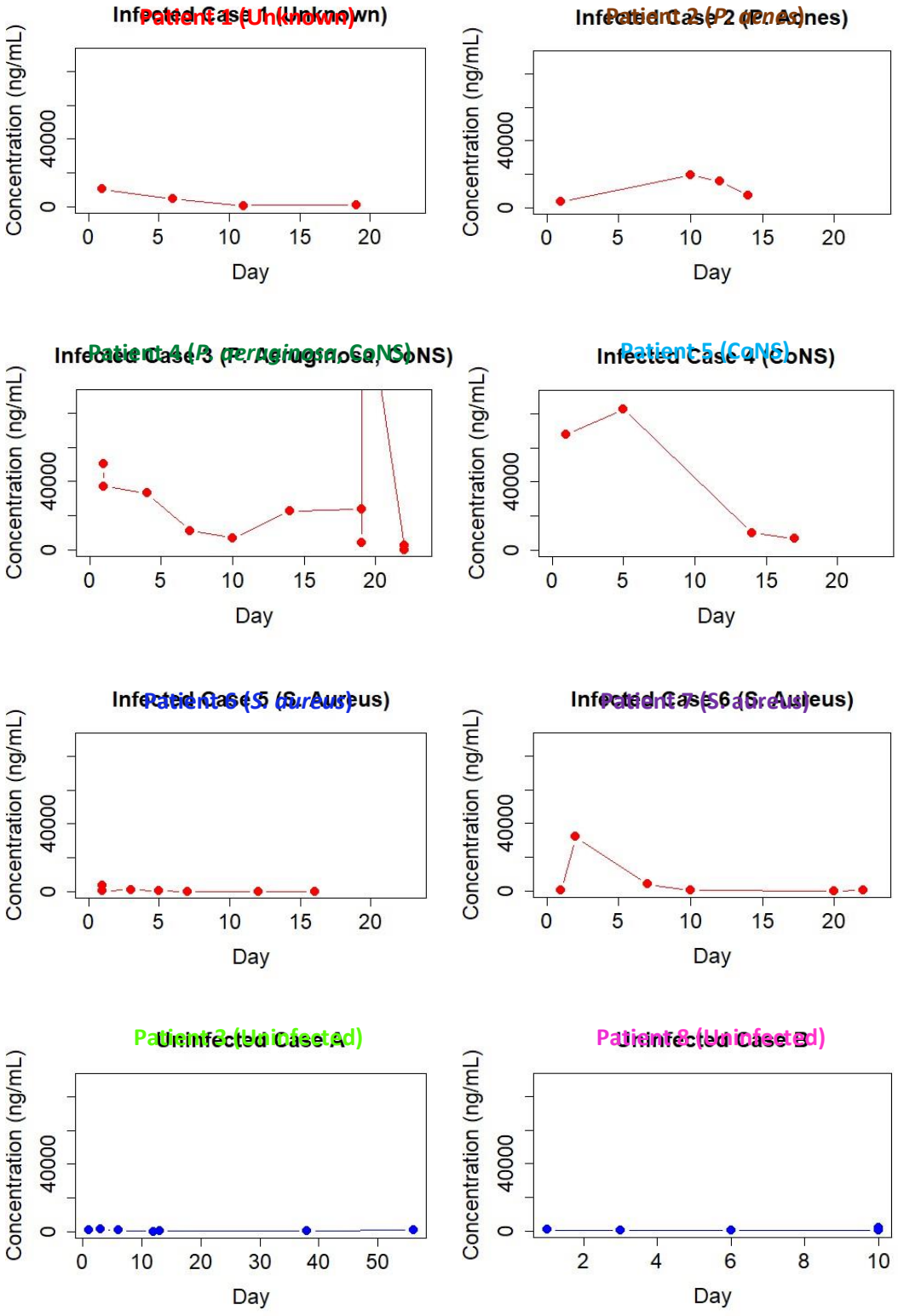

Figure 62 Results of ELISAs for Lactoferrin concentration (ng/mL) over the time for six patients with infection and two uninfected cases. As previously stated, patient 4 had more than one sample taken of several days. For clarity the 4th sample from day 19 has been excluded on the Patient 4 graph. CoNS= coagulase negative staphylococcus.

4.3.3 Proteins from meningitis literature

Of the biomarkers for meningitis that were discussed in Chapter 1, only CRP was identified in the LC-MS/MS data for these samples (Fig. 68). Neither lactate nor procalcitonin were identified in this data. The relative abundance data for CRP from LC-MS/MS is presented in Fig.68.

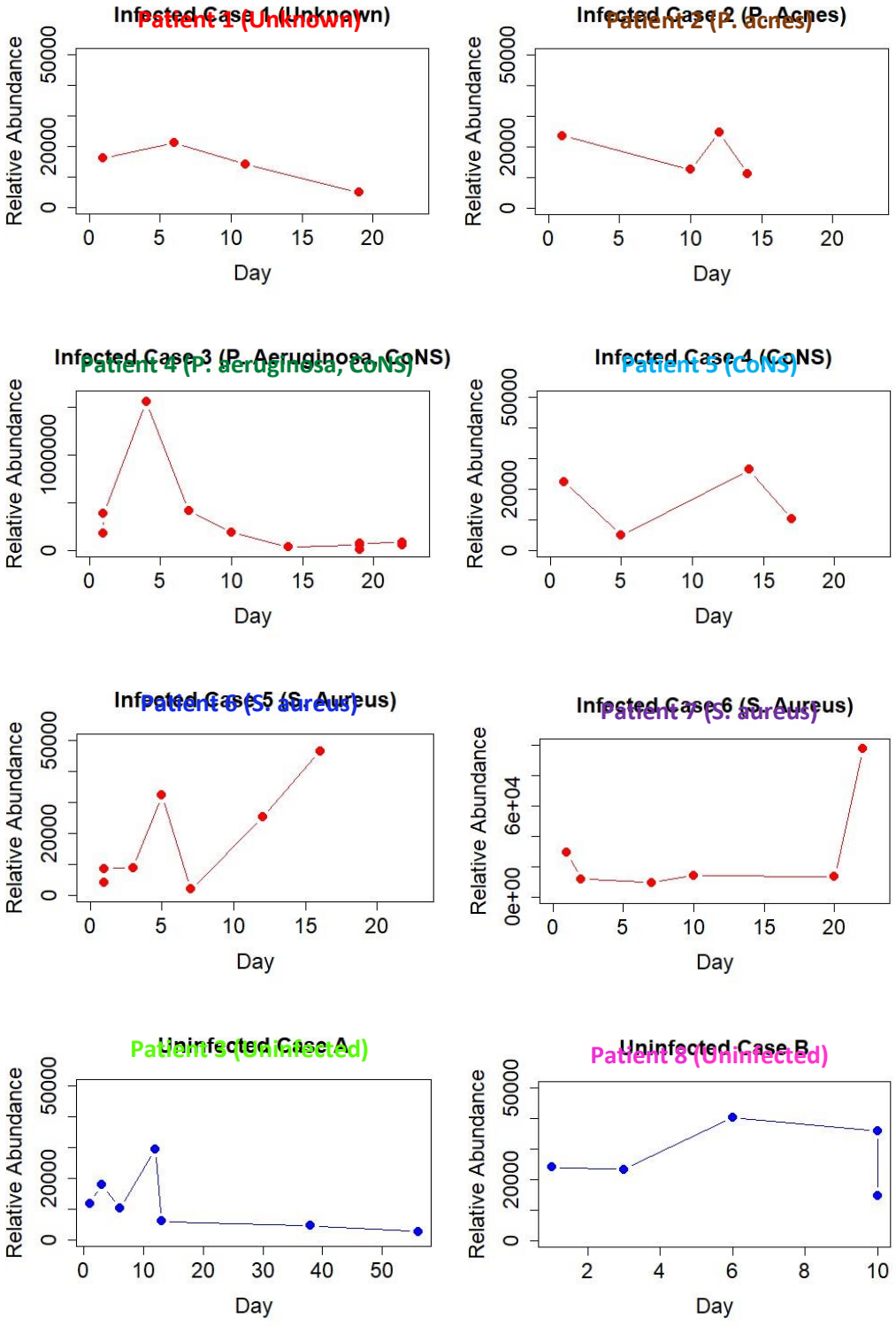

Figure 63 Relative abundance of CRP as measured by LC-MS/MS in eight patients CSF. CoNS= coagulase negative staphylococcus.

4.4 Discussion

When the analysis that was performed in Chapter 3 was performed on this data, overall, it appears that samples from an individual patient are more similar to other samples from that same patient. Even when the infected samples (clinical suspicion of infection, high WCC and culture positive) were compared only with the uninfected (no clinical suspicion of infection, low WCC and culture negative) samples, there does not appear to be a protein expression pattern that differentiates infected samples from uninfected samples.

On first inspection, the unsupervised cluster map of all the time course samples, Fig. 55 appears to not show any differentiation/clustering of the infected samples. When the heat map is more closely examined, which has been discussed for each patient in section 4.3.1, there does appear to be clustering of some infected samples (Patient 2, Patient 4 and Patient 5) with samples with high WCC (from Patient 4).

In contrast to this, is the Day 19 sample from Patient 1 which clusters with a Patient 3 sample- these samples would have been assumed to represent infected and uninfected samples. The CSF samples from Patient 1 came from two EVDs, each draining a different part of the ventricular system. Could this sample that clusters with the Patient 3 sample be from an EVD that is draining an uninfected CSF space that is not in continuity with the infected CSF (which is represented by the samples that grew bacteria on culture)?

The patients who did not develop infections have different proteomic profiles (Fig. 63). Which perhaps highlights the difference in the underlying pathologies. Patient 8 had a brain tumour whereas Patient 3 had a complicated shunt blockage. The effect of the tumour on the proteomic profile of the CSF would be expected to be significant. Is Patient 3 truly uninfected? This was a complex shunt revision case, where there was never any clinical suspicion of infection, and no sample ever grew an organism but as discussed in Chapter 1 there is always some doubt about shunt blockage being caused by an indolent infection.

It is interesting to note the difference in protein abundance by site of sampling within these samples. Patient 4, fig. 66, had two samples taken on day 1, four samples on day 19 and two samples on day 22. This was due to the patients having bilateral EVDs inserted but it serves to show how the CSF may not be in continuity within the cranium and that the clinician must be aware of the site of CSF sampling. If the CSF is sampled from a distant site or from a CSF compartment that is not in continuity with a potentially infected area, then the results may not be truly representative.

In reality, there are not enough samples here to identify a pattern. There was a mixture of different infections (*P. aeruginosa, S. aureus, CoNS*, possible *C. acnes*) and ages and pathologies. The six infected cases were not all straightforward infection, identified on Day

1, followed by treatment that definitively cleared that infection. Patient 4 developed a second infection on Day 19.

The analysis of this data was discussed at length with statisticians in the University of Liverpool. Given the small number of patients and the non-standard sampling time points (the samples were not taken at the same intervals for each patient) multivariate analysis was not possible.

Individual proteins

Examining the proteins identified in Chapter 3 in these samples was interesting, in that it tests the ability of LC-MS/MS to detect changes in protein over time in the same patient. This is possible, from what we can see on Fig. 66 that Lactoferrin is seen to change in relative abundance over time.

ELISA testing of protein concentration was performed for each of the proteins tested in Chapter 3. This produced mixed results (Fig.67) but highlights the need for verification of LC-MS/MS data with another more precise modality.

Conclusion

This is inarguably a small collection of samples to assess biological variability, but it does provide some interesting results. This proteomic analysis serves to highlight the difficulty and the nuance involved in interpreting neurosurgical CSF.

The relative abundance calculation produced by LC-MS/MS gives an indication of the concentration of proteins in a sample. How accurate is this relative abundance? Broadly speaking it appears that the two modalities produce similar but not identical results.

Proteomics is undoubtedly in its infancy but its utility as a mass screening tool for biomarkers is clear. Even if the price and throughput improve exponentially, it cannot replace the more accurate methods like ELISA for assessing concentration of proteins.

With greater resources if I were to do this experiment again, I would collect CSF prospectively and ensure that repeat CSF samples were taken every second day whilst CSF drainage was ongoing (whether there was an infection present or not).

If I were able to repeat the Chapter 3 experiment as previously discussed (i.e., 100 cases of each main causative bacterium and matching numbers on uninfected CSF samples to assess for the proteomic profile of each infection type and the differences between infected and uninfected CSF proteomes) I would have identified more candidate biomarkers of infection. I would therefore look to explore the concentrations of those proteins over the course of 100 cases of infection, to establish the behaviour of those markers over time.

Chapter 5. Bacterial genomic sequencing of neurosurgical CSF

5.1 Introduction

Thus far, the host's response to bacterial infection has been the focus of this project. Identifying the causative organism(s) of a neurosurgical CSF infection is equally important. As previously mentioned, the first test performed on a neurosurgical CSF sample is usually simple microscopy, where a CSF cell count and Gram stain is performed. This is followed by microbiological culture which can be further tested for sensitivity to antibiotics. The results of these tests can take between two and ten days to be reported to the clinician.

The interpretation of neurosurgical CSF cell parameters was explored in Chapter 1 (Section 1.5.4.6). A fifth of *infected* neurosurgical CSF samples have a "normal" white cell count(WCC) <5 cells/mm^3 [231]. We know that gram-positive bacteria are more common pathogens in neurosurgical patients (e.g., *S. aureus, S. epidermidis*) and that these bacteria often cause a less pronounced rise in WCC than gram-negative bacteria (e.g., *P. aeruginosa*)[237]. Up to 80% of CSF samples from definite neurosurgical CSF infections do not have detectable bacteria on Gram stain on initial examination [238] which can mean that there is a delay of days until a causative bacterium may be identified.

An essential step in managing an infection is the timely delivery of appropriate antimicrobials. Broad spectrum antibiotics are often prescribed when there is a reasonable clinical suspicion of neurosurgical CSF infection. These are later rationalised once culture results are confirmed (targeted antibiotic prescription is essential in the setting of rising bacterial resistance to antibiotics[506]). The duration of treatment is influenced by the

causative bacteria, gram-positive bacteria usually require treatment regimens of 10-14 days whereas gram-negative organisms require a longer, 21 day, course of antibiotics[507].

Multiplex PCR test kits for a panel of pathogens are available for community acquired meningitis/encephalitis but as seen in Chapter 1, (Section 1.5.4.6.4) these tests are not of much utility for neurosurgical CSF infection as they do not test for the bacteria that most commonly cause neurosurgical CSF infections. PCR tests use primers (targeting known sequence of bacteria/viruses known to cause meningitis) to identify whether a pathogen is present in a sample; an alternative approach would be the non-targeted sequencing of all genetic material in a sample with identification of any/all potential pathogens/ organisms present in the CSF.

5.1.1 Genome sequencing

The information needed for the formation and maintenance of every living organism is found in its genetic code, which is contained in the deoxyribonucleic acid (DNA) of the organism. DNA is a large molecule made up of smaller subunits, nucleotides which when bound together form chains (polynucleotide chains) (Fig.69). In bacteria, genomic information is contained in circular molecules of double stranded DNA, with some bacteria also containing additional DNA in plasmids [508].

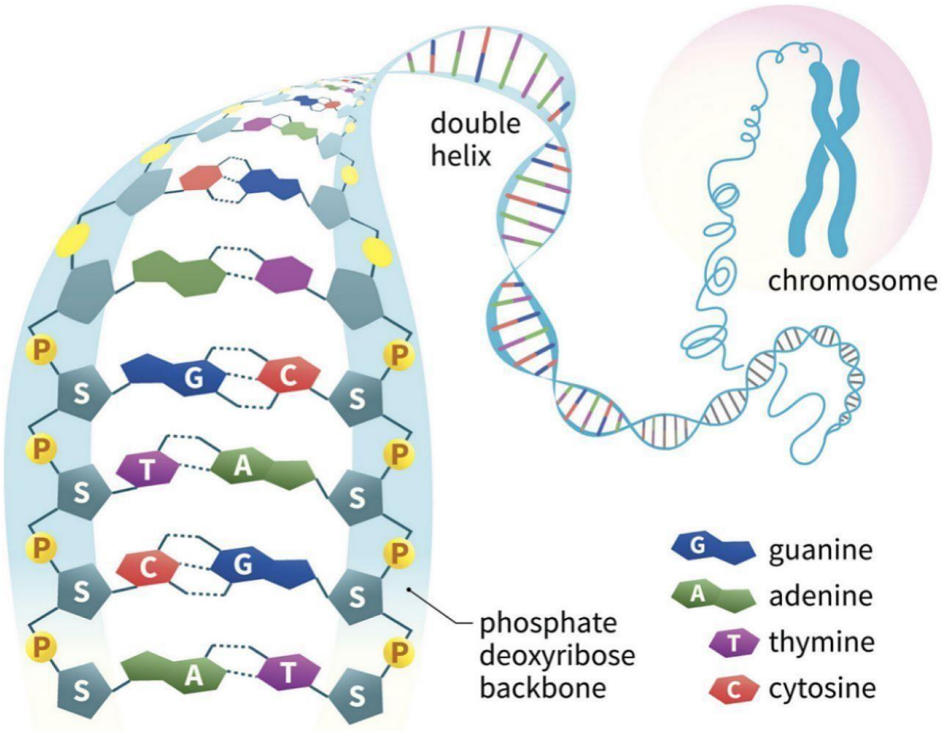

Figure 64 DNA structure: The nucleotides/bases are guanine (dark blue), adenine (green), thymine (purple) and cytosine (red). The double-helix of DNA is made up of two polynucleotide chains. These chains are bound by the hydrogen bonds formed between the nitrogen containing bases of the nucleotides (adenine- A with thymine-T and cytosine-C with guanine- G). DNA was discovered in 1869 by the Swiss chemist Friedrich Miescher, the double-helix was described by Watson and Crick in 1953 earning them a Nobel prize [500], which overlooked the brilliant Rosalind Franklin whose x-ray images of DNA were pivotal but not credited [509].

The order of the nucleotides in DNA is the DNA *sequence* of an organism. Sequencing, the process of determining the DNA sequence, was initially a slow and labour-intensive task. The dominant technique for sequencing in the 80's and 90's was Sanger sequencing. Sanger sequencing is a chain termination technique where small quantities of a chemically altered nucleotide is included, which when incorporated stops further polymerisation of the chain (Fig. 70). The addition of the chain terminating nucleotide occurs at random and so a mixture of chains of varying lengths is produced. The fragments can be separated by gel or capillary electrophoresis and the sequence inferred from the position of the terminating nucleotide. Initially the nucleotides were radiolabelled with a radioisotope, this has mostly been supplanted by fluorescent dyes.[510]

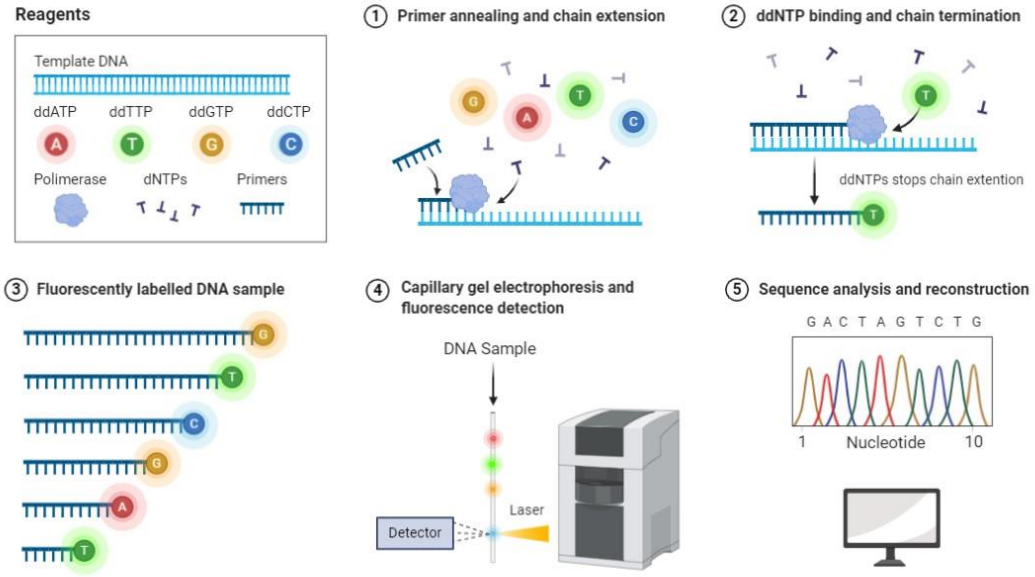

Figure 65 Diagram of Sanger sequencing. For this method there are four differentially fluorescent dye-labelled nucleotides that have been chemically altered (dideoxynucleotides: ddNTPs), one for each base (A, T, C, G; ddATP, ddTTP, ddGTP, ddCTP). Each reaction includes the template DNA to be sequenced (light blue), polymerase enzyme to catalyse the reaction, nucleotides (dNTPs), primers and ddNTPs. In step ①, the primer attaches to the denatured DNA (the double stranded DNA is heated to separate the strands and expose the bases). Polymerase catalyses the addition of nucleotides to the primer (chain extension). In step ② ddNTP is added to the chain, this lacks a hydroxyl group necessary for further nucleotides to be added and so the chain is terminated. The ddNTPs are incorporated at random and so chains of varying lengths are produced (Step ③). In step ④ capillary gel electrophoresis is used to separate the chains by size and the ddNTPs are excited by a laser to produce a colour signal which the detector records. The sequence of bases can be computed from the data collected, step ⑤.

Sanger sequencing is limited to DNA fragments ~750 bp but is cheap and reliable and continues to be used to this day[511]. In fact, an automated form of Sanger sequencing was used for the Human Genome Project. The International Human Genome Sequencing Consortium completed a draft sequence of the human genome on the 26th of June 2000, the final version of the sequence was released in April 2003. Approximately three billion nucleotides were sequenced, over 13 years at a cost of $2.7 billion. Technologies progressed rapidly during the project and aided it coming in ahead of time and below budget[512, 513].

Specific to bacterial identification is a method called 16S sequencing. The 16S ribosomal ribonucleic acid (rRNA) gene encodes for 16S rRNA which is a structural component of a bacterial and archaeal ribosomal subunit which is essential for the initiation of protein synthesis amongst other functions[514]. The gene is highly conserved and 16S Sanger sequencing (and other iterations of sequencing technologies) has been used for the identification of bacterial species for decades but it has biases and limitations[515], which influenced our decision to eschew it as a modality for this experiment:

- 16S is poorly adapted to identify more than one bacterial species (an issue for polymicrobial infections)
- The choice of primers can significantly impact the sensitivity and specificity of the amplification
- Differentiation at species level for some bacterial genera is difficult, e.g., *Staphylococci, Enterococci*
- 16S cannot identify genes associated with antibiotic resistance

In subsequent years, next generation sequencing (NGS) which is also called massively parallel sequencing developed. *Illumina* has dominated this market in the recent past with their sequencing by synthesis platform. The basic process for sequencing by synthesis is briefly explained in Fig. 71. The process of read alignment is improved by paired-end sequencing. These paired-end reads provide high-quality alignment particularly across DNA regions containing repetitive sequences [516].

Illumina has a range of sequencing platforms available which have different capabilities and capacities, summarised in Table 48.3.

Table 48 Illumina *NGS platforms. Some of the current sequencers available from* Illumina.*[516]*

	iSeq 100	MiniSeq	MiSeq Series	NextSeq 550 Series	NextSeq 1000&2000
Run Time	9.5–19 hrs	4–24 hours	4–55 hours	12–30 hours	11-48 hours
Maximum Output	1.2 Gb	7.5 Gb	15 Gb	120 Gb	330 Gb*
Maximum Reads Per Run	4 million	25 million	25 million †	400 million	1.1 billion*
Maximum Read Length	2 × 150 bp	2 × 150 bp	2 × 300 bp	2 × 150 bp	2 × 150 bp

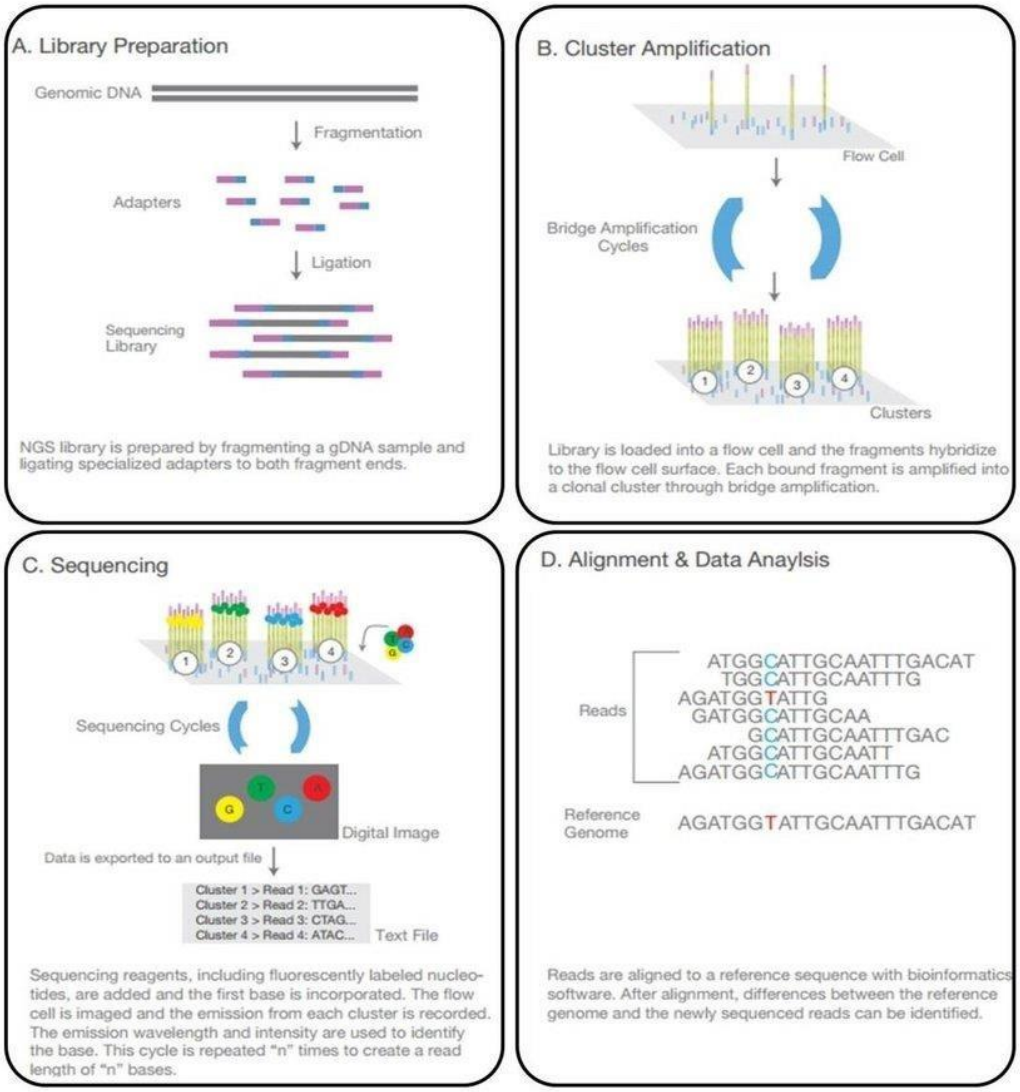

Figure 66 Sequencing by synthesis summary by Illumina *Inc.[516]. Samples are processed prior to sequencing with a library preparation step (A). In this step DNA is fragmented, sorted by size and adaptor sequences are added. When the sample is added to the flow cell the adapter binds to an oligonucleotide anchor (the flow cell is covered in a "lawn" of oligonucleotide anchors) as seen in (B) above. The bound DNA fragments are then amplified in situ: cluster amplification. With these clusters in place, sequencing then occurs by adding nucleotides (which have fluorescent labels). The emission wavelength of the nucleotide added is measured which identifies the base that has been incorporated (i.e., G/C/A/T). This process is repeated over numerous cycles resulting in millions of "reads" of bases (the DNA fragment sequences). These data are then cleaned- removing the known adaptor sequence and aligning the reads informatically to form a long read of the genetic sequence (D). The discovered DNA sequence may then be compared with known DNA sequence to identify the organism- e.g., human/viral/bacterial DNA databases.*

The main alternative to sequencing by synthesis currently, is nanopore sequencing (Fig. 72). In this method a nanopore (a nanometre sized protein which forms a pore) is embedded in a membrane with differential electrolyte solution on either side. Electrical current is measured continuously as a single molecule (e.g., DNA) passes through the nanopore. As each base passes through, there is a characteristic decrease in the current amplitude- thus allowing base calling. This method does not require amplification of the target DNA or labelling and produces longer sequence reads[517].

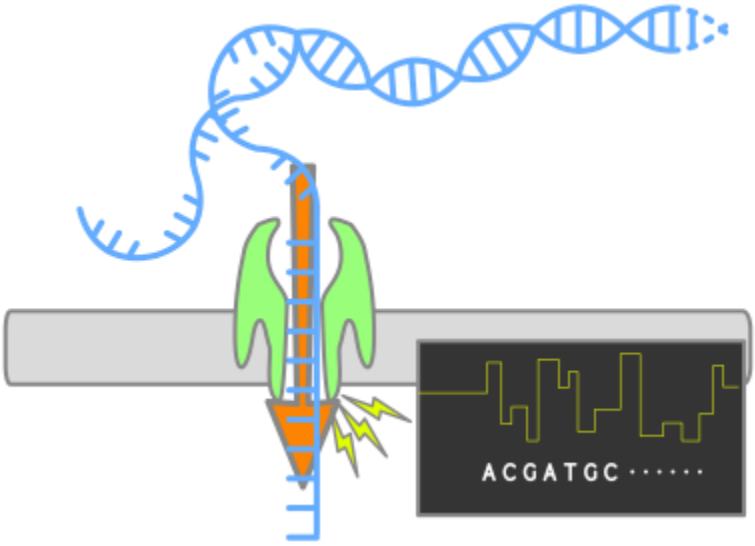

Figure 67 Illustration of the process of nanopore sequencing. The DNA molecule (blue helix) is denatured to a single strand. This passes through the nanopore (green) embedded in a membrane (grey). The current is continuously monitored as the single stranded DNA passes through. The change in current amplitude is seen as a yellow line in the black output box[518].

For the purposes of this project *Illumina*, sequencing by synthesis was used to sequence clinical CSF samples. This was performed by the Centre for Genomic Research (CGR) at the University of Liverpool.

5.1.2 Metagenomics for CSF infection

The plan for this experiment was to sequence all nucleic acid in clinical CSF samples. The resulting sequences would then be compared against a human reference genome. All human sequence would be removed bioinformatically. The remaining sequence would then be compared to known bacterial sequences in a bid to identify organisms. This is a metagenomic approach; that is the study of a community of organisms [519].

Metagenomics is fast developing as a clinically useful testing strategy, beyond the world of the research laboratory.[520]

The first report of a case where the diagnosis of CSF infection was confirmed using metagenomics was published in 2014 by *Wilson et al*- neuroleptospirosis was identified on NGS for a critically ill patient where all conventional testing had been negative. This was achieved in a clinically actionable timeframe which affected the treatment regimen [521]. Since then, metagenomic analysis of CSF infection in the clinical setting has continued to be employed for cases where diagnosis has been especially difficult (Table 50) [522, 523];

Table 49 Case reports of causative pathogens identified by metagenomics in cases of meningitis

Viral	Bacterial	Fungal	Other
Cache valley virus **[524]**	*Capnocytophaga canimorsus [525]*	*Aspergillus oryzae*[526]	*Taenia solium [526, 527]*
Chikungunya virus **[528]**	*H. influenzae [529]*	*Candida dubliniensis [526]*	
Echovirus 17 **[530]**	Neurobrucellosis [531]	Cryptococcal meningitis [526, 532]	
HIV **[526]**	*Nocardia farcinica* [533]	*Histoplasma capsulatum [526]*	
Powassan virus **[534]**	*C. acnes* [535]		
Torque teno virus **[536]**	*Psychrobacter Spp*. [537]		
Toscana virus **[538]**	*Ureaplasma parvum [539]*		
West nile virus **[540]**			

Neurosurgical CSF infections are, as laid out in Chapter 1, not common but they are a serious problem both biologically and economically. Current testing often fails to identify a causative organism, or the result is delayed by two to ten days. Could metagenomics potentially fill this diagnostic gap?

Can we identify the bacteria grown on routine culture via sequencing? If we cannot identify bacteria grown on the gold standard culture, then what utility can NGS have for culture negative samples?

Can we identify bacteria in culture negative samples that have a high WCC and a clinical diagnosis of infection with NGS?

5.2 Materials & Methods

5.2.1 CSF

All CSF samples used in this experiment were from the salvaged CSF collection. Four infected CSF samples and 4 uninfected CSF samples were used to assess if adequate *bacterial* DNA could be extracted for further sequencing (Table 50). In addition to these CSF samples sterile water and DES were also extracted as negative controls and two aliquots of *S. aureus* broth (provided by Dr Tessa Prince, post-doctoral researcher with the Liverpool Brain Infection Group, University of Liverpool) were extracted as positive controls.

Table 50 Samples used to assess if bacterial DNA is extractable from stored CSF samples.

Sample	Culture	WCC	RCC
1	*S. haemolyticus*	355	253
2	*E. faecalis*	434	62
3	*S. epidermidis & S. haemolyticus*	538	96
4	*E. cloacae*	850	90
5		<1	4
6		<1	12
7		1	<1
8		<1	140
9	H2O		
10	DES		
11	*S. aureus*		
12	*S. aureus*		

For the main sequencing experiment there were ten samples from cases where there was a *Definite Infection* (clinical infection noted, high WCC and a positive culture). Ten samples had high WCC but there was no growth on CSF culture and were included as *Possible Infections*. A further ten samples were from cases where there was no infection suspected (*Uninfected*), nothing grew on culture and the WCC was low (Table 51). The culture results

and cell counts for these samples were supplied with the samples from the LCL. How bacterial identification is confirmed by LCL are detailed in Chapter 2, section 2.2.1.

Table 51 CSF samples for NGS. The bacteria identified on culture are presented as reported by the microbiology laboratory to the treating clinicians (e.g., Definite Infection 8 grew a Pseudomonas *but the species was not reported).*

Sample	Culture	WCC	RCC
Definite Infection 1	*S. haemolyticus*	588	80
Definite Infection 2	*E. faecalis*	434	62
Definite Infection 3	*S. simulans*	Clotted	
Definite Infection 4	*S. epidermidis*	1580	2500
Definite Infection 5	*S. haemolyticus & S. epidermidis*	570	80
Definite Infection 6	*E. faecalis*	434	62
Definite Infection 7	*S. aureus*	3960	720
Definite Infection 8	*Pseudomonas*	Clotted	
Definite Infection 9	*S. aureus*	3960	720
Definite Infection 10	*E. coli*	292	6020
Possible Infection 11		140	6
Possible Infection 12		906	220
Possible Infection 13		1230	12
Possible Infection 14		3388	280
Possible Infection 15		1420	<1
Possible Infection 16		244	78
Possible Infection 17		532	8
Possible Infection 18		12540	1440
Possible Infection 19		2644	10
Possible Infection 20		5940	120
Uninfected 21		<1	4
Uninfected 22		<1	20
Uninfected 23		2	26
Uninfected 24		<1	4
Uninfected 25		1	<1
Uninfected 26		<1	4
Uninfected 27		<1	<1
Uninfected 28		<1	<1
Uninfected 29		<1	12
Uninfected 30		<1	2

5.2.2 Nucleic Acid Extraction

DNA was extracted from CSF using the Fast DNA Spin Kit for Soil (SKU:116560200-CF, MP Biomedicals). The procedure for this is described in detail in Chapter 2 section 2.3.4.

All DNA extracts were checked for DNA concentration using Qubit high sensitivity dsDNA kit (Q33230, ThermoFisher Scientific). DNA extract was added to buffer/dye mix. This was mixed thoroughly and gently and placed in the Qubit fluorimeter, which had been calibrated with high and low concentration standards using ds DNA machine settings (Chapter 2, section 2.3.4).

5.2.3 Assessment of bacterial DNA extract

To assess whether adequate *bacterial* DNA would be extractable from the stored salvaged CSF, eight samples had DNA extracted as above. Extracted DNA was amplified using 16S primers (V3/V4 region; oligos 319F, 806R, HPLC; Integrated DNA Technologies, USA) and the RoVI (Rotavirus Vaccine Immunogenicity: Impact of maternal antibodies & microbiota Study) standard operating procedure. This is described in section 2.3.4. This protocol was used as it was originally developed in the University of Liverpool as part of a larger study which assessed the microbiome in breast milk and faeces (samples with very different quantities of genetic material present)[319]. Breastmilk is a paucicellular fluid where bacteria are not normally found in significant numbers (Total cell count for breast milk is ~30-8000 cells/mm^3[541]).

A PCR mix was first prepared; *NEBNext* Q5 Hot Start HiFi PCR Mastermix (New England Biolabs Inc, M0544S), 10 µM 319F primer, 10 µM 806R primer, BSA and nuclease free water. Then the PCR mix was added to the whole DNA in a labelled PCR tube and briefly spun. PCR was performed in an Eppendorf Thermal Cycler (conditions seen in Chapter 2, section 2.3.4, Table 29).

Gel Electrophoresis

Extracted and amplified DNA was visualised using gel electrophoresis. This was done to ensure that usable DNA fragments had been extracted from the samples. A gel was prepared with agar, 0.5% TBE buffer and SYBR™ safe DNA gel stain (ThermoFisher

Scientific, USA, S33102) as described in section 2.3.3.3. E-Gel™ 1 Kb Plus DNA Ladder (5 µL, ThermoFisher Scientific, USA, catalogue number 10488090) was added to the first and last wells of the gel. For each sample 1 µL of GelPilot DNA Loading Dye (Qiagen, Germany, catalogue number 239901) and 5 µL of sample was carefully mixed and pipetted into a well and the position recorded.

The gel was placed in an electrophoresis chamber (Appleton Woods, UK), TBE was topped up to cover the surface of the gel, Thermo EC 250-90 positive and negative electrodes were attached, and machine was set to 100 V for one hour. The gel was then removed and placed in an UV trans-illuminator (Syngene Ingenius, UK).

Sanger Sequencing

Extracted and amplified DNA was further assessed by Sanger sequencing using the Eurofins Sanger sequencing service (see Chapter 2, section 2.3.3.4). This was not used to confirm whether bacterial DNA was present, this was done to ensure that the extraction process had yielded DNA of enough quality/quantity to allow for deep sequencing. Nanodrop analysis is available in our laboratory, but Sanger sequencing was felt to give more reliable results.

5.2.6 Next Generation Sequencing

DNA for sequencing was transferred to the CGR, University of Liverpool on dry ice. The extracted DNA from 10 Definite Infection samples, 10 Possible Infection and 10 Uninfected samples were used. No separate positive/negative controls were used for the sequencing experiment. This was due to budgetary constraints and it was felt that the Uninfected samples would act as a negative control.

The 30 genomic DNA samples were submitted for library preparation (using *Illumina NEBNext* Ultra II FS), completed by Edith Vamos. Following the manufacturer's protocol, 20ng of DNA was used as input material where available, followed by size selection of adaptor-ligated DNA. The libraries were purified after ten cycles of amplification using Ampure XP beads. Qubit was used to quantify each library and the Fragment analyser was used to assess the size distribution.

Equimolar amounts of the final DNA libraries were then pooled (using the Qubit and Bioanalyzer data). Bioanalyzer and then qPCR (using the *Illumina* Library Quantification Kit from Kapa (KK4854) on a Roche Light Cycler LC480II according to manufacturer's instructions) were used to assess the quantity and quality of each pool.

PCR thermal cycling conditions consisted of initial denaturation at 95°C for 5 minutes, 35 cycles of 95°C for 30 seconds (denaturation) and 60°C for 45 seconds (annealing and extension), melt curve analysis to 95°C (continuous) and cooling at 37°C (*LightCycler*® LC48011, Roche Diagnostics Ltd, Burgess Hill, UK).

The molarity was calculated using the qPCR data. Then template DNA was diluted to 300pM and denatured for eight minutes at room temperature using freshly diluted 0.2 N sodium hydroxide (NaOH), which was terminated by the addition of 400mM TrisCl, pH=8.
1% PhiX was spiked in to improve sequencing quality control.

The libraries were sequenced on an *Illumina*® *NovaSeq 6000* (*Illumina*®, San Diego, USA) by Charlotte Nelson of the CGR, following the XP workflow on 1 lane of an S4 flow cell and generating 2 x 150 bp paired-end reads.

5.2.7 Data Analysis

Bioinformatic analysis was performed by Matthew Gemmell of the CGR, University of Liverpool.

Initial data processing

Sequencing data underwent processing and quality assessment using a pipeline developed in-house in the CGR by Richard Gregory. This used the proprietary *Illumina* software CASAVA, version 1.8.2 to convert the colorimetric signal of sequencing to base calls, demultiplex indexed reads and convert data to the *FASTQ* format. *Cutadapt* version 1.2.1 [321] was then used to trim the Raw *FASTQ* data files- removing the *Illumina* adapter sequences. *Sickle* version 1.200 was used to further trim data of any low-quality bases (window quality score <20).

Bacterial identification

Bacterial identification was performed using *Kraken 2* and the relative abundance of each identified bacterium was estimated using *Bracken* (Bayesian Re-estimation of Abundance with Kraken)[323, 542, 543]. For these processes it was necessary to exclude sequence with

read lengths less than 100 base pairs, which was achieved by filtering read lengths with the tool *fastp* with the option "--length-required 100"[322].

A database for use with *Kraken 2* was then created including the "bacteria", "viral", "archaea", and "human" *Kraken* libraries. This database had a default k-mer length of 35. From this database a *Bracken* database was built. An ideal read length of 100 was used, hence the 100bp minimum length filtering. Paired reads were classified with *Kraken 2* using the *Kraken 2* database. [323] *Kraken 2* carries out taxonomic classification of short DNA reads by examining the k-mers within a read and querying a database with those k-mers.

Bracken (Bayesian Re-estimation of Abundance with KrakEN) was used with the results of the *Kraken 2* read classification to compute the abundance of classified species (Lu et al, 2017). *Bracken* output only contains the name at the specified taxa level (e.g., species) and taxon id. Therefore, the tool Taxonkit was used in conjunction with the taxon id to generate the lineages of each classified species [324, 325].

5.3 Results

5.3.1 Nucleic Acid Extraction

Seven of the ten Infected samples, half of the Possible samples and one of the Uninfected samples had measurable concentrations of DNA extracted (Table 52).

Table 52 Qubit measurement of concentration of ds DNA (ng/ mL) Seven of the ten infected CSF samples had a measurable concentration of DNA, half of the ten possible infection CSF samples and only one uninfected had measurable DNA on qubit (high sensitivity dsDNA kit, Q33230, ThermoFisher Scientific) which can quantify dsDNA in concentrations from 10 pg/µL to 100 ng/µL. "Low" results were either below the limits of detection of this assay or no dsDNA was present.

Status	Culture	WCC	RCC	Qubit result (pg/µL)
Definite Infection 1	*S. haemolyticus*	588	80	Low
Definite Infection 2	*E. faecalis*	434	62	Low
Definite Infection 3	*S. simulans*	Clotted		6.07
Definite Infection 4	*S. epidermidis*	1580	2500	23.2
Definite Infection 5	*S. haemolyticus & S. epidermidis*	570	80	1.19
Definite Infection 6	*E. faecalis*	434	62	Low
Definite Infection 7	*S. aureus*	3960	720	20.5
Definite Infection 8	*Pseudomonas*	Clotted		19.2
Definite Infection 9	*S. aureus*	3960	720	20.5
Definite Infection 10	*E. coli*	292	6020	11.8
Possible Infection 11		140	6	Low
Possible Infection 12		906	220	Low

Possible Infection 13		1230	12	2.13
Possible Infection 14		3388	280	0.7
Possible Infection 15		1420	<1	23.8
Possible Infection 16		244	78	Low
Possible Infection 17		532	8	0.8
Possible Infection 18		12540	1440	45.5
Possible Infection 19		2644	10	Low
Possible Infection 20		5940	120	Low
Uninfected 21		<1	4	Low
Uninfected 22		<1	20	Low
Uninfected 23		2	26	Low
Uninfected 24		<1	4	Low
Uninfected 25		1	<1	Low
Uninfected 26		<1	4	Low
Uninfected 27		<1	<1	Low
Uninfected 28		<1	<1	1.31
Uninfected 29		<1	12	Low
Uninfected 30		<1	2	Low

5.3.2 Assessment of bacterial DNA

Separate to the samples for full sequencing, eight CSF samples underwent DNA extraction. This DNA was amplified with V3/V4 primers and run on a gel, Fig. 73. DNA extract was also sent for Sanger sequencing, this is included in the Appendix C.

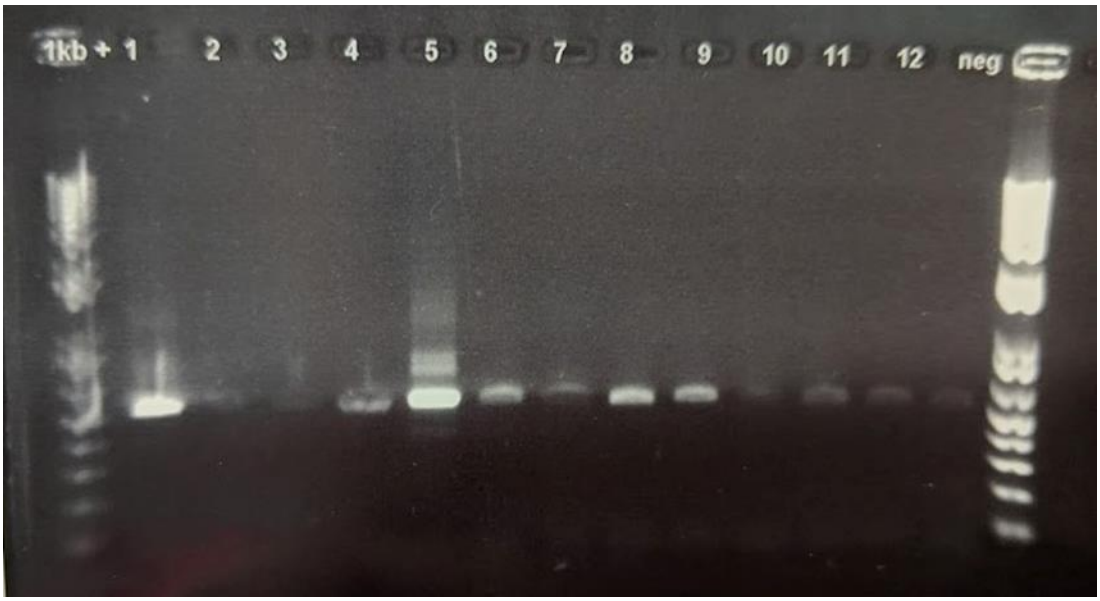

Figure 68 Extracted DNA, amplified with 16S V3/V4 primers and separated on gel by electrophoresis. The first and last channels have DNA ladders (fragments of DNA of known length- 100-1000 base pairs). Lanes 1-4 have DNA extracted from Infected *CSF samples, 5-8 are* Uninfected *samples, 9 & 10 are positive controls (9 is a community microbial standard, 10 is S. aureus broth) and 11 & 12 are negative controls (11 is water, 12 is DNA extraction solution). Whilst samples 5-8 are uninfected, they are human CSF samples from neurosurgical*

patients and as such will contain cells/cell fragments/proteins, which is likely why there is a visible band for these. Sample 2 and 3 (infected) have disappointing bands for samples that are meant to have high cell counts. The positive control (sample 9, community microbial standard) appears to have worked well. The S. aureus *broth extraction does not appear to have worked well. In fact, the band visible on the "negative" controls is clearer that the "positive" control,* S. aureus *broth extraction. This may be due to my lack of experience with the processes or running the gel electrophoresis.*

5.3.3 NGS library preparation

None of the Uninfected samples passed library preparation. Samples Possible Infection 11, Possible Infection 12 and Possible Infection 19 failed library preparation (Fig. 74).

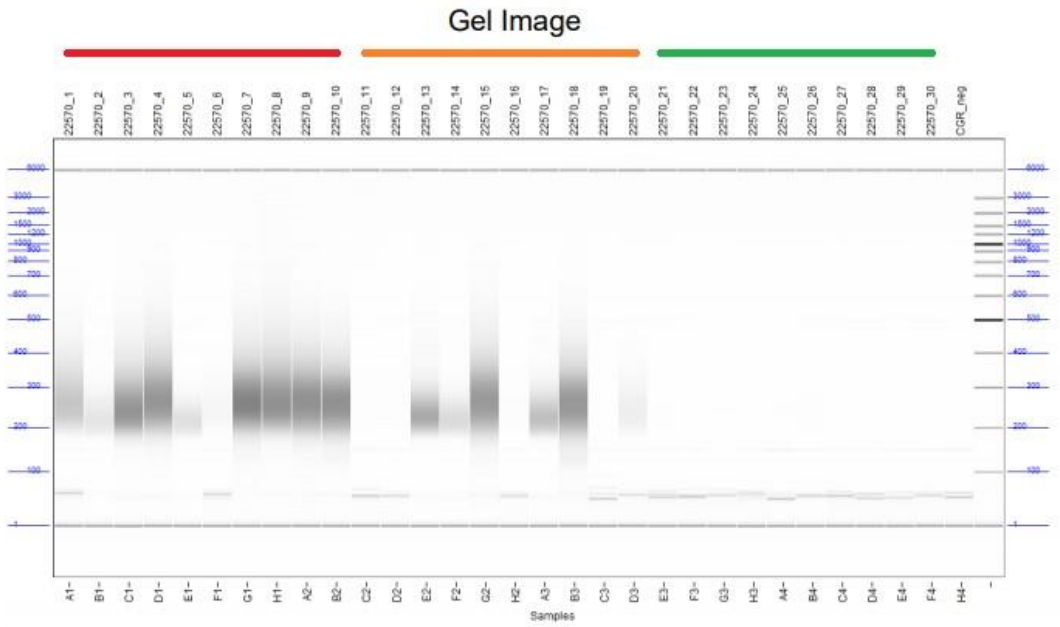

Figure 69 Analysis of DNA fragments (i.e., of library preparation of samples) performed using Fragment Analyser, PROSize 3.0 (Aligent, United States). This analyses DNA fragments between 1 and 6000 base pairs. The ten lanes below the ***red*** *bar are samples 1-10 (*Definite Infection*), the ten lanes below the* ***orange*** *bar are samples 11-20 (*Possible Infection*) and the lanes below the* ***green*** *bar are samples 21-30 (*Uninfected*). Samples 11, 12, 19 and all the uninfected samples (21-30) failed library preparation.*

5.3.4 Sequencing

All 30 samples were sequenced. There was a difference in the read count between the *Uninfected* group and the *Definite Infection*/*Possible Infection* group samples, see Fig. 75.

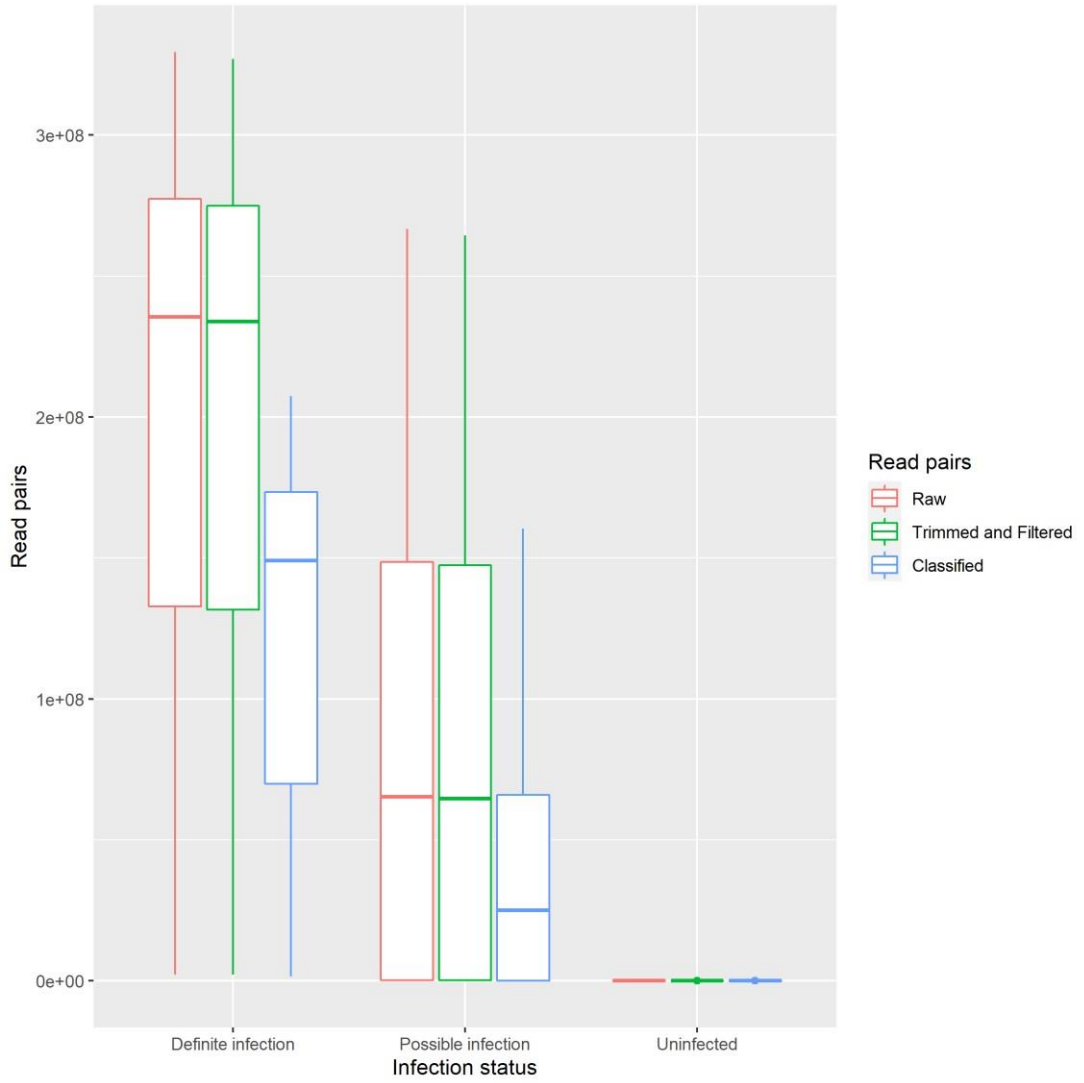

Figure 70 Read counts by group. Definite Infection= clinically and laboratory confirmed infection, samples 1-10. Possible Infection= Suspicious for infection, high WCC but culture negative, samples 11-20. Uninfected samples= no clinical or laboratory suspicion of infection, samples 21-30.

Table 53 shows the number of reads retained after length filtering (removing all read pairs with less than 100 base pairs). Most of the *Uninfected* samples (S21-30) had a high amount of filtering (<70% of trimmed reads retained). The majority of trimmed and filtered reads were classified. For the *Definite Infection* samples (S1-S10) and *Possible Infection* (S11-S20) each sample had > 89% classification with most at >98%. The *Uninfected* samples (S21-S30) had lower classifications (57.45%-98.9%) with most having a % classification between 70 and 90.

All 30 samples had multiple bacteria identified. To more clearly present the bacteria identified and their relative abundance in the *Definite Infection* and *Possible Infection* groups, these groups of samples are presented without the *Uninfected* group in Fig. 76.

The top ten bacteria by relative abundance for *Definite Infection*, *Possible Infection* and *Uninfected* groups are presented in Table 54, 55 and 56.

Table 53 Reads retained after length filtering. RP= read pairs

Sample	Trimmed Read Pairs (R1/R2)	Number Length Filtered Read Pairs (% of Trimmed RP)	Classified Read Pairs (% of Length Filtered RP Classified)
Definite Infection 1	186,599,861	144,936,712 (77.67)	143,628,878 (99.1)
Definite Infection 2	113,417,557	50,932,429 (44.91)	50,252,881 (98.67)
Definite Infection 3	222,985,734	130,368,704 (58.47)	129,048,581 (98.99)
Definite Infection 4	259,143,097	177,160,831 (68.36)	175,722,826 (99.19)
Definite Infection 5	100,414,013	31,958,820 (31.83)	31,439,926 (98.38)
Definite Infection 6	2,222,863	1,522,558 (68.5)	1,503,162 (98.73)
Definite Infection 7	244,573,206	155,934,840 (63.76)	154,613,390 (99.15)
Definite Infection 8	282,287,961)	185,569,986 (65.74	183,821,195 (99.06)
Definite Infection 9	327,017,015	209,196,458 (63.97)	207,369,499 (99.13)
Definite Infection 10	280,225,881	168,324,796 (60.07)	166,515,897 (98.93)
Possible Infection 11	51,571	36,860 (71.47)	35,219 (95.55)
Possible Infection 12	102,911	82,197 (79.87)	79,937 (97.25)
Possible Infection 13	153,966,421	69,195,374 (44.94)	68,092,227 (98.41)
Possible Infection 14	125,562,116	48,387,202 (38.54)	47,688,127 (98.56)
Possible Infection 15	264,420,965	161,920,525 (61.24)	160,479,879 (99.11)
Possible Infection 16	408,404	264,569 (64.78)	261,277 (98.76)
Possible Infection 17	127,672,128	60,316,269 (47.24)	59,584,707 (98.79)
Possible Infection 18	214,435,606	140,552,576 (65.55)	139,192,677 (99.03)
Possible Infection 19	16,667	10,506 (63.03)	9,372 (89.21)
Possible Infection 20	3,800,580	2,475,022 (65.12)	2,447,739 (98.9)
Uninfected 21	4,974	3,486 (70.08)	2,680 (76.88)
Uninfected 22	47,300	37,155 (78.55)	35,874 (96.55)
Uninfected 23	8,823	8,130 (92.15)	7,098 (87.31)
Uninfected 24	8,995	5,052 (56.16)	3,547 (70.21)
Uninfected 25	3,707	2,771 (74.75)	1,592 (57.45)
Uninfected 26	26,462	16,157 (61.06)	14,110 (87.33)
Uninfected 27	11,037	5,725 (51.87)	4,476 (78.18)
Uninfected 28	5,354	3,448 (64.4)	2,606 (75.58)

Uninfected 29	20,188	12,412 (61.48)	10,046 (80.94)
Uninfected 30	6,914	3,498 (50.59)	2,752 (78.67)

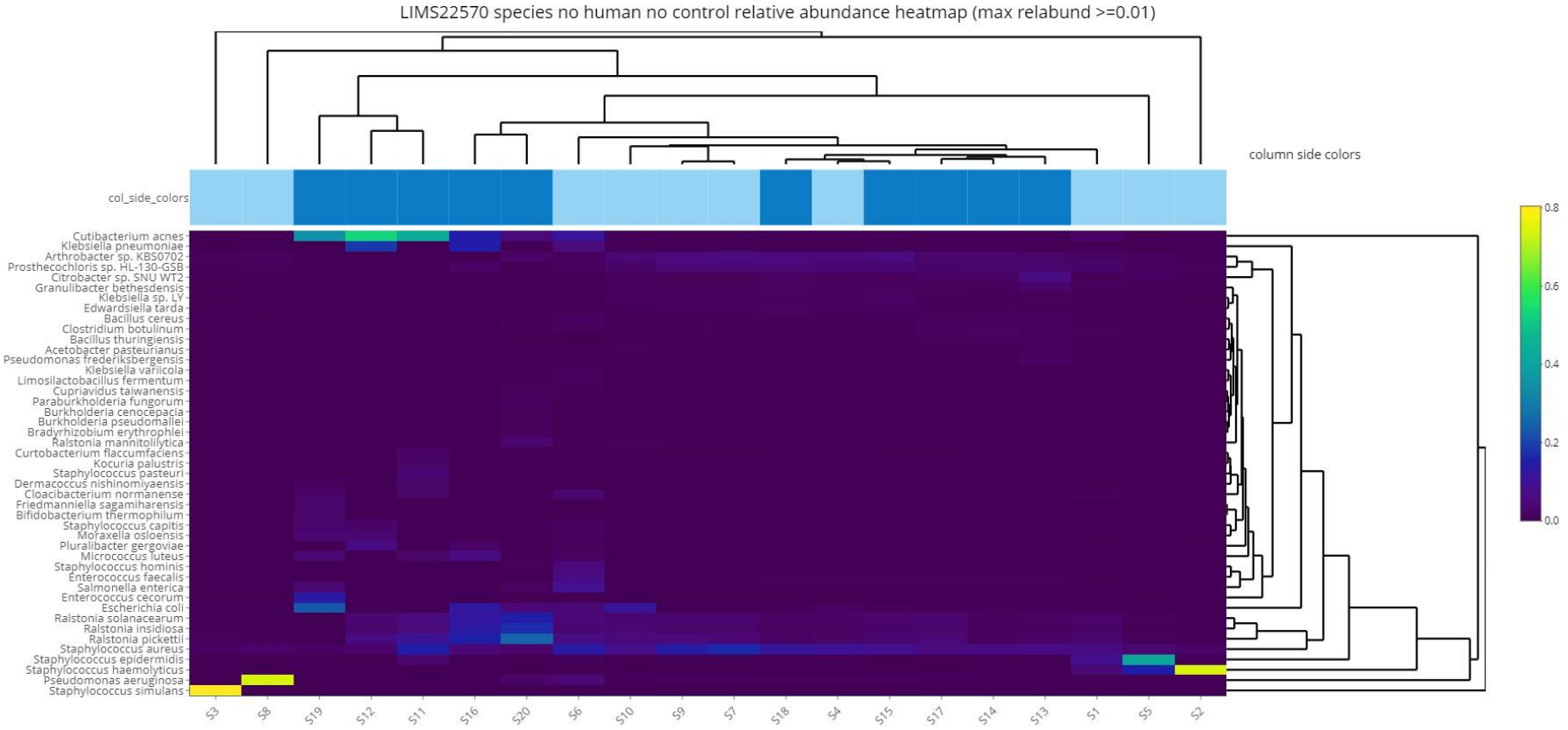

Figure 71 Heat map of bacterial sequence abundances. The first coloured row indicates the sample type- darker blue are samples 1-10, definite infections and light blue are samples 11-20 where infection was possible, but culture was negative. The colour legend to the right indicates the relative abundance of the bacterial sequence identified- higher relative abundance on the yellow end of the scale and lower relative abundance on the indigo end. The uninfected samples were not included in this figure.

Table 54 Top ten bacteria as identified by NGS for samples 1-10. Bacteria coloured yellow are the same as the bacteria identified on the original clinical culture. The number to the right of each identified bacterium is the percentage of the read count that mapped to that bacterium.

	Definite Infection 1		Definite Infection 2		Definite Infection 3		Definite Infection 4		Definite Infection 5	
1	*S. epidermidis*	1.03E-04	*S. haemolyticus*	3.38E-03	***S. simulans***	3.21E-03	*S. aureus*	6.25E-05	***S. epidermidis***	1.22E-03

2	*S. aureus*	8.05E-05	*S. aureus*	1.19E-04	*S. aureus*	7.98E-05	*Arthrobacter sp.* KBS0702	3.12E-05	***S. haemolyticus***	4.50E-04
3	***S. haemolyticus***	5.74E-05	Prosthecochloris sp. HL-130-GSB	3.91E-05	*R. pickettii*	3.91E-05	*Prosthecochloris sp.* HL-130-GSB	2.45E-05	*S. aureus*	1.16E-04
4	*Ralstonia pickettii*	4.60E-05	*S. hominis*	3.53E-05	*Arthrobacter sp.* KBS0702	3.36E-05	*R. pickettii*	1.66E-05	*Citrobacter sp.* SNU WT2	4.09E-05
5	Prosthecochloris sp. HL-130-GSB	3.20E-05	Arthrobacter sp. KBS0702	3.19E-05	R. solanacearum	3.04E-05	*R. solanacearum*	1.51E-05	*Arthrobacter sp.* KBS0702	3.89E-05
6	*R. solanacearum*	3.12E-05	*Citrobacter sp.* SNU WT2	2.67E-05	*Prosthecochloris sp.* HL-130-GSB	2.57E-05	*R. insidiosa*	1.17E-05	*Prosthecochloris sp.* HL-130-GSB	3.58E-05
7	*R. insidiosa*	3.11E-05	*R. pickettii*	2.44E-05	*R. insidiosa*	2.57E-05	*E. coli*	1.01E-05	*R. pickettii*	3.16E-05
8	*C. acnes*	3.07E-05	*R. solanacearum*	2.00E-05	*Citrobacter sp.* SNU WT2	9.80E-06	*Citrobacter sp.* SNU WT2	9.56E-06	*R. solanacearum*	2.44E-05
9	*Arthrobacter sp.* KBS0702	2.31E-05	*S. epidermidis*	1.97E-05	*S. haemolyticus*	8.38E-06	*G. bethesdensis*	8.52E-06	*R. insidiosa*	2.27E-05
10	*C. botulinum*	1.09E-05	*R. insidiosa*	1.76E-05	*Klebsiella sp.* LY	7.76E-06	*Klebsiella sp.* LY	8.20E-06	*C. botulinum*	2.00E-05
	Definite Infection 6		**Definite Infection 7**		**Definite Infection 8**		**Definite Infection 9**		**Definite Infection 10**	
1	*S. aureus*	3.19E-04	***S. aureus***	1.25E-04	***P. aeruginosa***	1.88E-03	***S. aureus***	1.19E-04	***E. coli***	1.15E-04
2	*C. acnes*	2.64E-04	*Arthrobacter sp.* KBS0702	4.10E-05	*S. aureus*	6.46E-05	*Arthrobacter sp.* KBS0702	4.41E-05	*S. aureus*	7.60E-05
3	*S. enterica*	2.14E-04	*Prosthecochloris sp.* HL-130-GSB	3.31E-05	Arthrobacter sp. KBS0702	3.73E-05	*R. pickettii*	4.06E-05	*R. pickettii*	5.31E-05
4	*R. pickettii*	1.55E-04	*R. pickettii*	3.29E-05	*Prosthecochloris sp.* HL-130-GSB	2.38E-05	*Prosthecochloris sp.* HL-130-GSB	3.56E-05	*Arthrobacter sp.* KBS0702	4.21E-05
5	***E. faecalis***	1.47E-04	*R. solanacearum*	2.63E-05	*R. solanacearum*	1.78E-05	*R. solanacearum*	2.90E-05	*R. solanacearum*	3.81E-05
6	*K. pneumoniae*	1.31E-04	*R. insidiosa*	2.09E-05	R. pickettii	1.70E-05	R. insidiosa	2.44E-05	R. insidiosa	3.55E-05
7	*S. hominis*	1.22E-04	*G. bethesdensis*	8.67E-06	*R. insidiosa*	1.23E-05	*G. bethesdensis*	9.41E-06	*Prosthecochloris sp.* HL-130-GSB	2.52E-05
8	*E. coli*	1.11E-04	*Klebsiella sp. LY*	8.36E-06	*G. bethesdensis*	1.02E-05	*Klebsiella sp.* LY	9.35E-06	*Citrobacter sp.* SNU WT2	1.22E-05
9	*P. aeruginosa*	1.06E-04	*Edwardsiella tarda*	7.48E-06	*Pseudomonas sp.* FDAARGOS_761	7.90E-06	*Edwardsiella tarda*	8.25E-06	*G. bethesdensis*	1.13E-05
10	*R. solanacearum*	1.05E-04	*P. aeruginosa*	6.76E-06	*Klebsiella sp.* LY	7.87E-06	*Citrobacter sp.* SNU WT2	6.90E-06	*Klebsiella sp.* LY	1.09E-05

Table 55 Top ten bacteria identified by NGS for samples 11-20. The number to the right of each identified bacterium is the percentage of the read count that mapped to that bacterium.

	Possible Infection 11		Possible Infection 12		Possible Infection 13		Possible Infection 14		Possible Infection 15	
1	*C. acnes*	9.33E-03	*C. acnes*	3.19E-03	*S. aureus*	7.57E-05	*S. aureus*	6.69E-05	*S. aureus*	6.22E-05
2	*S. aureus*	3.36E-03	*K. pneumoniae*	1.12E-03	*Citrobacter sp.* SNU WT2	6.84E-05	*Prosthecochloris sp.* HL-130-GSB	3.20E-05	*Arthrobacter sp.* KBS0702	4.09E-05
3	*R. pickettii*	2.20E-03	*R. pickettii*	3.90E-04	*Prosthecochloris sp.* HL-130-GSB	3.53E-05	*Arthrobacter sp.* KBS0702	3.13E-05	*R. pickettii*	2.69E-05
4	*R. insidiosa*	1.25E-03	*Pluralibacter gergoviae*	3.77E-04	*G. bethesdensis*	2.91E-05	*Citrobacter sp.* SNU WT2	2.30E-05	*Prosthecochloris sp.* HL-130-GSB	2.65E-05
5	*R. solanacearum*	1.22E-03	*Moraxella osloensis*	2.26E-04	*Arthrobacter sp.* KBS0702	2.64E-05	*C. botulinum*	1.75E-05	*R. solanacearum*	2.23E-05
6	*Staphylococcus pasteuri*	8.11E-04	*R. solanacearum*	2.14E-04	*R. pickettii*	2.44E-05	*R. pickettii*	1.66E-05	*R. insidiosa*	1.87E-05
7	*S. epidermidis*	7.53E-04	*R. insidiosa*	1.76E-04	*Pseudomonas frederiksbergensis*	2.06E-05	*R. solanacearum*	1.58E-05	*Klebsiella sp.* LY	1.15E-05
8	*Dermacoccus nishinomiyaensis*	6.08E-04	*S. aureus*	1.64E-04	*R. solanacearum*	1.91E-05	*Bacillus thuringiensis*	1.38E-05	*G. bethesdensis*	1.06E-05
9	*Kocuria palustris*	5.79E-04	*S. capitis*	1.51E-04	*R. insidiosa*	1.64E-05	*Bacillus cereus*	1.32E-05	*Citrobacter sp.* SNU WT2	8.23E-06
10	*Cloacibacterium normanense*	5.50E-04	*Pandoraea faecigallinarum*	0.00E+00	*Bacillus cereus*	1.24E-05	*R. insidiosa*	1.28E-05	*Edwardsiella tarda*	8.18E-06
	Possible Infection 16		**Possible Infection 17**		**Possible Infection 18**		**Possible Infection 19**		**Possible Infection 20**	
1	*R. pickettii*	2.80E-04	*S. aureus*	5.75E-05	*S. aureus*	7.59E-05	*C. acnes*	2.90E-02	*R. pickettii*	6.23E-04
2	*K. pneumoniae*	2.68E-04	*R. pickettii*	4.57E-05	*Arthrobacter sp.* KBS0702	3.50E-05	*E. coli*	1.94E-02	*R. insidiosa*	4.17E-04
3	*C. acnes*	2.65E-04	*R. solanacearum*	3.43E-05	*Prosthecochloris sp.* HL-130-GSB	3.13E-05	*Enterococcus cecorum*	1.16E-02	*R. solanacearum*	3.60E-04
4	*R. insidiosa*	2.42E-04	*R. insidiosa*	2.96E-05	*R. solanacearum*	1.36E-05	*S. enterica*	3.44E-03	*C. acnes*	1.20E-04
5	*E. coli*	2.22E-04	*Arthrobacter sp.* KBS0702	2.85E-05	*G. bethesdensis*	1.28E-05	*Micrococcus luteus*	3.33E-03	*E. coli*	1.07E-04
6	*R. solanacearum*	2.11E-04	*Prosthecochloris sp.* HL-130-GSB	2.60E-05	*R. pickettii*	1.25E-05	*Moraxella osloensis*	3.21E-03	*Ralstonia mannitolilytica*	8.96E-05
7	*Micrococcus luteus*	1.19E-04	*Citrobacter sp.* SNU WT2	2.06E-05	*Citrobacter sp.* SNU WT2	1.23E-05	*Friedmanniella sagamiharensis*	2.64E-03	*S. aureus*	7.77E-05
8	*S. aureus*	8.05E-05	*C. botulinum*	1.17E-05	*Klebsiella sp.* LY	1.00E-05	*Bifidobacterium thermophilum*	2.52E-03	*P. aeruginosa*	6.09E-05

9	*Pluralibacter gergoviae*	4.22E-05	*Bacillus cereus*	1.02E-05	*R. insidiosa*	9.76E-06	*Cloacibacterium normanense*	2.41E-03	*Arthrobacter sp.* KBS0702	5.52E-05
10	Prosthecochloris sp. HL-130-GSB	3.84E-05	*G. bethesdensis*	9.37E-06	*Edwardsiella tarda*	9.56E-06	*S. capitis*	2.29E-03	*S. enterica*	3.60E-05

Table 56 Top ten bacteria identified by NGS for samples 21-30. The number to the right of each identified bacterium is the percentage of the read count that mapped to that bacterium.

	Uninfected 21		Uninfected 22		Uninfected 23		Uninfected 24		Uninfected 25	
1	*C. acnes*	7.96E-02	*C. acnes*	8.02E-03	*R. pickettii*	3.17E-02	*C. acnes*	4.04E-02	*C. acnes*	9.49E-02
2	*Acinetobacter johnsonii*	2.79E-02	*A. baumannii*	7.59E-03	*C. acnes*	1.86E-02	*S. enterica*	3.78E-02	*K. pneumoniae*	9.41E-02
3	*Pseudomonas synxantha*	1.49E-02	*Cloacibacterium normanense*	2.49E-03	*R. insidiosa*	1.63E-02	*K. pneumoniae*	3.23E-02	*P. aeruginosa*	3.16E-02
4	*Micrococcus luteus*	1.12E-02	*R. pickettii*	1.22E-03	*K. pneumoniae*	1.60E-02	*E. coli*	2.13E-02	*S. enterica*	2.27E-02
5	*Moraxella osloensis*	9.78E-03	*Streptococcus mitis*	8.78E-04	*R. solanacearum*	1.41E-02	*P. aeruginosa*	1.94E-02	*R. pickettii*	2.19E-02
6	*Corynebacterium jeikeium*	7.45E-03	*S. aureus*	5.95E-04	*Ralstonia mannitolilytica*	3.73E-03	*Cloacibacterium normanense*	1.75E-02	*Pluralibacter gergoviae*	1.46E-02
7	*Pandoraea faecigallinarum*	0.00E+00	*Streptococcus gordonii*	5.10E-04	*Pandoraea faecigallinarum*	0.00E+00	*S. aureus*	1.62E-02	*S. aureus*	1.38E-02
8	*Helicobacter cholecystus*	0.00E+00	*R. insidiosa*	4.25E-04	*Helicobacter cholecystus*	0.00E+00	*K. grimontii*	1.23E-02	*Pandoraea faecigallinarum*	0.00E+00
9	*Haloquadratum walsbyi*	0.00E+00	*Veillonella parvula*	3.68E-04	*Haloquadratum walsbyi*	0.00E+00	*A. baumannii*	1.20E-02	*Helicobacter cholecystus*	0.00E+00
10	*Halomonas sp.* N3-2A	0.00E+00	*Gemella haemolysans*	2.83E-04	*Halomonas sp.* N3-2A	0.00E+00	*Micrococcus luteus*	1.13E-02	*Haloquadratum walsbyi*	0.00E+00
	Uninfected 26		Uninfected 27		Uninfected 28		Uninfected 29		Uninfected 30	
1	*C. granulosum*	1.12E-01	*Cloacibacterium normanense*	4.21E-02	*S. aureus*	5.43E-02	*S. enterica*	4.42E-02	*K. pneumoniae*	8.87E-02
2	*C. acnes*	2.27E-02	*E. coli*	4.13E-02	*C. acnes*	4.70E-02	*P. aeruginosa*	3.36E-02	*C. acnes*	6.64E-02
3	*K. pneumoniae*	1.67E-02	*C. acnes*	4.00E-02	*P. aeruginosa*	4.29E-02	*C. acnes*	3.28E-02	*S. enterica*	5.53E-02
4	*S. aureus*	1.28E-02	*P. aeruginosa*	1.88E-02	*E. coli*	3.92E-02	*K. pneumoniae*	2.66E-02	*Pluralibacter gergoviae*	3.30E-02

5	*P. aeruginosa*	1.19E-02	*S. enterica*	1.54E-02	*K. pneumoniae*	3.88E-02	*E. coli*	2.58E-02	*P. aeruginosa*	2.85E-02
6	*S. enterica*	1.15E-02	*R. pickettii*	1.15E-02	*Lactococcus lactis*	3.47E-02	*C. granulosum*	1.02E-02	*K. grimontii*	2.41E-02
7	*E. coli*	7.05E-03	*S. aureus*	7.84E-03	*S. enterica*	2.83E-02	*E. faecalis*	9.18E-03	*Cloacibacterium normanense*	2.14E-02
8	*Cloacibacterium normanense*	4.95E-03	*C. granulosum*	7.32E-03	*Streptococcus thermophilus*	1.78E-02	*S. aureus*	9.08E-03	*A. baumannii*	1.65E-02
9	*K. grimontii*	4.95E-03	*R. solanacearum*	6.27E-03	*Pluralibacter gergoviae*	1.41E-02	*K. grimontii*	6.70E-03	*Streptococcus thermophilus*	1.52E-02
10	*R. pickettii*	4.05E-03	*E. faecalis*	4.97E-03	*Micrococcus luteus*	1.32E-02	*Cloacibacterium normanense*	6.05E-03	*S. aureus*	1.34E-02

Table 57 Concordance between CSF culture and NGS. Samples where the bacterium identified as the top scoring match on NGS is the same as the bacterium identified on culture are coloured in green, samples where the bacterium identified on culture was within the top ten bacteria are coloured in yellow and the remaining samples coloured in blue had the bacterium identified on culture identified on NGS but not within the top ten.

	Culture	NGS
Definite Infection 1	*S. haemolyticus*	*S. epidermidis*
Definite Infection 2	*E. faecalis*	*S. haemolyticus*
Definite Infection 3	*S. simulans*	*S. simulans*
Definite Infection 4	*S. epidermidis*	*S. aureus*
Definite Infection 5	*S. haemolyticus & S. epidermidis*	*S. epidermidis*
Definite Infection 6	*E. faecalis*	*S. aureus*
Definite Infection 7	*S. aureus*	*S. aureus*
Definite Infection 8	*Pseudomonas spp.*	*P. aeruginosa*
Definite Infection 9	*S. aureus*	*S. aureus*
Definite Infection 10	*E. coli*	*E. coli*

5.4 Discussion

Bacteria identified by NGS

Using metagenomics, we were able to identify the bacteria grown on culture for all the samples included here. In six of the ten *Definite Infection* CSF samples the bacterium identified on culture was the same as the top scoring bacterium identified by NGS. *Definite Infection 1* and *Definite Infection 6* had the bacterium that was seen on culture identified by NGS but that bacterium was within the top ten bacteria identified. Whilst the top ten bacteria identified for *Definite Infection 2* and *Definite Infection 4* did not include the cultured bacterium, this is not to say that NGS failed to identify that pathogen. *E. coli* and *S. epidermidis* were identified by NGS for *Definite Infection 2* and *Definite Infection 4* respectively but their relative abundance did not rank them in the top 10 bacteria identified (Tables 54, 55, 56 and summarised in Table 57).

Prosthecochloris sp. HL-130-GSB was identified in the top ten most abundant bacteria for nine of the *Definite Infection* samples (Table 54). Prosthecochloris sp. HL-130-GSB was sequenced by *Thiel et al* from Pennsylvania State University, USA in 2017. It was isolated from a microbial mat in a salt lake in Washington, USA and is a slightly thermotolerant, anaerobic, photoautotrophic green sulphur bacterium[544].Six of the ten *Possible Infection* CSF samples had *Prosthecochloris* identified on their top ten NGS identified bacteria but none of the *Uninfected* CSF samples did (Table 55 and 56). Why would this be the case? The taxonomic classification of bacteria identified by NGS was achieved with a stringent and widely used method: *Kraken 2*. If it was a contaminant, then why is it not found in the uninfected samples? All 30 CSF samples used in this experiment are from the same hospital, taken using the same protocol, stored for very similar lengths of time, and prepared for sequencing in the same way. Why *Prosthecochloris* has been identified in the *Definite Infection* and *Possible Infection* groups and not the *Uninfected* group remains to be elucidated.

Within the *Possible Infection* group there were no cultured bacteria identified to compare the NGS results to. Five of the samples had *S. aureus* identified, three had *C. acnes* and the remaining two had *Ralstonia pickettii (Table 55).* All the *Definite Infection* samples had *R. pickettii* identified in their top ten bacteria (Table 54), nine out of the ten *Possible Infection*

samples similarly identified it in their top ten (Table 55), whereas five of the ten *Uninfected* samples identified it (Table 56).

Ralstonia spp. are aerobic, gram-negative, oxidase-positive, non-fermentative rods that are found in water and soil[545]. *R. pickettii* has been implicated in outbreaks of infection caused by contaminated sterile fluids; respiratory care solution [546], water for injection [547], chlorhexidine skin cleansing solution [548], heparin flushes [549], and saline solution [550, 551]. *R. pickettii* has also been associated with implant related infections- intravascular catheters [552, 553], silicone breast implants [554], and hip and knee implants [555].

Ralstonia spp. have traditionally been thought to be opportunistic pathogens, which cause infection in immunocompromised patients. It is possible that postoperative neurosurgical patients, in a relatively immunocompromised state due to steroid treatment or primary disease could contract *R. pickettii.* A particular concern for neurosurgeons implanting an indwelling neurosurgical drain or shunt is that *R. pickettii* is well known to produce a biofilm[556] and is frequently resistant to many antibiotics (aminoglycosides, aztreonam, colistin, ceftazidime, piperacillin–tazobactam, imipenem–cilastatin, ciprofloxacin, and sulphamethoxazole-trimethoprim) [557]. In fact, there is emerging evidence that *R. pickettii* infection with biofilm formation in breast implants may be associated with B-cell lymphomas [558, 559].

It is difficult to interpret the bacteria identified in *Uninfected* samples as the number of reads for these samples are very low (Figure 75, Table 53). The mean number of read pairs for the *Uninfected* samples was 14,375 (in comparison to the *Definite Infection* samples mean: 303,621,448 and *Possible Infection* mean: 89,043,737). The bacteria identified in the *Uninfected* group are likely to be contamination accrued by handling from the time of sampling in hospital to the microbiology laboratory to the sequencing facility.

Bacterial identification by culture is not perfect. Whole genome sequencing is the most precise way of identifying any organism and it provides ample data for further analysis of antimicrobial resistance (there are known gene adaptations that are associated with resistance).

In culture, bacteria are identified by a combination of Gram stain, morphology and biochemical reactions which can result in bacteria that look/behave similarly being misidentified. Many bacteria are difficult to culture or are currently unculturable[560]. As of

2020, there were only 3,252 bacterial species identified by culture from humans [561]. Bacterial genomics continues to surprise investigators with the evident biological diversity of the bacterial world[560]. It also challenges the traditional taxonomy of bacteria- a great example of this is the fact that *Shigella* (traditionally a genus in its own right, with 4 species) belongs genetically to the very diverse *E. coli* species[562].

We are also biased by the history of how we have come to understand infections. The process of microbiological culture is so fundamental to the diagnosis of infection and the assumption of most clinicians is that infection is caused by a single pathogenic bacterium in most infections. How can we be sure this is the reality? The process of bacterial culture is a very artificial set-up, much removed from the in vivo reality of the human body. Polymicrobial infections may be a more common problem than we believe. Our current strategy for treating infection is very generalised- many patients are started on broad spectrum antibiotics initially, with some rationalisation of the agents used once culture and sensitivity reports are available. Are we truly engaging in targeted treatment of infection or are we aiding the body in fighting a polymicrobial infection?

More precise identification of bacteria is here, sequencing offers huge amounts of data. A better understanding of the metagenomic profile of CSF, will establish the expected/acceptable amounts of bacterial DNA present in uninfected CSF. The CSF microbiome of both uninfected and infected CSF needs to be thoroughly explored. In the future we will be able to sequence clinical samples in real-time. Even at the moment if we were able to sequence samples on the day of sample collection, we could have results within 24 hours- which is quicker than most standard microbiological culture. We would also have information about the presence or absence of antimicrobial resistance genes which would guide antibiotic choice. This would be far quicker than standard sensitivity testing of bacterial strains grown on standard culture that then have to be re-plated on a sensitivity screening plate and allowed to grow again (often taking several days to yield results).

Samples

The CSF samples used here are representative of neurosurgical infections seen in scientific literature (Chapter 1, section 1.5.4.3). The *Definite Infection* CSF samples used in this experiment predominantly grew gram-positive bacteria on routine culture (80%). This is

very similar to the proportion of gram-positive bacteria seen in Chapter 2 (79% grampositive). This proportion of 4:1 gram-positive to gram-negative is again seen in the bacteria identified by NGS for the *Possible Infection* CSF samples. These samples were not chosen on purpose to maintain this proportion, they were merely the samples available with sufficient volume to use.

To assess if bacterial DNA was extractable from these clinical CSF samples 16S V3/V4 primers were used to amplify any bacterial sequence present in the DNA extracted from eight preliminary samples. The amplicons were then subjected to gel electrophoresis and Sanger sequencing. Bacterial DNA appeared to be present- the amplicon of each sample separated by gel electrophoresis showed- Fig. 73, Section 5.3.2. Sanger sequencing was reassuring that there was bacterial DNA in adequate amounts/ of adequate quality to allow for sequencing (data in Appendix C).

For the main experiment, the 30 CSF samples used had DNA extracted but no amplification of *16S* was performed- to allow for as unbiased an analysis as possible. The *Definite Infection* CSF samples had measurable concentrations of DNA on Qubit whereas the *Uninfected* samples did not. The *Possible Infection* samples lay somewhere in between (Table 52). Beyond DNA extraction all sample preparation and processing was undertaken by the CGR team. Whilst only *Possible Infection* Samples 11, 12, 19 and all the *Uninfected* samples (21-30) failed quality assessment, it can be seen on the gel image in Fig. 74 (section 5.3.3) that *Definite Infection 2, Definite Infection 6, Possible Infection 16,* and *Possible Infection 20* appear to have performed less well than the other infected samples. All the *Uninfected* samples failed pre-sequencing quality assessment; it is not clear why there was a measurable concentration of DNA in Uninfected 28 on qubit (which had very low numbers of reads as seen in Table 53). All samples went forward for sequencing.

Identifying a pathogen from a clinical sample has been described as a “needle in a haystack endeavour” as typically less than 1% of reads are non-human and only a subset of those correspond to potential pathogens [520]. Human tissue samples are understandably heavily dominated by human DNA. CSF is paucicellular by nature and is an attractive candidate for sequencing. Once the human sequence was identified in these samples and bioinformatically removed from the data, we were left with the microbiome sequence of the CSF tested. But how can a truly infecting bacteria be characterised and separated from environmental bacterial contaminant?

Kraken 2 compares sequence reads of a set length to a genome database to classify sequence reads (Fig. 77), *Bracken* (Bayesian Re-estimation of Abundance after Classification with KrakEN) probabilistically redistributes reads from the taxonomic tree created by *Kraken* to allow read abundance estimation at the species level. If sequence reads map to a strain of a bacterial species, for example, *Bracken* will redistribute these reads upwards along the taxonomic tree to the species level. Where a number of reads are assigned to a genus, *Bracken* will calculate the probable portion of those reads that are likely to be from each species within that genus[324]. This process allows the creation of a heat map like that seen in Figure 76. As yet, there is no universally agreed threshold of read count to establish an identified bacterium as causative of a presumed infection.

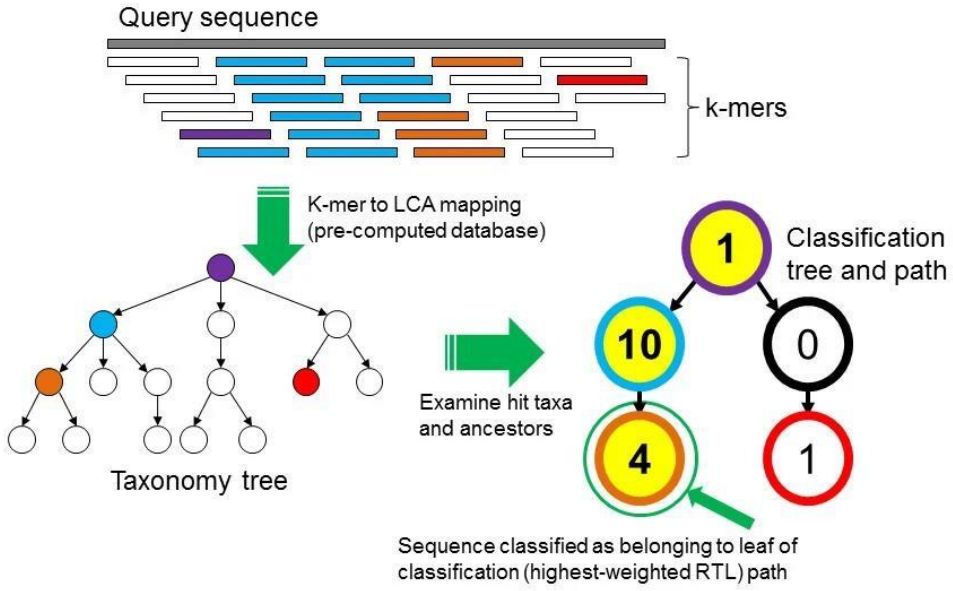

Figure 72 The Kraken sequence classification algorithm. Each section of sequence (set at a minimum length of nucleotides- k, this is referred to as a k-mer) is compared to a database of known genomic sequences (query sequence). The k-mers are mapped to a known sequence and to the lowest common ancestor of the genomes that contain that k-mer. So that, if a k-mer is present in multiple species they will also be mapped to their common genus for example. A taxonomic tree is built of all the sequence k-mers, as well as those k-mers ancestors with each node weighted to the number of k-mers associated with that taxon[543].

The read counts for the samples are reflective of the cell counts and therefore mostly the human genetic material present. The dominance of human cells in a clinical sample is known to reduce the sensitivity of mNGS for identifying pathogens. The read counts for the three groups are reassuring, in that, the *Uninfected* CSF samples had low read counts, which is to be expected with a virtually acellular sample.

Ji et al showed improved sensitivity for the identification of *TB* and *Cryptococci* in meningitis by centrifugation of samples prior to analysis of the supernatant. [563] Whilst depleting samples of human DNA is attractive , *Oechslin et al* showed that their approach (consisting of selective host cell lysis using a bead-beater tissue homogenizer with a soft tissue homogenizing lysing kit, followed by enzymatic degradation of released nucleic acid) increased read numbers in experimental CSF it failed to confer a benefit when applied to clinical CSF samples [564]. A bead beating step was included in the DNA extraction process for these samples due to the predominance of gram-positive organisms in neurosurgical CSF infections, but this was applied to improve the yield of gram-positive bacterial DNA not in preparation for human DNA depletion methods.

In the proteomics chapters it was noted that the generally accepted guidance is that you should avoid using bloody specimens for analysis. If we define a “bloody” CSF sample as one where the RCC >500, there were five bloody samples as well as two clotted samples included in the cohort used for this experiment. *Miller et al* have shown that bloody CSF samples did not reduce sensitivity for DNA pathogens, though bloody samples did result in decreased sensitivity for RNA virus detection [531]. Bloody CSF samples are a fact of life in neurosurgical practice and if a test cannot perform on bloody CSF, it will have limited utility in clinical practice. Also, as noted in Chapter 1, section 1.5.4.3, viral infections are exceptionally rare in neurosurgery.

If I were to re-do this experiment, I would include many more samples for each group, again they would be collected prospectively, and clinical data would be collected contemporaneously. My experiment would include a separate positive and negative control so that the samples could be compared with them. I cannot be sure that the low read numbers seen in the Uninfected samples in this experiment are comparable with a negative control. I would also include a series of samples where there was a definite confirmed infection with a cultured bacteria followed by samples taken from the same cases on a subsequent day (on antibiotics with high cell counts but culture negative). It would be interesting to see if the bacteria identified by culture could still be identified by NGS despite

antibiotic treatment. This could allow us to more confidently examine culture negative CSF with NGS in groups like the *Possible Infection* used here.

No experiment involving clinical samples will be perfect. Our "gold standard" test for causative organism of an infection, i.e., culture, has its limitations but it is the best test we have and so we have to compare any new method to it.

NGS for clinical practice

The high cost of metagenomics, to date, has meant that it has only performed only when all avenues were explored and found to be fruitless. The expertise and equipment required to perform and analyse metagenomic studies have kept metagenomics within the large university research hospitals. Some laboratories have retrospectively applied the approach to CSF samples from patients with meningitis/encephalitis [565, 566], including TB meningitis [567, 568], viral meningoencephalitis [523], cryptococcal meningitis [532] and more particularly for outbreak investigation (enterovirus D68 [569], *N. meningitidis* [570]).

With the costs of NGS plummeting (see Fig. 78) and with increasing automation and speed, NGS will likely become a routine clinical test in the future. Exemplified by an increasing number of groups now trying to implement NGS prospectively [522, 571-573].

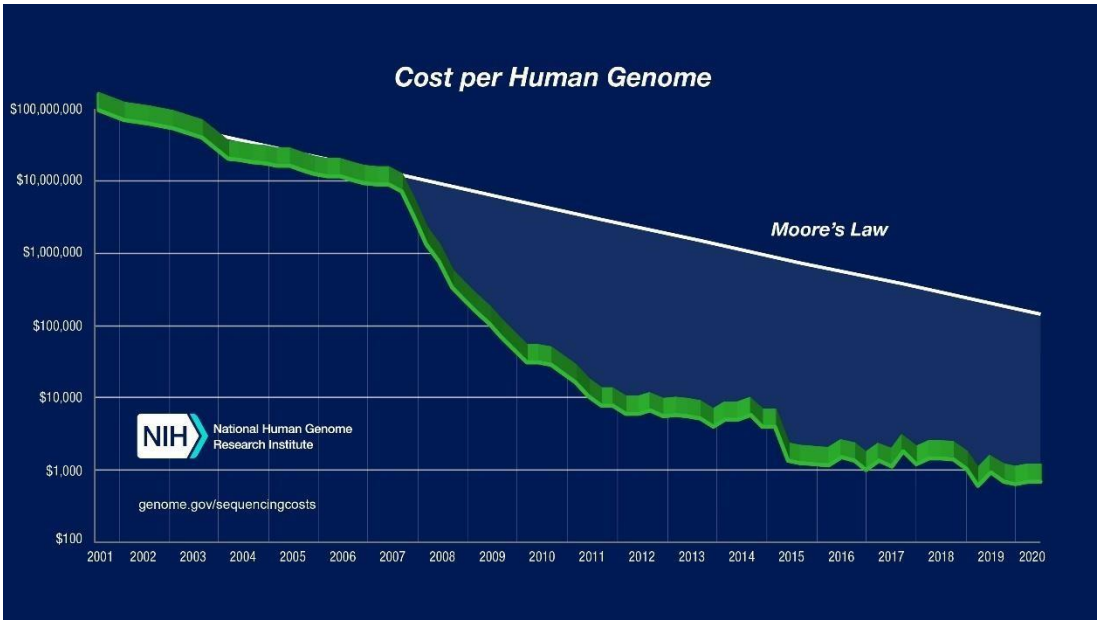

Figure 73 The estimated cost of sequencing the human genome between 2001 and 2020. Graph taken from NHGRI via genome.gov[574]

In my experience, the only way metagenomic sequencing will become part of routine diagnostics will be if a sample can be inserted into a testing instrument which automatically processes and sequences the sample. An automated extraction and sequencing machine would remove any further risk of contamination with human DNA. The bacteria identified by sequencing and their associated read numbers and sequence coverage would need to be provided as a concise report.

Ideally the cost of each test would be a similar price to current point of care tests like arterial blood gases or cardiac troponin (testing for myocardial infarction, see example of cost of POC troponin testing in Table 58 below). Point of care troponin testing is increasingly being adopted as standard in many emergency departments and even being trialled in the general practice setting[575]. Given the economic and clinical impact of diagnostic delays for meningitis and the increasing concern about antimicrobial resistance a higher price may be acceptable even to public health services.

Table 58 Cost comparison for point of care and standard laboratory Troponin testing. POC= point of care. cTn=cardiac troponin. Prices are in US dollars and were calculated in 2016 but serve as an example of the costs involved for a point of care test.[576]

	Device	Cost per Test	Average Lifetime of Device	Source
POC cTn testing strategies				
Stratus CS (Siemens)	$35,000	$8.50	8.5 years	Siemens
Cardio3 Panel (Alere)	$5,000	$20	7 years	Alere
i-STAT (Abbott)	$8,000	$14	5 years	Expert input (Ontario laboratory estimate)
Cost of staff for POC program (per annum)	$10,000			Expert Input (Ontario laboratory estimates)
Cost of calibration and quality control of POC cTn testing (per annum)	$600			
Number of annual POC tests	1,000			
Standard care				
Conventional cTn central laboratory testing, e.g., device, materials, staff (per test)	$10			Expert input (Alberta laboratory estimates)
Specimen procurement by central laboratory	$12			Expert input (Alberta laboratory estimates)

Conclusion

Ultimately, in an ideal world, we would know the CSF protein patterns of response seen for infections (due to different bacteria) and pair this with NGS findings as a fingerprint of infection. If NGS shows a bacterium but the host response is not that of infection then, it is

likely to be a contaminant. In classic culture if a bacterial colony was thought to be a contaminant a repeat sample could be sought. With the decreased costs for NGS it may well be an option in the future to repeat analyses.

Chapter 6. Discussion

This project was entitled the "Study of the feasibility and diagnostic accuracy of Proteomics and Next Generation Sequencing (NGS) for the investigation of neurosurgical cerebrospinal fluid infections." Is it feasible to use proteomics and NGS to investigate neurosurgical CSF infections? In a research laboratory, yes absolutely. In the clinical setting of a busy neurosurgical department embedded in the overstretched NHS, currently probably not but soon the cost of these techniques will be low enough that they will be.

Proteomic analyses will likely continue to be something that will be done in centres like the TDI in Oxford University. One conclusion I reached after this foray into proteomics is that biomarker exploration can only be undertaken on large numbers of samples. The biological variation of many, if not most, proteins is not clear but what is clear is that it cannot be ascertained from a handful of samples. The cost of LC-MS/MS is progressively declining but at the time of my experiments just analysing 30 samples cost ~£20,000. As costs fall, largescale screening of samples is becoming more feasible which will provide big data for computer learning algorithms. Ultimately a point of care test for a protein/ panel (ELISA or similar) of proteins could be developed to test for neurosurgical infection.

There may well be a proteomic profile(s) indicative of CSF infection, but this will only be discernible with the accrual of proteomic data of thousands of CSF samples. That proteomic data would also need to be paired to consistent, complete clinical data to allow for the clear definition of clinically infected CSF samples. Similarly, for the metagenomic exploration of neurosurgical CSF, ultimately there will need to be much larger studies of the microbiome of clinical CSF. This could define the sequence read thresholds required to confirm an infecting pathogen and develop a standard CSF NGS analysis protocol.

Salvaged CSF from the LCL turned out to be invaluable in this project and the main learning point I took from it is that if you can, you should integrate sample collection into routine practice. Indeed, the NHS Blood and Transplant service currently integrates research into its generic consent for blood donation. Blood that cannot be used for transfusion is used for research [321]. Obviously it would need public engagement and involvement but all neurosurgical units in university hospitals should include research in their generic consent processes.

Collecting samples prospectively was a very different experience, with many valuable lessons. The nature of suspected shunt/EVD infections is that they are not routine, they do not declare themselves neatly during office hours. It became clear as time went on in this study that CSF collection for research needs more than just one PhD student/neurosurgical registrar if you want a quality collection of prospectively collected samples with consistent and complete linked clinical data. With the best will in the world, the average neurosurgeon on call has too much to manage of an average day/night without even starting to think about the logistics of consenting for research, completing CRFs and ensuring appropriate storage of samples. In Alder Hey it was possible to remain in regular, almost continuous, contact with whoever was on call to ensure that most CSF sampling opportunities were captured. Parents and children were universally enthusiastic about helping with our research. Most likely as it was quickly obvious that it would not involve any additional risk or work from them.

Neurosurgical CSF infection is an uncommon event and so to collect this sort of biobank of samples and clinical data would require every neurosurgical centre to contribute CSF from all procedures where CSF samples are collected.

The sequence of an organism is the most accurate way of identifying it. Whole genome sequencing has received a lot of attention recently for the diagnosis of rare diseases, indeed the 100,000 genomes project has found that one in four patients who were sequenced had findings that affected their clinical management [577]. Sequencing is clearly becoming a more routine part of laboratory medicine. NGS/metagenomics is the future of microbiology. Its utility has been highlighted with the SARS-COV-2/ COVID-19 pandemic where sequencing has allowed us to track the evolution of the virus, its' mutations and its' movement through populations across the planet [578].

For both the proteomics and NGS experiments I did not personally run the main experiment. The Fischer group in Oxford performed the LC-MS/MS and The Darby group in Liverpool performed the metagenomic sequencing. Historically a PhD candidate would be expected to perform all experiments themselves. With the advances in science, the methods we use are becoming increasingly sophisticated and specialised. Both proteomic LC-MS/MS and metagenomic sequencing would take up the entirety of a PhD project for a candidate to become proficient in the technique to an independent level. Both techniques are vulnerable to operator introduced variability and the consumables used are costly.

I am primarily a clinician, and my future career will remain primarily clinical. I would see my role as being facilitative to basic and translational research and evangelical for evidencebased practice and high-quality research. I am not a career scientist, but I have the great privilege of having access to patients, many of whom are highly motivated to participate in research. It behoves us to ensure that any clinical specimens and data collected for research be used efficiently and effectively. Research questions should be driven by patient centred issues (see initiatives like the James Lindt Alliance) and research projects should plan from the beginning to adequately answer those research questions.

With each pathology dealt with by neurosurgery being so rare, every study that wishes to answer a research question struggles to collect adequate numbers of samples in a single centre. Patients undergoing neurosurgical procedures are often very motivated to participate in research. I would argue that every person undergoing a neurosurgical procedure should be approached for consent for any tissue samples that are surplus to requirements for routine clinical testing to be kept for research purposes. Indeed, there should be a research consent section incorporated into every neurosurgical consent form.

In my proteomics chapter there was an unexpected finding. The initial results of ELISA testing of CSF samples showed that some proteins identified by LC-MS/MS did not appear to produce the same changes in concentration of a protein in infected versus uninfected CSF. The relationship was reversed- where it was high concentration in *Infected* and low concentration in *Uninfected* for LC-MS/MS it was then low concentration in *Infected* and high concentration in *Uninfected* for ELISA. Presenting these results to a group of clinicians led to the exploration of the effect of protein digestion on CSF samples (included in the sample preparation for LC-MS/MS). Discussing this with scientists, they immediately saw that the chemicals used in the protein digestion could easily interfere with any further ELISA testing. We so often end up working in silos and in doing so, avoid the wealth of experience and knowledge that other specialties have. I did not include this step in my thesis, it being a mistake in many ways. But I think it was a great learning moment and serves to highlight the absolute necessity for scientists to be embedded in clinical research groups undertaking laboratory research.

Well designed and executed and communicated research is essential to maintain (and hopefully rebuild) public confidence in scientific evidence. Even before the COVID-19 pandemic and the ensuing tsunami of research projects, it was estimated that 85% of scientific evidence

was “wasted” due to poor research questions, poor study design, not assessing appropriate outcomes, failing to communicate the methodology clearly, reports not accessible and failure to publish findings in full [579]. With this in mind, if I ruled the world, I would give less money to solely clinician led research and insist on greater weighting for applications from projects that include scientists. Clinicians have access to patients and samples and get funding for projects relatively easily. We are not, however, trained scientists. There are some clinicians who have completed science degrees prior to a medical degree but this is unusual. The time pressures of clinical practice and the habits of swift plan making often carry over into the laboratory for clinicians. This often results in hastily planned experiments. I have had an unusual experience over the course of my PhD, in that I was primarily supervised by a clinician at the start but due to unforeseen circumstances I ended my project with a scientist as my primary supervisor. I am also married to a scientist who now works for a biotechnology company. Clinicians do not take the time to plan out an experiment with the same time and patience that scientists do. With research monies becoming ever more stretched it only stands to reason that we should be more discerning about research projects. Clinical research projects inevitably get published in more impactful journals and so scientists would gain valuable publications as well.

I think that all large clinical research projects should have a scientist attached to them and that this should be screened for at the IRAS (integrated research application system) stage. Large clinical research projects should also be routinely assessed to see if they achieved the goals set out by the application, which would encourage more careful planning and appropriate resourcing to ensure that those goals are met (much the same as is mandated for randomised control trials).

Bibliography

1. Piek, J., et al., *Stone Age Skull Surgery in Mecklenburg-Vorpommern: A Systematic Study.* Neurosurgery, 1999. **45**(1): p. 147-151.
2. HEE. *Neurosurgery*. Health Careers; Available from: https://www.healthcareers.nhs.uk/explore-roles/doctors/rolesdoctors/surgery/neurosurgery.
3. Liu, C.Y., et al., *The genesis of neurosurgery and the evolution of the neurosurgical operative environment: Part I - Prehistory to 2003.* Neurosurgery, 2003. **52**(1): p. 319.

4. Tatagiba, M., O.N. Ugarte, and M.A. Acioly, *Neurosurgery: Past, present, and future*, in *Handbook of Neuroethics*. 2015. p. 937-948.
5. Dewan, M.C., et al., *Global neurosurgery: the current capacity and deficit in the provision of essential neurosurgical care. Executive Summary of the Global Neurosurgery Initiative at the Program in Global Surgery and Social Change.* J Neurosurg, 2018: p. 1-10.
6. Carroll, E. and A. Lewis, *Prevention of surgical site infections after brain surgery: the prehistoric period to the present.* 2019. **47**(2): p. E2.
7. Netter, F.H., et al., *Atlas of human anatomy*. Seventh edition. ed. Netter basic science. Elsevier.
8. Hines, T. *Anatomy of the Brain*. 2018 19/02/2020]; Available from: https://mayfieldclinic.com/pe-anatbrain.htm.
9. Longstaff, A., *BIOS Instant Notes in Neuroscience*. 2011: Taylor & Francis Ltd - M.U.A.
10. Snell, R.S., *Clinical neuroanatomy: Seventh edition*. Clinical Neuroanatomy: Seventh Edition. 2011. 1-542.
11. Anthony Marmarou, A.B., *Physiology of the Cerebrospinal Fluid and Intracranial Pressure*, in *Youmans Neurological Surgery*, H.R. Winn, Editor. 2011, Elsevier. p. 169-182.
12. Johanson, C.E., *Choroid Plexus–Cerebrospinal Fluid Circulatory Dynamics: Impact on Brain Growth, Metabolism, and Repair*, in *Neuroscience in Medicine*, P.M. Conn, Editor. 2008, Humana Press: Totowa, NJ. p. 173-200.
13. Deisenhammer, F., et al., *Cerebrospinal fluid in clinical neurology*. Cerebrospinal Fluid in Clinical Neurology. 2015. 1-441.
14. Brinker, T., et al., *A new look at cerebrospinal fluid circulation.* Fluids and barriers of the CNS, 2014. **11**: p. 10-10.
15. Spector, R., S. Robert Snodgrass, and C.E. Johanson, *A balanced view of the cerebrospinal fluid composition and functions: Focus on adult humans.* Exp Neurol, 2015. **273**: p. 57-68.
16. Iliff, J.J., et al., *A paravascular pathway facilitates CSF flow through the brain parenchyma and the clearance of interstitial solutes, including amyloid β.* Science Translational Medicine, 2012. **4**(147).
17. Magendie, F., *Recherches physiologiques et cliniques sur le liquide céphalorachidien ou cerebro-spinal*. 1842: LIBRAIRIE MÉDICALE DE MÉQUIGNON-MARVIS FILS.
18. Orešković, D. and M. Klarica, *The formation of cerebrospinal fluid: Nearly a hundred years of interpretations and misinterpretations.* Brain Research Reviews, 2010. **64**(2): p. 241-262.
19. Redzic, Z.B. and M.B. Segal, *The structure of the choroid plexus and the physiology of the choroid plexus epithelium.* Advanced Drug Delivery Reviews, 2004. **56**(12): p. 1695-1716.
20. Johanson, C.E., et al., *Multiplicity of cerebrospinal fluid functions: New challenges in health and disease.* Cerebrospinal Fluid Research, 2008. **5**(1): p. 10.
21. Brodbelt, A. and M. Stoodley, *CSF pathways: A review.* British Journal of Neurosurgery, 2007. **21**(5): p. 510-520.
22. J. Gordon McComb, S.Y., *Cerebral Fluid Physiology*, in *Youmans Neurological Surgery*. 2011, Elsevier. p. 1993-2001.

23. Pollay, M. and F. Curl, *Secretion of cerebrospinal fluid by the ventricular ependyma of the rabbit.* American Journal of Physiology-Legacy Content, 1967. **213**(4): p. 1031-1038.
24. Kimelberg, H.K., *Water homeostasis in the brain: Basic concepts.* Neuroscience, 2004. **129**(4): p. 851-860.
25. Redzic, Z.B., et al., *The Choroid Plexus-Cerebrospinal Fluid System: From Development to Aging*, in *Current Topics in Developmental Biology*. 2005. p. 1-52.
26. Sambrook, M.A., *The relationship between cerebrospinal fluid and plasma electrolytes in patients with meningitis.* Journal of the Neurological Sciences, 1974. **23**(2): p. 265-273.
27. Mokri, B., *The Monro-Kellie hypothesis: applications in CSF volume depletion.* Neurology, 2001. **56**(12): p. 1746-8.
28. Winn, H.R. and J.R. Youmans, *Youmans & Winn Neurological Surgery. Vol 1. 7th edition.* 2017: p. 1638-1643.
29. Nicole c. Keong, M.C., Zofia Czosnyka, John D. Pickard, *Clinical Evaluation of Adult Hydrocephalus*, in *Youmans Neurological Surgery*, H.R. Winn, Editor. 2011, Elsevier. p. 494-514.
30. Aschoff, A., et al., *The scientific history of hydrocephalus and its treatment.* Neurosurgical Review, 1999. **22**(2-3): p. 67-93.
31. Richards, G.D. and S.C. Anton, *Craniofacial configuration and postcranial development of a hydrocephalic child (ca. 2500 B.C.–500 A.D.): With a review of cases and comment on diagnostic criteria.* American Journal of Physical Anthropology, 1991. **85**(2): p. 185-200.
32. Oi, S., *Hydrocephalus research update--controversies in definition and classification of hydrocephalus.* Neurol Med Chir (Tokyo), 2010. **50**(9): p. 859-69.
33. Oreskovic, D., M. Rados, and M. Klarica, *New Concepts of Cerebrospinal Fluid Physiology and Development of Hydrocephalus.* Pediatr Neurosurg, 2017. **52**(6): p. 417-425.
34. Rekate, H.L., *The definition and classification of hydrocephalus: A personal recommendation to stimulate debate.* Cerebrospinal Fluid Research, 2008. **5**.
35. Mollan, S.P., et al., *Idiopathic intracranial hypertension: consensus guidelines on management.* Journal of Neurology, Neurosurgery & Psychiatry, 2018. **89**(10): p. 1088-1100.
36. Rekate, H.L., *Slit ventricle syndromes*, in *Pediatric Hydrocephalus: Second Edition*. 2019. p. 1365-1374.
37. Adams, R.D., et al., *Symptomatic Occult Hydrocephalus with Normal CerebrospinalFluid Pressure.* New England Journal of Medicine, 1965. **273**(3): p. 117-126.
38. Pudenz, R.H., *The surgical treatment of hydrocephalus--an historical review.* Surg Neurol, 1981. **15**(1): p. 15-26.
39. Gangopadhyay, A.N., V.D. Upadhyaya, and A. Pandey, *Hydrocephalus*, in *Handbook of Pediatric Surgery*, C.K. Sinha and M. Davenport, Editors. 2010, Springer London: London. p. 459-465.
40. Hodel, J., A. Rahmouni, and P. Decq, *MRI of Patients with Hydrocephalus*, in *Neuroendoscopy: Current Status and Future Trends*, S. Sgouros, Editor. 2014, Springer Berlin Heidelberg: Berlin, Heidelberg. p. 133-139.
41. Saleh AlSuhibani, S., A. Hamad Alabdulwahhab, and A. Ammar, *Radiological Diagnosis of Hydrocephalus*, in *Hydrocephalus: What do we know? And what do we*

still not know?, A. Ammar, Editor. 2017, Springer International Publishing: Cham. p. 127-141.
42. Dewan, M.C., et al., *Global hydrocephalus epidemiology and incidence: systematic review and meta-analysis.* 2018. **130**(4): p. 1065.
43. Organisation, W.H., *Urgent health challenges for the next decade*. 2020.
44. UNAIDS. *Global HIV & AIDS statistics — 2019 fact sheet*. 2019; Available from: https://www.unaids.org/en/resources/fact-sheet.
45. worldometer. *current World Population*. 2020 21/02/2020]; Available from: https://www.worldometers.info/world-population/.
46. Simon, T.D., et al., *Hospital care for children with hydrocephalus in the United States: Utilization, charges, comorbidities, and deaths.* Journal of Neurosurgery: Pediatrics, 2008. **1**(2): p. 131-137.
47. Kestle, J.R.W., *Hydrocephus in Children : Approach to the Patient*. Sixth ed. Youmans Neurological Surgery, ed. H.R. Winn. Vol. 2. 2011: Elsevier.
48. van Dommelen, P., et al., *Diagnostic Accuracy of Referral Criteria for Head Circumference to Detect Hydrocephalus in the First Year of Life.* Pediatric Neurology, 2015. **52**(4): p. 414-418.
49. Kahle, K.T., et al., *Hydrocephalus in children.* The Lancet, 2016. **387**(10020): p. 788799.
50. Chau, C.Y.C., et al., *The Evolution of the Role of External Ventricular Drainage in Traumatic Brain Injury.* J Clin Med, 2019. **8**(9).
51. Bratton, S.L., et al., *Guidelines for the management of severe traumatic brain injury. VII. Intracranial pressure monitoring technology.* J Neurotrauma, 2007. **24 Suppl 1**: p. S45-54.
52. Catapano, J.S., et al., *Standardized Ventriculostomy Protocol without an Occlusive Dressing: Results of an Observational Study in Patients with Aneurysmal Subarachnoid Hemorrhage.* World Neurosurgery, 2019. **131**: p. e433-e440.
53. Champey, J., et al., *Strategies to reduce external ventricular drain–related infections: a multicenter retrospective study.* 2018. **130**(6): p. 2034.
54. Cinibulak, Z., et al., *Current practice of external ventricular drainage: a survey among neurosurgical departments in Germany.* Acta Neurochirurgica, 2016. **158**(5): p. 847-853.
55. Clifton, W.E., A.C. Damon, and W.D. Freeman, *Development of a Lumbar Drain Simulator for Instructional Technique and Skill Assessment.* Neurocritical Care, 2020. **32**(3): p. 894-898.
56. Shastin, D., M. Zaben, and P. Leach, *Life with a cerebrospinal fluid (CSF) shunt.* BMJ, 2016. **355**: p. i5209.
57. Di Rocco, C., E. Marchese, and F. Velardi, *A survey of the first complication of newly implanted CSF shunt devices for the treatment of nontumoral hydrocephalus - Cooperative survey of the 1991-1992 Education Committee of the ISPN.* Child's Nervous System, 1994. **10**(5): p. 321-327.
58. Fernández-Méndez, R., et al., *Current epidemiology of cerebrospinal fluid shunt surgery in the UK and Ireland (2004–2013).* Journal of Neurology, Neurosurgery & Psychiatry, 2019. **90**(7): p. 747-754.
59. Patwardhan, R.V. and A. Nanda, *Implanted ventricular shunts in the United States: The billion-dollar-a- year cost of hydrocephalus treatment.* Neurosurgery, 2005. **56**(1): p. 139-144.

60. Zohreh, H., et al., *Suprahepatic space as an alternative site for distal catheter insertion in pseudocyst-associated ventriculoperitoneal shunt malfunction.* Journal of Neurosurgery: Pediatrics PED, 2020. **26**(3): p. 247-254.
61. Philipp, R.A., E.J. Hector, and A.P. Richard, *Ventriculogallbladder shunts in pediatric patients.* Journal of Neurosurgery: Pediatrics PED, 2008. **1**(4): p. 284-287.
62. Oliveira, M.F.d., et al., *Failed Ventriculoperitoneal Shunt: Is Retrograde Ventriculosinus Shunt a Reliable Option?* World Neurosurgery, 2016. **92**: p. 445453.
63. Lou, P., et al., *The clinical application of ventriculovesical shunts.* National Medical Journal of China, 2019. **99**(1): p. 41-43.
64. Pillai, A., et al., *Ventriculo-ureteral shunt insertion using percutaneous nephrostomy: A novel minimally invasive option in a patient with chronic hydrocephalus complicated by multiple distal ventriculoperitoneal shunt failures.* Journal of Neurosurgery, 2017. **127**(2): p. 255-259.
65. Konar, S.K., et al., *Robert H. Pudenz (1911-1998) and Ventriculoatrial Shunt: Historical Perspective.* World Neurosurg, 2015. **84**(5): p. 1437-40.
66. Ignelzi, R.J. and W.M. Kirsch, *Follow-up analysis of ventriculoperitoneal and ventriculoatrial shunts for hydrocephalus.* J Neurosurg, 1975. **42**(6): p. 679-82.
67. Vernet, O., R. Campiche, and N. de Tribolet, *Long-term results after ventriculoatrial shunting in children.* Childs Nerv Syst, 1993. **9**(5): p. 253-5.
68. Keucher, T.R. and J. Mealey, Jr., *Long-term results after ventriculoatrial and ventriculoperitoneal shunting for infantile hydrocephalus.* J Neurosurg, 1979. **50**(2): p. 179-86.
69. Martínez-Lage, J.F., et al., *Ventriculopleural shunting with new technology valves.* Child's Nervous System, 2000. **16**(12): p. 867-871.
70. Jones, R.F.C., B.G. Currie, and B.C.T. Kwok, *Ventriculopleural Shunts for Hydrocephalus: A Useful Alternative.* Neurosurgery, 1988. **23**(6): p. 753-755.
71. Elder, B.D., et al., *Hydrocephalus shunt procedures*, in *Adult Hydrocephalus*, D. Rigamonti, Editor. 2014, Cambridge University Press: Cambridge. p. 175-189.
72. Eid, S., et al., *Ventriculosubgaleal shunting—a comprehensive review and over twodecade surgical experience.* Child's Nervous System, 2018. **34**(9): p. 1639-1642.
73. Vogel, T.W., et al., *The role of endoscopic third ventriculostomy in the treatment of hydrocephalus.* 2013. **12**(1): p. 54.
74. Cinalli, G., et al., *The role of endoscopic third ventriculostomy in the management of shunt malfunction.* Neurosurgery, 1998. **43**(6): p. 1323-1329.
75. Kulkarni, A.V., et al., *Endoscopic Third Ventriculostomy in the Treatment of Childhood Hydrocephalus.* Journal of Pediatrics, 2009. **155**(2): p. 254-259.e1.
76. Kulkarni, A.V., et al., *Endoscopic Third Ventriculostomy in the Treatment of Childhood Hydrocephalus.* The Journal of Pediatrics, 2009. **155**(2): p. 254-259.e1.
77. Lepard, J.R., et al., *The CURE Protocol: Evaluation and external validation of a new public health strategy for treating paediatric hydrocephalus in low-resource settings.* BMJ Global Health, 2020. **5**(2).
78. Murphy, B.P., et al., *Posthaemorrhagic ventricular dilatation in the premature infant: Natural history and predictors of outcome.* Archives of Disease in Childhood: Fetal and Neonatal Edition, 2002. **87**(1): p. F37-F41.
79. Eisha, A.C., et al., *Trends in hospitalization of preterm infants with intraventricular hemorrhage and hydrocephalus in the United States, 2000–2010.* Journal of Neurosurgery: Pediatrics PED, 2016. **17**(3): p. 260-269.

80. Blount, J.P., J.A. Campbell, and S.J. Haines, *Complications in ventricular cerebrospinal fluid shunting.* Neurosurgery clinics of North America, 1993. **4**(4): p. 633-656.
81. Dossani, R.H., et al., *Ayub Khan Ommaya (1930-2008): Legacy and Contributions to Neurosurgery.* Neurosurgery, 2016. **80**(2): p. 324-330.
82. Ommaya, A., *SUBCUTANEOUS RESERVOIR AND PUMP FOR STERILE ACCESS TO VENTRICULAR CEREBROSPINAL FLUID.* The Lancet, 1963. **282**(7315): p. 983-984.
83. Whitelaw, A. and R. Lee-Kelland, *Repeated lumbar or ventricular punctures in newborns with intraventricular haemorrhage.* Cochrane Database of Systematic Reviews, 2017. **2017**(4).
84. Dandy, W.E., *EXTIRPATION OF THE CHOROID PLEXUS OF THE LATERAL VENTRICLES IN COMMUNICATING HYDROCEPHALUS.* Ann Surg, 1918. **68**(6): p. 569-79.
85. Zhu, X. and C. Di Rocco, *Choroid plexus coagulation for hydrocephalus not due to CSF overproduction: a review.* Child's Nervous System, 2013. **29**(1): p. 35-42.
86. Enchev, Y. and S. Oi, *Historical trends of neuroendoscopic surgical techniques in the treatment of hydrocephalus.* Neurosurgical Review, 2008. **31**(3): p. 249-262.
87. Kulkarni, A.V. and I. Shams, *Quality of life in children with hydrocephalus: results from the Hospital for Sick Children, Toronto.* J Neurosurg, 2007. **107**(5 Suppl): p. 358-64.
88. Gupta, N., et al., *Long-term outcomes in patients with treated childhood hydrocephalus.* Journal of Neurosurgery, 2007. **106**(5 SUPPL.): p. 334-339.
89. Punchak, M., et al., *The Incidence of Postoperative Seizures Following Treatment of Postinfectious Hydrocephalus in Ugandan Infants: A Post Hoc Comparison of Endoscopic Treatment vs Shunt Placement in a Randomized Controlled Trial.* Clinical Neurosurgery, 2019. **85**(4): p. E714-E721.
90. Casey, A.T., et al., *The long-term outlook for hydrocephalus in childhood. A ten-year cohort study of 155 patients.* Pediatr Neurosurg, 1997. **27**(2): p. 63-70.
91. Adams-Chapman, I., et al., *Neurodevelopmental outcome of extremely low birth weight infants with posthemorrhagic hydrocephalus requiring shunt insertion.* Pediatrics, 2008. **121**(5): p. e1167-77.
92. Melot, A., et al., *Neurodevelopmental long-term outcome in children with hydrocephalus requiring neonatal surgical treatment.* Neurochirurgie, 2016. **62**(2): p. 94-99.
93. Lacy, M., et al., *Intellectual functioning in children with early shunted posthemorrhagic hydrocephalus.* Pediatric Neurosurgery, 2008. **44**(5): p. 376-381.
94. Kulkarni, A.V., et al., *Quality of life in obstructive hydrocephalus: Endoscopic third ventriculostomy compared to cerebrospinal fluid shunt.* Child's Nervous System, 2010. **26**(1): p. 75-79.
95. Laurence, K.M. and S. Coates, *The natural history of hydrocephalus: Detailed analysis of 182 unoperated cases.* Archives of Disease in Childhood, 1962. **37**(194): p. 345-362.
96. Chi, J.H., H.J. Fullerton, and N. Gupta, *Time trends and demographics of deaths from congenital hydrocephalus in children in the United States: National Center for Health Statistics data, 1979 to 1998.* Journal of Neurosurgery, 2005. **103 PEDIATRICS**(SUPPL. 2): p. 113-118.
97. Gmeiner, M., et al., *Long-term mortality rates in pediatric hydrocephalus—a retrospective single-center study.* Child's Nervous System, 2017. **33**(1): p. 101-109.
98. Paulsen, A.H., T. Lundar, and K.-F. Lindegaard, *Pediatric hydrocephalus: 40-year outcomes in 128 hydrocephalic patients treated with shunts during childhood.*

Assessment of surgical outcome, work participation, and health-related quality of life. 2015. **16**(6): p. 633.
99. Beverly, C.W., et al., *Cerebrospinal fluid shunt infection.* Journal of Neurosurgery, 1984. **60**(5): p. 1014-1021.
100. Basil, M.C. and B.D. Levy, *Specialized pro-resolving mediators: endogenous regulators of infection and inflammation.* Nature Reviews Immunology, 2016. **16**(1): p. 51-67.
101. Ransohoff, R.M. and B. Engelhardt, *The anatomical and cellular basis of immune surveillance in the central nervous system.* Nature Reviews Immunology, 2012. **12**(9): p. 623-635.
102. Forrester, J.V., P.G. McMenamin, and S.J. Dando, *CNS infection and immune privilege.* Nature Reviews Neuroscience, 2018. **19**(11): p. 655-671.
103. Jeffrey M. Tessier, W.M.S., *Basic Science of Central Nervous System Infections*, in *Youmans Neurological Surgery*, H.R. Winn, Editor. 2011, Elsevier. p. 544-559.
104. McCutcheon, I.E., *Meningits and Encephalitis*. Sixth ed. Youmans Neurological Surgery. Vol. Sixth. 2011: Elsevier.
105. Overturf, G.D., *Defining bacterial meningitis and other infections of the central nervous system.* Pediatric Critical Care Medicine, 2005. **6**(3 SUPPL.): p. S14-S18.
106. Robertson, F.C., et al., *Epidemiology of central nervous system infectious diseases: A meta-analysis and systematic review with implications for neurosurgeons worldwide.* Journal of Neurosurgery, 2019. **130**(4): p. 1107-1126.
107. Venkatesan, A., et al., *Case Definitions, Diagnostic Algorithms, and Priorities in Encephalitis: Consensus Statement of the International Encephalitis Consortium.* Clinical Infectious Diseases, 2013. **57**(8): p. 1114-1128.
108. Granerod, J., et al., *New estimates of incidence of encephalitis in England.* Emerg Infect Dis, 2013. **19**(9).
109. Skoldenberg, B., et al., *Acyclovir versus vidarabine in herpes simplex encephalitis. Randomised multicentre study in consecutive Swedish patients.* Lancet, 1984. **2**(8405): p. 707-11.
110. Venkatesan, A., *Epidemiology and outcomes of acute encephalitis.* Current Opinion in Neurology, 2015. **28**(3): p. 277-282.
111. Glaser, C.A., et al., *In search of encephalitis etiologies: Diagnostic challenges in the California Encephalitis Project, 1998-2000.* Clinical Infectious Diseases, 2003. **36**(6): p. 731-742.
112. Granerod, J., et al., *Causes of encephalitis and differences in their clinical presentations in England: a multicentre, population-based prospective study.* The Lancet Infectious Diseases, 2010. **10**(12): p. 835-844.
113. Goethe, E.A., et al., *Cerebellitis as a neurosurgical disease in pediatrics.* Journal of Clinical Neuroscience, 2021. **85**: p. 57-63.
114. Horan, T.C., M. Andrus, and M.A. Dudeck, *CDC/NHSN surveillance definition of health care–associated infection and criteria for specific types of infections in the acute care setting.* American Journal of Infection Control, 2008. **36**(5): p. 309-332.
115. Sáez-Llorens, X. and J.N. Guevara, *Chapter 116 - Brain abscess*, in *Handbook of Clinical Neurology*, O. Dulac, M. Lassonde, and H.B. Sarnat, Editors. 2013, Elsevier. p. 1127-1134.
116. Nathoo, N., et al., *Brain Abscess: Management and Outcome Analysis of a Computed Tomography Era Experience with 973 Patients.* World Neurosurgery, 2011. **75**(5): p. 716-726.
117. Bodilsen, J., et al., *Long-term mortality and epilepsy in patients after brain abscess:*

A nationwide population-based matched cohort study. Clin Infect Dis, 2019.
118. Canale, D.J., *William Macewen and the treatment of brain abscesses: revisited after one hundred years.* 1996. **84**(1): p. 133.
119. Samson, D.S. and K. Clark, *A current review of brain abscess.* The American Journal of Medicine, 1973. **54**(2): p. 201-210.
120. Mathisen, G.E. and J.P. Johnson, *Brain Abscess.* Clinical Infectious Diseases, 1997. **25**(4): p. 763-779.
121. Brouwer, M.C., J.M. Coutinho, and D. van de Beek, *Clinical characteristics and outcome of brain abscess: systematic review and meta-analysis.* Neurology, 2014. **82**(9): p. 806-13.
122. Brouwer, M.C. and D. van de Beek, *Epidemiology, diagnosis, and treatment of brain abscesses.* Current Opinion in Infectious Diseases, 2017. **30**(1): p. 129-134.
123. Tekkök, I. and A. Erbengi, *Management of brain abscess in children: review of 130 cases over a period of 21 years.* Childs Nerv Syst, 1992. **8**: p. 411-466.
124. Brouwer, M.C., et al., *Brain Abscess.* New England Journal of Medicine, 2014. **371**(5): p. 447-456.
125. Leaper, D.J., et al., *Surgical site infection - A European perspective of incidence and economic burden.* International Wound Journal, 2004. **1**(4): p. 247-273.
126. Buckwold, F.J., R. Hand, and R.R. Hansebout, *Hospital acquired bacterial meningitis in neurosurgical patients.* Journal of Neurosurgery, 1977. **46**(4): p. 494-500.
127. Blomstedt, G.C., *Infections in neurosurgery: A retrospective study of 1143 patients and 1517 operations.* Acta Neurochirurgica, 1985. **78**(3-4): p. 81-90.
128. Buffet-Bataillon, S., et al., *Impact of surgical site infection surveillance in a neurosurgical unit.* Journal of Hospital Infection, 2011. **77**(4): p. 352-355.
129. Korinek, A.M., et al., *Risk factors for neurosurgical site infections after craniotomy: A critical reappraisal of antibiotic prophylaxis on 4578 patients.* British Journal of Neurosurgery, 2005. **19**(2): p. 155-162.
130. Korinek, A.M., *Risk factors for neurosurgical site infections after craniotorny: A prospective multicenter study of 2944 patients.* Neurosurgery, 1997. **41**(5): p. 10731081.
131. Maurice-Williams, R.S. and J. Pollock, *Topical antibiotics in neurosurgery: A reevaluation of the Malis technique.* British Journal of Neurosurgery, 1999. **13**(3): p. 312-315.
132. McClelland Iii, S. and W.A. Hall, *Postoperative central nervous system infection: Incidence and associated factors in 2111 neurosurgical procedures.* Clinical Infectious Diseases, 2007. **45**(1): p. 55-59.
133. Holloway, K.L., et al., *Antibiotic prophylaxis during clean neurosurgery: A large, multicenter study using cefuroxime.* Clinical Therapeutics, 1996. **18**(1): p. 84-94.
134. Savitz, M.H. and S.S. Katz, *Prevention of Primary Wound Infection in Neurosurgical Patients: A 10-Year Study.* Neurosurgery, 1986. **18**(6): p. 685-688.
135. McClelland, S., *Postoperative intracranial neurosurgery infection rates in North America versus Europe: A systematic analysis.* American Journal of Infection Control, 2008. **36**(8): p. 570-573.
136. Heipel, D., et al., *Surgical site infection surveillance for neurosurgical procedures: A comparison of passive surveillance by surgeons to active surveillance by infection control professionals.* American Journal of Infection Control, 2007. **35**(3): p. 200202.
137. Jamjoom, A.A.B., et al., *Prospective, multicentre study of external ventricular drainage-related infections in the UK and Ireland.* Journal of Neurology, Neurosurgery and Psychiatry, 2018. **89**(2): p. 120-126.

138. Dorresteijn, K.R.I.S., et al., *Factors and measures predicting external CSF drainassociated ventriculitis.* Neurology, 2019. **93**(22): p. 964.
139. Keong, N.C.H., et al., *The SILVER (silver impregnated line versus evd randomized trial): A double-blind, prospective, randomized, controlled trial of an intervention to reduce the rate of external ventricular drain infection.* Neurosurgery, 2012. **71**(2): p. 394-403.
140. George, R., L. Leibrock, and M. Epstein, *Long-term analysis of cerebrospinal fluid shunt infections. A 25-year experience.* Journal of Neurosurgery, 1979. **51**(6): p. 804-811.
141. Choux, M., et al., *Shunt implantation: Reducing the incidence of shunt infection.* Journal of Neurosurgery, 1992. **77**(6): p. 875-880.
142. Kestle, J., et al., *Long-term follow-up data from the Shunt Design Trial.* Pediatr Neurosurg, 2000. **33**(5): p. 230-236.
143. Mallucci, C.L., et al., *Antibiotic or silver versus standard ventriculoperitoneal shunts (BASICS): a multicentre, single-blinded, randomised trial and economic evaluation.* The Lancet, 2019. **394**(10208): p. 1530-1539.
144. Vinchon, M. and P. Dhellemmes, *Cerebrospinal fluid shunt infection: Risk factors and long-term follow-up.* Child's Nervous System, 2006. **22**(7): p. 692-697.
145. Simon, T.D., et al., *Patient and Treatment Characteristics by Infecting Organism in Cerebrospinal Fluid Shunt Infection.* Journal of the Pediatric Infectious Diseases Society, 2019. **8**(3): p. 235-243.
146. Pople, I.K., R. Bayston, and R.D. Hayward, *Infection of cerebrospinal fluid shunts in infants: a study of etiological factors.* J Neurosurg, 1992. **77**(1): p. 29-36.
147. Kulkarni, A.V., J.M. Drake, and M. Lamberti-Pasculli, *Cerebrospinal fluid shunt infection: A prospective study of risk factors.* Journal of Neurosurgery, 2001. **94**(2): p. 195-201.
148. Ochieng', N., et al., *Bacteria causing ventriculoperitoneal shunt infections in a Kenyan population.* Journal of Neurosurgery: Pediatrics PED, 2015. **15**(2): p. 150.
149. Hussein, K., et al., *Management of post-neurosurgical meningitis: narrative review.* Clinical Microbiology and Infection, 2017. **23**(9): p. 621-628.
150. Hengstman, G.J.D., et al., *Delayed cranial neuropathy after neurosurgery caused by herpes simplex virus reactivation: report of three cases.* Surgical Neurology, 2005. **64**(1): p. 67-69.
151. Ohata, K., et al., *Aetiology of delayed facial palsy after vestibular schwannoma surgery: Clinical data and hypothesis.* Acta Neurochirurgica, 1998. **140**(9): p. 913917.
152. Raper, D.M.S., et al., *Herpes simplex encephalitis following spinal ependymoma resection: Case report and literature review.* Journal of Neuro-Oncology, 2011. **103**(3): p. 771-776.
153. Kwon, J.W., et al., *Herpes simplex encephalitis after craniopharyngioma surgery.* J Neurosurg Pediatr, 2008. **2**(5): p. 355-8.
154. Jalloh, I., et al., *Reactivation and centripetal spread of herpes simplex virus complicating acoustic neuroma resection.* Surg Neurol, 2009. **72**(5): p. 502-4.
155. Filipo, R., et al., *Post-operative Herpes simplex virus encephalitis after surgical resection of acoustic neuroma: a case report.* J Laryngol Otol, 2005. **119**(7): p. 55860.
156. Mallory, G.W., et al., *Herpes simplex meningitis after removal of a vestibular schwannoma: case report and review of the literature.* Otol Neurotol, 2012. **33**(8): p. 1422-5.

157. Ploner, M., B. Turowski, and G. Wobker, *Herpes encephalitis after meningioma resection.* Neurology, 2005. **65**(10): p. 1674-5.
158. Álvarez de Eulate-Beramendi, S., et al., *Herpes simplex virus type 1 encephalitis after meningioma resection.* Neurología (English Edition), 2015. **30**(7): p. 455-457.
159. Kuhnt, D., et al., *Herpes simplex encephalitis after neurosurgical operations: Report of 2 cases and review of the literature.* Journal of Neurological Surgery, Part A: Central European Neurosurgery, 2012. **73**(2): p. 116-122.
160. Gianoli, G.J. and J.M. Kartush, *Delayed facial palsy after acoustic neuroma resection: The role of viral reactivation.* American Journal of Otology, 1996. **17**(4): p. 625-629.
161. O'Brien, D., et al., *Candida infection of the central nervous system following neurosurgery: a 12-year review.* Acta Neurochirurgica, 2011. **153**(6): p. 1347-1350.
162. Murthy, J.M.K. and C. Sundaram, *Fungal infections of the central nervous system*, in *Handbook of Clinical Neurology*. 2014. p. 1383-1401.
163. Brown, P., et al., *Iatrogenic Creutzfeldt-Jakob disease, final assessment.* Emerging infectious diseases, 2012. **18**(6): p. 901-907.
164. Bode, L.G.M., et al., *Preventing surgical-site infections in nasal carriers of Staphylococcus aureus.* New England Journal of Medicine, 2010. **362**(1): p. 9-17.
165. Ning, J., et al., *Nasal colonization of Staphylococcus aureus and the risk of surgical site infection after spine surgery: a meta-analysis.* Spine Journal, 2020. **20**(3): p. 448-456.
166. Lefebvre, J., et al., *Staphylococcus aureus screening and decolonization reduces the risk of surgical site infections in patients undergoing deep brain stimulation surgery.* Journal of Hospital Infection, 2017. **95**(2): p. 144-147.
167. Segers, P., et al., *Prevention of nosocomial infection in cardiac surgery by decontamination of the nasopharynx and oropharynx with chlorhexidine gluconate: A randomized controlled trial.* Journal of the American Medical Association, 2006. **296**(20): p. 2460-2466.
168. Akhtar Danesh, L., et al., *Elimination of Staphylococcus aureus nasal carriage in intensive care patients lowers infection rates.* European Journal of Clinical Microbiology and Infectious Diseases, 2020. **39**(2): p. 333-338.
169. Courville, X.F., et al., *Cost-effectiveness of preoperative nasal mupirocin treatment in preventing surgical site infection in patients undergoing total hip and knee arthroplasty: A cost-effectiveness analysis.* Infection Control and Hospital Epidemiology, 2012. **33**(2): p. 152-159.
170. Huang, S.S., et al., *Cost savings of universal decolonization to prevent intensive care unit infection: Implications of the REDUCE MRSA trial.* Infection Control and Hospital Epidemiology, 2014. **35**: p. S23-S31.
171. Hetem, D.J., et al., *Prevention of Surgical Site Infections: Decontamination with Mupirocin Based on Preoperative Screening for Staphylococcus aureus Carriers or Universal Decontamination?* Clinical Infectious Diseases, 2016. **62**(5): p. 631-636.
172. Stambough, J.B., et al., *Decreased Hospital Costs and Surgical Site Infection Incidence With a Universal Decolonization Protocol in Primary Total Joint Arthroplasty.* Journal of Arthroplasty, 2017. **32**(3): p. 728-734.e1.
173. Walcott, B.P., N. Redjal, and J.-V.C.E. Coumans, *Infection following operations on the central nervous system: deconstructing the myth of the sterile field.* 2012. **33**(5): p. E8.
174. Winston, K.R., *Hair and Neurosurgery.* Neurosurgery, 1992. **31**(2): p. 320-329.

175. Sebastian, S., *Does preoperative scalp shaving result in fewer postoperative wound infections when compared with no scalp shaving? A systematic review.* Journal of Neuroscience Nursing, 2012. **44**(3): p. 149-156.
176. Excellence, N.I.o.C., *Surgical Site Infections: Prevention and Treatment*. 2019: nice.org.uk.
177. Cronquist, A.B., et al., *Relationship between Skin Microbial Counts and Surgical Site Infection after Neurosurgery.* Clinical Infectious Diseases, 2001. **33**(8): p. 13021308.
178. Davies, B.M. and H.C. Patel, *Does chlorhexidine and povidone-iodine preoperative antisepsis reduce surgical site infection in cranial neurosurgery?* Annals of the Royal College of Surgeons of England, 2016. **98**(6): p. 405-408.
179. Alotaibi, A.F., et al., *The Efficacy of Antibacterial Prophylaxis Against the Development of Meningitis After Craniotomy: A Meta-Analysis.* World Neurosurgery, 2016. **90**: p. 597-603.e1.
180. Bratzler, D.W., et al., *Clinical practice guidelines for antimicrobial prophylaxis in surgery.* American Journal of Health-System Pharmacy, 2013. **70**(3): p. 195-283.
181. Holloway, K.L., et al., *Antibiotic prophylaxis during clean neurosurgery: a large, multicenter study using cefuroxime.* Clinical Therapeutics, 1996. **18**(1): p. 84-94.
182. Ratilal, B., J. Costa, and C. Sampaio, *Antibiotic prophylaxis for surgical introduction of intracranial ventricular shunts: a systematic review.* Journal of Neurosurgery. Pediatrics., 2008. **1**(1): p. 48-56.
183. Haines, S.J. and B.C. Walters, *Antibiotic prophylaxis for cerebrospinal fluid shunts: A metanalysis.* Neurosurgery, 1994. **34**(1): p. 87-92.
184. Noble, W.C., *Dispersal of skin microorganisms.* British Journal of Dermatology, 1975. **93**(4): p. 477-485.
185. Hospodsky, D., et al., *Human occupancy as a source of indoor airborne bacteria.* PloS one, 2012. **7**(4): p. e34867-e34867.
186. Lidwell, O.M., et al., *Effect of ultraclean air in operating rooms on deep sepsis in the joint after total hip or knee replacement: A randomised study.* British Medical Journal, 1982. **285**(6334): p. 10-14.
187. Chidambaram, S., et al., *Impact of Operating Room Environment on Postoperative Central Nervous System Infection in a Resource-Limited Neurosurgical Center in South Asia.* World Neurosurgery, 2018. **110**: p. e239-e244.
188. von Vogelsang, A.C., et al., *Effect of mobile laminar airflow units on airborne bacterial contamination during neurosurgical procedures.* Journal of Hospital Infection, 2018. **99**(3): p. 271-278.
189. Montagna, M.T., et al., *Evaluation of air contamination in orthopaedic operating theatres in hospitals in Southern Italy: The IMPACT project.* International Journal of Environmental Research and Public Health, 2019. **16**(19).
190. Brandt, C., et al., *Operating room ventilation with laminar airflow shows no protective effect on the surgical site infection rate in orthopedic and abdominal surgery.* Annals of Surgery, 2008. **248**(5): p. 695-700.
191. Sadrizadeh, S., et al., *Influence of staff number and internal constellation on surgical site infection in an operating room.* Particuology, 2014. **13**(1): p. 42-51.
192. Agodi, A., et al., *Operating theatre ventilation systems and microbial air contamination in total joint replacement surgery: Results of the GISIO-ISChIA study.* Journal of Hospital Infection, 2015. **90**(3): p. 213-219.
193. Scaltriti, S., et al., *Risk factors for particulate and microbial contamination of air in operating theatres.* Journal of Hospital Infection, 2007. **66**(4): p. 320-326.

194. Sørensen, P., et al., *Bacterial contamination of surgeons gloves during shunt insertion: A pilot study.* British Journal of Neurosurgery, 2008. **22**(5): p. 675-677.
195. Tulipan, N. and M.A. Cleves, *Effect of an intraoperative double-gloving strategy on the incidence of cerebrospinal fluid shunt infection.* J Neurosurg, 2006. **104**(1 Suppl): p. 5-8.
196. Makama, J.G., et al., *Glove Perforation Rate in Surgery: A Randomized, Controlled Study to Evaluate the Efficacy of Double Gloving.* Surgical Infections, 2016. **17**(4): p. 436-442.
197. Haynes, A., et al., *A surgical safety checklist to reduce morbidity and mortality in a global population.* N Engl J Med, 2009. **360**: p. 491-499.
198. Lepänluoma, M., et al., *Analysis of neurosurgical reoperations: use of a surgical checklist and reduction of infection-related and preventable complication-related reoperations.* 2015. **123**(1): p. 145.
199. Bayston, R. and S.R. Penny, *Excessive production of mucoid substance in staphylococcus SIIA: a possible factor in colonisation of Holter shunts.* Developmental medicine and child neurology. Supplement, 1972. **27**: p. 25-28.
200. Bayston, R., et al., *Biofilm formation by Propionibacterium acnes on biomaterials in vitro and in vivo: Impact on diagnosis and treatment.* Journal of Biomedical Materials Research - Part A, 2007. **81**(3): p. 705-709.
201. Lajcak, M., et al., *Infection rates of external ventricular drains are reduced by the use of silver-impregnated catheters.* Acta Neurochirurgica, 2013. **155**(5): p. 875881.
202. Atkinson, R.A., et al., *Silver-impregnated external-ventricular-drain-related cerebrospinal fluid infections: A meta-analysis.* Journal of Hospital Infection, 2016. **92**(3): p. 263-272.
203. Nilsson, A., et al., *Silver-Coated Ventriculostomy Catheters Do Not Reduce Rates of Clinically Diagnosed Ventriculitis.* World Neurosurgery, 2018. **117**: p. e411-e416.
204. John, R.W.K., et al., *A new Hydrocephalus Clinical Research Network protocol to reduce cerebrospinal fluid shunt infection.* Journal of Neurosurgery: Pediatrics PED, 2016. **17**(4): p. 391-396.
205. Brian, T.R., R.B. Samuel, and H.S. Richard, *Surgical shunt infection: significant reduction when using intraventricular and systemic antibiotic agents.* Journal of Neurosurgery JNS, 2006. **105**(2): p. 242-247.
206. Bokhari, R., et al., *Effect of Intrawound Vancomycin on Surgical Site Infections in Nonspinal Neurosurgical Procedures: A Systematic Review and Meta-Analysis.* World Neurosurgery, 2019. **123**: p. 409-417.e7.
207. Ken, R.W., A.M. Lori, and D. Anwar, *Bandages, dressings, and cranial neurosurgery.* Journal of Neurosurgery: Pediatrics PED, 2007. **106**(6): p. 450-454.
208. Safdar, N., et al., *Chlorhexidine-Impregnated Dressing for Prevention of CatheterRelated Bloodstream Infection: A Meta-Analysis*.* Read Online: Critical Care Medicine | Society of Critical Care Medicine, 2014. **42**(7): p. 1703-1713.
209. Scheithauer, S., et al., *Significant Reduction of External Ventricular Drainage–Associated Meningoventriculitis by Chlorhexidine-Containing Dressings: A BeforeAfter Trial.* Clinical Infectious Diseases, 2015. **62**(3): p. 404-405.
210. Roethlisberger, M., et al., *Effectiveness of a chlorhexidine dressing on silver-coated external ventricular drain–associated colonization and infection: A prospective single-blinded randomized controlled clinical trial.* Clinical Infectious Diseases, 2018. **67**(12): p. 1868-1877.
211. Palese, A., et al., *Post-operative shampoo effects in neurosurgical patients: A pilot experimental study.* Surgical Infections, 2015. **16**(2): p. 133-138.

212. Yeom, I., et al., *Effect of Unshaven Hair with Absorbable Sutures and Early Postoperative Shampoo on Cranial Surgery Site Infection.* Pediatric Neurosurgery, 2017. **53**(1): p. 18-23.
213. Lavallée, J.F., et al., *The effects of care bundles on patient outcomes: a systematic review and meta-analysis.* Implementation Science, 2017. **12**(1): p. 142.
214. Sieg, E.P., et al., *Impact of an External Ventricular Drain Placement and Handling Protocol on Infection Rates: A Meta-Analysis and Single Institution Experience.* World Neurosurgery, 2018. **115**: p. e53-e58.
215. Leverstein-Van Hall, M.A., et al., *A bundle approach to reduce the incidence of external ventricular and lumbar drain-related infections: Clinical article.* Journal of Neurosurgery, 2010. **112**(2): p. 345-353.
216. Flint, A.C., et al., *A simple protocol to prevent external ventricular drain infections.* Neurosurgery, 2013. **72**(6): p. 993-999.
217. Talibi, S.S., et al., *The implementation of an external ventricular drain care bundle to reduce infection rates.* British Journal of Neurosurgery, 2020: p. 1-6.
218. Omrani, O., et al., *Effect of introduction of a standardised peri-operative protocol on CSF shunt infection rate: a single-centre cohort study of 809 procedures.* Child's Nervous System, 2018. **34**(12): p. 2407-2414.
219. Jay, R.-C., et al., *Risk factors for shunt malfunction in pediatric hydrocephalus: a multicenter prospective cohort study.* Journal of Neurosurgery: Pediatrics PED, 2016. **17**(4): p. 382-390.
220. Vinchon, M. and P. Dhellemmes, *Cerebrospinal fluid shunt infection: risk factors and long-term follow-up.* Childs Nerv Syst, 2006. **22**(7): p. 692-7.
221. Simon, T.D., et al., *Infection rates following initial cerebrospinal fluid shunt placement across pediatric hospitals in the United States: Clinical article.* Journal of Neurosurgery: Pediatrics, 2009. **4**(2): p. 156-165.
222. Simon, T.D., et al., *Risk Factors for First Cerebrospinal Fluid Shunt Infection: Findings from a Multi-Center Prospective Cohort Study.* The Journal of Pediatrics, 2014. **164**(6): p. 1462-1468.e2.
223. Sherise, D.F., M. Nancy, and M.F. David, *Observations regarding failure of cerebrospinal fluid shunts early after implantation.* Neurosurgical Focus FOC, 2007. **22**(4): p. 1-5.
224. Castle-Kirszbaum, M.D., et al., *Obesity in Neurosurgery: A Narrative Review of the Literature.* World Neurosurgery, 2017. **106**: p. 790-805.
225. Lietard, C., et al., *Risk factors for neurosurgical site infections: An 18-month prospective survey - Clinical article.* Journal of Neurosurgery, 2008. **109**(4): p. 729734.
226. Jeelani, N.U.O., et al., *Postoperative cerebrospinal fluid wound leakage as a predictor of shunt infection: A prospective analysis of 205 cases: Clinical article.* Journal of Neurosurgery: Pediatrics, 2009. **4**(2): p. 166-169.
227. Simon, T.D., et al., *Risk factors for first cerebrospinal fluid shunt infection: Findings from a multi-center prospective cohort study.* Journal of Pediatrics, 2014. **164**(6): p. 1462-1468.e2.
228. Linzey, J.R., et al., *The effect of surgical start time on complications associated with neurological surgeries.* Clinical Neurosurgery, 2018. **83**(3): p. 501-507.
229. Matthew, R.T., et al., *Relationship of causative organism and time to infection among children with cerebrospinal fluid shunt infection.* Journal of Neurosurgery: Pediatrics PED, 2019. **24**(1): p. 22-28.

230. Brown, E.M., et al., *The management of neurosurgical patients with postoperative bacterial or aseptic meningitis or external ventricular drain-associated ventriculitis. Infection in Neurosurgery Working Party of the British Society for Antimicrobial Chemotherapy.* British Journal of Neurosurgery, 2000. **14**(1): p. 7-12.
231. Conen, A., et al., *Characteristics and treatment outcome of cerebrospinal fluid shunt-associated infections in adults: A retrospective analysis over an 11-year period.* Clinical Infectious Diseases, 2008. **47**(1): p. 73-82.
232. Zervos, T. and B.C. Walters, *Diagnosis of Ventricular Shunt Infection in Children: A Systematic Review.* World Neurosurgery, 2019. **129**: p. 34-44.
233. UK, C.R. *Surgery to remove fluid*. Brain Tumours 2019 03//11/2020]; Available from: https://about-cancer.cancerresearchuk.org/about-cancer/braintumours/treatment/surgery/remove-fluid.
234. Greenberg, M.S.M.D., *Handbook of neurosurgery*. 9th ed. ed.: Thieme.
235. Martin, R.M., et al., *Diagnostic Approach to Health Care- and Device-Associated Central Nervous System Infections.* Journal of Clinical Microbiology, 2018. **56**(11): p. e00861-18.
236. Lenfestey, R.W., et al., *Predictive value of cerebrospinal fluid parameters in neonates with intraventricular drainage devices.* 2007. **107**(3): p. 209.
237. Daniel, H.F., et al., *Progression of cerebrospinal fluid cell count and differential over a treatment course of shunt infection.* Journal of Neurosurgery: Pediatrics PED, 2011. **8**(6): p. 613-619.
238. Schade, R.P., et al., *Lack of value of routine analysis of cerebrospinal fluid for prediction and diagnosis of external drainage-related bacterial meningitis.* Journal of Neurosurgery, 2006. **104**(1): p. 101-108.
239. Apostolakis, S., *Use of Focused Ultrasound (Sonication) for the Diagnosis of Infections in Neurosurgical Operations: A Systematic Review and Meta-Analysis.* World Neurosurgery, 2020. **136**: p. 364-373.e2.
240. Rath, P.M., et al., *Value of multiplex PCR using cerebrospinal fluid for the diagnosis of ventriculostomy-related meningitis in neurosurgery patients.* Infection, 2014. **42**(4): p. 621-627.
241. Rekate, H.L., T. Ruch, and F.E. Nulsen, *Diphtheroid infections of cerebrospinal fluid shunts. The changing pattern of shunt infection in Cleveland.* J Neurosurg, 1980. **52**: p. 553-556.
242. Arnell, K., et al., *Cerebrospinal fluid shunt infections in children over a 13-year period: Anaerobic cultures and comparison of clinical signs of infection with Propionibacterium acnes and with other bacteria.* Journal of Neurosurgery: Pediatrics, 2008. **1**(5): p. 366-372.
243. Education, N. *Polymerase chain reaction/ PCR*. Scitable 2014 [cited 2021 10/07/2021]; Definition]. Available from: https://www.nature.com/scitable/definition/polymerase-chain-reaction-pcr-110/.
244. Mostyn, A., et al., *Assessment of the FilmArray® multiplex PCR system and associated meningitis/encephalitis panel in the diagnostic service of a tertiary hospital.* Infection Prevention in Practice, 2020. **2**(2): p. 100042.
245. Leber, A.L., et al., *Multicenter Evaluation of BioFire FilmArray Meningitis/Encephalitis Panel for Detection of Bacteria, Viruses, and Yeast in Cerebrospinal Fluid Specimens.* Journal of Clinical Microbiology, 2016. **54**(9): p. 2251-2261.
246. Vetter, P., et al., *Diagnostic challenges of central nervous system infection:*

extensive multiplex panels versus stepwise guided approach. Clinical Microbiology and Infection, 2020. **26**(6): p. 706-712.
247. Notomi, T., et al., *Loop-mediated isothermal amplification of DNA.* Nucleic Acids Research, 2000. **28**(12): p. e63-e63.
248. D'Inzeo, T., et al., *Implementation of the eazyplex® CSF direct panel assay for rapid laboratory diagnosis of bacterial meningitis: 32-month experience at a tertiary care university hospital.* European Journal of Clinical Microbiology & Infectious Diseases, 2020. **39**(10): p. 1845-1853.
249. bioMérieux. *BIOFIRE® FILMARRAY® ME Panel*

BIOFIRE FILMARRAY Meningitis/Encephalitis Panel. Commercial website and marketing materials]. Available from: https://www.biomerieux-diagnostics.com/filmarraymeningitis-encephalitis-me-panel.
250. Inc, S. *Allplex™*

Meningitis Panel Assays. Available from: http://www.seegene.com/assays/allplex_meningitis_panel_assays.
251. Durand, M.L., et al., *Acute Bacterial Meningitis in Adults – A Review of 493 Episodes.* New England Journal of Medicine, 1993. **328**(1): p. 21-28.
252. Brenna, J.T., *Natural intramolecular isotope measurements in physiology: Elements of the case for an effort toward high-precision position-specific isotope analysist.* Rapid Communications in Mass Spectrometry, 2001. **15**(15): p. 1252-1262.
253. Group, F.-N.B.W., in *BEST (Biomarkers, EndpointS, and other Tools) Resource*. 2016, Food and Drug Administration (US) National Institutes of Health (US): Silver Spring (MD)

Bethesda (MD).
254. Puttgen, H.A. and J.N. Shah, *Dire straits for biomarkers of neurosurgery-associated meningitis.* Critical Care Medicine, 2015. **43**(11): p. 2513-2514.
255. Desiderio, C., et al., *Cerebrospinal fluid top-down proteomics evidenced the potential biomarker role of LVV- and VV-hemorphin-7 in posterior cranial fossa pediatric brain tumors.* Proteomics, 2012. **12**(13): p. 2158-2166.
256. Schuhmann, M.U., et al., *Peptide screening of cerebrospinal fluid in patients with glioblastoma multiforme.* European Journal of Surgical Oncology, 2010. **36**(2): p. 201-207.
257. King, M.D., et al., *Elucidating novel mechanisms of brain injury following subarachnoid hemorrhage: An emerging role for neuroproteomics.* Neurosurgical Focus, 2010. **28**(1): p. E10.1-E10.10.
258. Connor, D.E., et al., *Variations in the cerebrospinal fluid proteome following traumatic brain injury and subarachnoid hemorrhage.* Pathophysiology, 2017. **24**(3): p. 169-183.
259. Fernández-Irigoyen, J., et al., *New insights into the human brain proteome: Protein expression profiling of deep brain stimulation target areas.* Journal of Proteomics, 2015. **127**: p. 395-405.
260. Zsigmond, P., S.A. Ljunggren, and B. Ghafouri, *Proteomic Analysis of the Cerebrospinal Fluid in Patients With Essential Tremor Before and After Deep Brain Stimulation Surgery: A Pilot Study.* Neuromodulation, 2020. **23**(4): p. 502-508.
261. Fredricks, D.N. and D.A. Relman, *Sequence-based identification of microbial pathogens: A reconsideration of Koch's postulates.* Clinical Microbiology Reviews, 1996. **9**(1): p. 18-33.

262. Leib, S.L., et al., *Predictive value of cerebrospinal fluid (CSF) lactate level versus CSF/blood glucose ratio for the diagnosis of bacterial meningitis following neurosurgery.* Clinical Infectious Diseases, 1999. **29**(1): p. 69-74.
263. Posner, J.B. and F. Plum, *Independence of Blood and Cerebrospinal Fluid Lactate.* Archives of Neurology, 1967. **16**(5): p. 492-496.
264. Bland, R.D., R.C. Lister, and J.P. Ries, *Cerebrospinal Fluid Lactic Acid Level and pH in Meningitis: Aids in Differential Diagnosis.* American Journal of Diseases of Children, 1974. **128**(2): p. 151-156.
265. Sakushima, K., et al., *Diagnostic accuracy of cerebrospinal fluid lactate for differentiating bacterial meningitis from aseptic meningitis: A meta-analysis.* Journal of Infection, 2011. **62**(4): p. 255-262.
266. McGill, F., et al., *The UK joint specialist societies guideline on the diagnosis and management of acute meningitis and meningococcal sepsis in immunocompetent adults.* Journal of Infection, 2016. **72**(4): p. 405-438.
267. Grille, P., et al., *Clinical research Value of cerebrospinal fluid lactate for the diagnosis of bacterial meningitis in postoperative neurosurgical patients.* Neurocirugia, 2012. **23**(4): p. 131-135.
268. Li, Y., et al., *The diagnostic value of cerebrospinal fluids procalcitonin and lactate for the differential diagnosis of post-neurosurgical bacterial meningitis and aseptic meningitis.* Clinical Biochemistry, 2015. **48**(1-2): p. 50-54.
269. Maskin, L.P., et al., *Cerebrospinal fluid lactate in post-neurosurgical bacterial meningitis diagnosis.* Clinical Neurology & Neurosurgery, 2013. **115**(9): p. 1820-5.
270. Roth, J., et al., *The value of CSF lactate levels in diagnosing shunt infections in pediatric patients.* World Neurosurgery, 2019.
271. Zhang, Y., et al., *Diagnostic accuracy of routine blood examinations and CSF lactate level for post-neurosurgical bacterial meningitis.* International Journal of Infectious Diseases, 2017. **59**: p. 50-54.
272. Tavares, W.M., et al., *CSF markers for diagnosis of bacterial meningitis in neurosurgical postoperative patients.* Arquivos de Neuro-Psiquiatria, 2006. **64**(3A): p. 592-5.
273. Xiao, X., et al., *The diagnostic value of cerebrospinal fluid lactate for postneurosurgical bacterial meningitis: A meta-analysis.* BMC Infectious Diseases, 2016. **16**(1).
274. Roth, J., et al., *Value of Cerebrospinal Fluid Lactate Levels in Diagnosing Shunt Infections in Pediatric Patients.* World Neurosurgery, 2019. **129**: p. e207-e215.
275. Bhimraj, A., *Healthcare-acquired meningitis and ventriculitis*, in *CNS Infections: A Clinical Approach: Second Edition*. 2018. p. 31-48.
276. Ortiz, O.H.H., et al., *Development of a prediction rule for diagnosing postoperative meningitis: A cross-sectional study.* Journal of Neurosurgery, 2018. **128**(1): p. 262271.
277. Becker, K.L., R. Snider, and E.S. Nylen, *Procalcitonin in sepsis and systemic inflammation: a harmful biomarker and a therapeutic target.* British journal of pharmacology, 2010. **159**(2): p. 253-264.
278. Brunkhorst, F.M., U. Heinz, and Z.F. Forycki, *Kinetics of procalcitonin in iatrogenic sepsis.* Intensive Care Medicine, 1998. **24**(8): p. 888-889.
279. Dandona, P., et al., *Procalcitonin increase after endotoxin injection in normal subjects.* J Clin Endocrinol Metab, 1994. **79**(6): p. 1605-8.

280. Feezor, R.J., et al., *Molecular Characterization of the Acute Inflammatory Response to Infections with Gram-Negative versus Gram-Positive Bacteria.* Infection and Immunity, 2003. **71**(10): p. 5803-5813.
281. Alons, I.M.E., et al., *Procalcitonin in cerebrospinal fluid in meningitis: a prospective diagnostic study.* Brain and Behavior, 2016. **6**(11).
282. Viallon, A., et al., *High sensitivity and specificity of serum procalcitonin levels in adults with bacterial meningitis.* Clinical Infectious Diseases, 1999. **28**(6): p. 13131316.
283. Schwarz, S., et al., *Serum procalcitonin levels in bacterial and abacterial meningitis.* Critical Care Medicine, 2000. **28**(6): p. 1828-1832.
284. Dubos, F., et al., *Serum procalcitonin and other biologic markers to distinguish between bacterial and aseptic meningitis.* Journal of Pediatrics, 2006. **149**(1): p. 7276.
285. Martínez, R., et al., *Serum procalcitonin monitoring for differential diagnosis of ventriculitis in adult intensive care patients.* Intensive Care Medicine, 2002. **28**(2): p. 208-210.
286. Choi, S.H. and S.H. Choi, *Predictive performance of serum procalcitonin for the diagnosis of bacterial meningitis after neurosurgery.* Infection and Chemotherapy, 2013. **45**(3): p. 308-314.
287. Black, S., I. Kushner, and D. Samols, *C-reactive protein.* Journal of Biological Chemistry, 2004. **279**(47): p. 48487-48490.
288. Volanakis, J.E., *Human C-reactive protein: Expression, structure, and function.* Molecular Immunology, 2001. **38**(2-3): p. 189-197.
289. Corrall, C.J., et al., *C-Reactive protein in spinal fluid of children with meningitis.* The Journal of Pediatrics, 1981. **99**(3): p. 365-369.
290. Gerdes, L.U., et al., *C-reactive protein and bacterial meningitis: a meta-analysis.* Scand J Clin Lab Invest, 1998. **58**(5): p. 383-93.
291. Malla, K.K., et al., *Is cerebrospinal fluid C-reactive protein a better tool than blood creactive protein in laboratory diagnosis of meningitis in children?* Sultan Qaboos University Medical Journal, 2013. **13**(1): p. 93-99.
292. Javadinia, S., et al., *C - reactive protein of cerebrospinal fluid, as a sensitive approach for diagnosis of neonatal meningitis.* African Health Sciences, 2019. **19**(3): p. 2372-2377.
293. Kashaki, M., et al., *Is there any correlation between cerebrospinal fluid and serum creactive protein in neonates suspected to meningitis?* Journal of Kerman University of Medical Sciences, 2020. **27**(5): p. 389-393.
294. Thakur, S., et al., *Csf c-reactive protein in meningitis.* Journal, Indian Academy of Clinical Medicine, 2020. **21**(3-4): p. 123-126.
295. Mishra, N.R., B.K. Sahoo, and R.R. Das, *Role of CSF C-reactive protein for rapid diagnosis and differentiation of different forms of meningitis in children.* Journal of Clinical and Diagnostic Research, 2018. **12**(8): p. SC05-SC08.
296. Song, B., et al., *Relevant analyses of pathogenic bacteria and inflammatory factors in neonatal purulent meningitis.* Experimental and Therapeutic Medicine, 2018. **16**(2): p. 1153-1158.
297. Nadeem, M., M.S. Alam, and M. Singh, *Role of CSF-CRP in diagnosis of acute bacterial and aseptic meningitis in children.* Pakistan Journal of Medical and Health Sciences, 2018. **12**(2): p. 720-723.

298. Zhang, X.F., et al., *Application value of procalcitonin in patients with central nervous system infection.* European review for medical and pharmacological sciences, 2017. **21**(17): p. 3944-3949.
299. Belagavi, A.C. and M. Shalini, *Cerebrospinal fluid C reactive protein and adenosine deaminase in meningitis in adults.* Journal of Association of Physicians of India, 2011. **59**(9): p. 557-560.
300. Martin, U.S., et al., *The value of C-reactive protein in the management of shunt infections.* Journal of Neurosurgery: Pediatrics, 2005. **103**(3): p. 223-230.
301. Santotoribio, J.D., J.F. Cuadros-Muñoz, and N. García-Casares, *Comparison of C reactive protein and procalcitonin levels in cerebrospinal fluid and serum to differentiate bacterial from viral meningitis.* Annals of Clinical and Laboratory Science, 2018. **48**(4): p. 506-510.
302. Aharwar, S., et al., *A study of CSF C-reactive protein levels in patients of meningitis.* Journal, Indian Academy of Clinical Medicine, 2016. **17**(2): p. 105-110.
303. Sharouf, F., et al., *C-reactive protein kinetics post elective cranial surgery. A prospective observational study.* British Journal of Neurosurgery, 2020. **34**(1): p. 4650.
304. Clarridge Iii, J.E., *Impact of 16S rRNA gene sequence analysis for identification of bacteria on clinical microbiology and infectious diseases.* Clinical Microbiology Reviews, 2004. **17**(4): p. 840-862.
305. Organization, W.H. *Ten threats to global health in 2019*. 2019; Available from: https://www.who.int/vietnam/news/feature-stories/detail/ten-threats-to-globalhealth-in-2019.
306. Dong, J., et al., *Emerging Pathogens: Challenges and Successes of Molecular Diagnostics.* The Journal of Molecular Diagnostics, 2008. **10**(3): p. 185-197.
307. Koch, R., *Ueber bakteriologische forschung.* Über bakteriologische Forschung., 1891. **1**: p. 35-47.
308. Lewis, A., et al., *Ventriculostomy-related infections: The performance of different definitions for diagnosing infection.* British Journal of Neurosurgery, 2016. **30**(1): p. 49-56.
309. Teunissen, C.E., et al., *Biobanking of CSF: International standardization to optimize biomarker development.* Clinical Biochemistry, 2014. **47**(4-5): p. 288-292.
310. Schilling, B., et al., *CHAPTER 7 MS1 Label-free Quantification Using Ion Intensity Chromatograms in Skyline (Research and Clinical Applications)*, in *Quantitative Proteomics*. 2014, The Royal Society of Chemistry. p. 154-174.
311. Cox, J. and M. Mann, *MaxQuant enables high peptide identification rates, individualized p.p.b.-range mass accuracies and proteome-wide protein quantification.* Nature Biotechnology, 2008. **26**(12): p. 1367-1372.
312. Cox, J., et al., *A practical guide to the MaxQuant computational platform for SILACbased quantitative proteomics.* Nature Protocols, 2009. **4**(5): p. 698-705.
313. Tyanova, S., et al., *The Perseus computational platform for comprehensive analysis of (prote)omics data.* Nature Methods, 2016. **13**(9): p. 731-740.
314. Eisen, M.B., et al., *Cluster analysis and display of genome-wide expression patterns.* Proceedings of the National Academy of Sciences of the United States of America, 1998. **95**(25): p. 14863-14868.
315. Keil, C.L., Robert William; Faizaan, Shaik Mohammed; Bezawada, Srikanth; Parsons, Lance; Baryshnikova, Anastasia. *Treeview 3.0 (beta 1) - Visualization and analysis of large data matrices*. Available from: https://bitbucket.org/TreeView3Dev/treeview3/src/master/.

316. Earls, J.C., et al., *AUREA: An open-source software system for accurate and userfriendly identification of relative expression molecular signatures.* BMC Bioinformatics, 2013. **14**.
317. Team, R., *RStudio*, in *RStudio*, R.I. Development, Editor. 2020, RStudio Team: PBC, Boston, MA. p. Environment for R. .
318. Key, M., *A tutorial in displaying mass spectrometry-based proteomic data using heat maps.* BMC bioinformatics, 2012. **13 Suppl 16**(Suppl 16): p. S10-S10.
319. Parker, E.P.K., et al., *Impact of maternal antibodies and microbiota development on the immunogenicity of oral rotavirus vaccine in African, Indian, and European infants.* Nature Communications, 2021. **12**(1): p. 7288.
320. Altschul, S.F., et al., *Basic local alignment search tool.* J Mol Biol, 1990. **215**(3): p. 403-10.
321. Martin, M., *Cutadapt removes adapter sequences from high-throughput sequencing reads.* 2011, 2011. **17**(1): p. 3.
322. Chen, S., et al., *fastp: an ultra-fast all-in-one FASTQ preprocessor.* Bioinformatics, 2018. **34**(17): p. i884-i890.
323. Wood, D.E., J. Lu, and B. Langmead, *Improved metagenomic analysis with Kraken 2.* Genome Biology, 2019. **20**(1).
324. Lu, J., et al., *Bracken: Estimating species abundance in metagenomics data.* PeerJ Computer Science, 2017. **2017**(1).
325. Shen, W. and J. Xiong, *TaxonKit: a cross-platform and efficient NCBI taxonomy toolkit*. 2019.
326. Galili, T., et al., *heatmaply: an R package for creating interactive cluster heatmaps for online publishing.* Bioinformatics, 2018. **34**(9): p. 1600-1602.
327. Geisow, M.J., *Proteomics: one small step for a digital computer, one giant leap for humankind.* Nat Biotechnol, 1998. **16**(2): p. 206.
328. Wilkins, M.R., et al., *From Proteins to Proteomes: Large Scale Protein Identification by Two-Dimensional Electrophoresis and Arnino Acid Analysis.* Bio/Technology, 1996. **14**(1): p. 61-65.
329. International Human Genome Sequencing, C., *Finishing the euchromatic sequence of the human genome.* Nature, 2004. **431**(7011): p. 931-945.
330. Gstaiger, M. and R. Aebersold, *Applying mass spectrometry-based proteomics to genetics, genomics and network biology.* Nature Reviews Genetics, 2009. **10**(9): p. 617-627.
331. Smejkal, G.B., *Genomics and proteomics: of hares, tortoises and the complexity of tortoises.* Expert Review of Proteomics, 2012. **9**(5): p. 469-472.
332. Shen, L.X., J.P. Basilion, and V.P. Stanton, Jr., *Single-nucleotide polymorphisms can cause different structural folds of mRNA.* Proceedings of the National Academy of Sciences of the United States of America, 1999. **96**(14): p. 7871-7876.
333. Chu, D. and L. Wei, *Nonsynonymous, synonymous and nonsense mutations in human cancer-related genes undergo stronger purifying selections than expectation.* BMC Cancer, 2019. **19**(1): p. 359.
334. Clancy, S.B., W. . *Translation: DNA to mRNA to Protein*. Nucleic acid structure and function 2013 17/01/2021]; Available from: https://www.nature.com/scitable/topicpage/translation-dna-to-mrna-to-protein393/.
335. Nilsen, T.W. and B.R. Graveley, *Expansion of the eukaryotic proteome by alternative splicing.* Nature, 2010. **463**(7280): p. 457-463.

336. Chen, J. and W.A. Weiss, *Alternative splicing in cancer: implications for biology and therapy.* Oncogene, 2015. **34**(1): p. 1-14.
337. Maloy, S. and K. Hughes, *Brenner's Encyclopedia of Genetics: Second Edition*. Brenner's Encyclopedia of Genetics: Second Edition. 2013. 1-3905.
338. Wang, Y.-C., S.E. Peterson, and J.F. Loring, *Protein post-translational modifications and regulation of pluripotency in human stem cells.* Cell Research, 2014. **24**(2): p. 143-160.
339. Zhang, J., *Proteomics of human cerebrospinal fluid - The good, the bad, and the ugly.* Proteomics - Clinical Applications, 2007. **1**(8): p. 805-819.
340. Zhang, Y., et al., *A comprehensive map and functional annotation of the normal human cerebrospinal fluid proteome.* Journal of Proteomics, 2015. **119**: p. 90-99.
341. Walker, D.G., in *Clinical Methods: The History, Physical, and Laboratory Examinations*, H.K. Walker, W.D. Hall, and J.W. Hurst, Editors. 1990, Butterworths

342. *Proteomics for Biomarker Discovery Methods and Protocols*, ed. J.M. Walker. 2019: Humana Press, Springer. 291.
343. Pedrero-Prieto, C.M., et al., *A comprehensive systematic review of CSF proteins and peptides that define Alzheimer's disease.* Clinical Proteomics, 2020. **17**(1).
344. Wang, H., et al., *Integrated analysis of ultra-deep proteomes in cortex, cerebrospinal fluid and serum reveals a mitochondrial signature in Alzheimer's disease.* Molecular Neurodegeneration, 2020. **15**(1).
345. Muraoka, S., et al., *Proteomic Profiling of Extracellular Vesicles Derived from Cerebrospinal Fluid of Alzheimer's Disease Patients: A Pilot Study.* Cells, 2020. **9**(9).
346. Ausó, E., V. Gómez-Vicente, and G. Esquiva, *Biomarkers for alzheimer's disease early diagnosis.* Journal of Personalized Medicine, 2020. **10**(3): p. 1-27.
347. Reus, L.M., et al., *Degree of genetic liability for Alzheimer's disease associated with specific proteomic profiles in cerebrospinal fluid.* Neurobiology of Aging, 2020. **93**: p. 144.e1-144.e15.
348. Whelan, C.D., et al., *Multiplex proteomics identifies novel CSF and plasma biomarkers of early Alzheimer's disease.* Acta Neuropathologica Communications, 2019. **7**(1).
349. Hayashi, N., et al., *Proteomic analysis of exosome-enriched fractions derived from cerebrospinal fluid of amyotrophic lateral sclerosis patients.* Neuroscience Research, 2020. **160**: p. 43-49.
350. Oeckl, P., et al., *Proteomics in cerebrospinal fluid and spinal cord suggests UCHL1, MAP2 and GPNMB as biomarkers and underpins importance of transcriptional pathways in amyotrophic lateral sclerosis.* Acta Neuropathologica, 2020. **139**(1): p. 119-134.
351. Thompson, A.G., et al., *Cerebrospinal fluid macrophage biomarkers in amyotrophic lateral sclerosis.* Annals of Neurology, 2018. **83**(2): p. 258-268.
352. Rotunno, M.S., et al., *Cerebrospinal fluid proteomics implicates the granin family in Parkinson's disease.* Scientific Reports, 2020. **10**(1).
353. Sinha, A., et al., *Identification of differentially displayed proteins in cerebrospinal fluid of Parkinson's disease patients: A proteomic approach.* Clinica Chimica Acta, 2009. **400**(1-2): p. 14-20.
354. Maarouf, C.L., et al., *Cerebrospinal fluid biomarkers of neuropathologically diagnosed Parkinson's disease subjects.* Neurological Research, 2012. **34**(7): p. 669676.

355. Shi, M., et al., *Cerebrospinal fluid peptides as potential parkinson disease biomarkers: A staged pipeline for discovery and validation.* Molecular and Cellular Proteomics, 2015. **14**(3): p. 544-555.
356. Constantinescu, R., et al., *Proteomic profiling of cerebrospinal fluid in parkinsonian disorders.* Parkinsonism and Related Disorders, 2010. **16**(8): p. 545-549.
357. Van Steenoven, I., et al., *Identification of novel cerebrospinal fluid biomarker candidates for dementia with Lewy bodies: a proteomic approach.* Molecular Neurodegeneration, 2020. **15**(1).
358. Dieks, J.K., et al., *Low-abundant cerebrospinal fluid proteome alterations in dementia with Lewy bodies.* Journal of Alzheimer's Disease, 2013. **34**(2): p. 387-397.
359. Kessler, T., et al., *Cerebrospinal fluid proteomic profiling in nusinersen-treated patients with spinal muscular atrophy.* Journal of Neurochemistry, 2020. **153**(5): p. 650-661.
360. Mellinger, A.L., E.H. Griffith, and M.S. Bereman, *Peptide variability and signatures associated with disease progression in CSF collected longitudinally from ALS patients.* Analytical and Bioanalytical Chemistry, 2020. **412**(22): p. 5465-5475.
361. Dumont, D., et al., *Proteomic analysis of cerebrospinal fluid from multiple sclerosis patients.* Proteomics, 2004. **4**(7): p. 2117-2124.
362. Noben, J.P., et al., *Lumbar cerebrospinal fluid proteome in multiple sclerosis: Characterization by ultrafiltration, liquid chromatography, and mass spectrometry.* Journal of Proteome Research, 2006. **5**(7): p. 1647-1657.
363. Lehmensiek, V., et al., *Cerebrospinal fluid proteome profile in multiple sclerosis.* Multiple Sclerosis, 2007. **13**(7): p. 840-849.
364. Anderson, N.L. and N.G. Anderson, *The human plasma proteome: history, character, and diagnostic prospects.* Molecular & cellular proteomics : MCP, 2002. **1**(11): p. 845-867.
365. Surinova, S., et al., *On the Development of Plasma Protein Biomarkers.* Journal of Proteome Research, 2011. **10**(1): p. 5-16.
366. O'Farrell, P.H., *High resolution two dimensional electrophoresis of proteins.* Journal of Biological Chemistry, 1975. **250**(10): p. 4007-4021.
367. Griffiths, J., *A Brief History of Mass Spectrometry.* Analytical Chemistry, 2008. **80**(15): p. 5678-5683.
368. Mann, M., R.C. Hendrickson, and A. Pandey, *Analysis of Proteins and Proteomes by Mass Spectrometry.* Annual Review of Biochemistry, 2001. **70**(1): p. 437-473.
369. Karas, M. and F. Hillenkamp, *Laser desorption ionization of proteins with molecular masses exceeding 10,000 daltons.* Analytical Chemistry, 1988. **60**(20): p. 2299-2301.
370. Fenn, J., et al., *Electrospray ionization for mass spectrometry of large biomolecules.* Science, 1989. **246**(4926): p. 64-71.
371. Shimadzu. *Principle of MALDI/TOFMS*. 17/01/2021]; Available from: https://www.shimadzu.com/an/products/maldi/ms-applications/principle-ofmalditofms/index.html.
372. Alymatiri, C.M., M.G. Kouskoura, and C.K. Markopoulou, *Decoding the signal response of steroids in electrospray ionization mode (ESI-MS).* Analytical Methods, 2015. **7**(24): p. 10433-10444.
373. Domon, B. and R. Aebersold, *Mass Spectrometry and Protein Analysis.* Science, 2006. **312**(5771): p. 212-217.
374. Consortium, T.U., *UniProt: a worldwide hub of protein knowledge.* Nucleic Acids Research, 2018. **47**(D1): p. D506-D515.

375. Zhang, Y., et al., *Protein analysis by shotgun/bottom-up proteomics.* Chemical Reviews, 2013. **113**(4): p. 2343-2394.
376. Gillet, L.C., A. Leitner, and R. Aebersold, *Mass Spectrometry Applied to Bottom-Up Proteomics: Entering the High-Throughput Era for Hypothesis Testing.* Annual Review of Analytical Chemistry, 2016. **9**(1): p. 449-472.
377. Bennett, K.L. *A Fusion of Proteomic Practices: The Indisputable Complementarity of "Bottom-Up" and "Top-Down" Approaches*. Proteomics & Metabolomics, 2020.
378. Szabo, Z. and T. Janaky, *Challenges and developments in protein identification using mass spectrometry.* TrAC Trends in Analytical Chemistry, 2015. **69**: p. 76-87.
379. Blackstock, W.P. and M.P. Weir, *Proteomics: quantitative and physical mapping of cellular proteins.* Trends in Biotechnology, 1999. **17**(3): p. 121-127.
380. Geman, D., et al., *Classifying gene expression profiles from pairwise mRNA comparisons.* Statistical applications in genetics and molecular biology, 2004. **3**: p. Article19-Article19.
381. UniProt Consortium, T., *UniProt: the universal protein knowledgebase.* Nucleic Acids Research, 2018. **46**(5): p. 2699-2699.
382. Uhlén, M., et al., *Tissue-based map of the human proteome.* Science, 2015. **347**(6220): p. 1260419.
383. Sorensen, M. and S. Sorensen, *Compte rendu des Travaux du Laboratoire de Carlsberg.* The Proteins in Whey, 1939.
384. Johansson, B., *Isolation of an iron-containing red protein from human milk.* Acta Chem. Scand., 1960. **14**: p. 510-512.
385. Masson, P.L., J.F. Heremans, and C.H. Dive, *An iron-binding protein common to many external secretions.* Clinica Chimica Acta, 1966. **14**(6): p. 735-739.
386. Weinberg, E.D., *Antibiotic properties and applications of lactoferrin.* Current Pharmaceutical Design, 2007. **13**(8): p. 801-811.
387. Weinberg, E.D., *Iron availability and infection.* Biochimica et Biophysica Acta - General Subjects, 2009. **1790**(7): p. 600-605.
388. Masson, P.L. and J.F. Heremans, *Lactoferrin in milk from different species.* Comparative Biochemistry and Physiology -- Part B: Biochemistry and, 1971. **39**(1): p. 119-"122,IN11-IN14,123-129".
389. Bennett, R.M. and T. Kokocinski, *Lactoferrin Content of Peripheral Blood Cells.* British Journal of Haematology, 1978. **39**(4): p. 509-521.
390. Rosa, L., et al., *Lactoferrin: A Natural Glycoprotein Involved in Iron and Inflammatory Homeostasis.* International journal of molecular sciences, 2017. **18**(9): p. 1985.
391. Lönnerdal, B. and S. Iyer, *Lactoferrin: Molecular Structure and Biological Function.* Annual Review of Nutrition, 1995. **15**(1): p. 93-110.
392. Singh, P.K., et al., *A component of innate immunity prevents bacterial biofilm development.* Nature, 2002. **417**(6888): p. 552-555.
393. Bellamy, W., et al., *Identification of the bactericidal domain of lactoferrin.* Biochimica et Biophysica Acta (BBA) - Protein Structure and Molecular Enzymology, 1992. **1121**(1): p. 130-136.
394. Fillebeen, C., et al., *Receptor-mediated transcytosis of lactoferrin through the blood-brain barrier.* Journal of Biological Chemistry, 1999. **274**(11): p. 7011-7017.
395. Nasri, H., et al., *New concepts in nutraceuticals as alternative for pharmaceuticals.* International journal of preventive medicine, 2014. **5**(12): p. 1487-1499.
396. Sherman, M.P., et al., *Randomized Controlled Trial of Talactoferrin Oral Solution in Preterm Infants.* Journal of Pediatrics, 2016. **175**: p. 68-73.e3.

397. Manzoni, P., et al., *Bovine Lactoferrin Supplementation for Prevention of Late-Onset Sepsis in Very Low-Birth-Weight Neonates: A Randomized Trial.* JAMA, 2009. **302**(13): p. 1421-1428.
398. Kaur, G. and G. Gathwala, *Efficacy of bovine lactoferrin supplementation in preventing late-onset sepsis in low birth weight neonates: A randomized placeboControlled clinical trial.* Journal of Tropical Pediatrics, 2015. **61**(5): p. 370-376.
399. Lykova, O.F., et al., *Level of lactoferrin in serum and cerebrospinal fluid of patients with meningitis.* Zhurnal mikrobiologii, epidemiologii, i immunobiologii, 2007(2): p. 80-84.
400. Hällgren, R., A. Terént, and P. Venge, *Lactoferrin, lysozyme, and β<inf>2</inf>Microglobulin levels in cerebrospinal fluid - Differential indices of CNS inflammation.* Inflammation, 1982. **6**(3): p. 291-304.
401. Gutteberg, T.J., T. Flaegstad, and T. Jorgensen, *Lactoferrin, C-reactive protein, α-1antitrypsin and immunoglobulin GA in cerebrospinal fluid in meningitis.* Acta Paediatrica Scandinavica, 1986. **75**(4): p. 569-572.
402. Visakorpi, T., et al., *Cerebrospinal fluid lactoferrin in bacterial and viral meningitis.* Acta Paediatrica Scandinavica, 1987. **76**(6): p. 987-988.
403. Maffei, F.A., et al., *Levels of antimicrobial molecules defensin and lactoferrin are elevated in the cerebrospinal fluid of children with meningitis.* Pediatrics, 1999. **103**(5 I): p. 987-992.
404. Steinberg, A.V., V.I. Korzhenevich, and E.V. Mihailova, *Optimization of a diagnostic procedure for children with preliminary diagnosis of "meningitis".* Journal of Pediatric Infectious Diseases, 2010. **5**(1): p. 57-63.
405. Dastych, M., J. Gottwaldová, and Z. Čermáková, *Calprotectin and lactoferrin in the cerebrospinal fluid; Biomarkers utilisable for differential diagnostics of bacterial and aseptic meningitis?* Clinical Chemistry and Laboratory Medicine, 2015. **53**(4): p. 599-603.
406. Bottazzi, B., et al., *An Integrated View of Humoral Innate Immunity: Pentraxins as a Paradigm.* Annual Review of Immunology, 2010. **28**(1): p. 157-183.
407. Wang, Z., et al., *The Basic Characteristics of the Pentraxin Family and Their Functions in Tumor Progression.* Frontiers in Immunology, 2020. **11**(1757).
408. Dodds, D.C., et al., *Neuronal pentraxin receptor, a novel putative integral membrane pentraxin that interacts with neuronal pentraxin 1 and 2 and taipoxin-associated calcium-binding protein 49.* Journal of Biological Chemistry, 1997. **272**(34): p. 21488-21494.
409. Chen, B. and J.L. Bixby, *Neuronal pentraxin with chromo domain (NPCD) is a novel class of protein expressed in multiple neuronal domains.* Journal of Comparative Neurology, 2005. **481**(4): p. 391-402.
410. Kirkpatrick, L.L., et al., *Biochemical interactions of the neuronal pentraxins. Neuronal pentraxin (NP) receptor binds to taipoxin and taipoxin-associated calciumbinding protein 49 via NP1 and NP2.* Journal of Biological Chemistry, 2000. **275**(23): p. 17786-17792.
411. Tillett, W.S. and T. Francis, *Serological reactions in pneumonia with a nonprotein somatic fraction of pneumococcus.* Journal of Experimental Medicine, 1930. **52**(4): p. 561-571.
412. Cummings, D.M., et al., *Neuronal and Peripheral Pentraxins Modify Glutamate Release and may Interact in Blood-Brain Barrier Failure.* Cerebral Cortex, 2017. **27**(6): p. 3437-3448.

413. Boles, N.C., et al., *NPTX1 Regulates Neural Lineage Specification from Human Pluripotent Stem Cells.* Cell Reports, 2014. **6**(4): p. 724-736.
414. Sia, G.M., et al., *Interaction of the N-Terminal Domain of the AMPA Receptor GluR4 Subunit with the Neuronal Pentraxin NP1 Mediates GluR4 Synaptic Recruitment.* Neuron, 2007. **55**(1): p. 87-102.
415. Xu, D., et al., *Narp and NP1 form heterocomplexes that function in developmental and activity-dependent synaptic plasticity.* Neuron, 2003. **39**(3): p. 513-528.
416. Pribiag, H. and D. Stellwagen, *Neuroimmune regulation of homeostatic synaptic plasticity.* Neuropharmacology, 2014. **78**(C): p. 13-22.
417. Kanda, M., et al., *Therapeutic monoclonal antibody targeting of neuronal pentraxin receptor to control metastasis in gastric cancer.* Molecular Cancer, 2020. **19**(1).
418. Bartolini, A., et al., *The neuronal pentraxin-2 pathway is an unrecognized target in human neuroblastoma, which also offers prognostic value in patients.* Cancer Research, 2015. **75**(20): p. 4265-4271.
419. Andreiuolo, F., et al., *Neuronal differentiation distinguishes supratentorial and infratentorial childhood ependymomas.* Neuro-Oncology, 2010. **12**(11): p. 11261134.
420. Lim, B., et al., *Decreased cerebrospinal fluid neuronal pentraxin receptor is associated with PET-Aβ load and cerebrospinal fluid Aβ in a pilot study of Alzheimer's disease.* Neuroscience Letters, 2020. **731**.
421. Lim, B., et al., *Cerebrospinal fluid neuronal pentraxin receptor as a biomarker of long-term progression of Alzheimer's disease: a 24-month follow-up study.* Neurobiology of Aging, 2020. **93**: p. 97.e1-97.e7.
422. Lim, B., et al., *Liquid biopsy of cerebrospinal fluid identifies neuronal pentraxin receptor (NPTXR) as a biomarker of progression of Alzheimer's disease.* Clinical Chemistry and Laboratory Medicine, 2019.
423. Begcevic, I., et al., *Neuronal pentraxin receptor-1 is a new cerebrospinal fluid biomarker of Alzheimer's disease progression [version 1; peer review: 4 approved].* F1000Research, 2018. **7**.
424. Hendrickson, R.C., et al., *High resolution discovery proteomics reveals candidate disease progression markers of Alzheimer's disease in human cerebrospinal fluid.* PLoS ONE, 2015. **10**(8).
425. Avramopoulos, D., et al., *Gene expression reveals overlap between normal aging and Alzheimer's disease genes.* Neurobiology of Aging, 2011. **32**(12): p. 2319.e272319.e34.
426. Remnestål, J., et al., *Altered levels of CSF proteins in patients with FTD, presymptomatic mutation carriers and non-carriers.* Translational Neurodegeneration, 2020. **9**(1).
427. van der Ende, E.L., et al., *Novel CSF biomarkers in genetic frontotemporal dementia identified by proteomics.* Annals of Clinical and Translational Neurology, 2019. **6**(4): p. 698-707.
428. Van Der Ende, E.L., et al., *Neuronal pentraxin 2: A synapse-derived CSF biomarker in genetic frontotemporal dementia.* Journal of Neurology, Neurosurgery and Psychiatry, 2020. **91**(6): p. 612-621.
429. Barschke, P., et al., *Different CSF protein profiles in amyotrophic lateral sclerosis and frontotemporal dementia with C9orf72 hexanucleotide repeat expansion.* Journal of Neurology, Neurosurgery and Psychiatry, 2020. **91**(5): p. 503-511.

430. Baker, A.H., D.R. Edwards, and G. Murphy, *Metalloproteinase inhibitors: biological actions and therapeutic opportunities.* Journal of Cell Science, 2002. **115**(19): p. 3719.
431. Stetler-Stevenson, W.G., H.C. Krutzsch, and L.A. Liotta, *Tissue inhibitor of metalloproteinase (TIMP-2). A new member of the metalloproteinase inhibitor family.* Journal of Biological Chemistry, 1989. **264**(29): p. 17374-17378.
432. Seo, D.W., et al., *TIMP-2 mediated inhibition of angiogenesis: An MMP-independent mechanism.* Cell, 2003. **114**(2): p. 171-180.
433. Albini, A., et al., *Angiogenic potential in vivo by Kaposi's sarcoma cell-free supernatants and HIV-1 tat product: Inhibition of KS-like lesions by tissue inhibitor of metalloproteinase-2.* AIDS, 1994. **8**(9): p. 1237-1244.
434. Valente, P., et al., *TIMP-2 over-expression reduces invasion and angiogenesis and protects B16F10 melanoma cells from apoptosis.* International Journal of Cancer, 1998. **75**(2): p. 246-253.
435. Egeblad, M. and Z. Werb, *New functions for the matrix metalloproteinases in cancer progression.* Nature Reviews Cancer, 2002. **2**(3): p. 161-174.
436. Meersch, M., et al., *Urinary TIMP-2 and IGFBP7 as early biomarkers of acute kidney injury and renal recovery following cardiac surgery.* PLoS ONE, 2014. **9**(3).
437. Wetz, A.J., et al., *Quantification of urinary TIMP-2 and IGFBP-7: An adequate diagnostic test to predict acute kidney injury after cardiac surgery?* Critical Care, 2015. **19**(1).
438. Gocze, I., et al., *Urinary biomarkers TIMP-2 and IGFBP7 early predict acute kidney injury after major surgery.* PLoS ONE, 2015. **10**(3).
439. Gunnerson, K.J., et al., *TIMP2•IGFBP7 biomarker panel accurately predicts acute kidney injury in high-risk surgical patients.* Journal of Trauma and Acute Care Surgery, 2016. **80**(2): p. 243-249.
440. Yamashita, T., et al., *Evaluation of urinary tissue inhibitor of metalloproteinase-2 in acute kidney injury: A prospective observational study.* Critical Care, 2014. **18**(1).
441. McCullough, P.A., et al., *Serial Urinary Tissue Inhibitor of Metalloproteinase-2 and Insulin-Like Growth Factor-Binding Protein 7 and the Prognosis for Acute Kidney Injury over the Course of Critical Illness.* CardioRenal Medicine, 2019. **9**(6): p. 358369.
442. Kashani, K., et al., *Discovery and validation of cell cycle arrest biomarkers in human acute kidney injury.* Critical Care, 2013. **17**(1): p. R25.
443. Pianta, T.J., et al., *Evaluation of biomarkers of cell cycle arrest and inflammation in prediction of dialysis or recovery after kidney transplantation.* Transplant International, 2015. **28**(12): p. 1392-1404.
444. Bank, J.R., et al., *Urinary TIMP-2 Predicts the Presence and Duration of Delayed Graft Function in Donation after Circulatory Death Kidney Transplant Recipients.* Transplantation, 2019. **103**(5): p. 1014-1023.
445. Knafl, D., et al., *The urine biomarker panel [IGFBP7]x[TIMP-2] (NephroCheck® parameter) does not correlate with IGFBP7 and TIMP-2 gene expression in urinary sediment.* PLoS ONE, 2017. **12**(11).
446. Bar-Or, A., et al., *Analyses of all matrix metalloproteinase members in leukocytes emphasize monocytes as major inflammatory mediators in multiple sclerosis.* Brain, 2003. **126**(12): p. 2738-2749.
447. Rosenberg, G.A., et al., *TIMP-2 reduces proteolytic opening of blood-brain barrier by type IV collagenase.* Brain Research, 1992. **576**(2): p. 203-207.

448. Sulik, A. and L. Chyczewski, *Immunohistochemical analysis of MMP-9, MMP-2 and TIMP-1, TIMP-2 expression in the central nervous system following infection with viral and bacterial meningitis.* Folia Histochemica et Cytobiologica, 2008. **46**(4): p. 437-442.
449. Leppert, D., et al., *Matrix metalloproteinase (MMP)-8 and MMP-9 in cerebrospinal fluid during bacterial meningitis: Association with blood-brain barrier damage and neurological sequelae.* Clinical Infectious Diseases, 2000. **31**(1): p. 80-84.
450. Li, Y.J., et al., *Elevated Matrix Metalloproteinase Concentrations Offer Novel Insight into Their Role in Pediatric Tuberculous Meningitis.* Journal of the Pediatric Infectious Diseases Society, 2019. **9**(1): p. 82-86.
451. Yee, D., *IGF 1 and IGF 2*, in *Cancer Therapeutic Targets*, J.L. Marshall, Editor. 2017, Springer New York: New York, NY. p. 739-743.
452. O'Dell, S.D. and I.N.M. Day, *Molecules in focus Insulin-like growth factor II (IGF-II).* The International Journal of Biochemistry & Cell Biology, 1998. **30**(7): p. 767-771.
453. Yakar, S., H. Werner, and C.J. Rosen, *Insulin-like growth factors: actions on the skeleton.* J Mol Endocrinol, 2018. **61**(1): p. T115-t137.
454. Pollak, M., *The insulin and insulin-like growth factor receptor family in neoplasia: an update.* Nature Reviews Cancer, 2012. **12**(3): p. 159-169.
455. Nielsen, F.C., *The molecular and cellular biology of insulin-like growth factor II.* Progress in Growth Factor Research, 1992. **4**(3): p. 257-290.
456. Johanson, C., et al., *Traumatic brain injury and recovery mechanisms: peptide modulation of periventricular neurogenic regions by the choroid plexus–CSF nexus.* Journal of Neural Transmission, 2011. **118**(1): p. 115-133.
457. Funatsu, N., et al., *Characterization of a Novel Rat Brain Glycosylphosphatidylinositol-anchored Protein (Kilon), a Member of the IgLON Cell Adhesion Molecule Family.* Journal of Biological Chemistry, 1999. **274**(12): p. 82248230.
458. Marg, A., et al., *Neurotractin, A Novel Neurite Outgrowth-promoting Ig-like Protein that Interacts with CEPU-1 and LAMP.* Journal of Cell Biology, 1999. **145**(4): p. 865876.
459. Schäfer, M., et al., *Neurotractin/kilon promotes neurite outgrowth and is expressed on reactive astrocytes after entorhinal cortex lesion.* Molecular and Cellular Neuroscience, 2005. **29**(4): p. 580-590.
460. Ntougkos, E., et al., *The IgLON family in epithelial ovarian cancer: Expression profiles and clinicopathologic correlates.* Clinical Cancer Research, 2005. **11**(16): p. 5764-5768.
461. Willer, C.J., et al., *Six new loci associated with body mass index highlight a neuronal influence on body weight regulation.* Nature Genetics, 2009. **41**(1): p. 25-34.
462. Lee, P.H., et al., *Genomic Relationships, Novel Loci, and Pleiotropic Mechanisms across Eight Psychiatric Disorders.* Cell, 2019. **179**(7): p. 1469-1482.e11.
463. Li, S., et al., *Regulatory mechanisms of major depressive disorder risk variants.* Molecular Psychiatry, 2020. **25**(9): p. 1926-1945.
464. Wang, X., et al., *Integrating genome-wide association study and expression quantitative trait loci data identifies NEGR1 as a causal risk gene of major depression disorder.* Journal of Affective Disorders, 2020. **265**: p. 679-686.
465. Hyde, C.L., et al., *Identification of 15 genetic loci associated with risk of major depression in individuals of European descent.* Nature Genetics, 2016. **48**(9): p. 1031-1036.

466. Gamero-Villarroel, C., et al., *Impact of NEGR1 genetic variability on psychological traits of patients with eating disorders.* Pharmacogenomics Journal, 2015. **15**(3): p. 278-283.
467. Szczurkowska, J., et al., *NEGR1 and FGFR2 cooperatively regulate cortical development and core behaviours related to autism disorders in mice.* Brain, 2018. **141**(9): p. 2772-2794.
468. Lachén-Montes, M., et al., *Deployment of label-free quantitative olfactory proteomics to detect cerebrospinal fluid biomarker candidates in synucleinopathies*, in *Methods in Molecular Biology*. 2019. p. 273-289.
469. Jesse, S., et al., *A proteomic approach for the diagnosis of bacterial meningitis.* PLoS ONE, 2010. **5**(4).
470. Goonetilleke, U.R., et al., *Proteomic analysis of cerebrospinal fluid in pneumococcal meningitis reveals potential biomarkers associated with survival.* Journal of Infectious Diseases, 2010. **202**(4): p. 542-550.
471. Cordeiro, A.P., et al., *Comparative proteomics of cerebrospinal fluid reveals a predictive model for differential diagnosis of pneumococcal, meningococcal, and enteroviral meningitis, and novel putative therapeutic targets.* BMC Genomics, 2015. **16**(5).
472. Njunge, J.M., et al., *Cerebrospinal fluid markers to distinguish bacterial meningitis from cerebral malaria in children.* Wellcome Open Research, 2017. **2**.
473. Gómez-Baena, G., et al., *Quantitative Proteomics of Cerebrospinal Fluid in Paediatric Pneumococcal Meningitis.* Scientific Reports, 2017. **7**(1).
474. Thanh, T.T., et al., *Value of lipocalin 2 as a potential biomarker for bacterial meningitis.* Clinical Microbiology and Infection, 2020.
475. Wall, E.C., et al., *CSF Levels of Elongation Factor Tu Is Associated With Increased Mortality in Malawian Adults With Streptococcus pneumoniae Meningitis.* Frontiers in Cellular and Infection Microbiology, 2020. **10**.
476. Bakochi, A., et al., *Cerebrospinal fluid proteome maps detect pathogen-specific host response patterns in meningitis.* eLife, 2021. **10**.
477. Frank Klont, P.H., Natalia Govorukhina, Rainer Bischoff, *Pre- and Post-analytical Factors in Biomarker Discovery*, in *Proteomics for Biomarker Discovery Methods and Protocols*, Y.C. Virginie Brun, Editor. 2019, Humana Press, Springer Science+Business Media. p. 1-22.
478. Dayon, L., et al., *Proteomes of Paired Human Cerebrospinal Fluid and Plasma: Relation to Blood-Brain Barrier Permeability in Older Adults.* Journal of Proteome Research, 2019. **18**(3): p. 1162-1174.
479. Reiber, H., *Dynamics of brain-derived proteins in cerebrospinal fluid.* Clin Chim Acta, 2001. **310**(2): p. 173-86.
480. McCudden, C.R., et al., *Cerebrospinal Fluid Total Protein Reference Intervals Derived from 20 Years of Patient Data.* Clinical Chemistry, 2020. **63**(12): p. 1856-1865.
481. Nilsson, C., et al., *Circadian variation in human cerebrospinal fluid production measured by magnetic resonance imaging.* American Journal of Physiology - Regulatory Integrative and Comparative Physiology, 1992. **262**(1 31-1): p. R20-R24.
482. Zhang, J., D.R. Goodlett, and T.J. Montine, *Proteomic biomarker discovery in cerebrospinal fluid for neurodegenerative diseases.* Journal of Alzheimer's Disease, 2005. **8**(4): p. 377-386.
483. Roche, S., A. Gabelle, and S. Lehmann, *Clinical proteomics of the cerebrospinal fluid: Towards the discovery of new biomarkers.* Proteomics - Clinical Applications, 2008. **2**(3): p. 428-436.

484. Blennow, K., et al., *Protein Analyses in Cerebrospinal Fluid.* European Neurology, 1993. **33**(2): p. 126-128.
485. Teunissen, C.E., et al., *A consensus protocol for the standardization of cerebrospinal fluid collection and biobanking.* Neurology, 2009. **73**(22): p. 1914-1922.
486. Hok-A-Hin, Y.S., et al., *Guidelines for CSF Processing and Biobanking: Impact on the Identification and Development of Optimal CSF Protein Biomarkers*, in *Cerebrospinal Fluid (CSF) Proteomics: Methods and Protocols*, E. Santamaría and J. FernándezIrigoyen, Editors. 2019, Springer New York: New York, NY. p. 27-50.
487. Marton, K.I. and M.I. Vender, *The lumbar puncture: patterns of use in clinical practice.* Medical Decision Making, 1981. **1**(4): p. 331-344.
488. Glatstein, M.M., et al., *Incidence of traumatic lumbar puncture: Experience of a large, tertiary care pediatric hospital.* Clinical Pediatrics, 2011. **50**(11): p. 10051009.
489. Bonadio, W.A., et al., *Distinguishing cerebrospinal fluid abnormalities in children with bacterial meningitis and traumatic lumbar puncture.* Journal of Infectious Diseases, 1990. **162**(1): p. 251-254.
490. Eskey an, C.J. and C.S. Ogilvy, *Fluoroscopy-guided Lumbar Puncture: Decreased Frequency of Traumatic Tap and Implications for the Assessment of CT-negative Acute Subarachnoid Hemorrhage.* American Journal of Neuroradiology, 2001. **22**(3): p. 571-576.
491. Shah, K.H., et al., *Incidence of traumatic lumbar puncture.* Academic Emergency Medicine, 2003. **10**(2): p. 151-154.
492. Greenberg, R.G., et al., *Traumatic lumbar punctures in neonates: Test performance of the cerebrospinal fluid white blood cell count.* Pediatric Infectious Disease Journal, 2008. **27**(12): p. 1047-1051.
493. Willemse, E., et al., *How to handle adsorption of cerebrospinal fluid amyloid β (1–42) in laboratory practice? Identifying problematic handlings and resolving the issue by use of the Aβ<inf>42</inf>/Aβ<inf>40</inf> ratio.* Alzheimer's and Dementia, 2017. **13**(8): p. 885-892.
494. Carrette, O., et al., *Truncated cystatin C in cerebrospiral fluid: Technical artefact or biological process?* Proteomics, 2005. **5**(12): p. 3060-3065.
495. Magalhães, B., et al., *Reviewing Mechanistic Peptidomics in Body Fluids Focusing on Proteases.* PROTEOMICS, 2018. **18**(18): p. 1800187.
496. Hu, S., J.A. Loo, and D.T. Wong, *Human body fluid proteome analysis.* PROTEOMICS, 2006. **6**(23): p. 6326-6353.
497. Hanash, S. and J.E. Celis, *The Human Proteome Organization.* A Mission to Advance Proteome Knowledge, 2002. **1**(6): p. 413-414.
498. Deutsch, E.W., et al., *Human Proteome Project Mass Spectrometry Data Interpretation Guidelines 3.0.* Journal of Proteome Research, 2019. **18**(12): p. 41084116.
499. Parker, C.E. and C.H. Borchers, *Mass spectrometry based biomarker discovery, verification, and validation – Quality assurance and control of protein biomarker assays.* Molecular Oncology, 2014. **8**(4): p. 840-858.
500. Sandin, M., A. Chawade, and F. Levander, *Is label-free LC-MS/MS ready for biomarker discovery?* PROTEOMICS – Clinical Applications, 2015. **9**(3-4): p. 289-294.
501. Güzel, C., et al., *Comparison of Targeted Mass Spectrometry Techniques with an Immunoassay: A Case Study for HSP90α.* PROTEOMICS – Clinical Applications, 2018. **12**(1): p. 1700107.
502. Clyne, B. and J.S. Olshaker, *The C-reactive protein.* Journal of Emergency Medicine, 1999. **17**(6): p. 1019-1025.

503. Kolb-Bachofen, V., *A Review on the Biological Properties of C-Reactive Protein.* Immunobiology, 1991. **183**(1): p. 133-145.
504. Pepys, M.B. and G.M. Hirschfield, *C-reactive protein: A critical update.* Journal of Clinical Investigation, 2003. **111**(12): p. 1805-1812.
505. Danesh, J., et al., *C-Reactive Protein and Other Circulating Markers of Inflammation in the Prediction of Coronary Heart Disease.* New England Journal of Medicine, 2004. **350**(14): p. 1387-1397.
506. Excellence, N.I.f.C. *NICE impact ; Antimicrobial Resistance*. 2018 [cited 2021; Available from: https://www.nice.org.uk/media/default/about/what-we-do/intopractice/measuring-uptake/niceimpact-antimicrobial-resistance.pdf.
507. Tunkel, A.R., et al., *2017 Infectious Diseases Society of America's Clinical Practice Guidelines for Healthcare-Associated Ventriculitis and Meningitis.* Clinical infectious diseases : an official publication of the Infectious Diseases Society of America, 2017. **64**(6): p. e34-e65.
508. Doron, S. and S.L. Gorbach, *Bacterial Infections: Overview.* International Encyclopedia of Public Health, 2008: p. 273-282.
509. Maddox, B., *The double helix and the 'wronged heroine'.* Nature, 2003. **421**(6921): p. 407-408.
510. Heather, J.M. and B. Chain, *The sequence of sequencers: The history of sequencing DNA.* Genomics, 2016. **107**(1): p. 1-8.
511. Schuster, S.C., *Next-generation sequencing transforms today's biology.* Nature Methods, 2008. **5**(1): p. 16-18.
512. Institute, N.H.G.R. *Human Genome Project FAQ*. 2020 24/02/2020 [cited 2021 27/07/2021]; Available from: https://www.genome.gov/human-genomeproject/Completion-FAQ.
513. Lander, E.S., et al., *Initial sequencing and analysis of the human genome.* Nature, 2001. **409**(6822): p. 860-921.
514. Jay, Z.J. and W.P. Inskeep, *The distribution, diversity, and importance of 16S rRNA gene introns in the order Thermoproteales.* Biol Direct, 2015. **10**: p. 35.
515. Lamoureux, C., et al., *Prospective Comparison Between Shotgun Metagenomics and Sanger Sequencing of the 16S rRNA Gene for the Etiological Diagnosis of Infections.* Frontiers in Microbiology, 2022. **13**.
516. Illumina. *An introduction to next-generation sequencing technology*. 2017 [cited 2021; Available from: https://emea.illumina.com/content/dam/illuminamarketing/documents/products/illumina_sequencing_introduction.pdf.
517. Branton, D., et al., *The potential and challenges of nanopore sequencing.* Nature Biotechnology, 2008. **26**(10): p. 1146-1153.
518. Harazono, Y. Wikimedia: Wikimedia.
519. Segre, J.A. *Metagenomics*. Genetics glossary [cited 2021 26/09/2021]; Available from: https://www.genome.gov/genetics-glossary/Metagenomics.
520. Chiu, C.Y. and S.A. Miller, *Clinical metagenomics.* Nature Reviews Genetics, 2019. **20**(6): p. 341-355.
521. Wilson, M.R., et al., *Actionable diagnosis of neuroleptospirosis by next-generation sequencing.* New England Journal of Medicine, 2014. **370**(25): p. 2408-2417.
522. Kufner, V., et al., *Two years of viral metagenomics in a tertiary diagnostics unit: Evaluation of the first 105 cases.* Genes, 2019. **10**(9).

523. Hong, N.T.T., et al., *Performance of metagenomic next-generation sequencing for the diagnosis of viral meningoencephalitis in a resource-limited setting.* Open Forum Infectious Diseases, 2020. **7**(3).
524. Wilson, M.R., et al., *A novel cause of chronic viral meningoencephalitis: Cache Valley virus.* Annals of Neurology, 2017. **82**(1): p. 105-114.
525. Asif, A.A., et al., *Capnocytophaga canimorsus meningitis diagnosed using next-generation sequencing of microbial cell-free DNA.* IDCases, 2021. **24**.
526. Wilson, M.R., et al., *Chronic meningitis investigated via metagenomic nextgeneration sequencing.* JAMA Neurology, 2018. **75**(8): p. 947-955.
527. Beck, E.S., et al., *Clinicopathology conference: 41-year-old woman with chronic relapsing meningitis.* Annals of Neurology, 2019. **85**(2): p. 161-169.
528. Saha, S., et al., *Unbiased metagenomic sequencing for pediatric meningitis in bangladesh reveals neuroinvasive chikungunya virus outbreak and other unrealized pathogens.* mBio, 2019. **10**(6).
529. Morsli, M., et al., *Haemophilus influenzae meningitis direct diagnosis by metagenomic next-generation sequencing: A case report.* Pathogens, 2021. **10**(4).
530. Morsli, M., et al., *Direct diagnosis of echovirus 12 meningitis using metagenomic next generation sequencing.* Pathogens, 2021. **10**(5).
531. Mongkolrattanothai, K., et al., *Neurobrucellosis: Unexpected answer from metagenomic next-generation sequencing.* Journal of the Pediatric Infectious Diseases Society, 2017. **6**(4): p. 393-398.
532. Xing, X.W., et al., *Apparent performance of metagenomic next-generation sequencing in the diagnosis of cryptococcal meningitis: A descriptive study.* Journal of Medical Microbiology, 2019. **68**(8): p. 1204-1210.
533. Zhou, C., et al., *Idiopathic thrombocytopenic purpura with brain abscess caused by Nocardia farcinica diagnosed using metagenomics next-generation sequencing of the cerebrospinal fluid: a case report.* BMC infectious diseases, 2021. **21**(1): p. 380.
534. Piantadosi, A., et al., *Rapid detection of powassan virus in a patient with encephalitis by metagenomic sequencing.* Clinical Infectious Diseases, 2018. **66**(5): p. 789-792.
535. Wylie, K.M., et al., *High-throughput sequencing of cerebrospinal fluid for diagnosis of chronic Propionibacterium acnes meningitis in an allogeneic stem cell transplant recipient.* Transplant Infectious Disease, 2016. **18**(2): p. 227-233.
536. Ikuta, Y., et al., *Aseptic meningitis caused by torque teno virus in an infant: A case report.* Journal of Medical Case Reports, 2019. **13**(1).
537. Joanna María, O.A., et al., *Fatal Psychrobacter sp. infection in a pediatric patient with meningitis identified by metagenomic next-generation sequencing in cerebrospinal fluid.* Archives of Microbiology, 2016. **198**(2): p. 129-135.
538. Tschumi, F., et al., *Meningitis and epididymitis caused by Toscana virus infection imported to Switzerland diagnosed by metagenomic sequencing: A case report.* BMC Infectious Diseases, 2019. **19**(1).
539. Wang, Q., et al., *Neonatal Ureaplasma parvum meningitis: A case report and literature review.* Translational Pediatrics, 2020. **9**(2): p. 174-179.
540. Wilson, M.R., et al., *Acute West Nile Virus Meningoencephalitis Diagnosed Via Metagenomic Deep Sequencing of Cerebrospinal Fluid in a Renal Transplant Patient.* American Journal of Transplantation, 2017. **17**(3): p. 803-808.
541. Trend, S., et al., *Leukocyte Populations in Human Preterm and Term Breast Milk Identified by Multicolour Flow Cytometry.* PLOS ONE, 2015. **10**(8): p. e0135580.

542. Davis, M.P.A., et al., *Kraken: A set of tools for quality control and analysis of highthroughput sequence data.* Methods, 2013. **63**(1): p. 41-49.
543. Wood, D.E. and S.L. Salzberg, *Kraken: ultrafast metagenomic sequence classification using exact alignments.* Genome Biology, 2014. **15**(3): p. R46.
544. Thiel, V., et al., *Genome sequence of Prosthecochloris sp. strain HL-130-GSB from the phylum Chlorobi.* Genome Announcements, 2017. **5**(24).
545. Gilligan, P.H., et al., *Burkholderia, Stenotrophomonas, Ralstonia, Brevundimonas, Comamonas, Delftia, Pandoraea and Acidovorax.* Manual of Clinical Microbiology, 2003: p. 729-748.
546. Labarca, J.A., et al., *A multistate nosocomial outbreak of Ralstonia pickettii colonization associated with an intrinsically contaminated respiratory care solution.* Clinical Infectious Diseases, 1999. **29**(5): p. 1281-1286.
547. Moreira, B.M., et al., *Ralstonia pickettii and Burkholderia cepacia complex bloodstream infections related to infusion of contaminated water for injection.* Journal of Hospital Infection, 2005. **60**(1): p. 51-55.
548. Kahan, A., et al., *Nosocomial infections by chlorhexidine solution contaminated with Pseudomonas pickettii (Biovar VA-1).* Journal of Infection, 1983. **7**(3): p. 256-263.
549. Kimura, A.C., et al., *Outbreak of Ralstonia pickettii bacteremia in a neonatal intensive care unit.* Pediatric Infectious Disease Journal, 2005. **24**(12): p. 1099-1103.
550. Chen, Y.Y., et al., *An Outbreak of Ralstonia pickettii Bloodstream Infection Associated with an Intrinsically Contaminated Normal Saline Solution.* Infection Control and Hospital Epidemiology, 2017. **38**(4): p. 444-448.
551. Bedir Demirdag, T., et al., *An outbreak of Ralstonia pickettii bloodstream infection among pediatric leukemia patients.* Journal of Microbiology, Immunology and Infection, 2021.
552. Zhang, L., M. Morrison, and C.M. Rickard, *Draft genome sequence of Ralstonia pickettii AU12-08, isolated from an intravascular catheter in Australia.* Genome Announcements, 2014. **2**(1).
553. Kismet, E., et al., *Two cases of Ralstonia pickettii bacteremias in a pediatric oncology unit requiring removal of the Port-A-Caths.* Journal of Pediatric Hematology/Oncology, 2005. **27**(1): p. 37-38.
554. Brindle, C.T., et al., *Preliminary Results of the Use of a Stabilized Hypochlorous Acid Solution in the Management of Ralstonia Pickettii Biofilm on Silicone Breast Implants.* Aesthetic Surgery Journal, 2018. **38**: p. S52-S61.
555. Birlutiu, R.M., et al., *Sonication contribution to identifying prosthetic joint infection with Ralstonia pickettii: A case report and review of the literature.* BMC Musculoskeletal Disorders, 2017. **18**(1).
556. Ryan, M.P., J.T. Pembroke, and C.C. Adley, *Ralstonia pickettii: a persistent gramnegative nosocomial infectious organism.* J Hosp Infect, 2006. **62**(3): p. 278-84.
557. Ferro, P., I. Vaz-Moreira, and C.M. Manaia, *Evolution of gentamicin and arsenite resistance acquisition in Ralstonia pickettii water isolates.* Research in Microbiology, 2021. **172**(1): p. 103790.
558. Hu, H., et al., *Bacterial Biofilm Infection Detected in Breast Implant–Associated Anaplastic Large-Cell Lymphoma.* Plastic and Reconstructive Surgery, 2016. **137**(6).
559. Evans, M.G., et al., *B-cell lymphomas associated with breast implants: Report of three cases and review of the literature.* Annals of Diagnostic Pathology, 2020. **46**.
560. Stewart, E.J., *Growing unculturable bacteria.* J Bacteriol, 2012. **194**(16): p. 4151-60.

561. Diakite, A., G. Dubourg, and D. Raoult, *Updating the repertoire of cultured bacteria from the human being.* Microbial Pathogenesis, 2021. **150**: p. 104698.
562. Lan, R. and P.R. Reeves, *Escherichia coli in disguise: molecular origins of Shigella.* Microbes and Infection, 2002. **4**(11): p. 1125-1132.
563. Ji, X.C., et al., *Reduction of Human DNA Contamination in Clinical Cerebrospinal Fluid Specimens Improves the Sensitivity of Metagenomic Next-Generation Sequencing.* Journal of Molecular Neuroscience, 2020. **70**(5): p. 659-666.
564. Oechslin, C.P., et al., *Limited Correlation of Shotgun Metagenomics Following Host Depletion and Routine Diagnostics for Viruses and Bacteria in Low Concentrated Surrogate and Clinical Samples.* Frontiers in cellular and infection microbiology, 2018. **8**: p. 375.
565. Miller, S., et al., *Laboratory validation of a clinical metagenomic sequencing assay for pathogen detection in cerebrospinal fluid.* Genome Research, 2019. **29**(5): p. 831-842.
566. Zhang, Y., et al., *Clinical application and evaluation of metagenomic nextgeneration sequencing in suspected adult central nervous system infection.* Journal of Translational Medicine, 2020. **18**(1).
567. Wang, S., et al., *The Feasibility of Metagenomic Next-Generation Sequencing to Identify Pathogens Causing Tuberculous Meningitis in Cerebrospinal Fluid.* Frontiers in Microbiology, 2019. **10**.
568. Yan, L., et al., *Metagenomic Next-Generation Sequencing (mNGS) in cerebrospinal fluid for rapid diagnosis of Tuberculosis meningitis in HIV-negative population.* International Journal of Infectious Diseases, 2020. **96**: p. 270-275.
569. Greninger, A.L., et al., *A novel outbreak enterovirus D68 strain associated with acute flaccid myelitis cases in the USA (2012-14): A retrospective cohort study.* The Lancet Infectious Diseases, 2015. **15**(6): p. 671-682.
570. Bozio, C.H., et al., *Outbreak of Neisseria meningitidis serogroup C outside the meningitis belt—Liberia, 2017: an epidemiological and laboratory investigation.* The Lancet Infectious Diseases, 2018. **18**(12): p. 1360-1367.
571. Wilson, M.R., et al., *Clinical metagenomic sequencing for diagnosis of meningitis and encephalitis.* New England Journal of Medicine, 2019. **380**(24): p. 2327-2340.
572. Xing, X.W., et al., *Metagenomic Next-Generation Sequencing for Diagnosis of Infectious Encephalitis and Meningitis: A Large, Prospective Case Series of 213 Patients.* Frontiers in Cellular and Infection Microbiology, 2020. **10**.
573. Zhang, X.X., et al., *The diagnostic value of metagenomic next-generation sequencing for identifying Streptococcus pneumoniae in paediatric bacterial meningitis.* BMC Infectious Diseases, 2019. **19**(1).
574. KA., W. *DNA Sequencing Costs: Data from the NHGRI Genome Sequencing Program (GSP)*. [cited 2021 21/07/2021]; Available from: www.genome.gov/sequencingcostsdata.
575. Kip, M.M.A., et al., *The cost-utility of point-of-care troponin testing to diagnose acute coronary syndrome in primary care.* BMC Cardiovascular Disorders, 2017. **17**(1): p. 213.
576. Ho C, C.K., Weeks L, et al. *Point-of-Care Troponin Testing in Patients With Symptoms Suggestive of Acute Coronary Syndrome: A Health Technology Assessment [Internet]*. 2016; (CADTH Optimal Use Report, No. 5.1b.) Table 5, Costs of Cardiac Troponin Testing Strategies.]. Available from: https://www.ncbi.nlm.nih.gov/books/NBK362825/table/T5/.

577. *100,000 Genomes Pilot on Rare-Disease Diagnosis in Health Care — Preliminary Report.* New England Journal of Medicine, 2021. **385**(20): p. 1868-1880.
578. Volz, E., et al., *Assessing transmissibility of SARS-CoV-2 lineage B.1.1.7 in England.* Nature, 2021. **593**(7858): p. 266-269.
579. Chalmers, I. and P. Glasziou, *Avoidable waste in the production and reporting of research evidence.* Lancet, 2009. **374**(9683): p. 86-9.

Appendices

Appendix A

A0A0A0MS09	A0A1W2PNV4
A0A0A0MSC4	A0A1W2PPI5
A0A0A0MSV6	A0A1W2PQ11
A0A0A0MSY7	A0A1W2PQB1
A0A0A0MTI5	A0A1X7SBT7
A0A0A0MTS2	A0A286YEY1
A0A0A6YYG9	A1AG1
A0A0B4J2B5	A1AG2
A0A0C4DFP6	A1AT
A0A0C4DG09	A1BG
A0A0C4DGN2	A2A2V1
A0A0C4DGX4	A2AP
A0A0G2JLV5	A2GL
A0A0G2JLV7	A2MG
A0A0G2JMB2	A4
A0A0G2JPD3	A6XGL3
A0A0G2JRQ6	A8MUA9
A0A0J9YXB8	A9UJN9
A0A0J9YY99	AACT
A0A0U1RQC5	AATC
A0A0U1RQQ4	ACTA
A0A0U1RQT8	ACTB
A0A0U1RR20	AFAM
A0A0U1RRM4	AHNK
A0A140T998	AJAP1
A0A1B0GUU9	AL1A1
A0A1B0GV23	ALBU

A0A1B0GW95	ALDOC

IDENTIFIER
6PGD
7B2
A0A024R0T9
A0A024R571
A0A024R6I7
A0A075B6H7
A0A075B6Z2
A0A075B7D0
A0A087WSY5
A0A087WTA1
A0A087WTA8
A0A087WTY6
A0A087WVD1
A0A087WVQ9
A0A087WWT2
A0A087WXK5
A0A087WXW9
A0A087WYL5
A0A087WZM2
A0A087X0I3
A0A087X0S5
A0A087X1J7
A0A096LPE2
A0A0A0MRJ6
A0A0A0MRJ7

A0A0A0MRV3

Table 59 Proteins identified by LC-MS/MS in Chapter 3

ALS
AMBP
AMD
ANFC
ANGI
ANGT
ANKH1
ANT3
ANXA1
APLP1
APOA1
APOA4
APOB
APOE
APOH
APOL1
APOM
ARGI1
ASC
ASPG
ATRN
ATS1
B0AZS6
B0QYF8
B0YIW2
B1AHL2
B2MG

B4GA1
B5MBX2
B5MC14
B5MCX6
B7ZKJ8
B7ZLJ8
B8ZZE5
BASP1
BGH3
BID
BLVRB
BPI
BTD
C1QA
C1QC
C1QT3
C1RL
C4BPA
C9J0J0
C9J8S2
C9J8Z4
C9JC84
C9JF17
C9JFR7
C9JGI3
C9JL85
C9JP35

CADH2
CADM4
CAH1
CAH2
CAH3
CALM1
CAP1
CAP7
CAPG
CART
CATA
CATB
CATG
CATZ
CAZA1
CBG
CBPE
CBPN
CBPQ
CCKN
CD14
CD166
CD2AP
CDC42
CEAM8
CELR2
CERU

B2R5W2
B4DG04
B4DPQ0
B4E1Z4

C9JV77
C9JYY6
CA2D1
CAD13

CFA58
CFAH
CGRE1
CH3L1

CH3L2
CLH2
CLUS
CMGA
CNDP1
CNTFR
CNTN1
CO1A1
CO2
CO3
CO3A1
CO4B
CO5
CO6
CO6A3
CO7
CO8A
CO9
COIA1
COL12
COR1A
COTL1
CPN2

D6RBV2
D6RC06
D6RD17
D6RER2
D6REY1
D6RF35
DAG1
DEF1
DESM
DHPR
DIAC
DIAP3
DNER
DYL2
E7EPK1
E7EQR8
E7ET33
E7EUF1
E9PEK4
E9PEW8
E9PG71
E9PHK0
E9PNW4

F13A
F13B
F16P1
F2Z2Y4
F5GY03
F5GY80
F5GZG1
F5GZZ9
F5H265
F6RFD5
F6SYF8
F8VR50
F8VSD4
F8VVB6
F8VXG0
F8VY04
F8VZ49
F8WCZ6
FA12
FABP5
FAM3C
FAT2
FBLN1

CRP
CSF1
CSTN3
CXCL7
CYTA
CYTB
CYTC
D6RA82

ECM1
EFNB2
ELNE
ENDD1
ENOA
ENPP5
ETBR2
EXTL2

FBLN3
FCG2A
FCGBP
FCN3
FETUB
FHR1
FHR3
FIBA

FIBB
FINC
FINC
FKB1A
FUCO2
G3P
G3PT
G3V164
G3V1A4
G3V1D7
G3V1N2
G3V1V0
G3V3X5
G3V4U0
G3V5M2
G3V5V4
G3XAM2
G3XAP6
GDIB

H0Y8G5
H0YAC1
H0YBX6
H0YDE5
H0YEA2
H0YGZ3
H0YID2
H0YIZ1
H0YJE6
H0YKL9
H0YL90
H0YMN7
H14
H15
H1X
H2A2A
H31T
H3BLU2
H3BRK3

HBG1
HBG2
HEM2
HEMO
HEP2
HERC5
HMGN2
HNRPK
HPRT
HPT
HPTR
HRG
HS71A
HSP7C
HTRA1
HV102
HV118
HV145
HV205

GDIR1
GDIR2
GELS
GLDN
GLRX1
GOLM1
GP158
GPNMB
GSTP1
H0Y2P0
H0Y512
H0Y5K2

H3BUA5
H4
H7BXD5
H7BY57
H7BZ67
H7C1M3
H7C3F9
H9KV31
HABP2
HBA
HBB
HBD

HV226
HV307
HV309
HV315
HV321
HV333
HV348
HV349
HV372
HV373
HV374
HV404

HV428
HV551
HV5X1
HV601
HV69D
HV70D
HVD82
I3L0K2
I3L397
IBP2
IBP4
IBP6
IBP7
IC1
ICAM5

J3KNB4
J3KNF6
J3KPG5
J3KPS3
J3KQ18
J3KQ66
J3KQE5
J3QLF6
J3QRJ3
J3QSE5
K2C1
K4DIA0
K7EJT1
K7ELW0
K7EM19

KV224
KV228
KV230
KV320
KV401
KV621
KVD08
KVD11
KVD13
KVD15
KVD20
KVD21
KVD29
KVD30
L1CAM

IGF2
IGHG1
IGHG2
IGHG3
IGHG4
IGKC
IGLC2
IGLL5
IGS21
IL1R2
IL6RB
ILEU
IMPA3
ITIH1
ITIH2
ITIH4

K7ERG9
K7ERI9
K7ES70
KAIN
KLHL5
KLK6
KNG1
KNG1
KPYM
KPYM
KV105
KV108
KV116
KV117
KV127
KV139

LAMB2
LAMP1
LAMP2
LBP
LDHA
LDHB
LEG1
LEG10
LEG3
LG3BP
LIGO1
LKHA4
LRC4B
LUM
LV136
LV147

LV151
LV208
LV214
LV218
LV223
LV310
LV319
LV321
LV325
LV39
LV746

MOES
MRC1
MUC18
NAMPT
NCAM1
NCAN
NCHL1
NDKB
NECT1
NEGR1
NEO1

PGBM
PGCB
PGK1
PGRP1
PGRP2
PHLD
PI16
PLBL1
PLD3
PLMN
PLSL

LV861
LY6H
LYOX
LYSC
LYVE1
M0QX47
MAG
MARCS
MASP1
MDHC
MEGF8
MGP
MIF
MIME
MIPT3
MMP2
MMP3
MMP9
MMRN2
MNDA

NPTX1
NPY
NRX1A
NRX2A
NTRI
NUCB1
OMGP
OPCM
OSTP
PAI1
PCOC1
PCP
PCSK1
PEBP1
PEBP4
PEDF
PENK
PERE
PERM
PGAM1

PLTP
PMGE
PNPH
PON1
POSTN
PPIA
PPIB
PRDX1
PRDX2
PRDX5
PRDX6
PROF1
PROS
PRRT3
PRVA
PSB1
PSME1
PTGDS
PTN6
PTPRG

PTPRN
PTPRS
PTPRZ
PXDC2
Q3KPI9
Q5H9A7
Q5HY54

SAP3
SBK1
SBP1
SCG1
SCG2
SCG3
SEM7A

THIO
THRB
TIAM1
TIMP2
TKT
TPIS
TRFE

Q5QPM7	SEPP1	TRFL
Q5SPY9	SFRP4	TSP1
Q5SQ08	SH3L1	TTHY
Q5SQ11	SHAN1	TYB4
Q5SR54	SHPS1	U3KPS2
Q5T123	SIAT2	U3KQK0
Q5T948	SMG1	V9GYM3
Q5TA02	SMS	VAS1
Q5VY30	SODC	VASN
QSOX1	SODE	VASP
R4GMR2	SORC2	VGF
RD23B	SORC3	VIME
RNAS2	SPAT5	VNN1
RNAS4	SPRL1	VSIG4
RNAS6	SPT6H	VTDB
ROA2	SPTA1	VTM2B
RPIA	SULF2	VTNC
S100A9	SYNE2	WDR1
S10A4	T132A	WFKN2
S10A8	TAGL	X6R3B1
S10AB	TALDO	X6R8F3
SAA1	TCO1	X6RJP6
SAA2	TGON2	ZA2G
SAHH	THBG	ZSWM9
ZZEF1		

LC-MS/MS data from the 10 proteins that were chosen for further investigation with ELISA testing are presented below

Lactoferrin

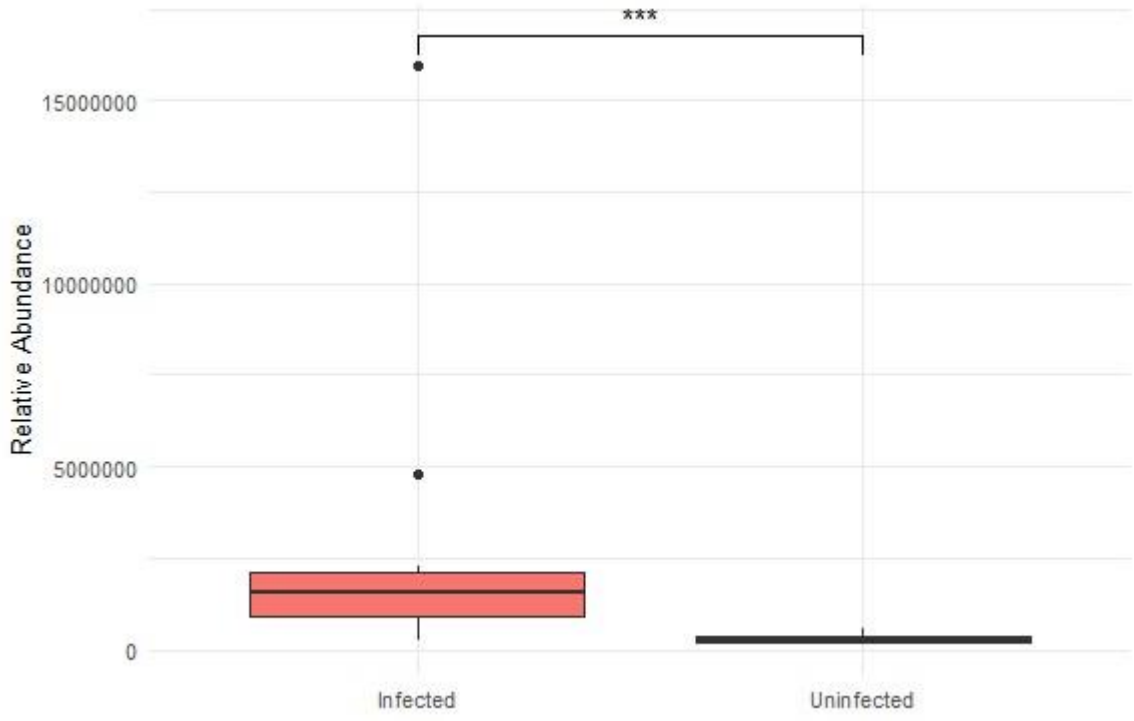

Figure 74 Lactoferrin relative abundance as measured by LC-MS/MS

The average "concentration" of Lactoferrin in infected samples as measured by LC-MS/MS was 1,287,919 (250,763-2,260,166). In uninfected samples the average was 287,998.7 (119,402.8-589507.1).

A Welch two sample t-test was applied to this data. T test statistic was 5.0342 with 11.602 degrees of freedom and p-value of 0.0003239 (confidence interval 565,499.2-1,434,342.3).

NPTXR

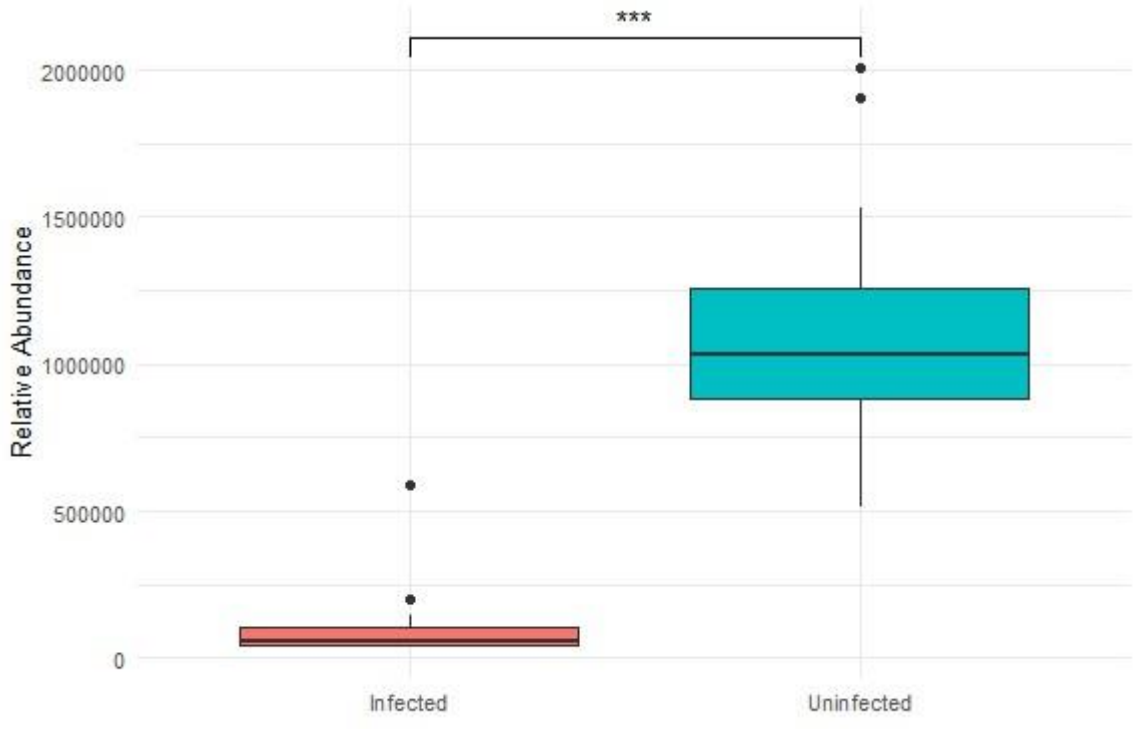

Figure 75 NPTXR relative abundance as measured by LC MS/MS

The average "concentration" of NPTXR in infected samples as measured by LC-MS/MS was 122,883.8 (34,432.83-592,361). In uninfected samples the average was 1,114,079.3 (511,076.3-2,008,770).

A Welch two sample t-test was applied to this data. T test statistic was -9.7241with 25.355 degrees of freedom and p-value of 0.0000000004877 (95 percent confidence interval: 1200979.2--781411.8).

TIMP2

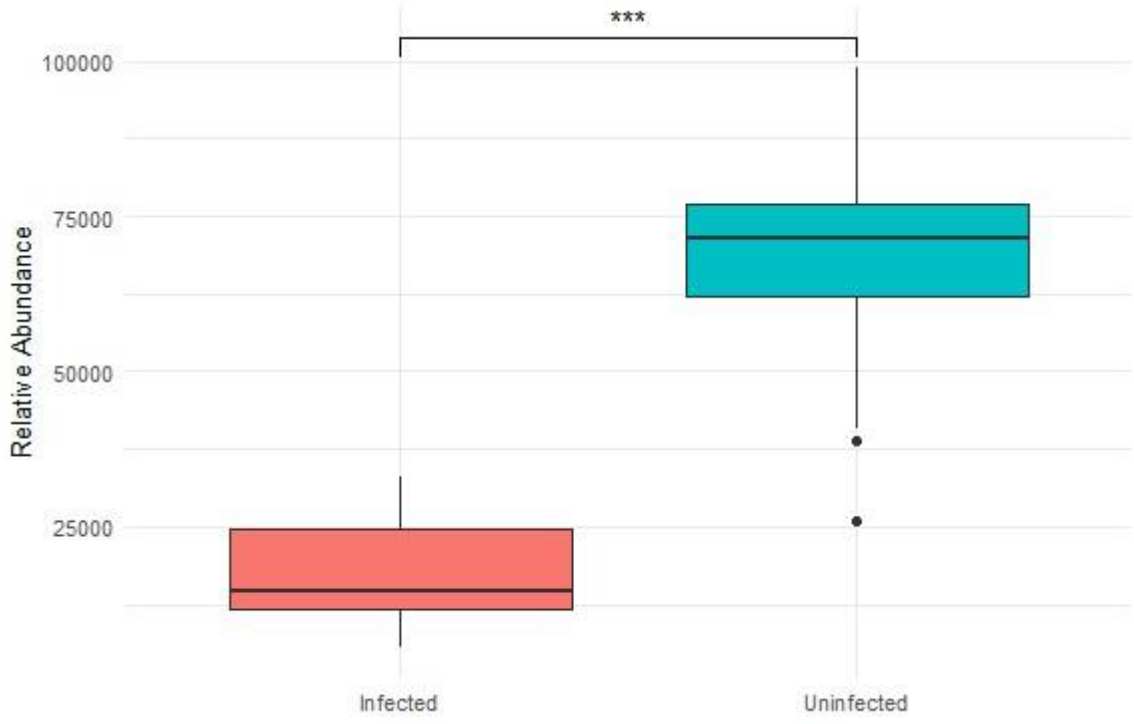

Figure 76 TIMP2 relative abundance as measured by LC-MS/MS

The average “concentration” in the infected group was 15,952.43 (range 5,442.7232,934.46) and the average in the uninfected group was 68,426.22 (range 26064.7599005.67).

Welch Two Sample t-test statistic was -10.763 with 26.976 degrees of freedom and a pvalue of 0.00000000002894 (95 percent confidence interval: -62477.41 -42470.15).

IGF2

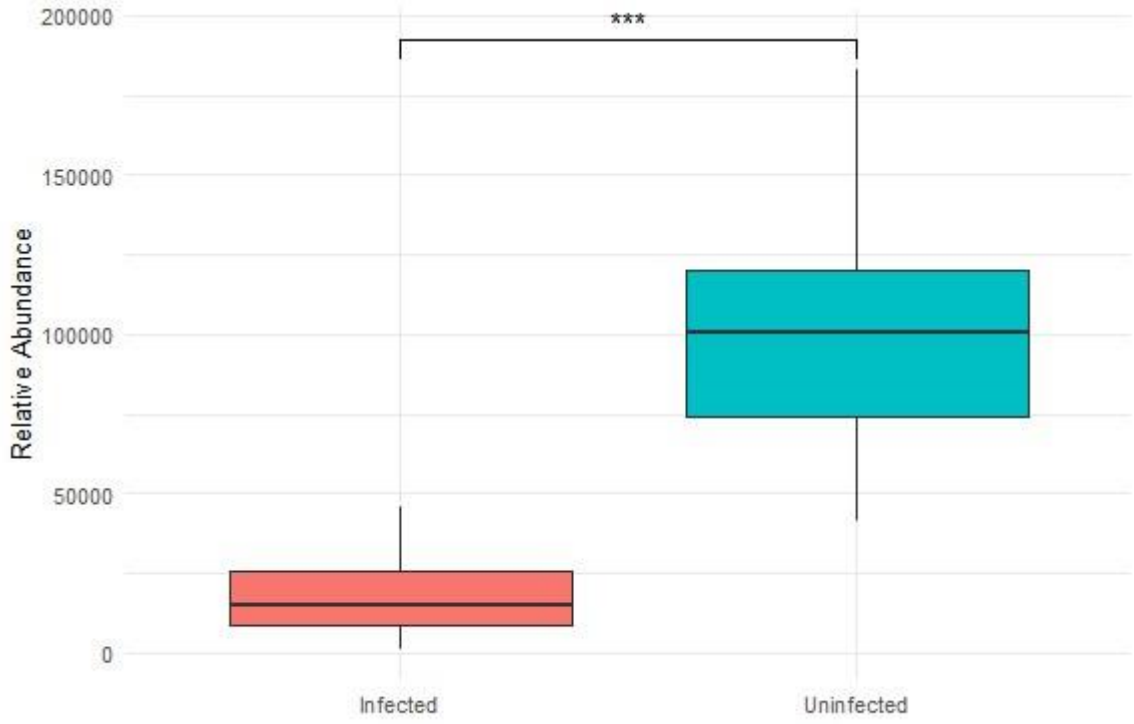

Figure 77 IGF2 relative abundance as measured by LC MS/MS

The average "concentration" of IGF2 in infected samples as measured by LC-MS/MS was 15,763.67 (range=927.01-37313.38). In uninfected samples the average was 98,497.46 (41,459.7-183,064.7).

Welch Two Sample t-test statistic was -9.6036, df = 23.056, p-value = 0.000000001593(95% confidence interval: -100,552.67 - -64,914.92).

NEGR1

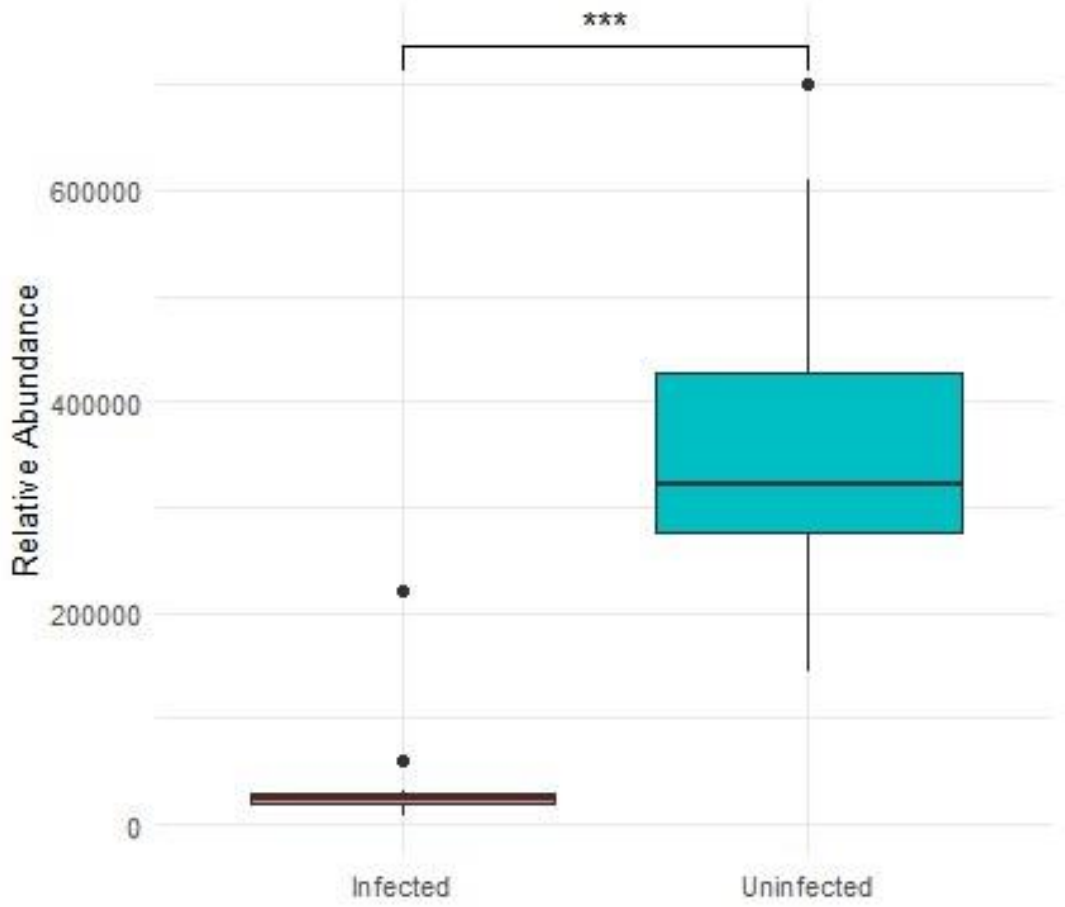

Figure 78 NEGR1 relative abundance as measured by LC MS/MS

The average "concentration" of NEGR1 in infected samples as measured by LC-MS/MS was 40,861.4 (6,617.66-221,804.4). In uninfected samples the average was 357,035.6 (145,187.9-700,848.4).

Welch Two Sample t-test value was -8.7325, df = 26.087, p-value = 0.000000003201(95% confidence interval: -390,585.9- -241,762.4).

FCGR3A

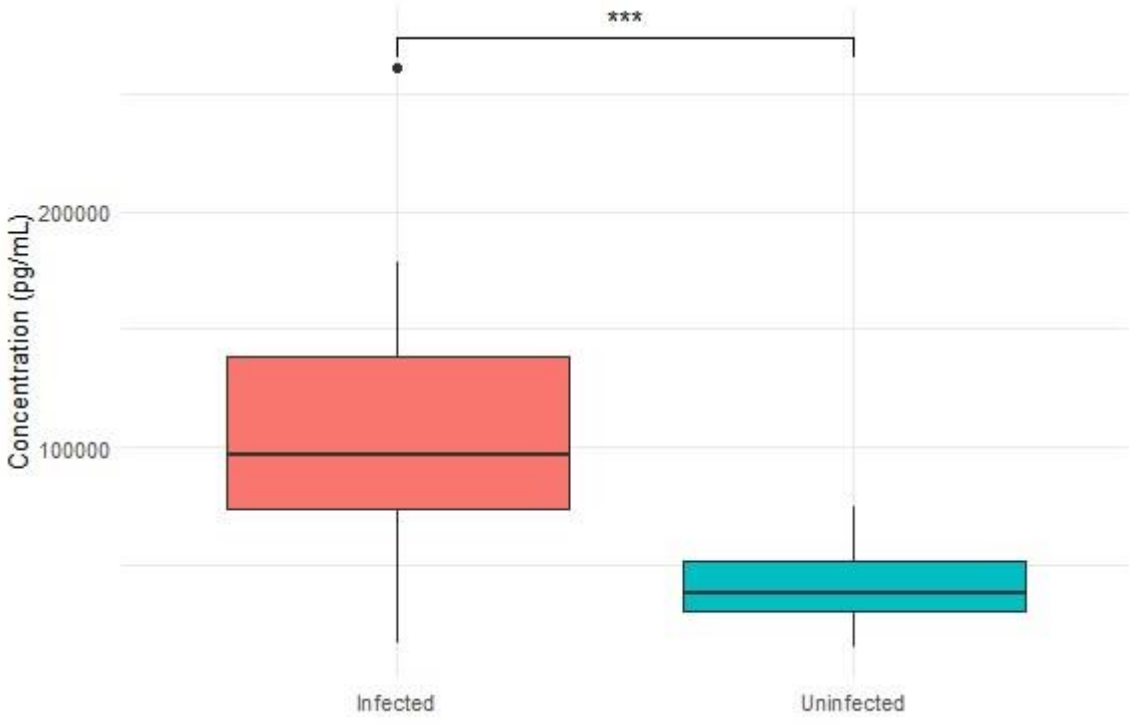

Figure 79 FCGR3A relative abundance as measured by LC MS/MS

The average "concentration" of FCGR3A in infected samples as measured by LC-MS/MS was 108,438.1 (range=16,323.46-261,619.6). In uninfected samples the average was 41,385.47 (range=14,288.12-74,602.62).

Welch Two Sample t-test statistic was 3.8674, df = 14.298, p-value = 0.001647(95% confidence interval:29,939.12-104,166.20).

VGF

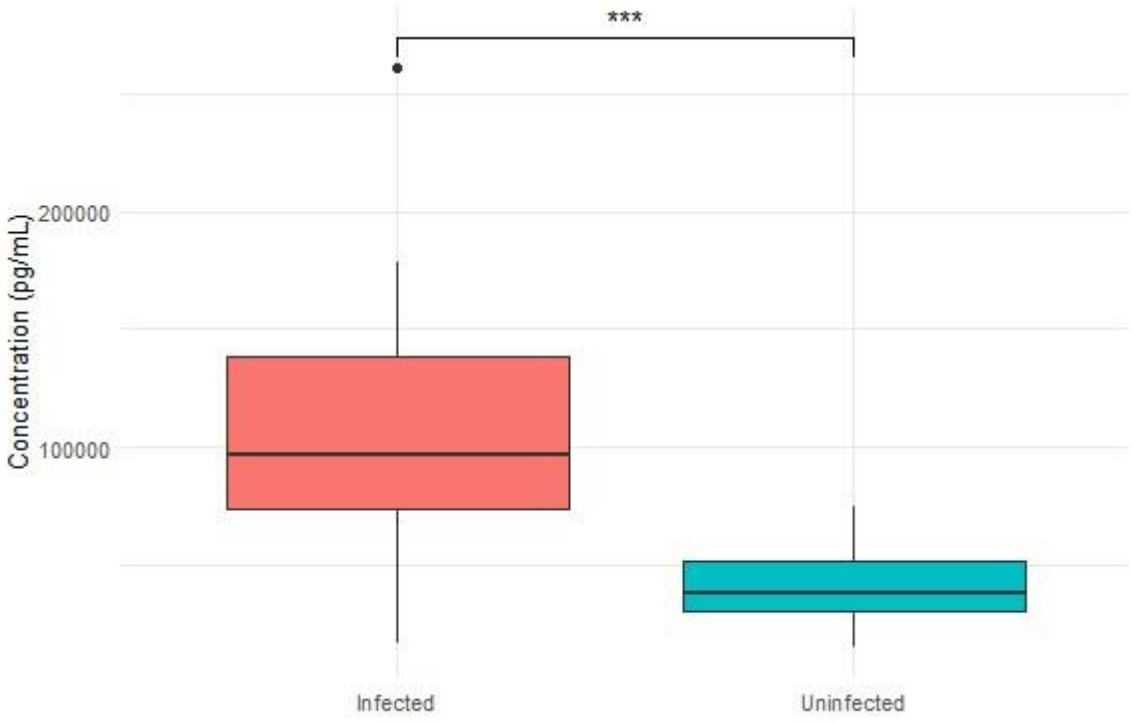

Figure 80 VGF relative abundance as measured by LC MS/MS

The average "concentration" of VGF in infected samples as measured by LC-MS/MS was 466,916.7 (range= 35,214.9-2,786,534). In uninfected samples the average was 4,990,136 (range= 1,991,230-12,571,619).

Welch Two Sample t-test statistic was -6.5284, df = 22.221, p-value = 0.000001376 (95% confidence interval: -5,959,279- -3,087,160).

SCG2

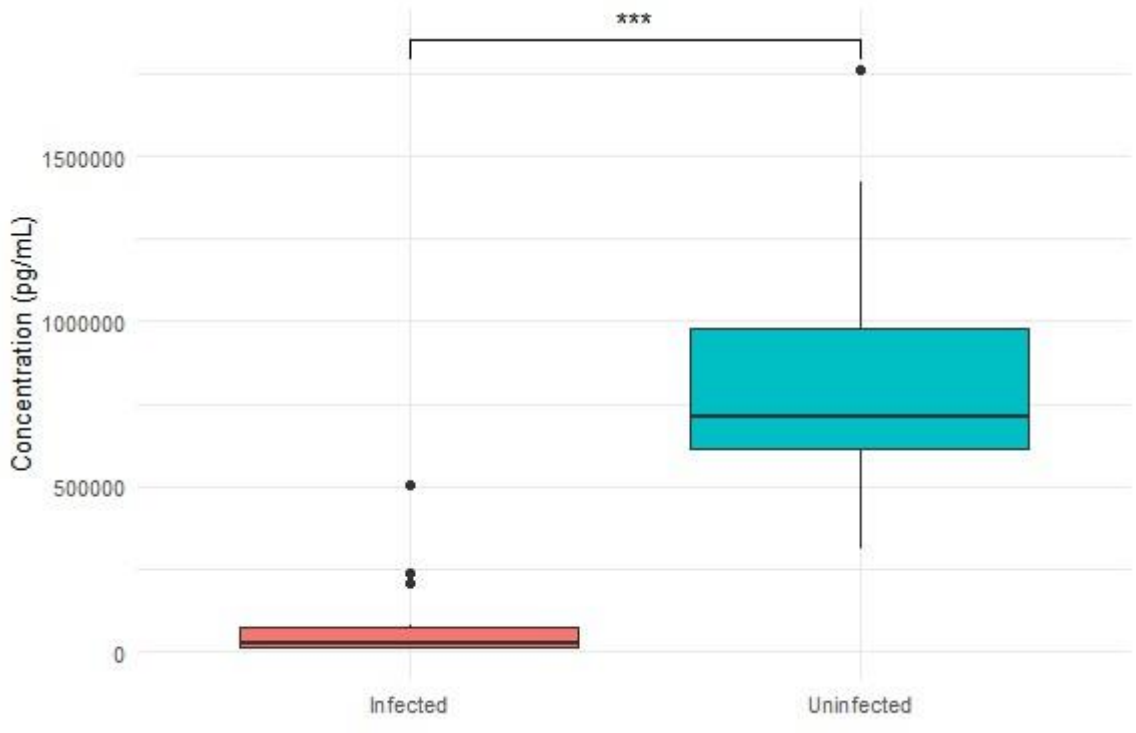

Figure 81 SCG2 relative abundance as measured by LC MS/MS

The average “concentration” of SCG2 in infected samples as measured by LC-MS/MS was 94,832.61 (range= 4,323.69-502,836.2).In uninfected samples the average was 804,046.8 (range= 310,746.9-1,762,695).

Welch Two Sample t-test statistic was -7.7739, df = 26.436, p-value = 0.0000000269 (95% confidence interval: -896590.8- -521837.5).

SCG5

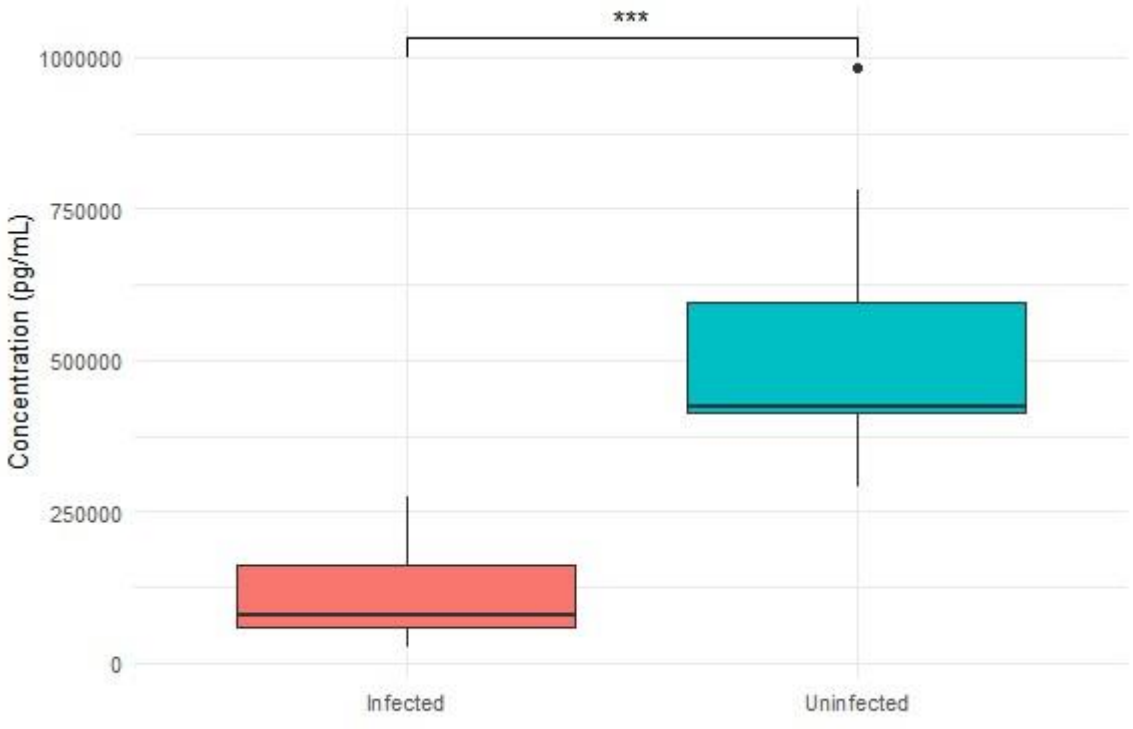

Figure 82 SCG5 relative abundance as measured by LC MS/MS

The average "concentration" of SCG5 in infected samples as measured by LC-MS/MS was 109,747.2 (range= 24,782.54-272,764.1). In uninfected samples the average was 508,613 (range= 292,293.2-983,209.4).

Welch Two Sample t-test statistic was -8.692, df = 26.425, p-value = 0.000000003147 (95% confidence interval: -493117.7- -304613.7).

Fibrinogen

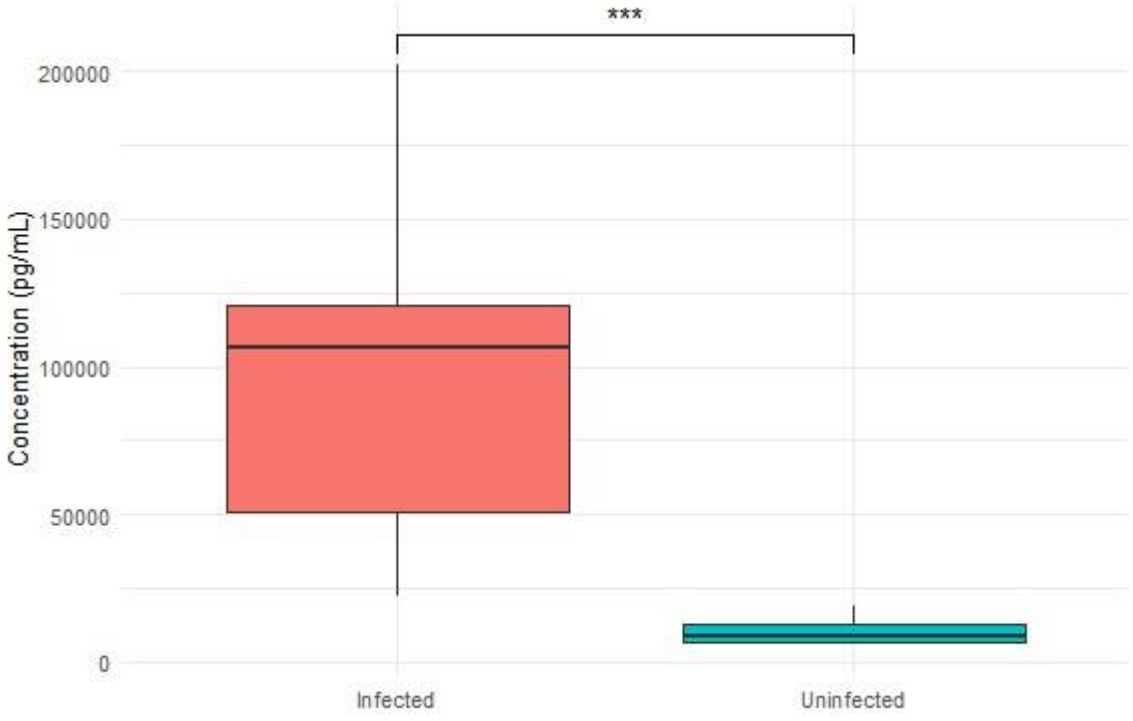

Figure 83 Fibrinogen relative abundance as measured by LC MS/MS

The average "concentration" of Fibrinogen in infected samples as measured by LC-MS/MS was 89,723.65 (range= 22,657.87-202,223.4). In uninfected samples the average was 10,233.73 (range= 5,824.76 19,007.87).

Welch Two Sample t-test statistic was 5.2415, df = 11.093, p-value = 0.0002686 (95% confidence interval: 46,145.35-112,834.50).

ELISAs using pooled CSF samples

Lactoferrin

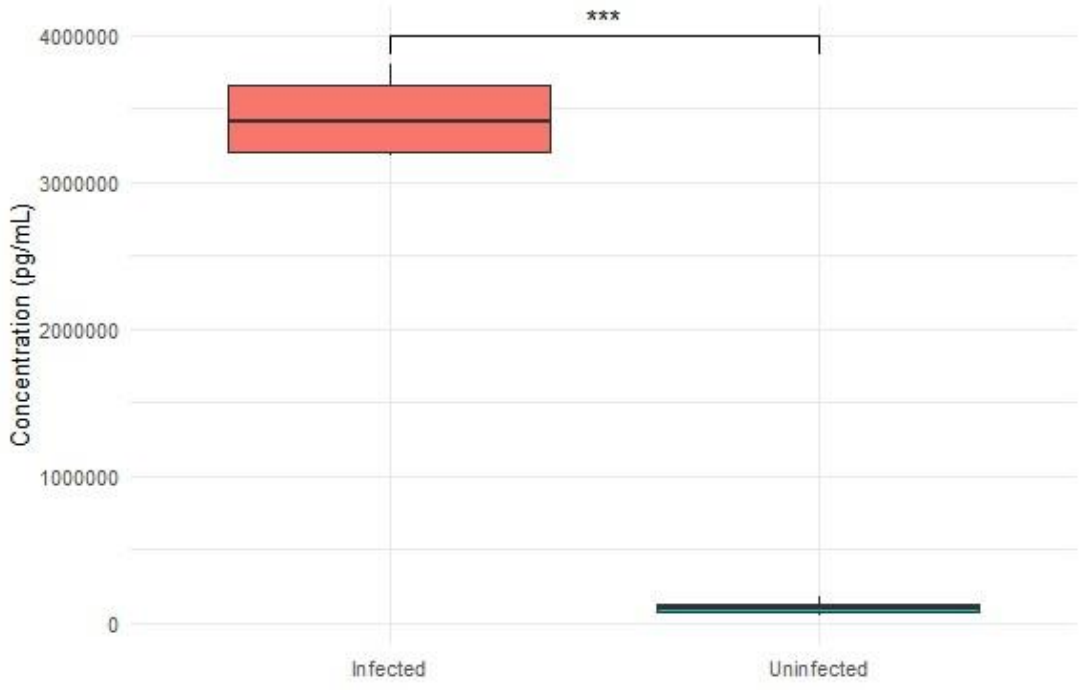

Figure 84 Lactoferrin ELISA results of testing pooled CSF samples

The average concentration of lactoferrin in the four different dilutions of CSF, corrected for dilution, was 3,451.5ng/mL (range=3,179-3,804ng/mL, SD 308.85) for infected samples and 102.95ng/mL (44.6-172.76ng/mL, SD 54.26) for uninfected samples.

Welch Two Sample t-test statistic was 21.357, df = 3.185, p-value = 0.0001512 (95% confidence interval: 2,865.574-3,831.531)

NPTXR

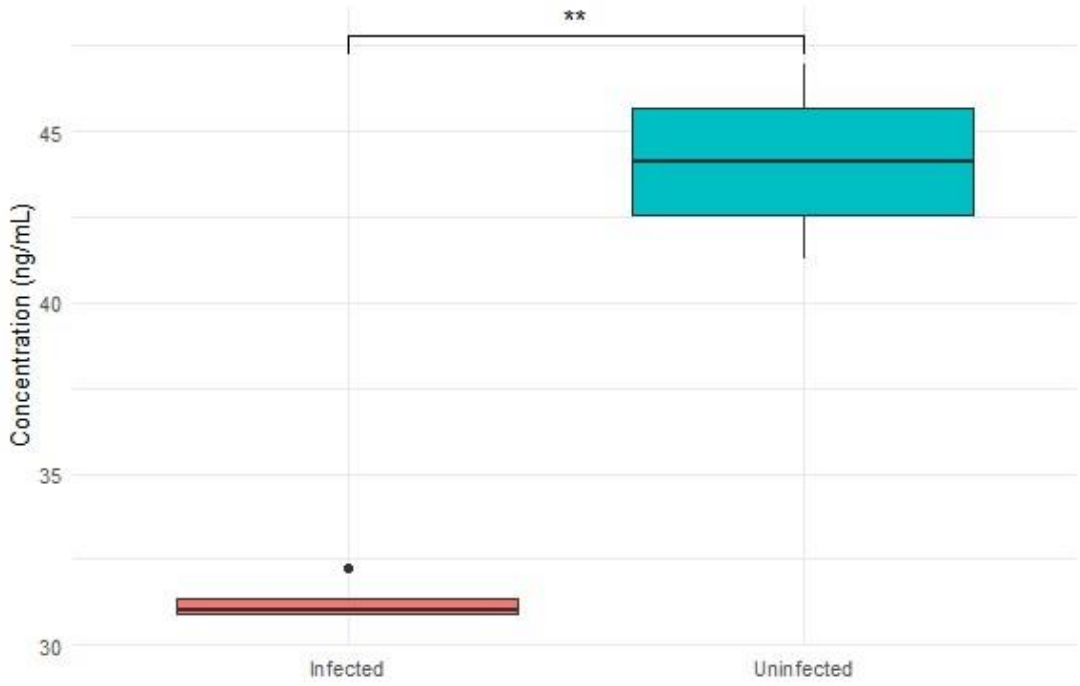

Figure 85 NPTXR ELISA results of pooled CSF samples

The average concentration of NPTXR in the four different dilutions of CSF, corrected for dilution, was 31.27ng/mL (range 30.83-32.26ng/mL, SD 0.67) for infected samples and 44.11ng/mL(41.25-46.96ng/mL, SD 2.51) for uninfected samples.

Welch Two Sample t-test statistic was -9.8715, df = 3.4181, p-value = 0.001248 (95% confidence interval: -16.71-8.97).

TIMP2

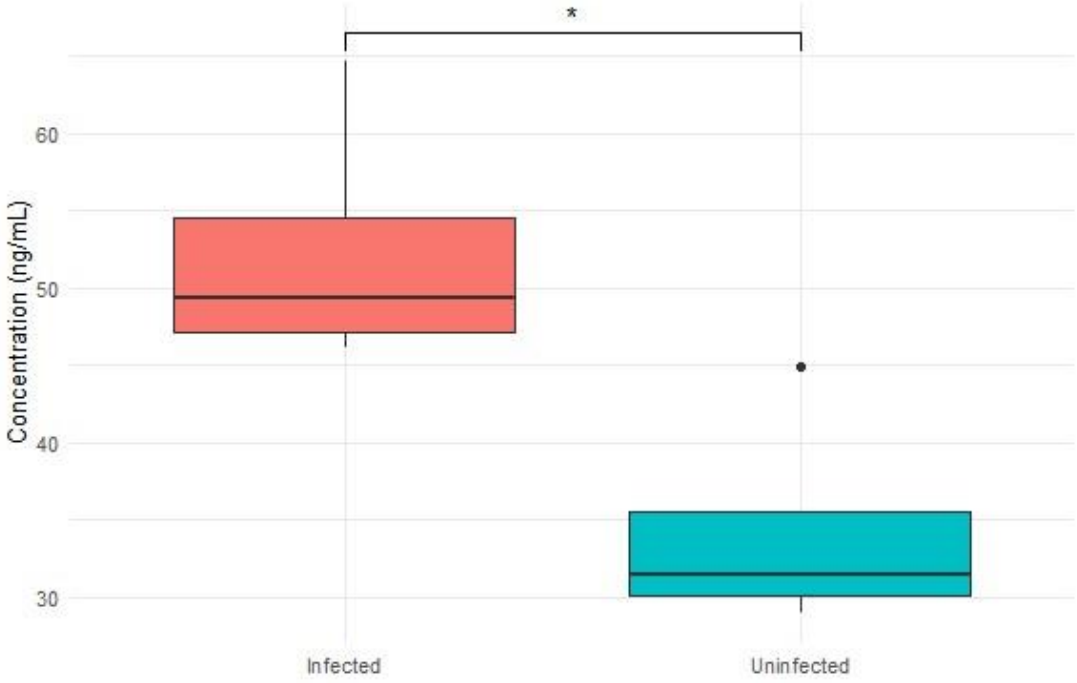

Figure 86 TIMP2 ELISA results of pooled CSF samples

The average concentration of TIMP2 in the four different dilutions of CSF, corrected for dilution, was 52.4ng/mL (range 46.1-64.7ng/mL, SD 8.46) for infected samples and 34.2ng/mL(29-44.95ng/mL, SD 7.3) for uninfected samples.

Welch Two Sample t-test statistic was 3.2469, df = 5.8737, p-value = 0.01807(95 percent confidence interval: 4.399-31.9)

IGF2

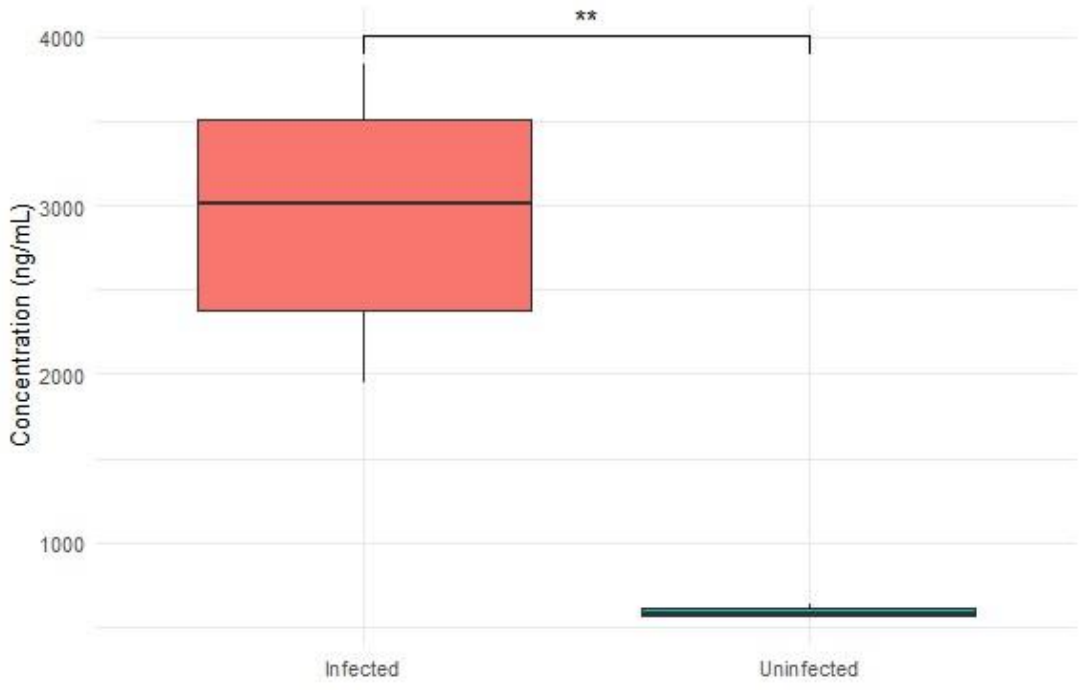

Figure 87 IGF2 ELISA results of pooled CSF samples

The average concentration of IGF2 in the five different dilutions of CSF, corrected for dilution, was 2,937.3 ng/mL (range 1,944.5-3,843.2ng/mL, SD 783.96) for infected samples and 592 ng/mL(range 562.5-638.5ng/mL, SD 34.21) for uninfected samples.

Welch Two Sample t-test statistic was 6.6832, df = 4.0152, p-value = 0.002571(95% confidence interval: 1,372.5-3,318.2).

NEGR1

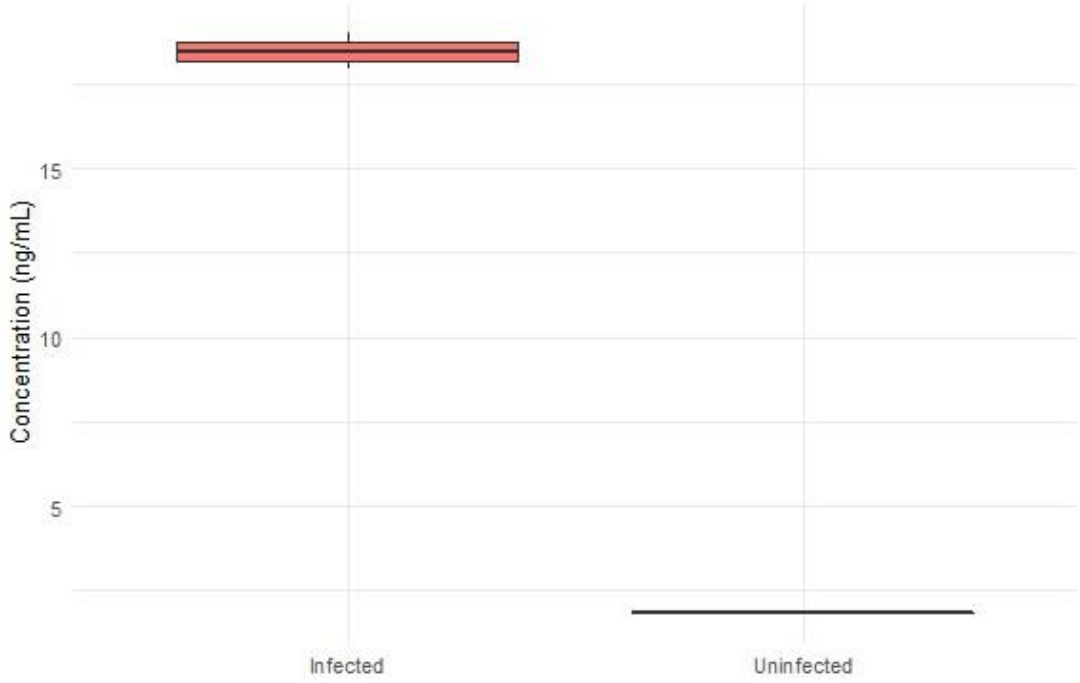

Figure 88 NEGR1 ELISA results of pooled CSF samples

NEGR1 concentration was measurable in the 1/10 dilution of CSF for both groups and in the 1/20 dilution in the infected group only. The average NEGR1 concentration, adjusting for dilution, of the infected pool was 18.5ng/mL (17.9-19ng/mL). In the 1/10 dilution of the uninfected pool the NEGR1 concentration was 1.8ng/mL.

There was no statistic for this difference due to their only being one uninfected value.

FCGR3A

All the test samples measured beyond the limits of the assay.

VGF

All the test samples measured beyond the limits of the assay.

SCG2

All the test samples measured beyond the limits of the assay.

SCG5

All the test samples measured beyond the limits of the assay.

Fibrinogen

The standards for the assay failed and as such no valid results were obtained.

ELISAs using individual CSF samples

ELISAs without protein digest step

Lactoferrin

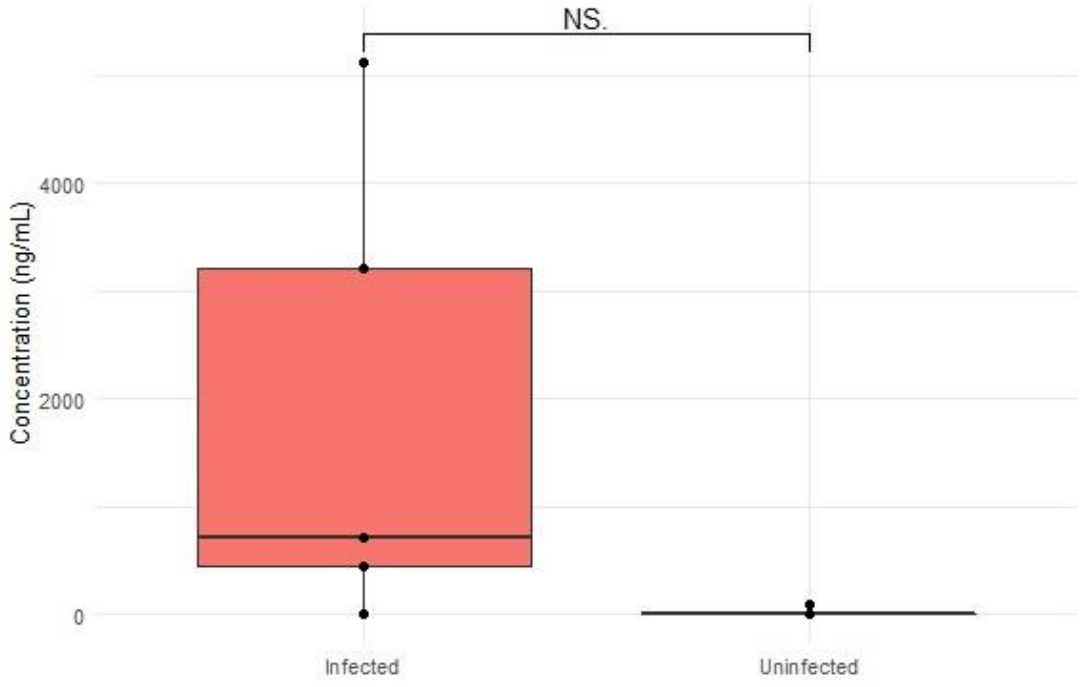

Figure 89 Lactoferrin ELISA results of individual CSF samples

The average Lactoferrin concentration for the infected samples was 1,895.44ng/mL, (05,121ng/mL, SD 2,192.69). Sample 2 was below the level of detection of the assay.

Excluding sample 2 from the infected group the average Lactoferrin concentration was 2369.3ng/mL, range 442-5121ng/mL.

In the uninfected group the average Lactoferrin concentration was 17.3ng/mL, range 086.3ng/mL, SD 38.6. Only sample 9 had a detectable level of Lactoferrin.

Welch Two Sample t-test statistic was 1.915, df = 4.0025, p-value = 0.128 (95% confidence interval: -844,155.3-4,600,523.3).

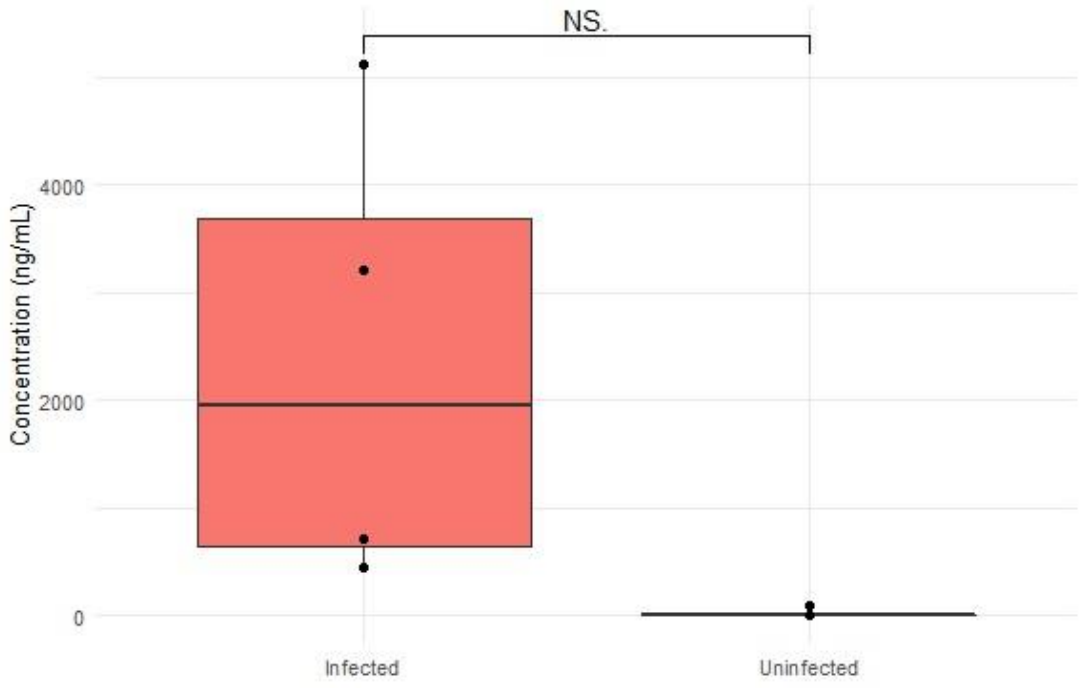

Figure 90 Lactoferrin ELISA results of individual samples, excluding sample 2

NPTXR

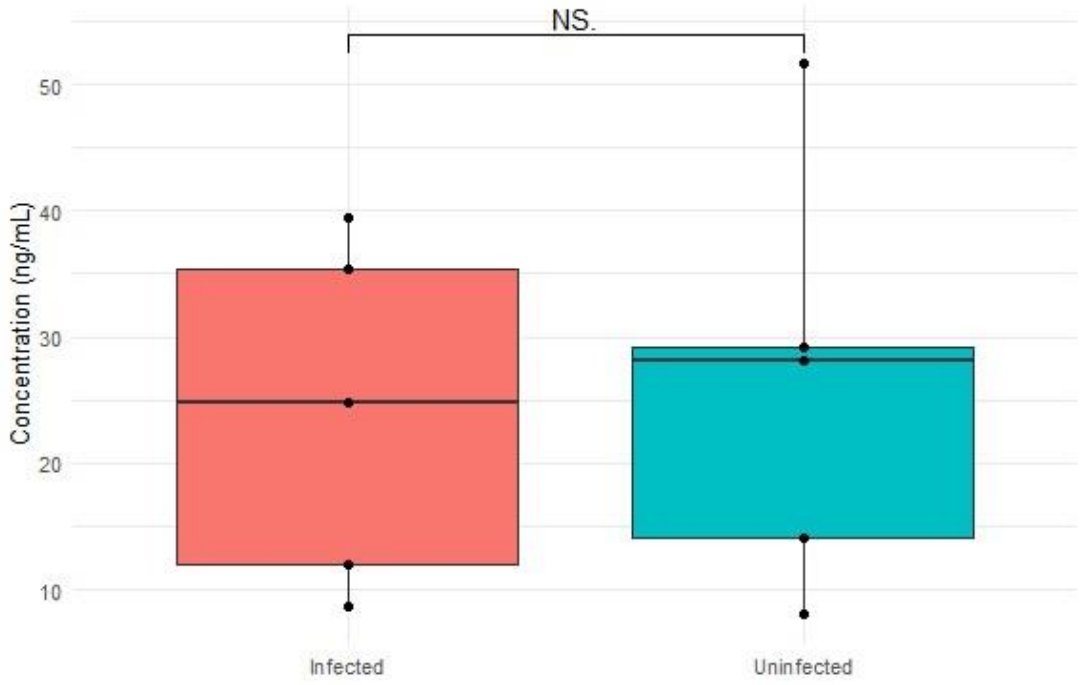

Figure 91 NPTXR ELISA results of individual CSF samples

The average NPTXR concentration for infected samples was 24.04ng/mL (range 8.739.4ng/mL, SD 13.65) whilst the average for uninfected samples was 26.21ng/mL (range 851.69ng/mL, SD 16.89).

Welch Two Sample t-test statistic was -0.22302, df = 7.6634, p-value = 0.8293 (95% confidence interval: -24.73184 -20.40024).

NEGR1

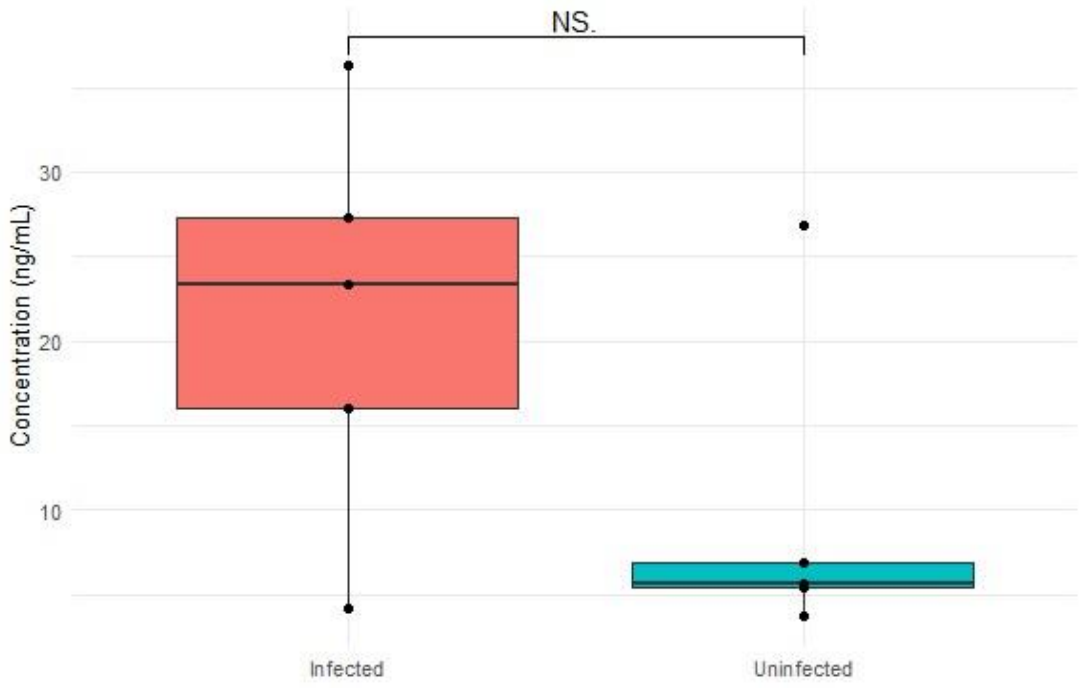

Figure 92 NEGR1 ELISA results of individual CSF samples

The average NEGR1 concentration in infected samples was 21.4ng/mL (range 4.236.3ng/mL, SD 21.43) and the average for uninfected samples was 9.7ng/mL (range 3.7-26.8ng/mL, SD 9.69).

Welch Two Sample t-test statistic was 1.6974, df = 7.6177, p-value = 0.13 (95% percent confidence interval: -4,351.259-27,838.459).

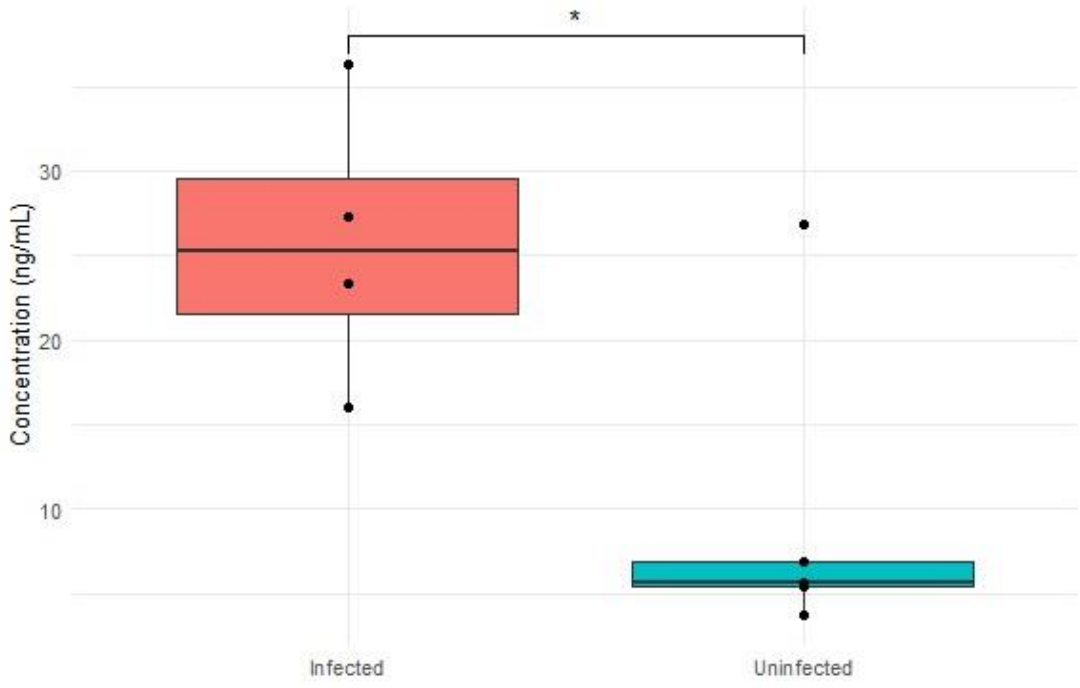

Figure 93 NEGR1 ELISA results of individual CSF samples excluding sample 2

Excluding sample two from analysis the average concentration of Lactoferrin for the infected group was 25.7ng/mL (16-36.3ng/mL).

Welch Two Sample t-test statistic was 2.6553, df = 6.8885, p-value = 0.03317 (95% confidence interval: 1.709582-30.385418).

ELISAs comparing protein digested CSF samples and untreated CSF

TIMP2

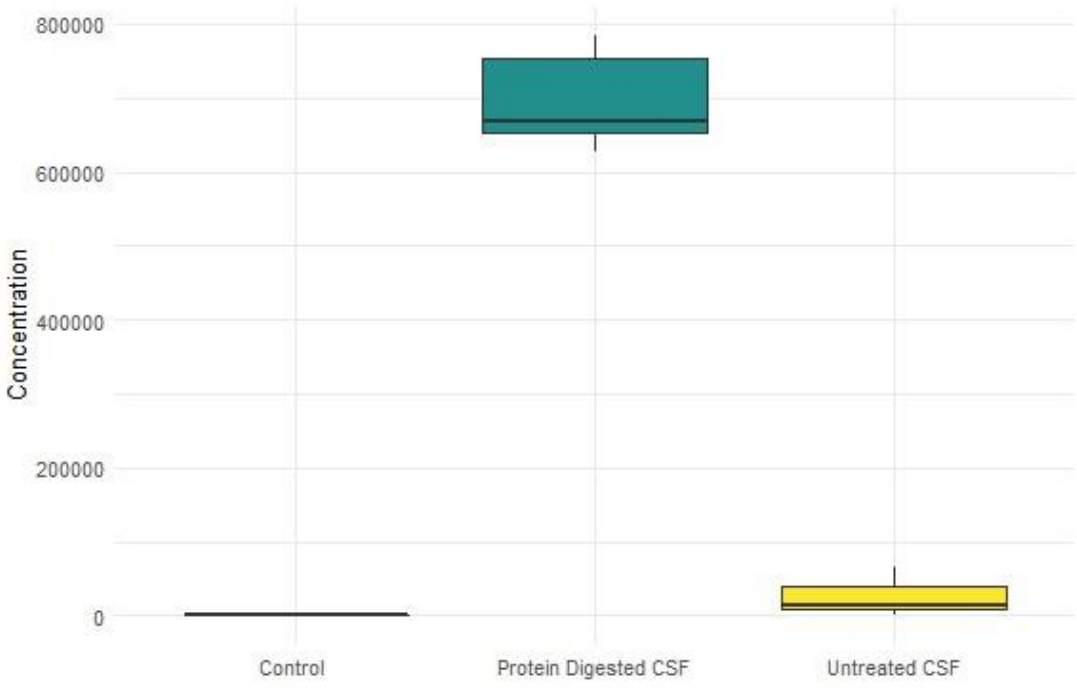

Figure 94 TIMP2 concentration of control, protein digested CSF and untreated CSF, Experiment 1

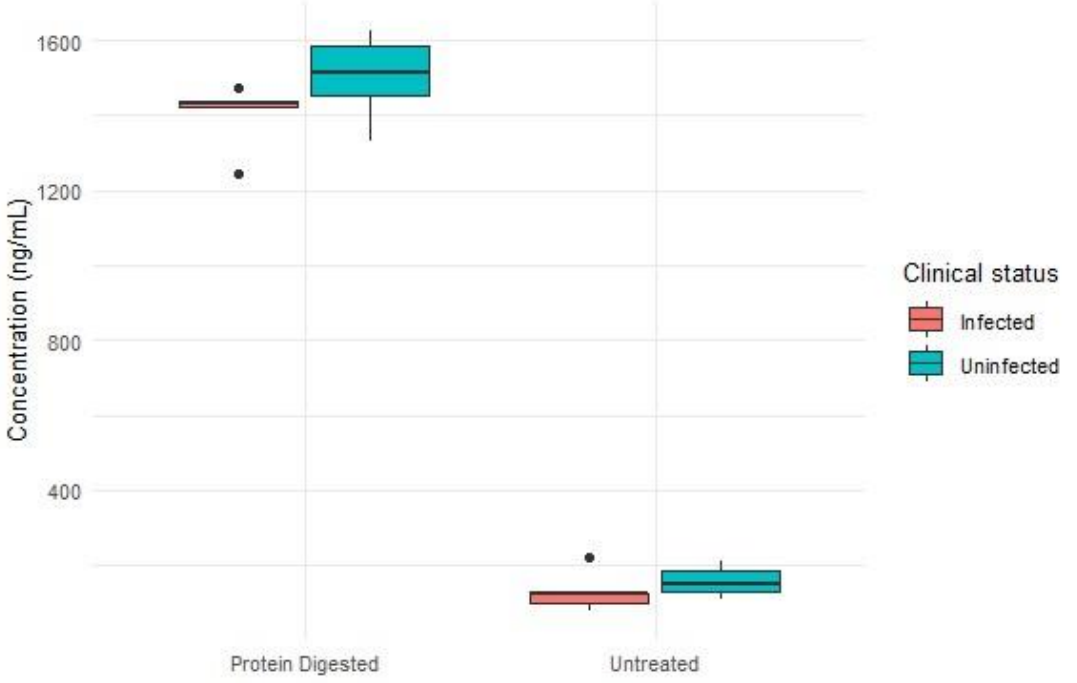

Figure 95 TIMP2 ELISA results of protein digested and untreated individual CSF samples, Experiment 1

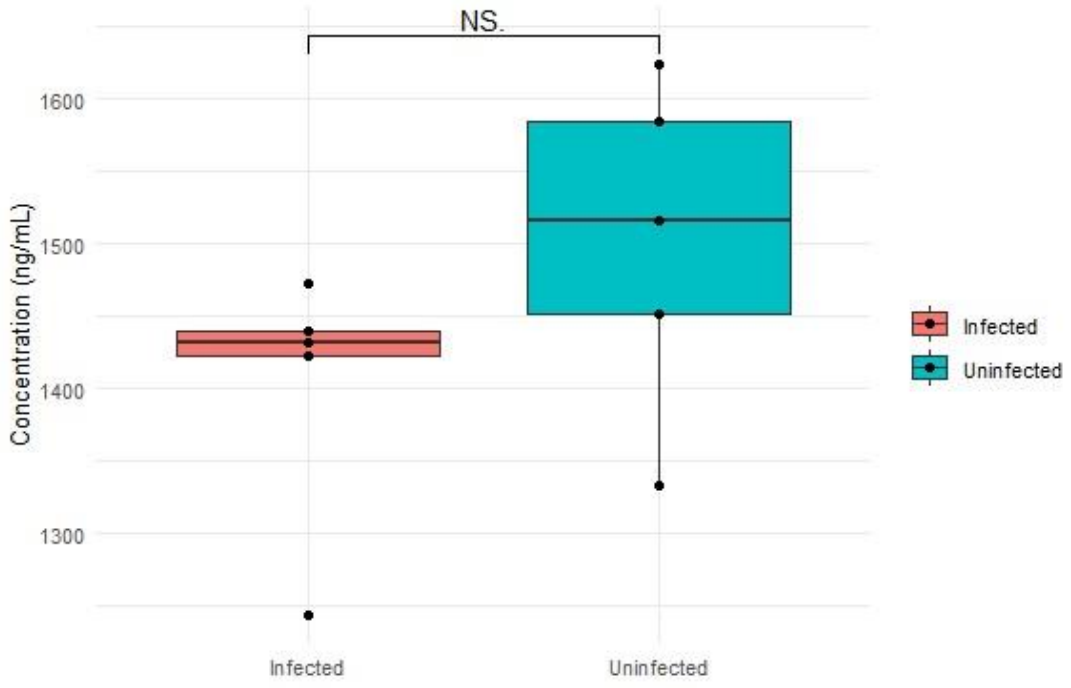

Figure 96 TIMP2 ELISA results of protein digested individual CSF samples, Experiment 1

In protein digested samples the average TIMP2 concentration in the infected samples was 1,401.4ng/mL (range 1,243-1,472ng/mL, SD 90.54). The average for uninfected samples was 1501.6ng/mL (range 1,333-1,624ng/mL, SD 115.07).

Welch Two Sample t-test statistic was -1.5302, df = 7.5804, p-value = 0.1666 (95% confidence interval: -252.666-52.266ng/mL).

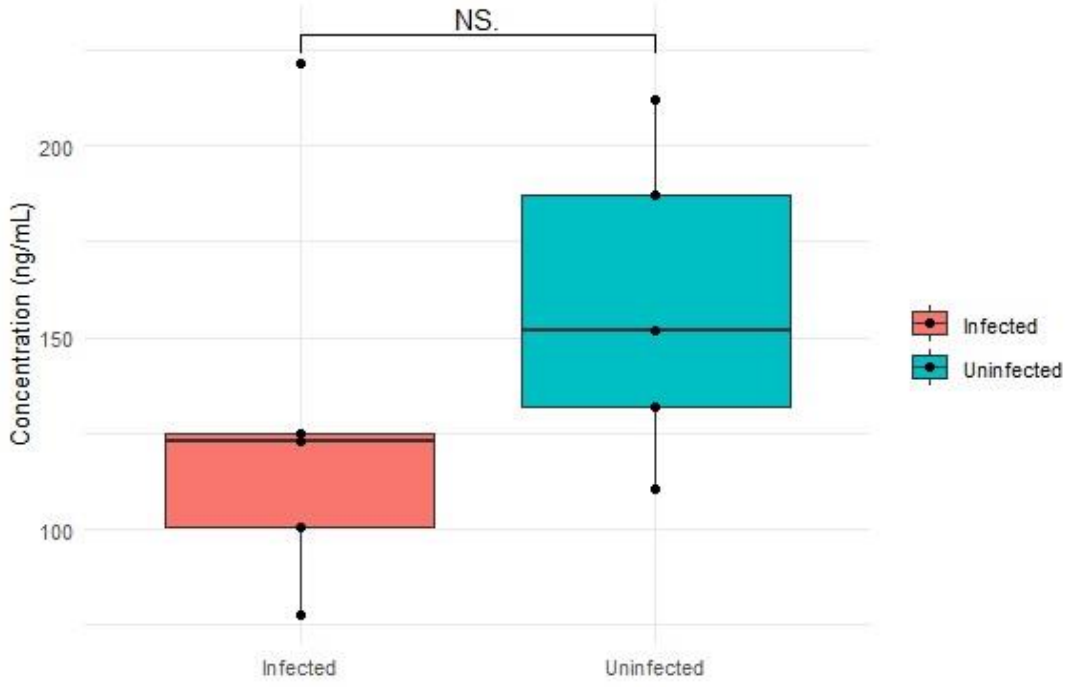

Figure 97 TIMP2 ELISA results of untreated individual CSF samples

In the untreated samples the average TIMP2 concentration in the infected samples was 129.5ng/mL (range 77.5-221.6ng/mL, SD 54.97). The average for uninfected samples was 158.7ng/mL (range 110.6-212.2ng/mL, 41.07).

Welch Two Sample t-test statistic was -0.95132, df = 7.4051, p-value = 0.3715 (95% confidence interval: -100.963-42.6ng/mL).

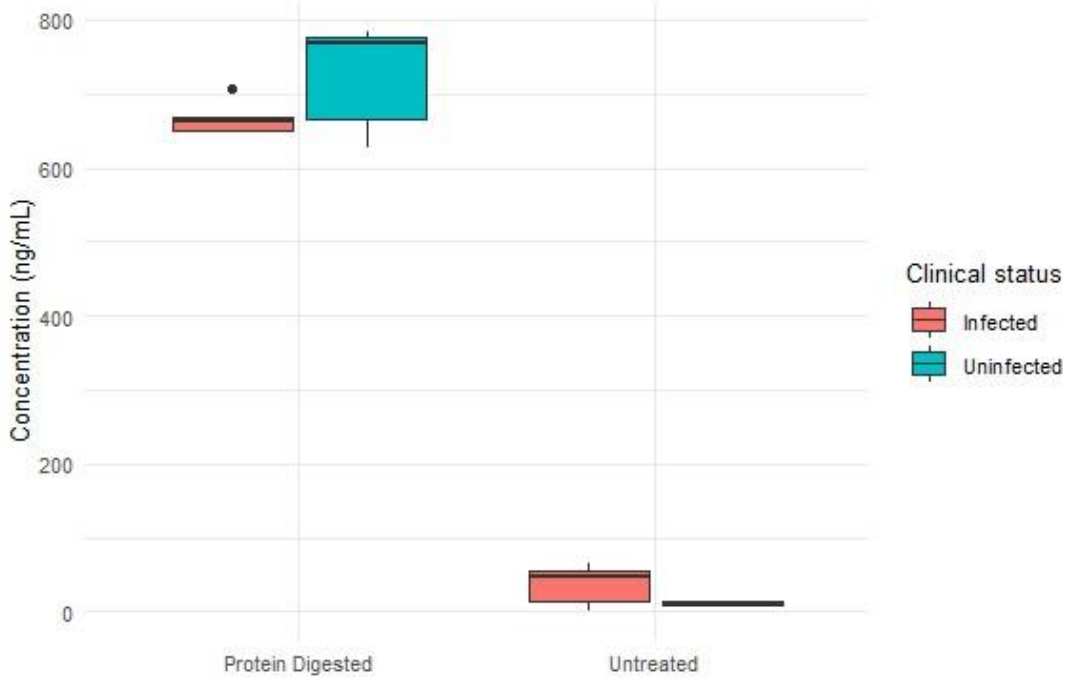

Figure 98 TIMP2 ELISA results of protein digested and untreated individual CSF samples, Experiment 2

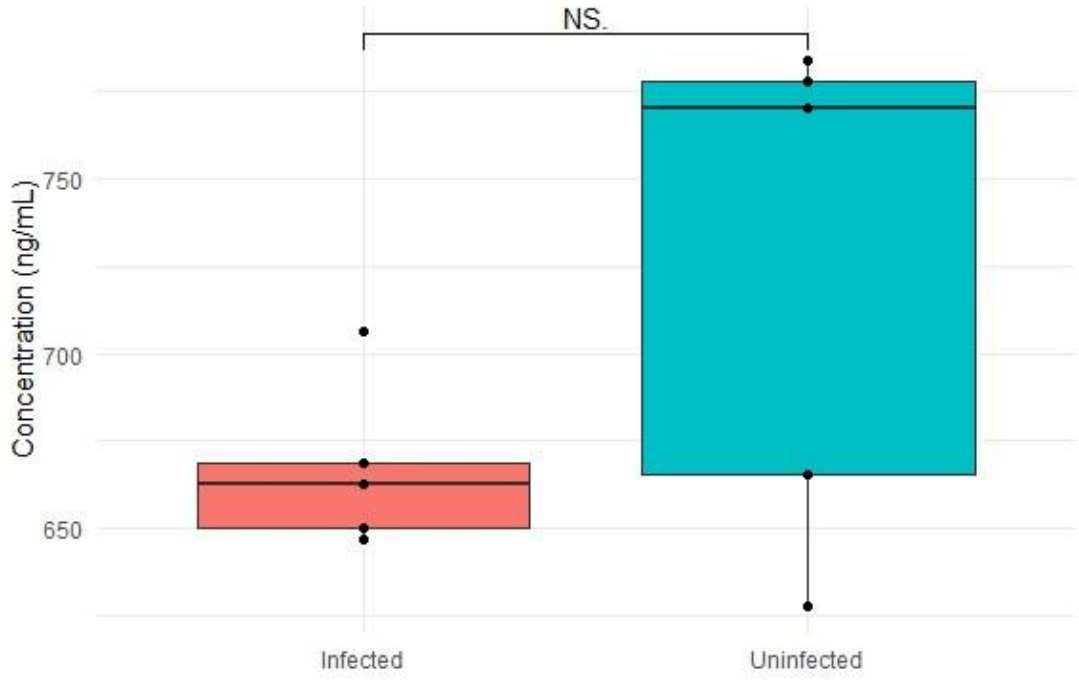

Figure 99 TIMP2 ELISA results of protein digested individual CSF samples, Experiment 2

In protein digested samples the average TIMP2 concentration in the infected samples was 666.9ng/mL (range 647.1-706ng/mL, SD 23.59). The average for uninfected samples was 724.9ng/mL (range 627.9-783.5ng/mL, SD 72.7).

Welch Two Sample t-test statistic was -1.6962, df = 4.8329, p-value = 0.1526 (95% confidence interval: -146.8-30.8ng/mL).

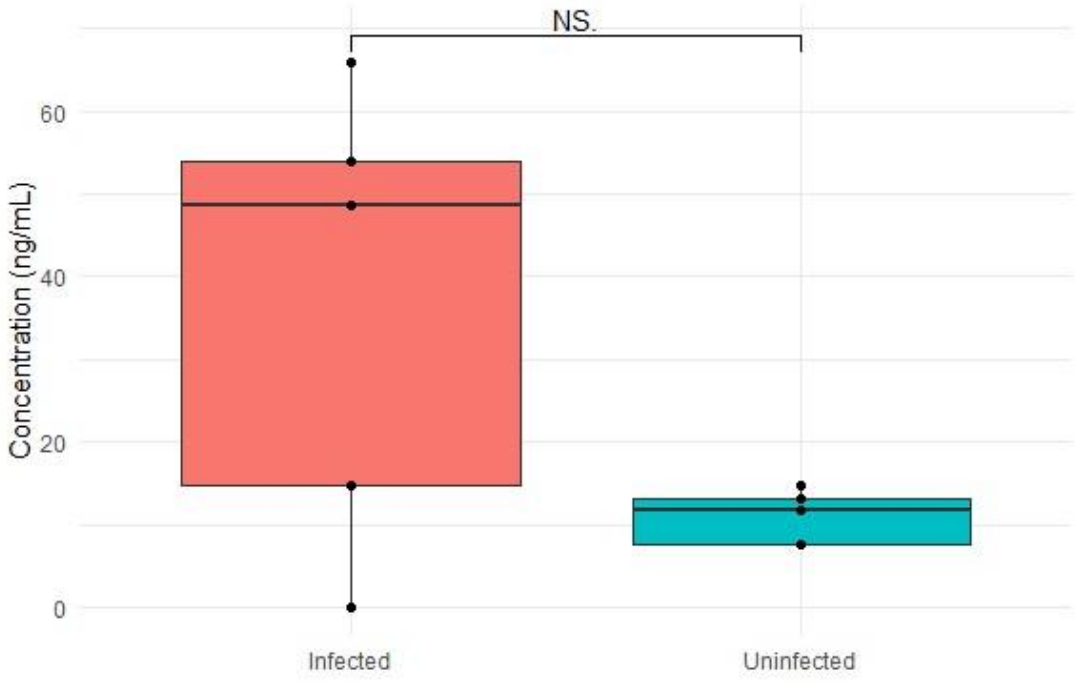

Figure 100 TIMP2 ELISA results of untreated individual CSF samples, repeat experiment

In the untreated samples the average TIMP2 concentration in the infected samples was 36.6ng/mL (range 0-65.9ng/mL, SD 27.94). The average for uninfected samples was 10.966ng/mL (range 7.6-14.6ng/mL, SD 3.26).

Welch Two Sample t-test statistic was 2.038, df = 4.1091, p-value = 0.1093 (95% confidence interval: -8.9-60.2ng/mL).

IGF2

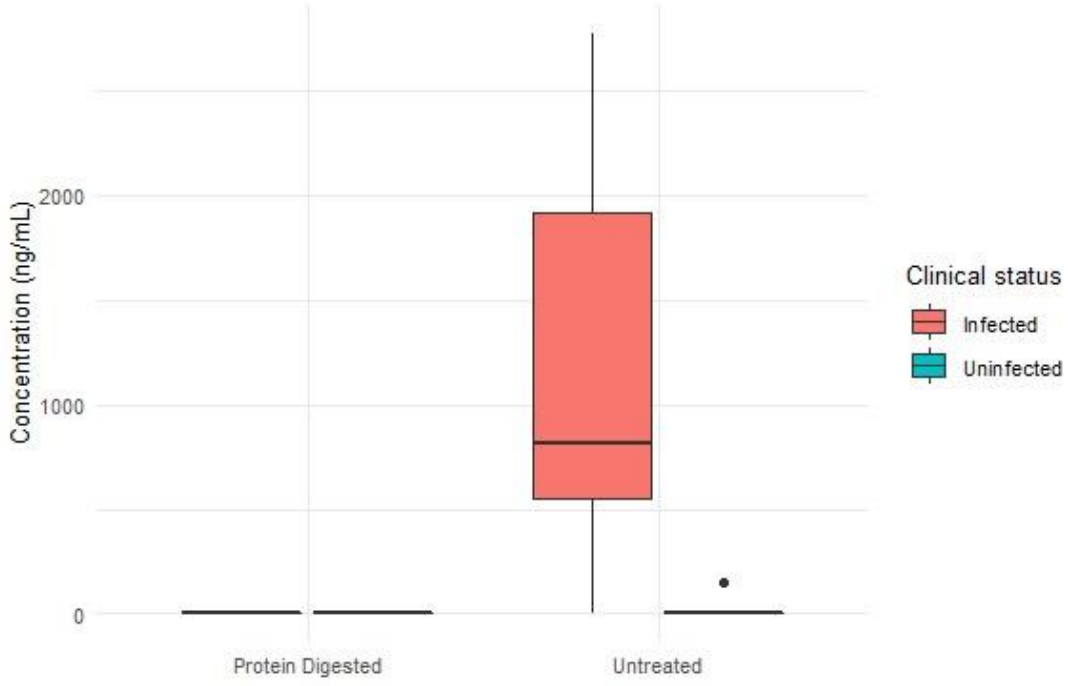

Figure 101 IGF2 ELISA results of protein digested and untreated individual CSF samples

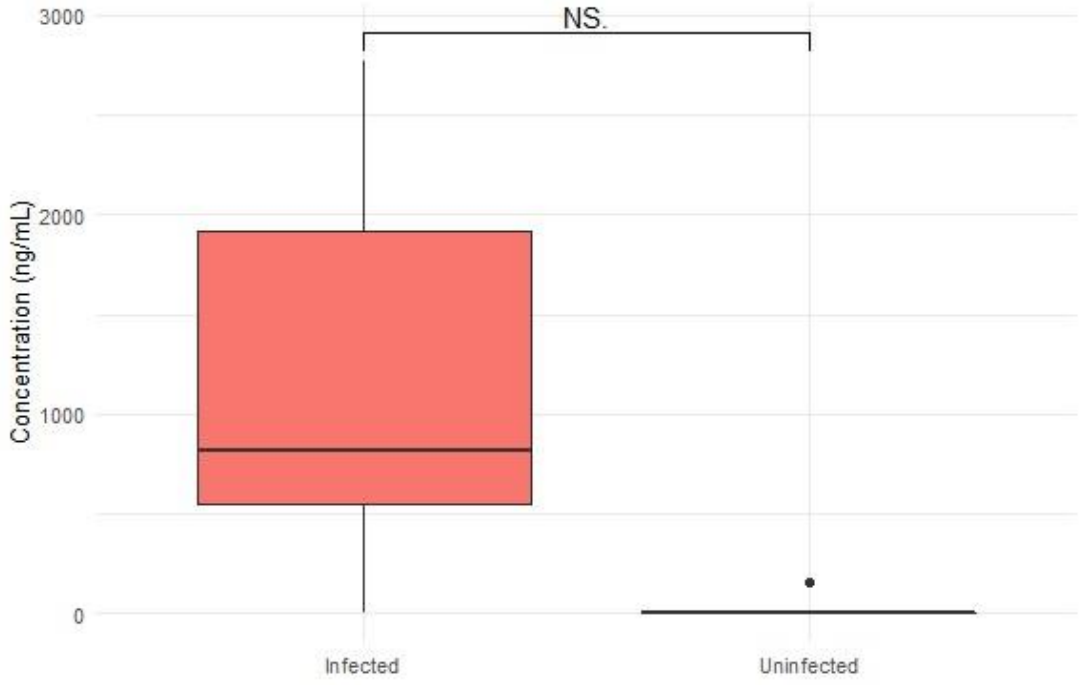

Figure 102 IGF2 ELISA results of individual untreated CSF samples

All samples that underwent protein digestion (low complexity matrix protocol) measured below the detection limits of the assay.

For untreated CSF samples the average IGF2 concentration for infected samples was 1,210.14ng/mL (range 0-2,771ng/mL, SD 1,117.96) and for uninfected samples 30.68ng/mL (range 0-153.4ng/mL, SD 68.6).

Welch Two Sample t-test statistic was 2.3546, df = 4.0301, p-value = 0.07763 (95% confidence interval: -207.2-2,566.1ng/mL).

Appendix B

ANXA1
ANXA2
ANXA3
ANXA5
ANXA6
APBB1IP
APCS
APEX1
APLP1
APLP2
APMAP
APOA1
APOA2
APOA4
APOB
APOBR
APOC1
APOC2
APOC3
APOD
APOE
APOF
APOH
APOL1
APOL3
APOM
APP
AQP4
ARCN1
ARF3
ARG1
ARHGAP1
ARHGDIA
ARHGDIB
ARPC1B
ARPC2
ARPC3

ATP5F1A
ATP5F1B
ATP5PD
ATP5PO
ATP6AP1
ATP6V1A
ATP6V1B2
ATP6V1E1
ATRN
AZGP1
AZU1
B2M
B4GALT1
B4GAT1
BANF1
BASP1
BBS5
BBS7
BCAN
BID
BLVRB
BOLA2
BPGM
BPI
BST1
BTD
C1QA
C1QB
C1QC
C1R
C1RL
C1S
C2
C2orf40
C3
C4A
C4B

A1BG
A2M
ABHD12B
ACAT1
ACO2
ACTB
ACTC1
ACTN1
ACTN4
ACTR2
ACTR3
ACYP2
ADA2
ADAMTS1
ADGRG3
ADSS
AFM
AGRN
AGT
AHCY
AHNAK
AHSA1
AHSG
AK1
AK2
AKR1A1
AKR7A2
ALAD
ALB
ALCAM
ALDH1A1
ALDOA
ALDOC
ALPL
ALYREF

ARPC4
ARPC5
ARR3

C4BPA
C5
C6

AMBP
AMER2
ANK1

Table 60 Proteins identified by LC-MS/MS in Chapter 4

C7
C8A
C8B
C8G
C9
CA1
CA2
CA3
CAB39
CACNA2D1
CADM1
CADM3
CADM4
CALM1
CAMP
CANX
CAP1
CAPZA1
CAPZB
CARTPT
CAST
CAT
CCDC78
CCT2
CCT3
CCT6A
CCT8
CD109
CD14
CD163
CD44
CD59
CD99L2
CDA
CDC42
CDH13

CFHR1
CFHR3
CFI
CFL1
CGREF1
CHGA
CHGB
CHI3L1
CHI3L2
CHIT1
CHL1
CKB
CKMT1A
CLC
CLEC3B
CLIC1
CLSTN1
CLTC
CLU
CNDP1
CNDP2
CNN2
CNRIP1
CNTN1
CNTN2
CNTNAP2
COL11A1
COL18A1
COL1A1
COL1A2
COL3A1
COL5A1
COL5A2
COL5A3
COL6A1
COL6A3

CPN2
CPNE3
CRISP3
CRISPLD1
CRKL
CRP
CRTAC1
CSF1R
CST3
CST7
CSTA
CSTB
CTBS
CTSB
CTSC
CTSD
CTSG
CUTA
CXADR
CXCL10
CXCL8
CXCL9
CYBB
CYCS
DAG1
DBI
DBN1
DCTN2
DDTL
DDX17
DEFA1
DERA
DKK3
DMXL2
DNER
DNM1

CDH2
CDH5
CEACAM1
CEACAM6
CEACAM8
CFB
CFD
CFH

COMP
CORO1A
CORO1C
COTL1
CP
CPB2
CPE
CPN1

DPYSL2
DPYSL3
DRAXIN
DSTN
DYNC2H1
DYNLL2
ECM1
EEF1A1

EEF1A2
EEF2
EFEMP1
EFHD1
EHD1
EIF5A
ELANE
ENDOD1
ENO1
ENO2
ENPP2
ENPP7
EPB41
EPHA4
EPHA5
ESD
EZR
F11
F12
F13A1
F13B
F2
F5
F9
FABP5
FABP7
FAM3C
FAM49B

FLOT1
FN1
FRMPD1
FSCN1
FSTL1
FUBP1
FXYD6
G6PD
GALNT15
GALNT2
GANAB
GAP43
GAPDH
GBP1
GBP2
GC
GCA
GDI2
GFAP
GLIPR2
GLO1
GLOD4
GLRX
GM2A
GNAI2
GNB2
GNG5
GNPTG

H2AFY
H2AFZ
HABP2
HADHA
HAGH
HBA1
HBB
HBD
HBG1
HCK
HCLS1
HEBP1
HEBP2
HGFAC
HINT1
HIST1H1B
HIST1H1E
HIST1H2AB
HIST1H4A
HIST2H2AA3
HIST2H2AB
HIST2H2BF
HIST3H3
HK3
HLA-A
HLA-A
HLA-C
HLTF

FBLN1
FBLN5
FBP1
FCGBP
FCGR3A
FCGR3B
FCN1
FCN2
FCN3
FERMT3
FETUB
FGA
FGB
FGG
FKBP1A
FLNA

GOLM1
GON4L
GOT2
GPI
GPLD1
GPR158
GPR37L1
GPX3
GRB2
GSN
GSS
GSTO1
GSTP1
GYG1
H1F0
H1FX

HMGB1P1
HMGB2
HMGN1
HMGN2
HMOX1
HNRNPA1
HNRNPA2B1
HNRNPAB
HNRNPCL4
HNRNPD
HNRNPF
HNRNPK
HP
HPR
HPRT1
HPX

HRG
HSP90AA1
HSP90AB1
HSPA1A
HSPA5
HSPA8
HSPD1
HSPE1
HSPG2
HTRA1
ICAM1
ICAM3
ICOSLG
IDH1
IGFALS
IGFBP2
IGFBP3
IGFBP4
IGFBP6
IGFBP7

IGHV3-48
IGHV3-49
IGHV3-64
IGHV3-7
IGHV3-72
IGHV3-9
IGHV4-28
IGHV4-30-2
IGHV4-34
IGHV4-39
IGHV4-4
IGHV4-61
IGHV5-10-1
IGHV5-51
IGHV6-1
IGHV7-4-1
IGKC
IGKJ1
IGKV1-16
IGKV1-17

IGLV2-18
IGLV2-23
IGLV2-8
IGLV3-10
IGLV3-12
IGLV3-19
IGLV3-21
IGLV3-25
IGLV3-27
IGLV3-9
IGLV4-3
IGLV4-60
IGLV4-69
IGLV5-37
IGLV6-57
IGLV7-43
IGLV7-46
IGLV8-61
IL1R2
IL1RN

IGHA1
IGHG2
IGHG3
IGHG4
IGHM
IGHV1-18
IGHV1-2
IGHV1-24
IGHV1-3
IGHV1-45
IGHV1-46
IGHV1-69D
IGHV1-8
IGHV2-26
IGHV2-5
IGHV2-70
IGHV2-70D
IGHV3-11
IGHV3-15
IGHV3-20
IGHV3-21
IGHV3-30
IGHV3-33
IGHV3-43

IGKV1-27
IGKV1-39
IGKV1-5
IGKV1-8
IGKV1D-13
IGKV1D-16
IGKV2-24
IGKV2-28
IGKV2-30
IGKV2D-29
IGKV3-15
IGKV3-20
IGKV3D-11
IGKV3D-15
IGKV3D-20
IGKV4-1
IGKV6D-21
IGLC2
IGLC7
IGLV10-54
IGLV1-40
IGLV1-47
IGLV1-51
IGLV2-14

IL6
ILF3
INHBC
IQGAP1
ISLR
ITGAM
ITGB2
ITIH1
ITIH2
ITIH3
ITIH4
JAML
JCHAIN
KCTD12
KHDRBS1
KLK6
KLKB1
KNG1
KRT1
KRT10
KRT77
KRT86
KRT9
L1CAM

LAIR1
LAMA1
LAMP2
LAP3
LASP1
LBP
LBR
LCAT
LCN2
LCP1
LDHA
LDHB

MCAM
MDH1
MDH2
MEGF8
MIF
MMP2
MMP8
MMP9
MNDA
MPO
MSLN
MSN

NRXN1
NRXN2
NRXN3
NSF
NTM
NUCB1
NXPH4
OGN
OLA1
OLFM4
OPCML
ORM1

LGALS1
LGALS3
LGALS3BP
LHPP
LILRA3
LMNB1
LOX
LRG1
LRRFIP1
LSAMP
LSP1
LTA4H
LTBP2
LTF
LUM
LY6H
LYNX1
LYVE1
LYZ
LZTS2
MAP1B
MAP1LC3B2
MAP2
MAPT
MARCKS
MARCKSL1
MARCO
MASP2
MAT2B
MB
MBL2
MBP

MT3
MTPN
MYH9
MYL12B
MYL6
MYO18B
NACA
NAGK
NAMPT
NAXE
NBL1
NCALD
NCAM1
NCAM2
NCAN
NCL
NECTIN1
NEFL
NELL2
NEO1
NFASC
NID2
NME1
NME2
NMI
NPC2
NPDC1
NPM1
NPTXR
NPY
NRCAM
NRGN

ORM2
OSBPL6
OSTF1
OTUB1
P4HB
PABPC1
PADI2
PADI4
PALM
PAM
PARK7
PCBP1
PCOLCE
PCSK1N
PDCD6IP
PDIA3
PEA15
PEBP1
PEBP4
PENK
PFDN5
PFKP
PFN1
PGAM1
PGD
PGK1
PGLS
PGLYRP1
PGLYRP2
PGM2
PHPT1
PI16

PIAS4
PIK3IP1
PKM
PLBD1
PLG

PSME2
PTGDS
PTN
PTPN6
PTPRG

RPS7
RPS8
S100A11
S100A12
S100A4

PLIN3
PLTP
PLXDC2
PLXNB2
PNP
PODXL2
PON1
POSTN
PPA1
PPBP
PPIA
PPIB
PPP2R1A
PRAM1
PRCP
PRDX1
PRDX2
PRDX3
PRDX5
PRDX6
PRG4
PRNP
PROC
PROCR
PROS1
PRSS1
PRSS3
PRTN3
PSAP
PSAT1
PSMA1
PSMA2
PSMA5
PSMA6
PSMA7
PSMB1
PSMB2
PSMB3
PSME1

PTPRS
PTPRZ1
PTX3
PVALB
PYCARD
PYGL
PYROXD2
PZP
QDPR
QSOX1
RAB10
RAB11B
RAB5B
RAB7A
RAC2
RAD23B
RALB
RAN
RAP1B
RARRES2
RBMXL2
RBP4
RELN
RHOA
RHOG
RNASE2
RNASE3
RNASE4
RNASET2
RNH1
RPL10A
RPL18
RPL29
RPL4
RPL6
RPLP0
RPLP2
RPS15
RPS27A

S100A6
S100A8
S100A9
S100B
S100P
SAA1
SAA2
SAA4
SCG2
SCG3
SCG5
SCRG1
SDCBP
SELENBP1
SELENOP
SELL
SEMA7A
SERBP1
SERPINA1
SERPINA2
SERPINA3
SERPINA4
SERPINA6
SERPINA7
SERPINB1
SERPINC1
SERPIND1
SERPINE1
SERPINF1
SERPINF2
SERPING1
SEZ6L
SH3BGRL
SH3BGRL3
SHANK1
SHBG
SHROOM3
SIAE
SIGLEC14

SIGLEC9	T	UBQLN4
SIRPA	T	UFM1
SLC14A2	T	UGP2
SLC9A3R1	T	UQCR11
SNAP91	T	USP1
SNCA	T	VASN
SNCG	T	VASP
SNRPE	T	VAT1
SOD1	T	VCAM1
SOD2	T	VCAN
SOD3	T	VCL
SPARC	T	VCP
SPARCL1	T	VGF
SPP1	T	VIM
SPTA1	T	VSIG4
SPTAN1	T	VSNL1
SPTB	T	VSTM2A
SRSF2	T	VSTM2B
SRSF3	T	VTN
SST	T	VWF
STIP1	T	WARS
STMN1	T	WDR1
STXBP1	T	WFIKKN2
STXBP2	T	XYLT1
SUB1	T	YBX1
SULF2	T	YIPF3
SUMO4	T	YWHAB
SUPT6H	T	YWHAE
SYN1	T	YWHAG
SYN2	T	YWHAH
SYNCRIP	T	YWHAZ
SYNE2	T	ZYX
TAGLN	T	ZZEF1
TAGLN2	U	
TALDO1	U	

FCGR3A

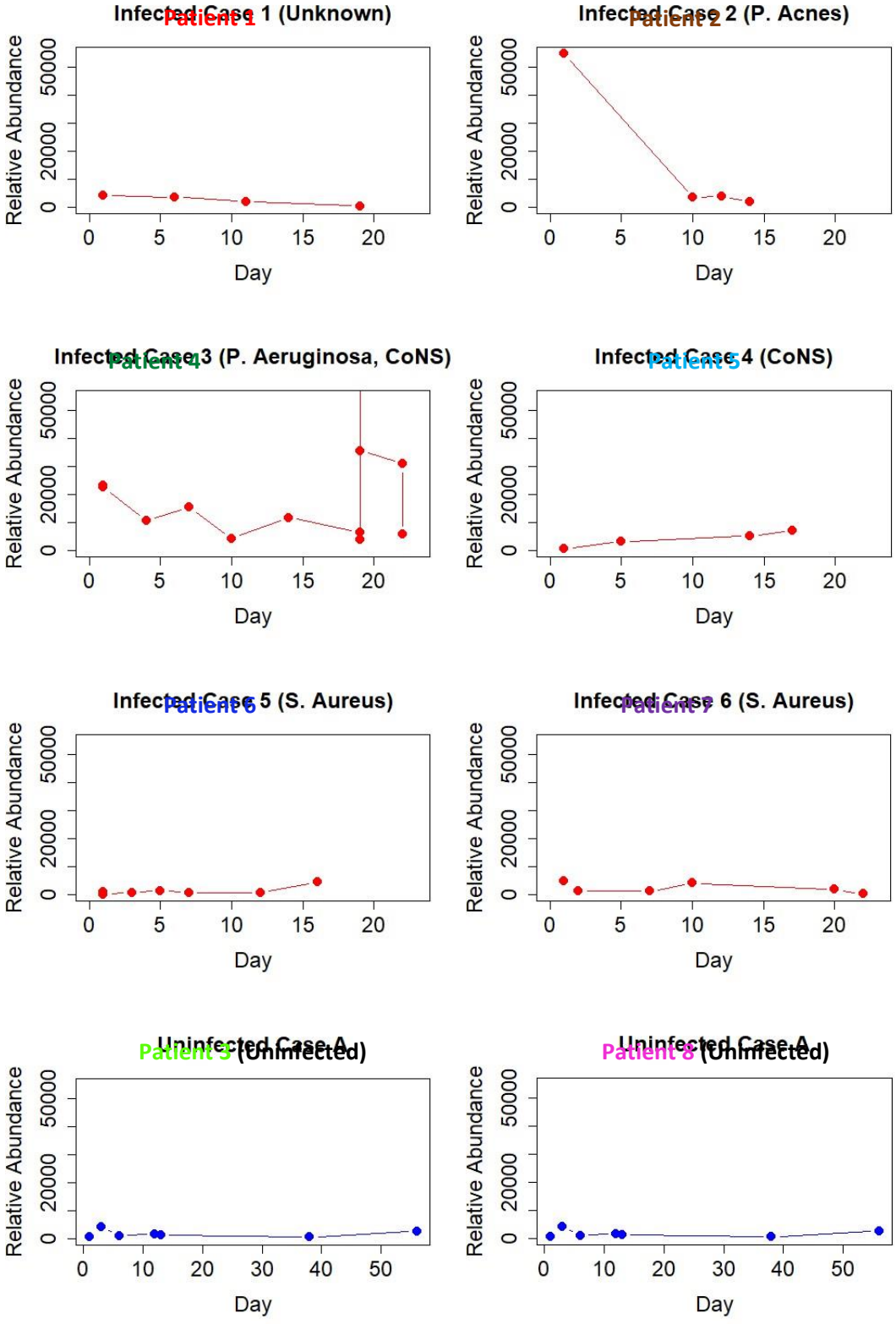

Figure 103 Relative abundance of FCGR3A as measured by LC-MS/MS

VGF

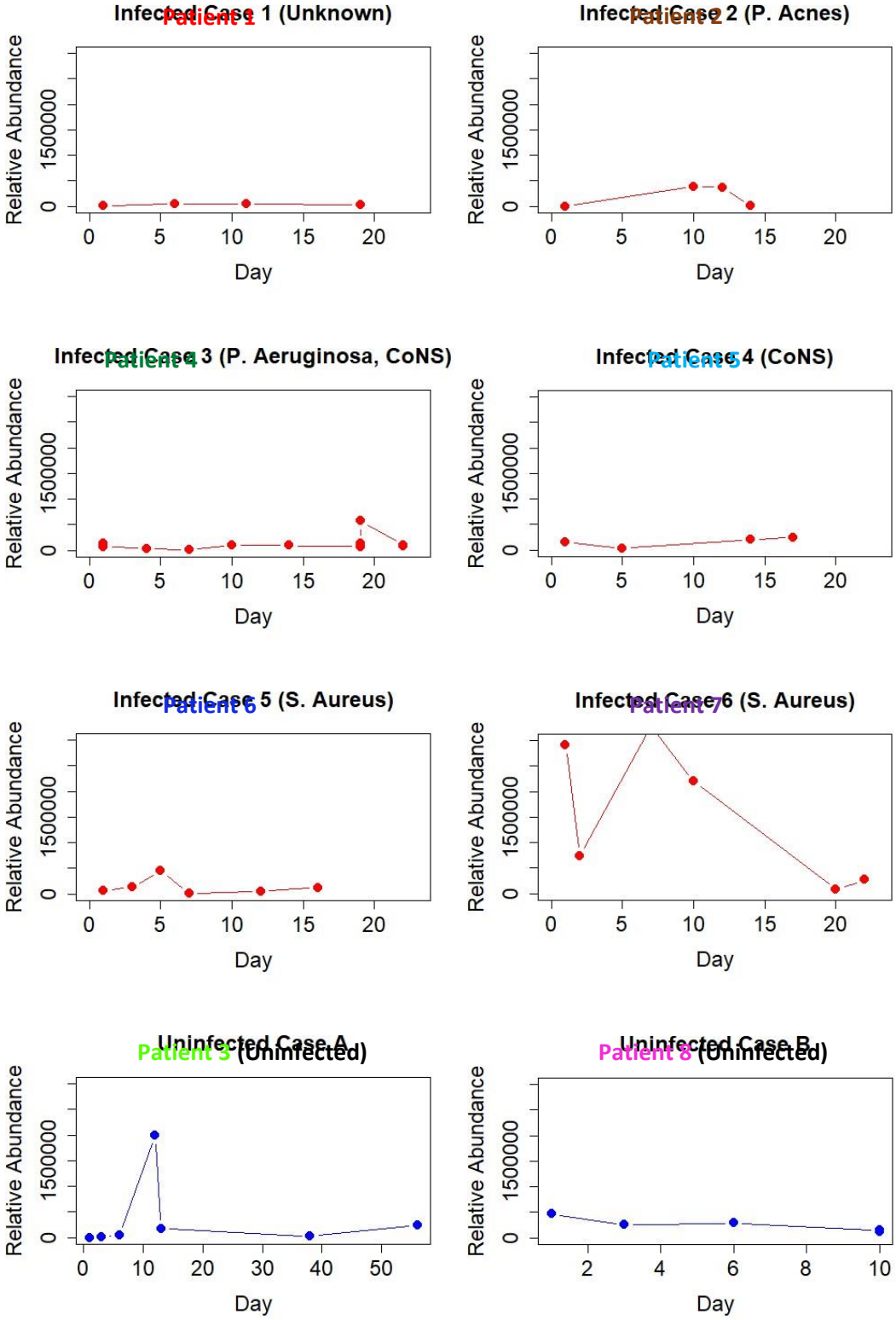

Figure 104 Relative abundance of VGF as measured by LC-MS/MS

SCG2

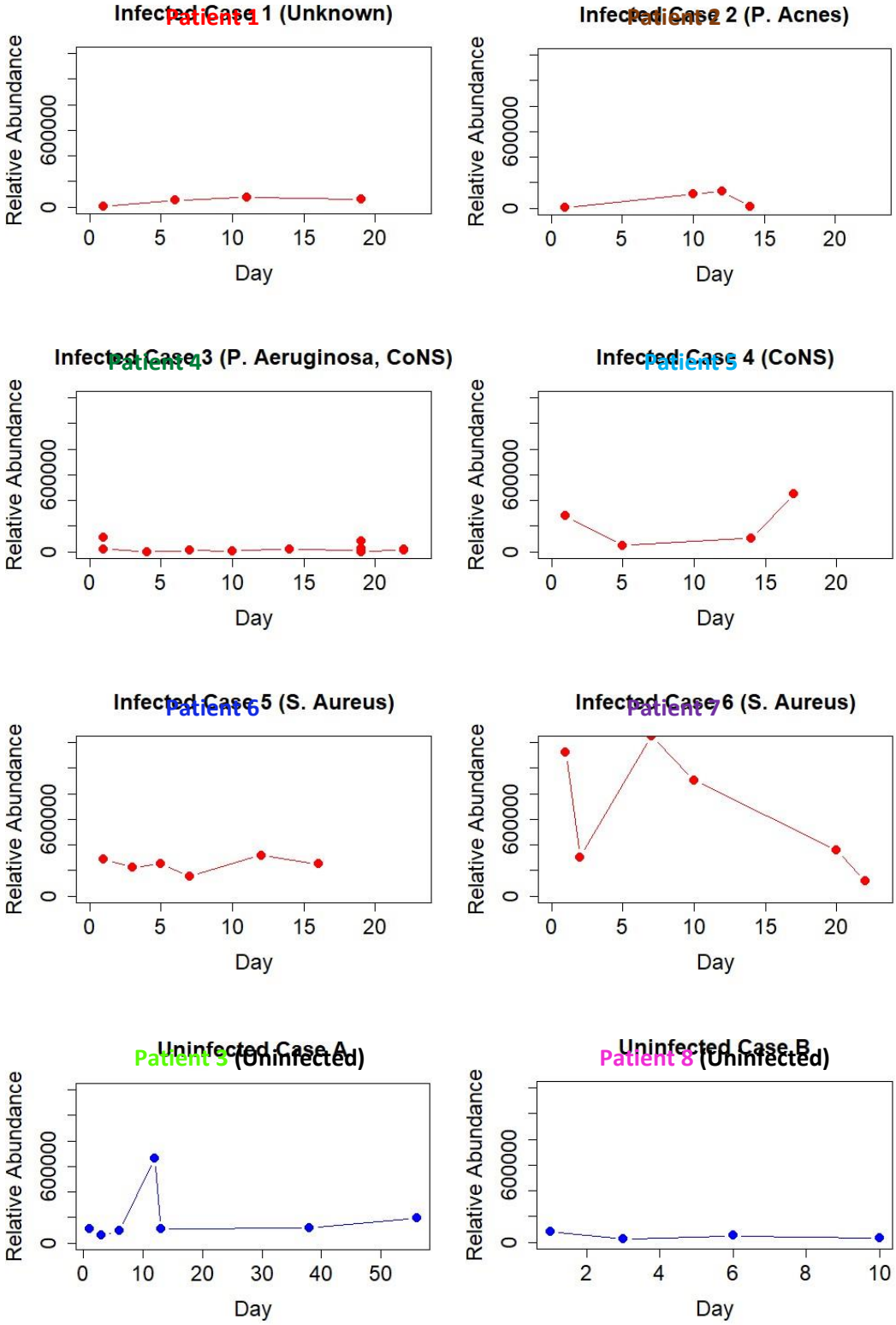

Figure 105

Relative abundance of SCG2 as measured by LC-MS/MS.

SCG5

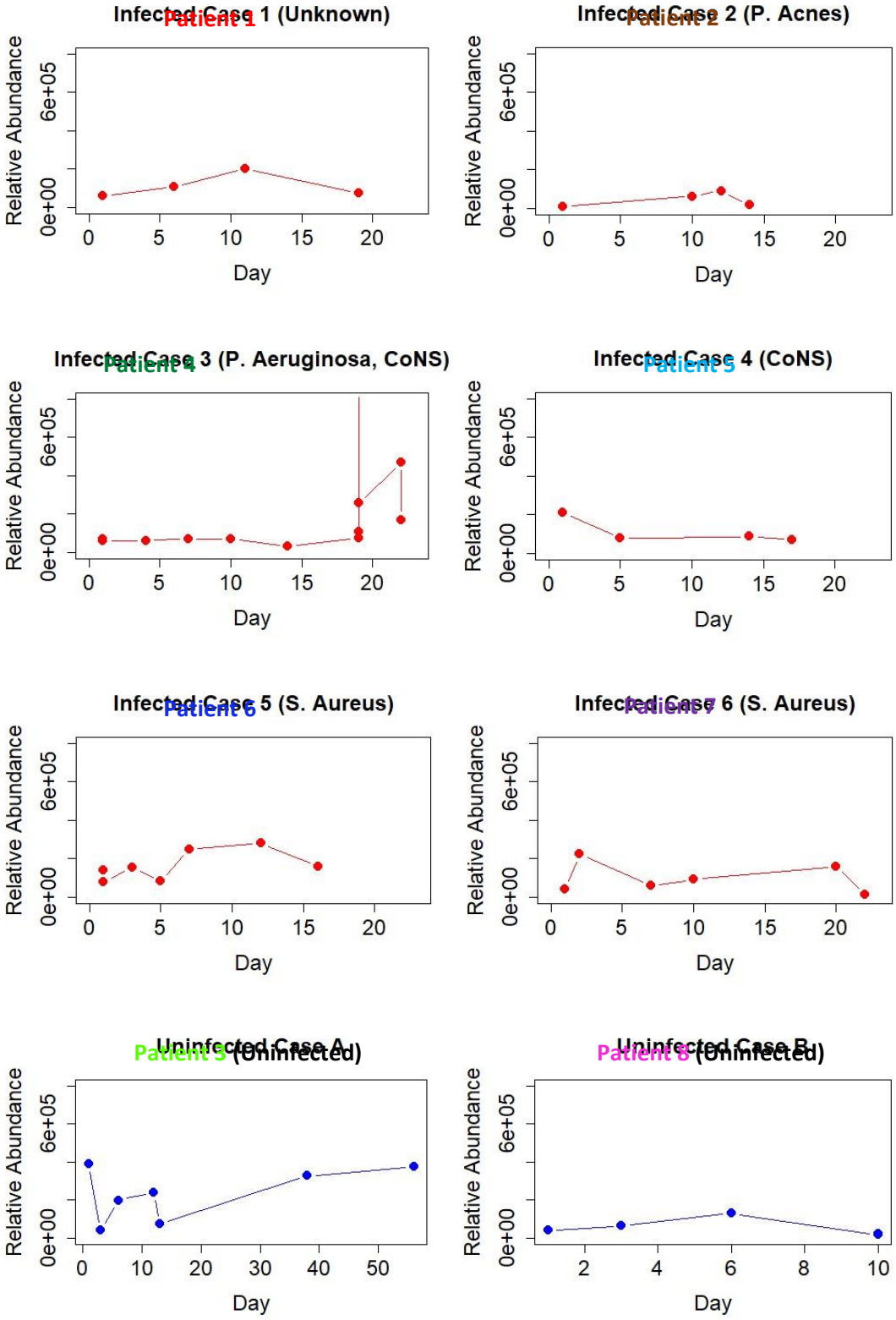

Figure 106 Relative abundance of SCG5 as measured by LC-MS/MS.

Fibrinogen

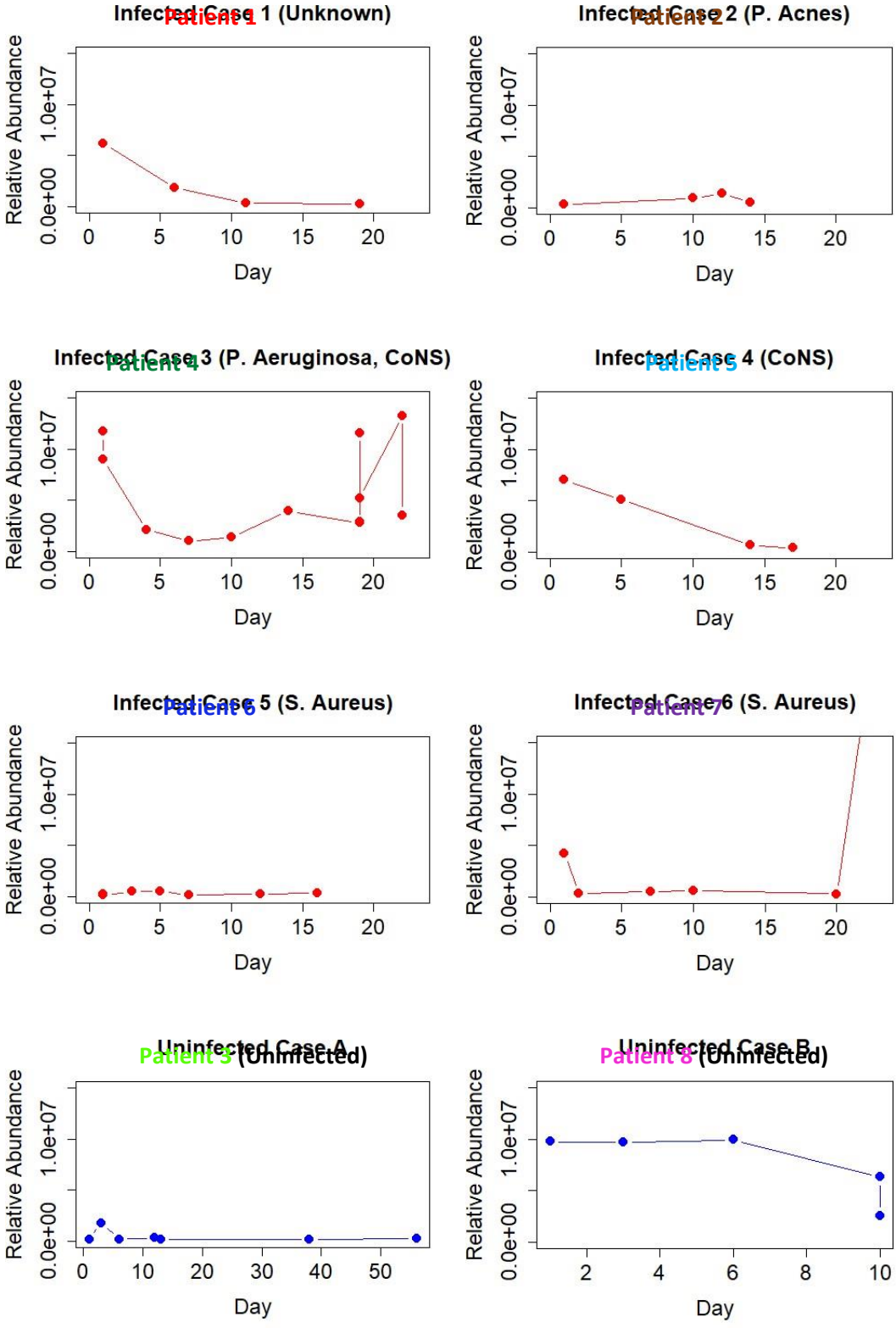

Figure 107 Relative abundance of Fibrinogen as measured by LC-MS/MS

Lipocalin

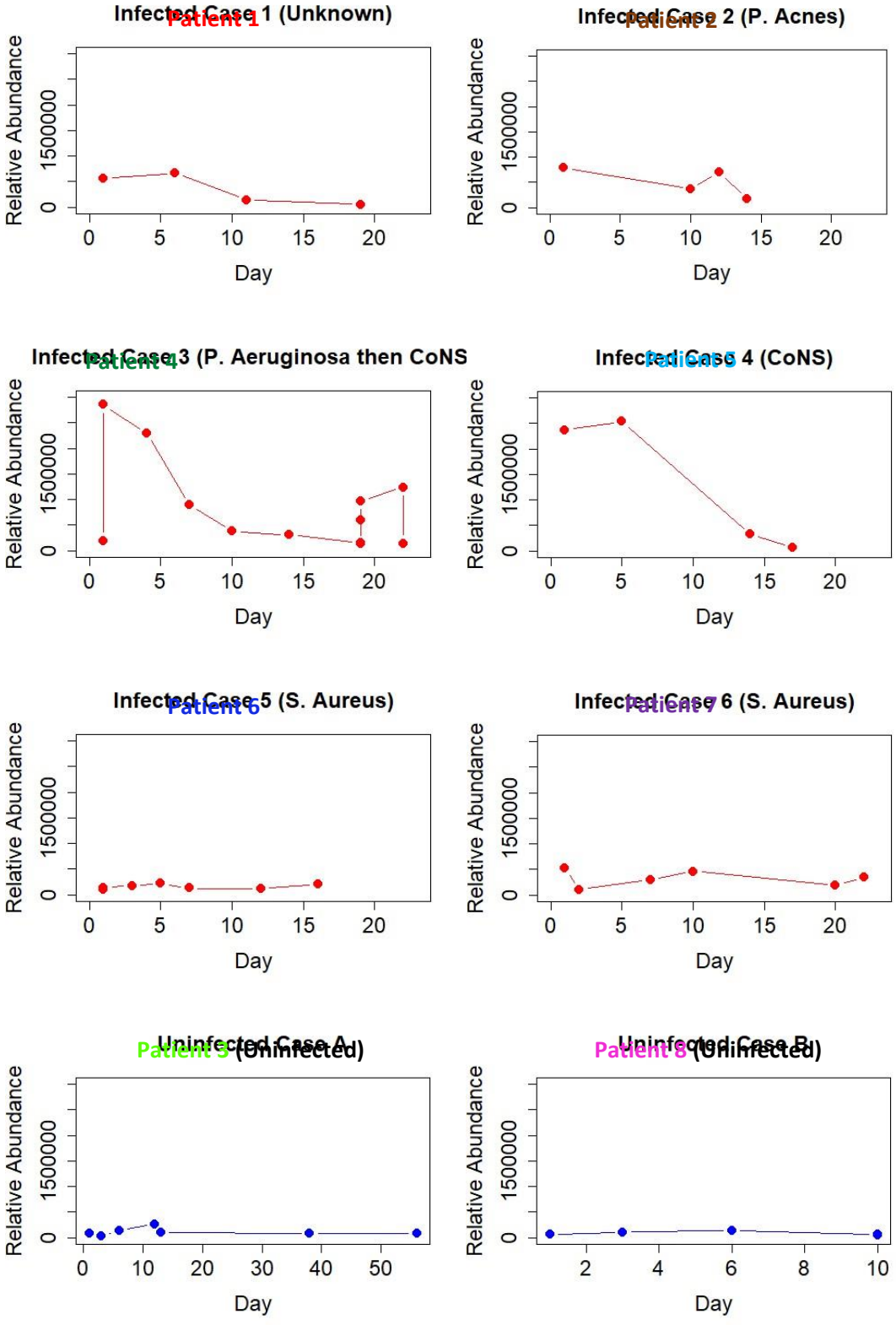

Figure 108 Relative abundance of Lipocalin as measured by LC-MS/MS in eight patients' CSF.

Calprotectin

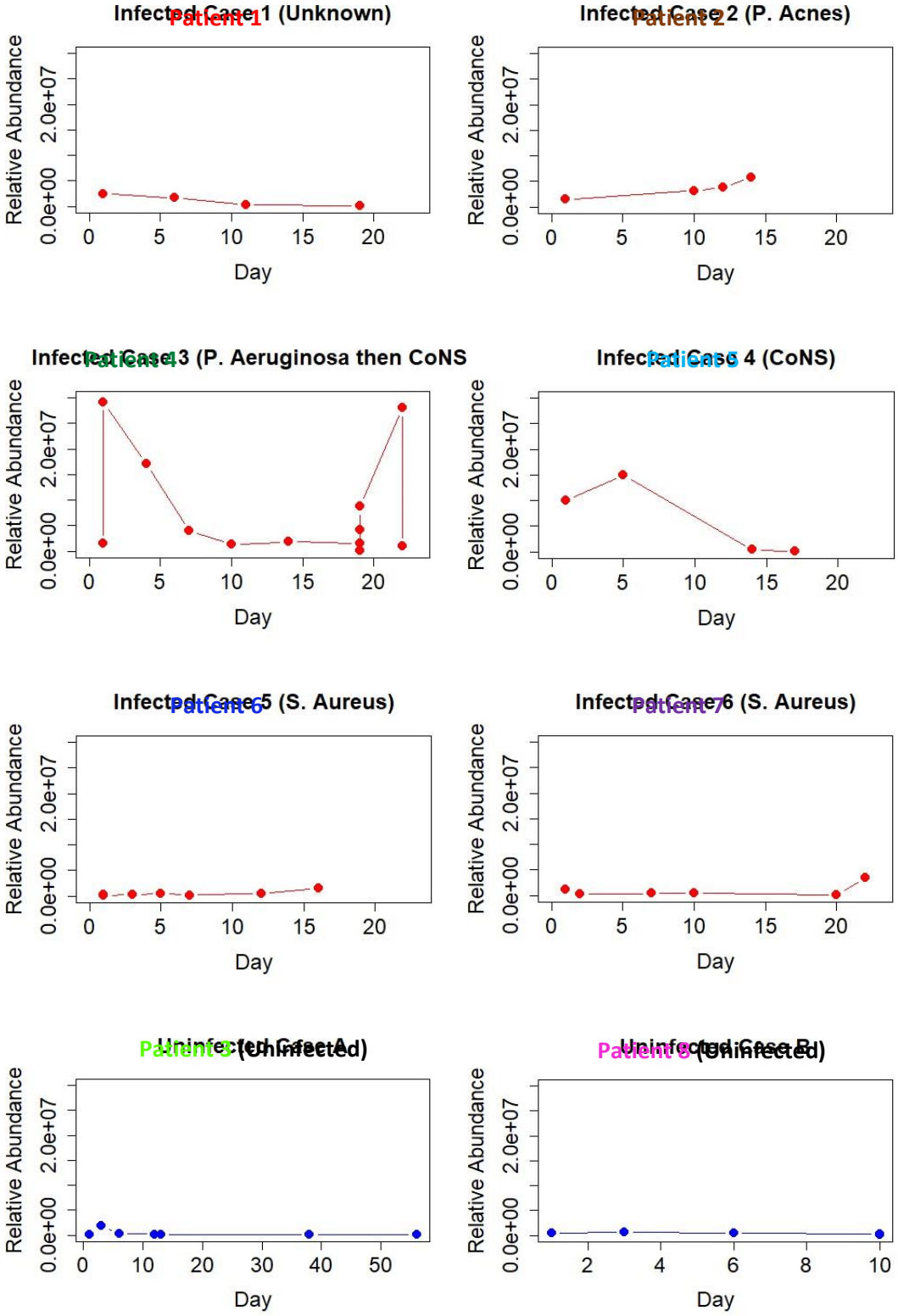

Figure 109 Relative abundance of Calprotectin as measured by LC-MS/MS in 8 patients

Appendix C

*Sample 1- Infected neurosurgical CSF (*S. haemolyticus*, WCC=355, RCC=253)*

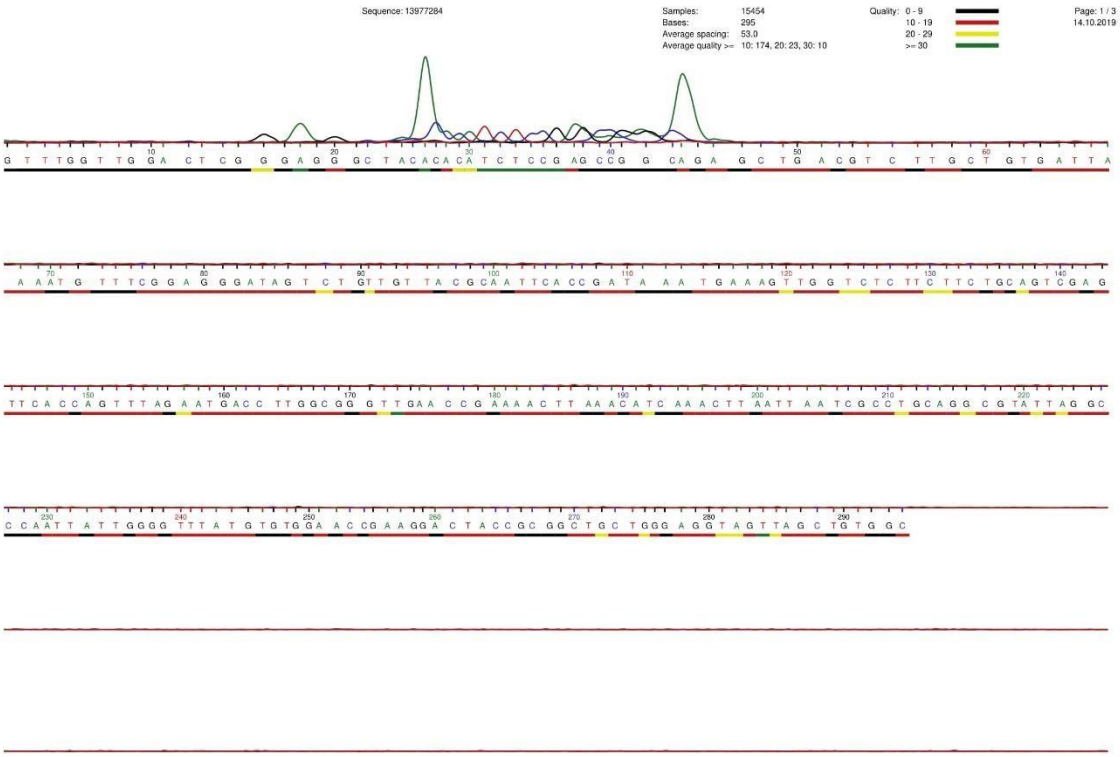

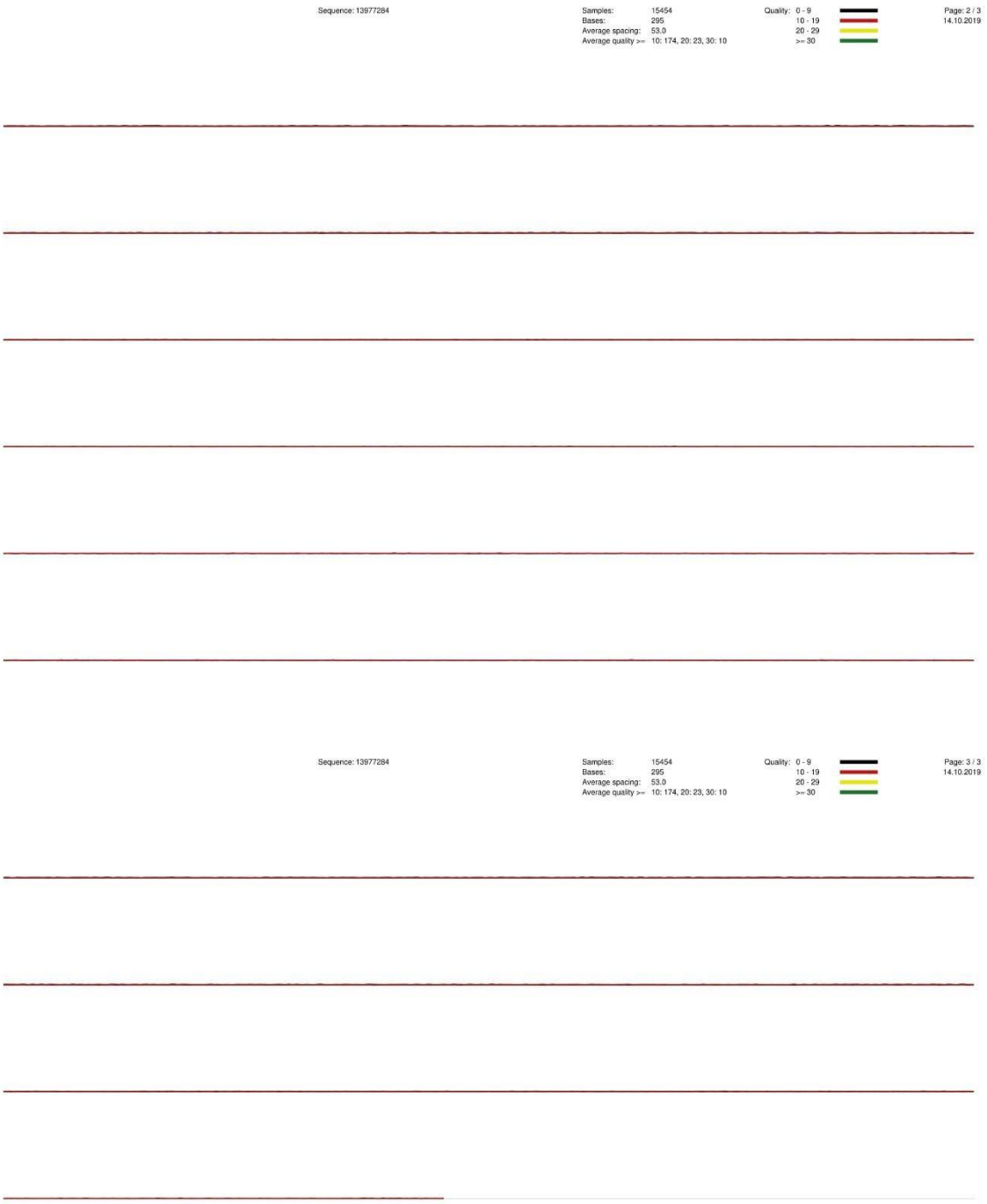

Sample 2- Infected neurosurgical CSF (E. faecalis, WCC=434, RCC= 62)

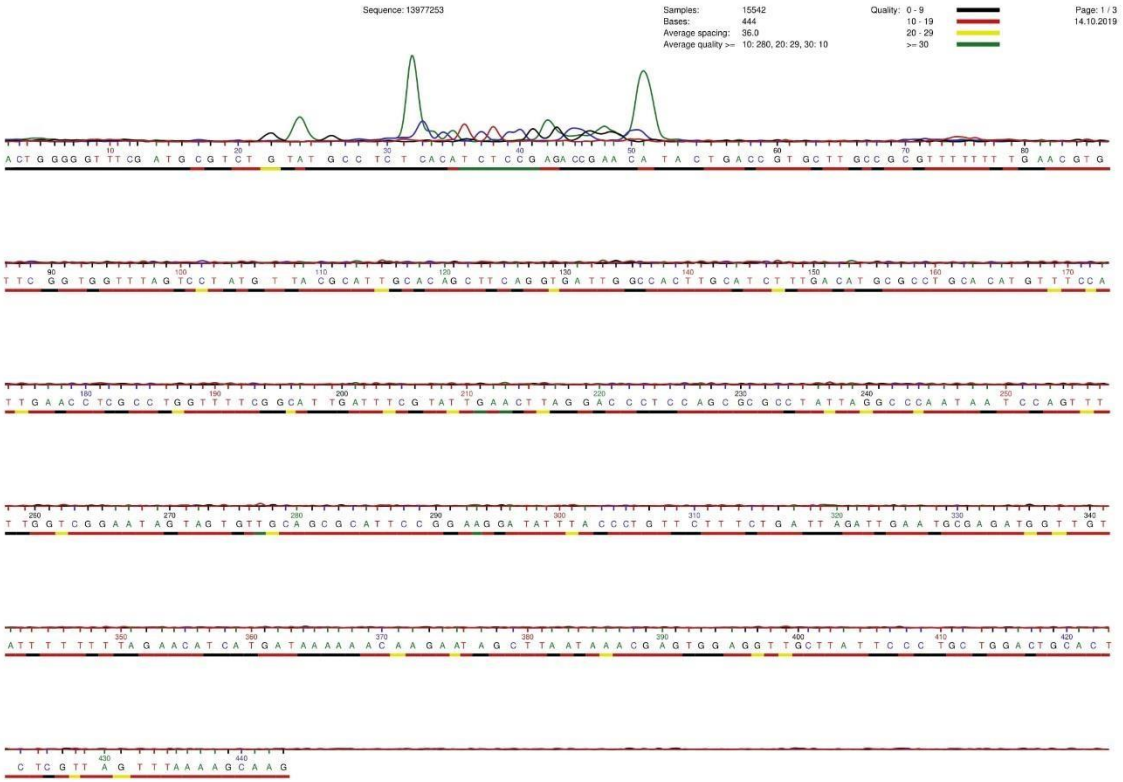
Sequence: 13977253
Samples: 15542
Bases: 444
Average spacing: 36.0
Average quality >= 10: 280, 20: 29, 30: 10
Quality: 0 - 9
10 - 19
20 - 29
>= 30
Page: 1 / 3
14.10.2019

*Sample 3- Infected neurosurgical CSF (*S. epidermidis & S. haemolyticus*, WCC=538, RCC=96)*

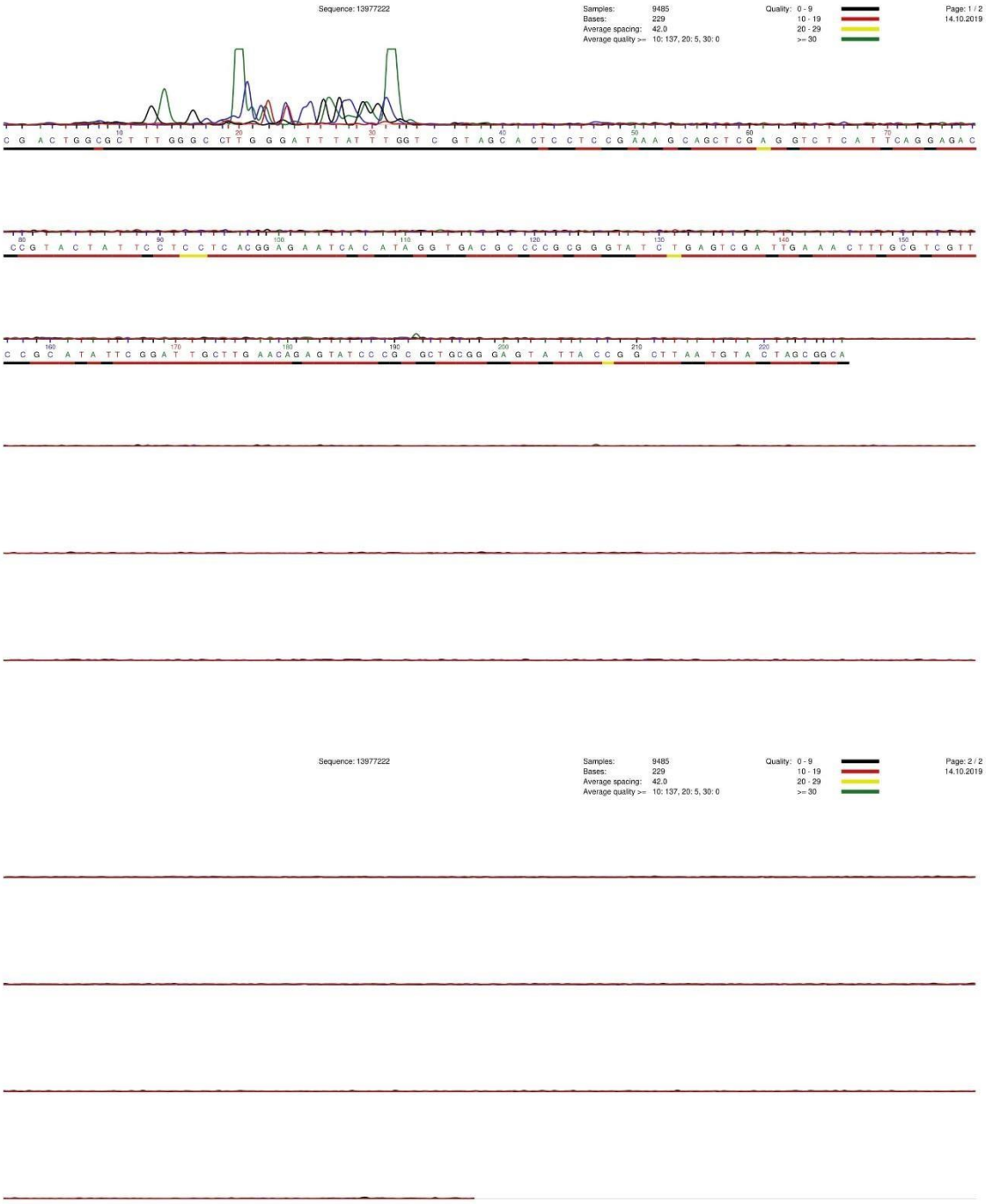

*Sample 4 Infected neurosurgical CSF (*E. cloacae, *WCC=850, RCC=90)*

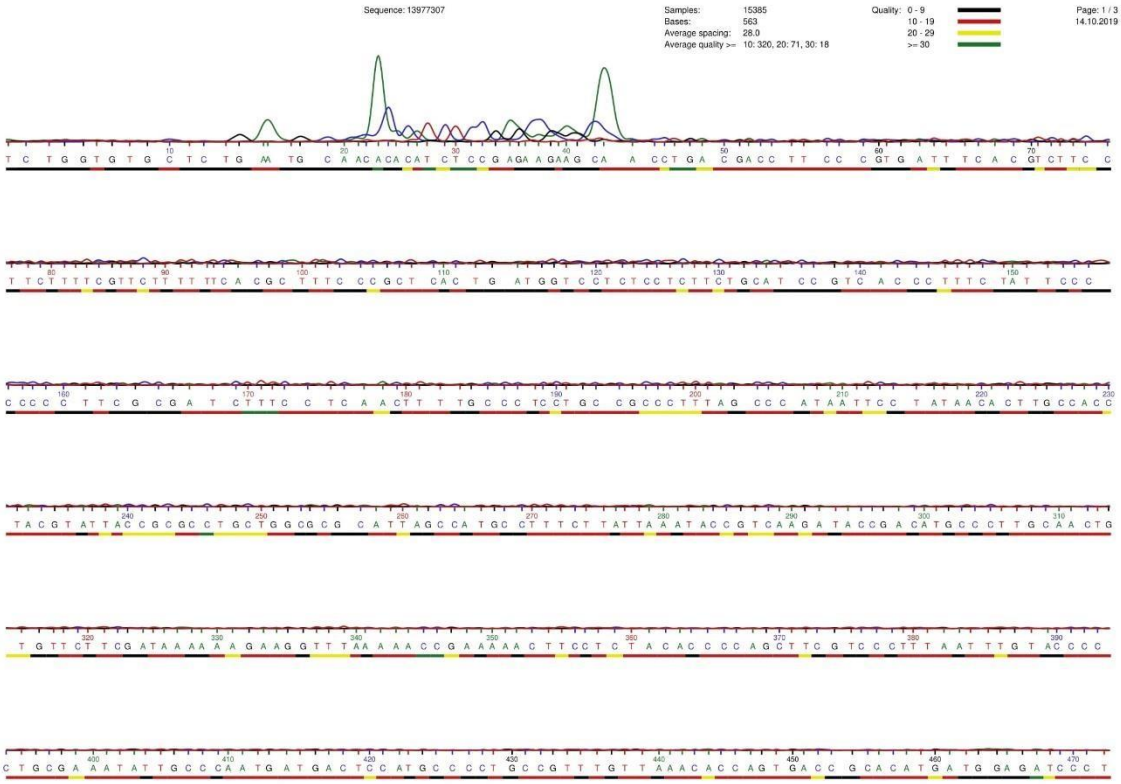

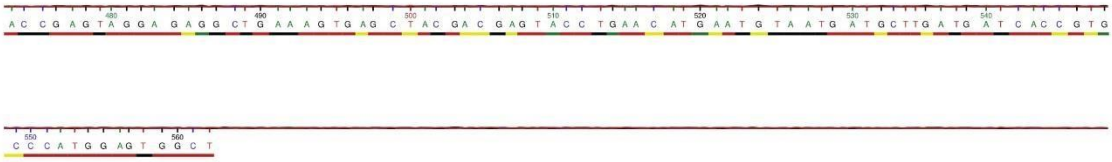
480
490
500
510
520
530
540
ACCGAGTAGGAGAGGCTGAAAAGTGAGCTACGACGAGTACCTGAACATGAATGTAATGATGCTTGATGATCACCGTG
550
560
CCCATGGAGTGGCT

Sample 5 Uninfected neurosurgical CSF (WCC<1, RCC=4)

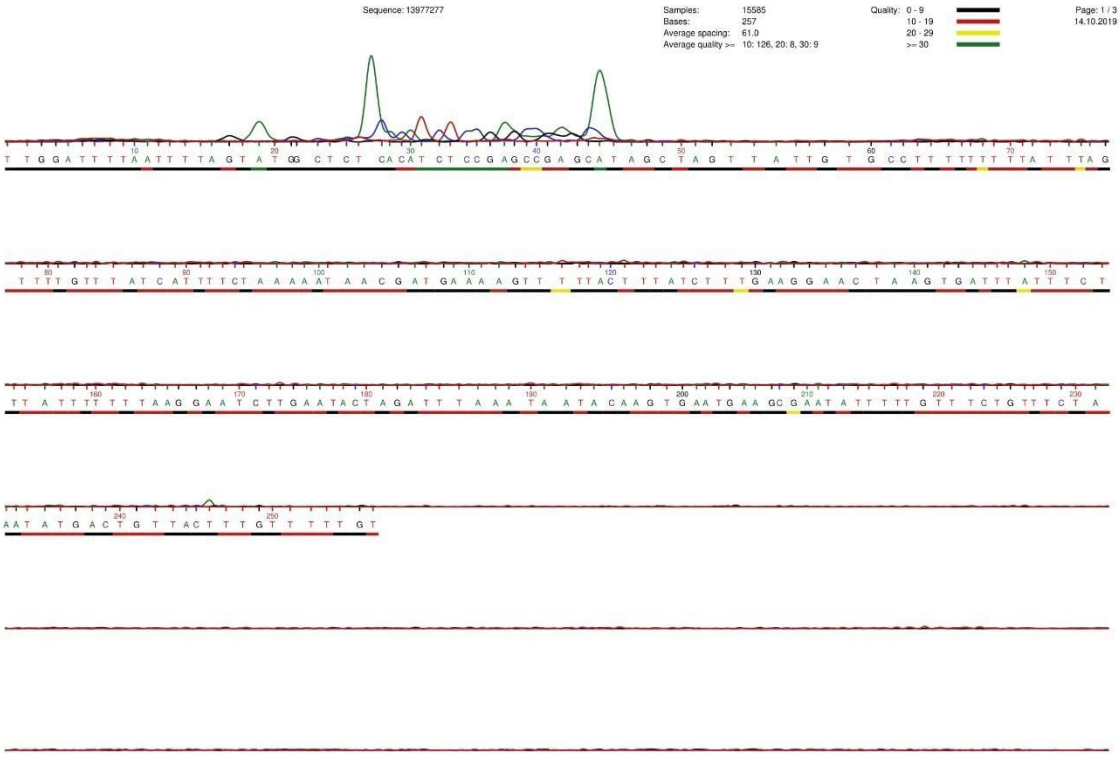

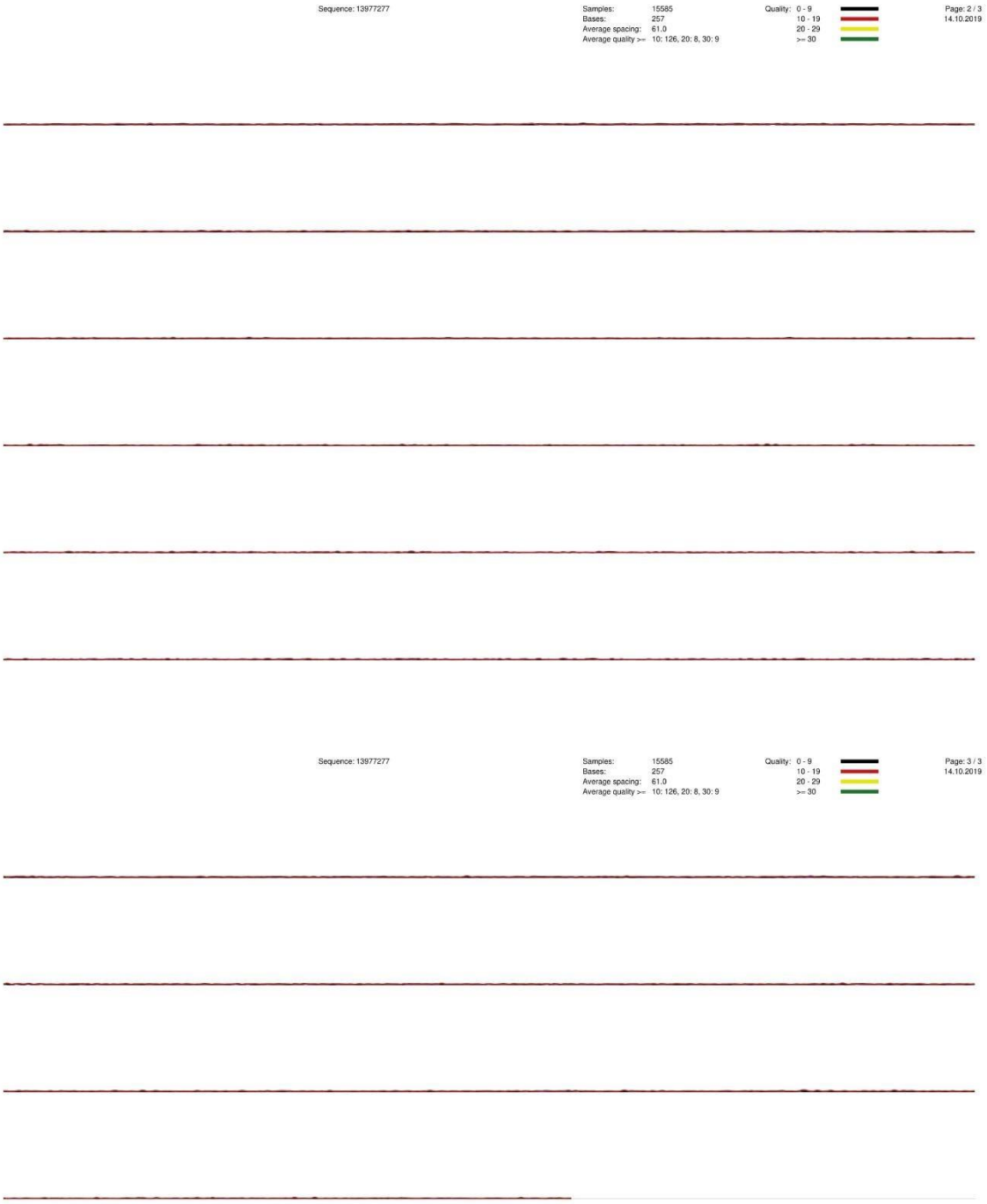
Sequence: 13977277
Samples: 15585
Bases: 257
Average spacing: 61.0
Average quality >= 10: 126, 20: 8, 30: 9
Quality: 0 - 9
10 - 19
20 - 29
>= 30
Page: 2 / 3
14.10.2019

Sequence: 13977277
Samples: 15585
Bases: 257
Average spacing: 61.0
Average quality >= 10: 126, 20: 8, 30: 9
Quality: 0 - 9
10 - 19
20 - 29
>= 30
Page: 3 / 3
14.10.2019

Sample 6 Uninfected neurosurgical CSF (WCC<1, RCC=12)

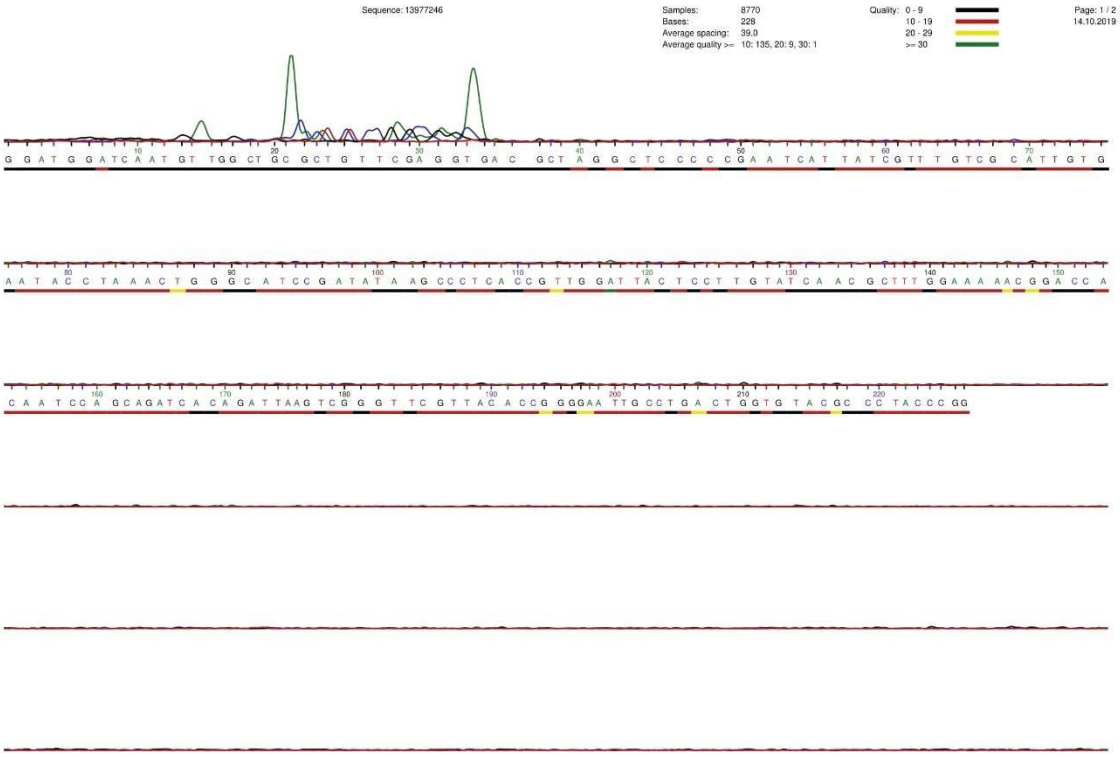

Sample 7 Uninfected neurosurgical CSF (WCC=1. RCC<1)

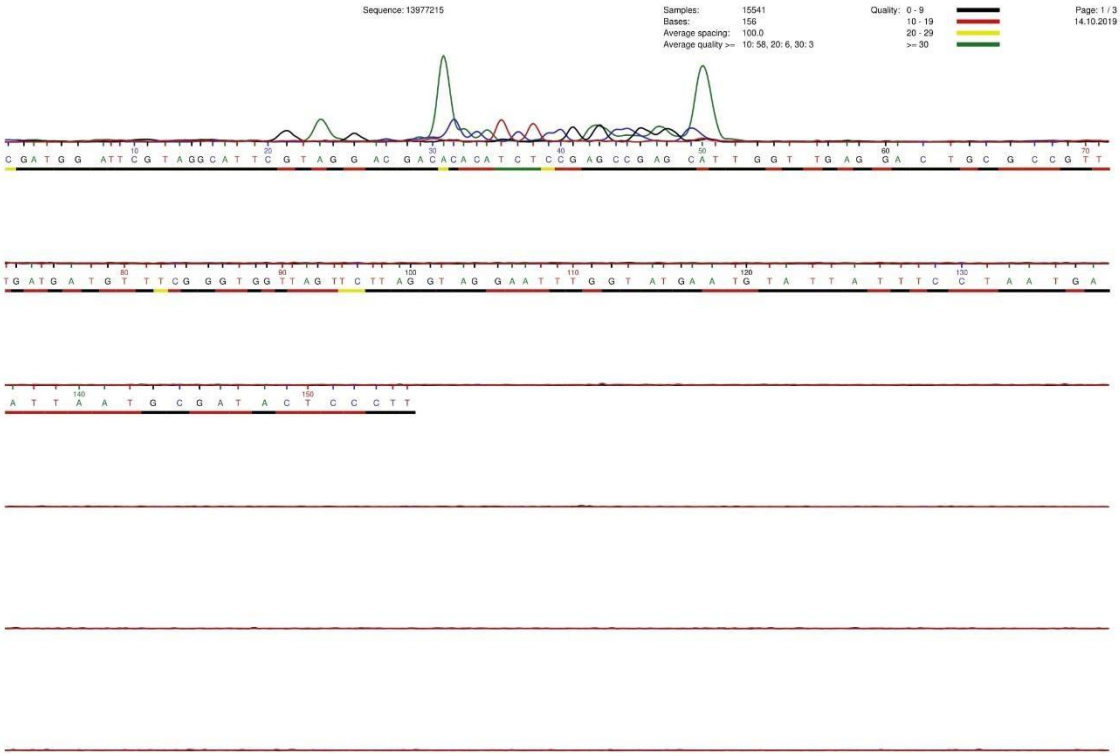

Sample 8 Uninfected neurosurgical CSF (WCC<1, RCC=140)

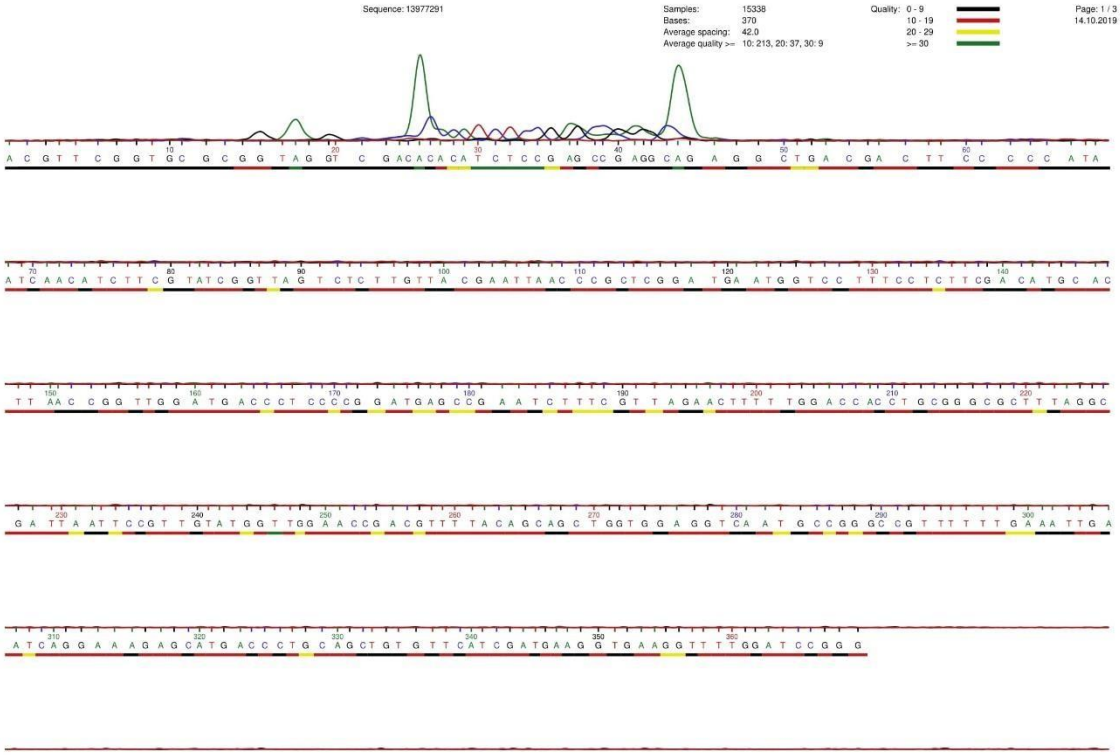

Sample 9 Laboratory grade water (H20) that underwent extraction and amplification

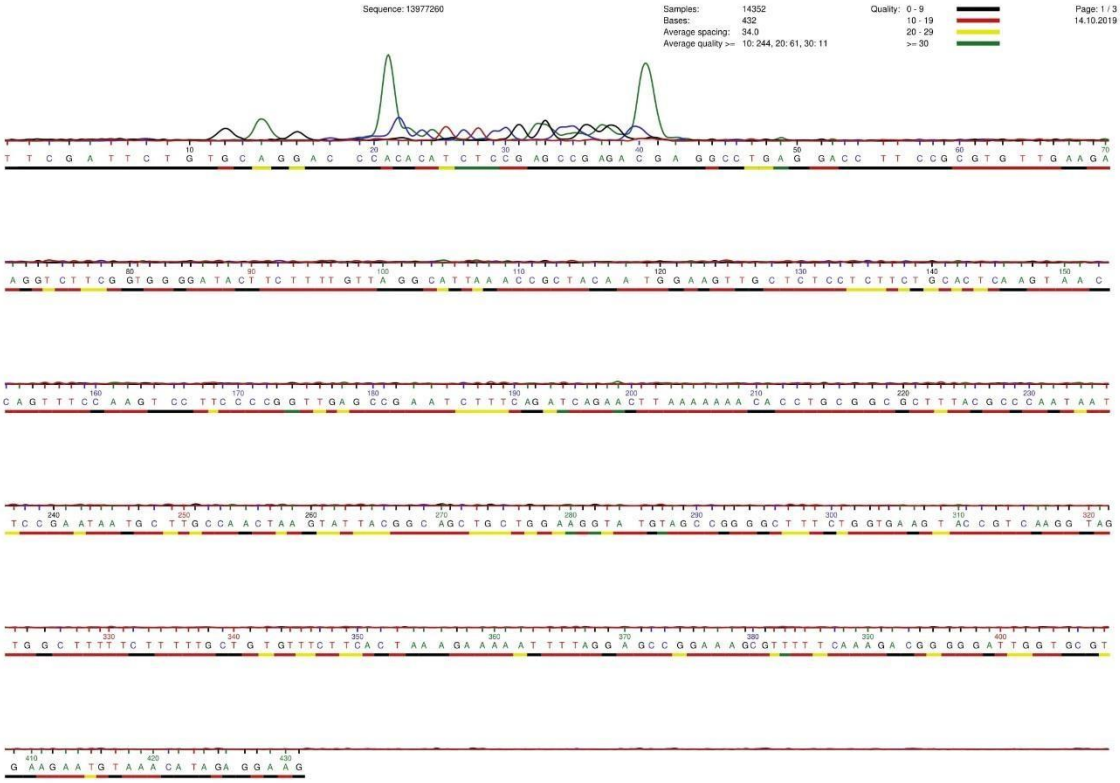

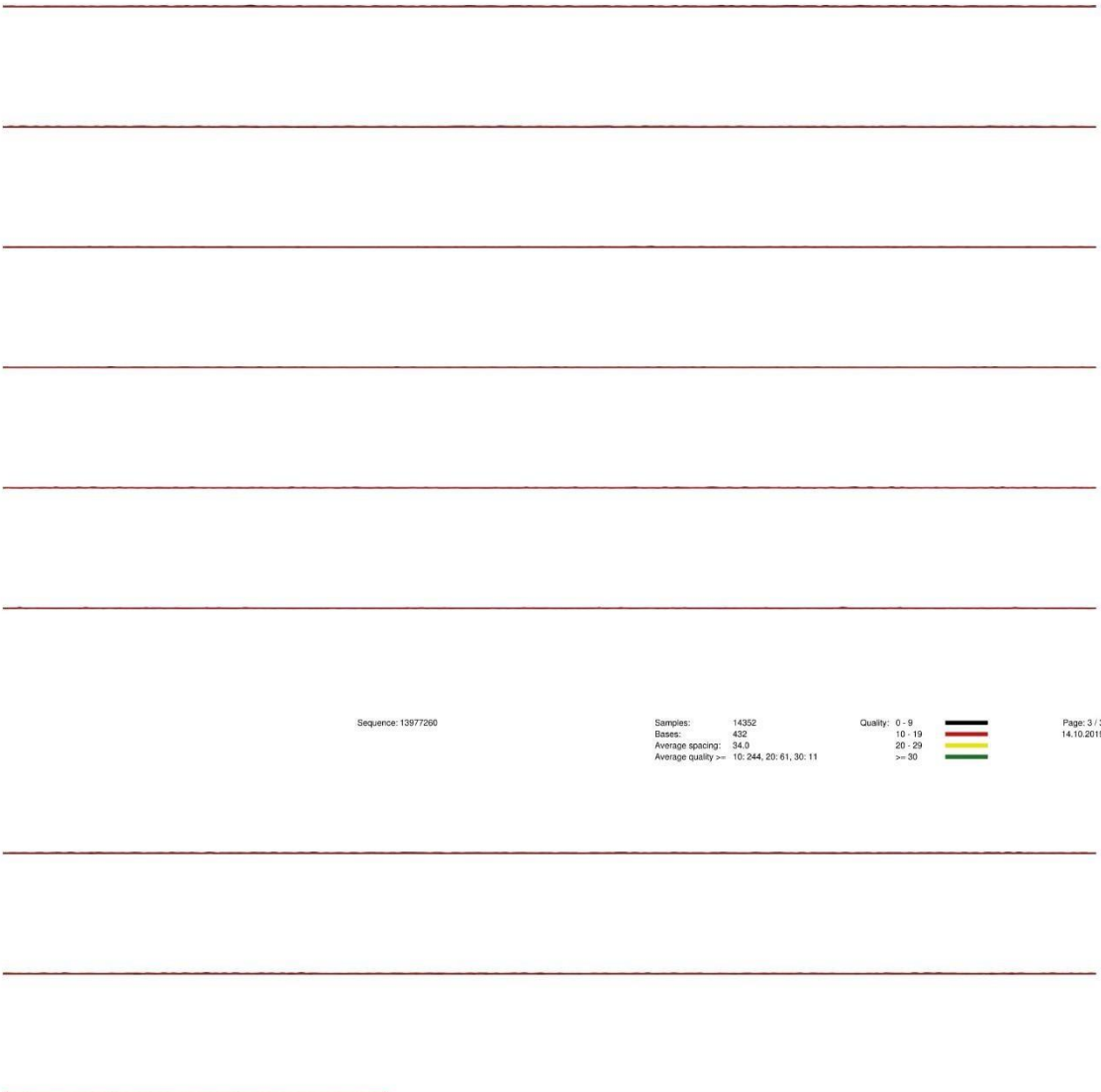

Sample 10- DES that underwent extraction and amplification

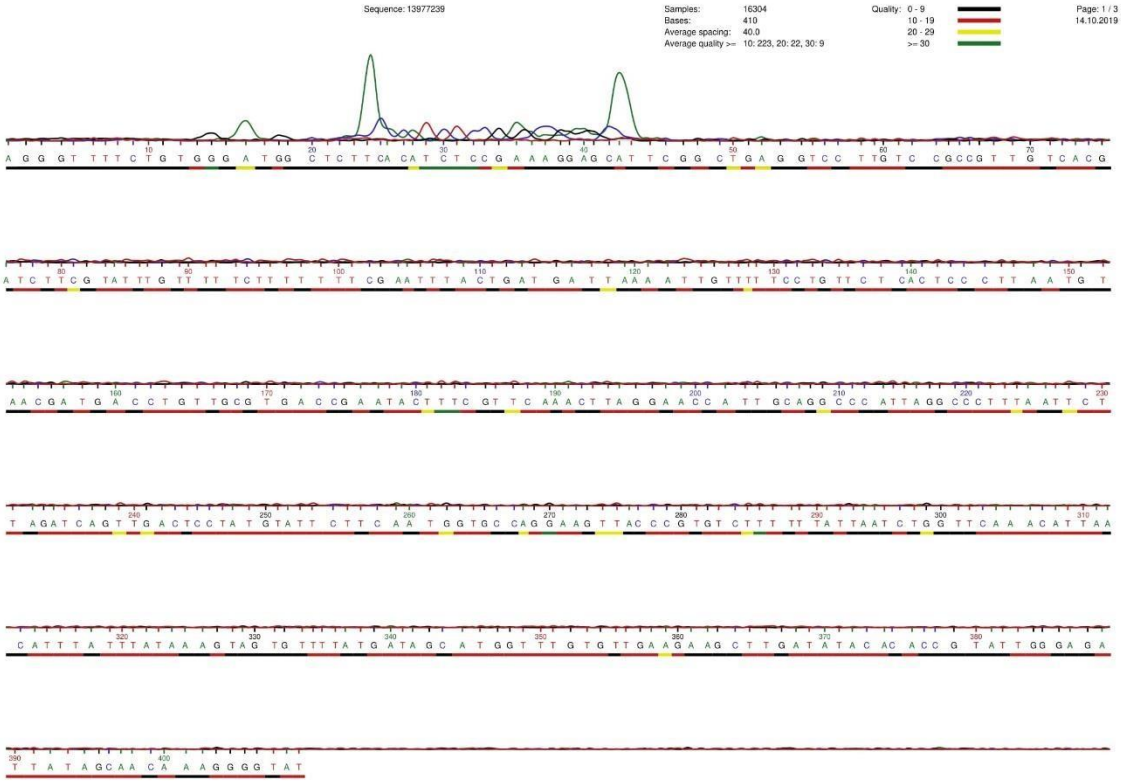

Negative control sample

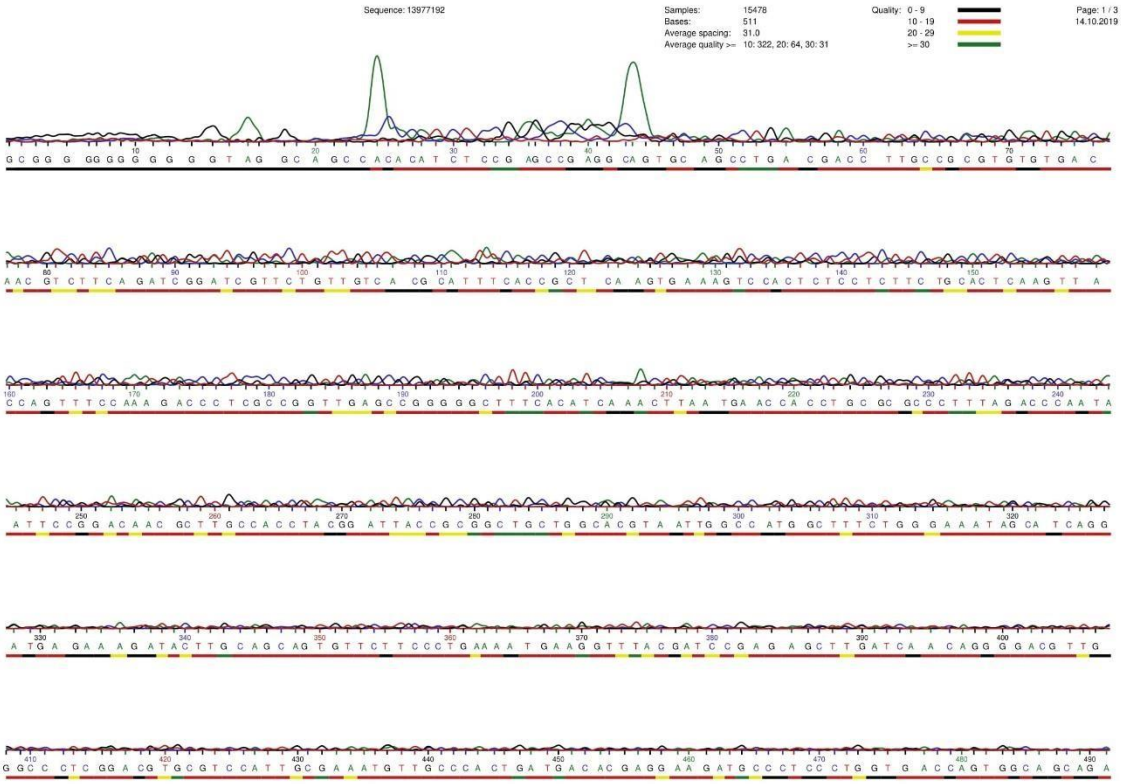

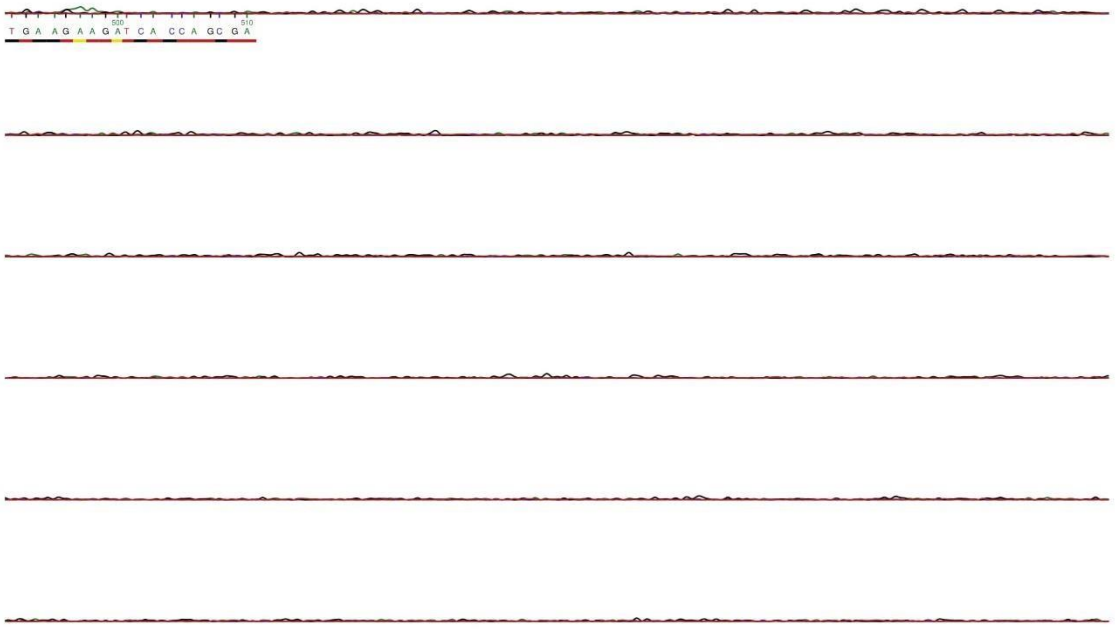
500
510
T G A A G A A G A T C A C C A G C G A